Novel insights into chemotrophic L-tryptophan metabolism of *Rubrivivax benzoatilyticus* JA2

Thesis Submitted to the University of Hyderabad for the award of

DOCTOR OF PHILOSHPY By

Shabbir Ahmad

(Reg. No: 13LPPH20)



Department of Plant Sciences School of Life Sciences University of Hyderabad Hyderabad - 500 046 INDIA

November, 2020

Acknowledgements

For Almighty ALLAH is all praise as He blessed me the strength and for the light that he bestowed me to finish this research.

I extend my gratitude to my supervisor Prof. Ch. V. Ramana for his constant guidance, encouragement and constant support throughout my doctoral research.

I thank the present head Prof. G. Padmaja and former heads of the Department of Plant Sciences i.e. Prof. A. R. Reddy, Prof. Ch. V. Ramana for providing me the departmental facilities.

I thank the present dean Prof. S. Dayananda and former deans i.e Prof. P. Reddana, Prof. KVA Ramaiha, Prof. Aparna Datta Gupta, School of Life Sciences for providing me the general facilities of the School.

I thank my Doctoral Committee members Prof. S. Rajagopal, Prof. Appa Rao Podile and Dr. K. Gopinath for their valuable suggestions.

I thank Prof. Ch. Sasikala, JNTU for extending her lab facilities.

I also thank all the faculty members of School of Life Sciences for extending their lab and for their valuable inputs in times of needs.

I would also like to thank my senior lab members Dr. Mujahid Muhammed, Dr. Lakshmi Prasuna for their tremendous guidance and for their invaluable insights and suggestions.

I would like to thank all my present (Dr. Suresh, Dr. Ganesh, Kim, Meesha, Smita, Indu, Anusha, Sreya, Gaurav, Jagdishwari, Ipsita, Krishnah, Ashif and Deepshikha) and former lab mates from HCU and JNTU for their help and cooperation throughout my research.

I thank all my friends and research scholars of School of Life Sciences for their cooperation and help me throughout the research periods.

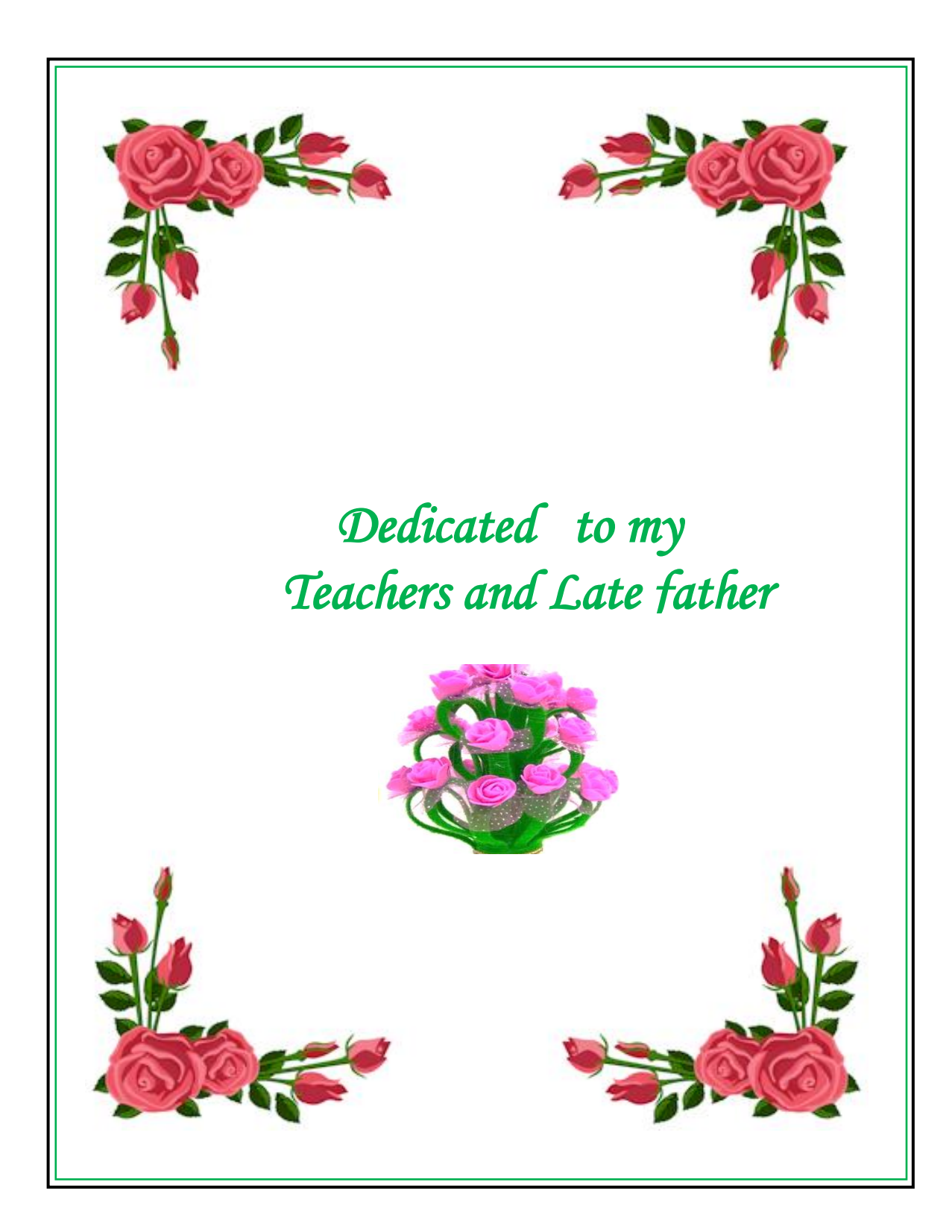
The help and cooperation of the non-teaching staff is highly acknowledged.

I acknowledge the UGC-MANF for financial aid. DST-FIST, UGC-SAP, DBT-CREEB for school and departmental facilities, and highly acknowledged TATA Innovation fellowship for Lab Funding.

I am extremely grateful to my mother, my brothers and family members for their unwavering love, support and patience throughout my life.

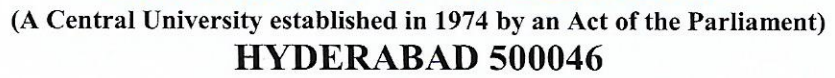
Above all, I thank Almighty for providing me everything.

Shabbir Ahmad.....





UNIVERSITY OF HYDERABAD





CERTIFICATE

This is to certify that this thesis entitled "Novel insights into chemotrophic L-tryptophan metabolism of Rubrivivax benzoatilyticus JA2" is a record of bonafide work done by Mr. Shabbir Ahmad, a research scholar for Doctor of Philosophy in Department of Plant Sciences, School of Life Sciences, University of Hyderabad, under my supervision and guidance.

HEAD MIN 12010
Dept. Plant Sciences

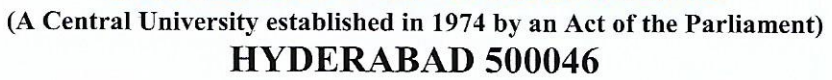
Dept. of Plant Sciences School of Life Sciences University of Hyderabad Hyderabad-500 046 INDIA DEAN
School of Life Sciences

DEAN School of Life Sciences University of Hyderabad Hyderabad - 500 046. SUPERVISOR Prof. Ch. V. Ramana

Prof. Ch. Venkata Ramaga Ph.s. Department of Plant Sciences School of Life Sciences University of Hyderabad, P.O. Central University, Hyderabad - 500 046, India



UNIVERSITY OF HYDERABAD





DECLARATION

I Shabbir Ahmad, hereby declare that this thesis entitled "Novel insights into chemotrophic L-tryptophan metabolism of Rubrivivax benzoatilyticus JA2" submitted by me under the guidance and supervision of Prof. Ch.Venkata Ramana is an original and independent research work. I hereby declare that this work is original and has not been submitted previously in part or in full to this University or any other University or Institution for the award of any degree or diploma.

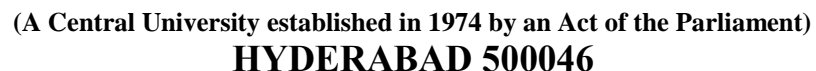
Shabbir Ahmad
(Ph.D student)

Supervisor Prof. Ch.V. Ramana

Prof. Ch. Venkata Ramana Ph.:
Department of Plant Sciences School of Life Sciences
University of Hyderabad, P.O. Central University,
Hyderabad - 500 046, India



UNIVERSITY OF HYDERABAD





CERTIFICATE

This is to certify that this thesis entitled "Novel insights into chemotrophic L-tryptophan metabolism of *Rubrivivax benzoatilyticus* JA2" is a record of submitted by Mr. Shabbir Ahmad, bearing registration number 13LPPH20 a research scholar for award of Doctor of Philosophy in Department of Plant Sciences, School of Life Sciences, University of Hyderabad, under my guidance and supervision. This thesis is free from plagiarism and has not been submitted in any part or to full to this or any other University or Institute for the award of any degree or diploma.

Parts of the thesis has been:

A. Published in following publication:

<u>Shabbir Ahmad</u>, Mujahid Mohammed, Lakshmi Prasuna Mekala, Chintalapati Sasikala and Venkata Ramana Chintalapati, (2020) Tryptophan, a non-canonical melanin precursor: new L-tryptophan based melanin production by *Rubrivivax benzoatilyticus* JA2. *Sci Rep*. 10:8925. doi: 10.1038/s41598-020-65803-6.

- B. Presented in the following conferences and award:
 - 1. Poster presentation Title "Novel melaniod-like pigment production by a Betaproteobacteria *Rubrivivax benzoatilyticus* JA2" Md. Shabbir Ahmad, M.Lakshmi Prasuna, M. Mujahid ,Ch. Sasikala Ch. V. Ramana 56th Annual Conference of Association of Microbiologists of India (AMI) Dec 07-10 2015.

- **Tester** presentation Title" Characterization of 5-hydroxytryptophan-based melanin and it's hydrolysis products in the photosynthetic bacterium Berivivax benzoatilyticus JA2T" Shabbir Ahmad, Lakshmi Prasuna, M, Muhammed and Ramana Ch.V. 59th Annual Conference of Association of Microbiologists of India (AMI) Dec 09-12, 2018.
- presentation Title "Characterization of novel L-Tryptophan based melanin from Rubrivivax benzoatilyticus JA2." Shabbir Ahmad and Prof. Venkata Ramana, Department of Plant Science, School Life Science Wersity of Hyderabad Telangana 500046. In 8th International Conference 30-03 Nov 2017.

AWARDED BEST ORAL PRESENTATION

student has passed the following courses toward the fulfillment requirement for Ph.D. degree.

San	Course	Name	Credits	Pass/Fail
L	PL801	Seminar I	1	Pass
2	PL802	Research ethics and management	2	Pass
五	PL803	Biostatics	2	Pass
×.	PL804	Analytical Technique	. 3	Pass
5.	PL805	Lab work	4	Pass

THE RESERVE

School of Life Sciences

SUPERVISOR Prof. Ch. V. Ramana

DEAN School of Life Sciences University of Hyderabad Hyderabad - 500 046.

Prof. Ch. Venkata Ramana Ph. Department of Plant Sciences School of Life Sciences University of Hyderabad, P.O. Central University, Hyderabad - 500 046, India

Table of Contents	
Abbreviations	vi-vii
e	viii- xv
1.0 Introduction	1-18
1.2. Metabolism of L-Tryptophan by prokaryotes	3
1.2.1. Catabolism of L-Tryptophan	3-4
1.2.2. Partial oxidation of L-Tryptophan under oxic and anoxic environments	4-5
1.2.2.1. Indole-3-pyruvic acid pathway [IPyA]	5
1.2.2.2. Indole-3-acetamide pathway	5
1.2.2.3. Tryptamine pathway	6
1.2.2.4. Indole-3-acetonitrile pathway	6-7
1.3. Kynurenine pathway of L-Tryptophan metabolism	7-8
1.4. L-Tryptophan biotransformation	8-9
1.5 Secondary metabolites	10
1.5.1. Indigo and Violacein	10-12
1.5.2. Melanins	12-13
1.5.2.1. Melanin biosynthesis in bacteria	13-14
1.5.4. Types of melanin and their biosynthesis	15-16
1.6. Definition of the problem	16-18
1.7. Objectives of the study	18
2.0. Materials and methods	19-48
2.1. Equipment and chemicals	19
2.1.1. Equipment	19
2.1.2. Water for solubalization	19
2.1.3. Stock chemical and reagents	19
2.1.4. Filtration units and equipment	19
2.1.5. Measurement of pH	19
2.1.6. Standard buffers	20
2.1.6.1. Normal buffers	20
2.1.7. Media and equipment sterilization	20
2.1.8. Mineral media preparation	20
2.1.8.1. Mineral medium [ingredientg.l ⁻¹]	20
2.1.8.2. Nutrient Agar [component g.l ⁻¹]	21

2.1.8.3. Standard chemical solutions	21
2.1.8.4. Buffers for whole cell proteome analysis	21
2.1.8.5. SDS-PAGE buffers and chemicals	21-22
2.2. Organisms and growth conditions	22
2.2.1. Light anaerobic [photoheterotrophic] and dark aerobic	
[chemotrophic] growth	22
2.2.2. Maintenance of stock cultures	22
2.2.3. Determination of purity of the cultures	22
2.2.4. Growth conditions	23
2.2.5. L-Tryptophan feeding	23
2.2.6. Glyphosate inhibitors studies	24
2.2.7. Pathway-specific inhibitors studies	24
2.3. Extraction of Metabolites	24
2.3.1. Extraction of aromatic compound	24-25
2.3.2. Extraction of brown pigments	25-26
2.3.2.1. Purification and characterization of brown pigment	26-27
2.3.3. Identification of pigments from the Fraction-I [methanolic fraction]	28
2.3.4. Extraction of extracellular metabolites [exo-metabolomics]	29
2.4. Analytical Technique	30
2.4.1. Thin Layer Chromatography [TLC]	30
2.4.2. High-Performance Liquid Chromatography [HPLC] analysis	30
2.4.3. Liquid Chromatography tandem mass spectrometry (LC-MS) analysis	31
2.4.4 Gas chromatography-mass spectrometry [GC-MS] analysis for indole der	ived
Metabolites	31-32
2.4.5. Nuclear magnetic resonance [NMR] analysis	32
2.4.5.1. Solid-state ¹³ C NMR	32
2.4.5.2. Solid-state ¹⁵ N NMR	33
2.4.6. Fourier Transform Infrared [FTIR] analysis	33
2.4.7. UV-Visible spectral analysis	33-34
2.4.8. Electron Spin Resonance [ESR/EPR] analysis	34
2.4.9. X-ray Diffraction [XRD analysis	35
2.5. Microscopic Technique	35
2.5.1. Scanning electron microscopy [SEM]	35

2.7. Melanin degradation and alkaline hydrolysis methods	35
2.7.1. Melanin (brown pigment) degradation	35
2.7.2. Chemical oxidation of melanin	36-38
2.6. Biochemical methods	38
2.6.1. Spectrophotometric assays	38
2.6.1.1 Estimation of total indole	38
2.6.1.2. Proteins determination	38
2.7. Enzyme activities	38
2.7.1. Preparation of cell-free extracts	38-39
2.7.2. Aromatic aminotransferase /Transaminase activity	39
2.7.3. Monooxygenase activity	39-40
2.7.4. <i>In-vitro</i> melanogenesis	40
2.8. Metabolomics studies	40
2.8.1 Stable isotope-labeled L-Tryptophan feeding experiments	40-41
2.8.2. Liquid chromatography-tandem mass spectrometry (LC-MS/MS)	
analysis	41-42
2.8.3 Data analysis and metabolite identification	42-44
2.9. Methodology used for proteomics studies	44
2.9.1. Isolation of total protein from cells of Rbx. benzoatilyticus	44-45
2.9.1.1. Isobaric tags relative and absolute quantitation [iTRAQ]	
labeling of proteome	45-46
2.9.1.2 Two-dimensional Nano Liquid chromatography-tandem mass	
spectroscopy (LCMS/MS) analysis [MudPIT]	46-47
2.9.1.3. MS data analysis, protein identification and quantification	47-48
3.0 Results	49-106
3.1. Chemotrophic growth kinetics of Rbx. benzoatilyticus	49
3.1.1. Growth, L-Tryptophan utilization and exo-metabolites	
production by Rbx. benzoatilyticus	49-50
3.1.2. Identification of indole derivatives metabolites	51
3.1.2.1. Metabolic profiling of control and L-Tryptophan fed supernatant by	
using TLC and HPTLC	51-52
3.1.2.2. Identification of pink and yellow pigment	
from a methanolic fraction	52-53

3.1.2.3. Mass spectral analysis of yellow pigment (yellow ⁻¹)	54
3.1.2.4. Comparative metabolite profiling of L-Tryptophan fed and	
control conditions by using HPLC	54-55
3.1.2.5. HPLC and LC-MS/MS-based metabolites identification of ethyl	acetate
fraction of L-Tryptophan fed culture supernatant\	
by Rbx. benzoatilyticus	55-57
3.1.2.6. GC-MS analysis of L-Tryptophan fed culture supernatant	
by Rbx. benzoatilyticus	57-58
3.1.2.7. LC-MS based exo-metabolite profiling of L-Tryptophan	
fed aerobic cultures	59-60
3.2. Stable isotope metabolite profiling (SIMP) of L-Tryptophan	
fed chemotrophic cultures of Rbx. benzoatilyticus	61
3.2.1. SIMP analysis of [13C11] L-Tryptophan fed cultures of	
Rbx. benzoatilyticus	61-62
3.2.2. Identification of indole footprints of [13C11] L-Tryptophan	
fed cultures of Rbx. benzoatilyticus	63-67
3.3. Chemotrophic metabolism of 5-hydroxytryptophan by	
Rbx. benzoatilyticus	68
3.3.1. Growth, 5-hydroxytryptophan consumption and pigment	
production by Rbx. benzoatilyticus	68-69
3.3.1.1. Exo-metabolite profiling of 5-hydroxytryptophan fed	
culture supernatant	69-70
3.3.1.2. Comparative exo-metabolite profiling of L-Tryptophan and	
5-hydroxytryptophan fed Rbx. benzoatilyticus	70-71
3.3.1.3. LC-MS based metabolite identification of ethyl acetate fraction of	
5-hydroxytryptophan fed culture supernatant	71-74
3.4. Characterization of brown pigment produced from L-Tryptophan/	
5-hydroxytryptophan fed cultures	75
3.4.1. Brown pigment production by <i>Rbx. benzoatilyticus</i> fed with	
L-Tryptophan/5- hydroxytryptophan	75-76
3.4.2. Physico-chemical properties of purified brown pigment	76-77
3.4.3. Structural characterization	78
3.4.3.1. Scanning electron microscope (SEM) analysis	78

3.4.3.2. UV-Visible spectroscopic analysis	79
3.4.3.3. ESR/EPR spectroscopic analysis	80
3.4.3.4. X-ray Diffraction (XRD) analysis	80
3.4.3.5. Fourier-transform infrared spectroscopy (FTIR) analysis	81
3.4.3.6. Solid state C-13 NMR spectroscopy	82
3.4.3.7. Solid state N-15 NMR spectroscopy	82-83
3.4.3.8. Identification of monomers of brown pigment	83-85
3.5. Melanogenesis in Rbx. benzoatilyticus	85
3.5.1 Brown pigment production	85-86
3.5.2. In-vitro melanogenesis	87-88
3.5.3. Enzyme studies	88
3.5.3.1. Aromatic aminotransferase	88-90
3.5.3.2. Monooxygenase	91
3.6. Global proteome analysis of L-Tryptophan fed cells of Rbx. benzoatily	ticus
cultivated under chemotrophic condition conditions	92
3.6.1 Proteomic inventory	92-96
3.6.2. Functional classification of proteins	97-99
3.6.3. Cellular response of L-Tryptophan fed by of Rbx. benzoatilyticus under	•
chemotrophic conditions	100
3.6.3.1. Membrane related proteins	100
3.6.3.2 Signal transduction related proteins	100
3.6.3.3 Transcription and translation-related proteins	101
3.6.3.4. Proteins related to metabolism	101-102
3.6.3.5. Proteins involved in replication and repair	102
3.6.3.6. Proteins related to stress	102
3.6.3.7. Molecular chaperones proteins	102
3.6.3.8. Proteins related to antioxidant	103
4.0 Discussion	108-123
5.0 Summary	124-126
6.0 Major finding	127
7.0 References	128-150

LIST OF ABBREVIATIONS

μg Microgram
μl Microliter
μs Microsecond

2D LC-MS Two dimensional liquid chromatography

ACN Acetonitrile

APB Anoxygenic photosynthetic bacteria

APS Ammonium persulfate

ATCC American Type Culture Collection BSTFA N,O-bis(trimethylsilyl)trifluoroacetamide

CFU Colony forming unit

CID Collision induced dissociation
CLSM Confocal laser scanning microscopy

CP/TOSS Cross polarization/total sideband suppression DAHP 3-deoxy-D-arabinoheptulosonate 7-phosphate

DCM Dichloromethane
DEPC Diethyl pyrocarbonate
DMSO Dimethyl sulfoxide
DTT Dithiothreitol

EDTA Ethylenediaminetetraacetic acid

ESI Electrospray ionization

FTIR Fourier transformation infra-red

g Force of gravity

GC-MS Gas chromatography mass spectrometry

GRAVY Grand average of hydropathy

h Hour

HEPES 4-(2-hydroxyethyl)-1-piperazineethanesulfonic acid

HOAc Acetic acid

HPLC High performance liquid chromatography

IAA Indole-3-acetic acid
IAld Indole-3-aldehyde
IAM Indole-3-acetamide
IAN Indole-3-acetonitrile

iTRAQ Isobaric tag for relative and absolute quantitation KEGG Kyoto encyclopedia of genes and genomes LC-MS Liquid chromatography and mass spectrometry

m/z Mass-to-charge ratio

MeOHMethanolmgMilligramminMinutesmlmilliliter

MS Mass spectrometry

MS/MS Tandem mass spectrometry

MudPIT Multidimensional protein identification technology
NIST National institute of standards and technology

nm Nanometer

NMR Nuclear magnetic resonance

PAGE Polyacrylamide gel electrophoresis PCA Principal component analysis

PDA Photodiode array
PEP Phosphoenolpyruvate
PHAs Polyhydroxyalkanoates
PLP Pyridoxal-phosphate

PLS-DA Partial least squares discriminant analysis

PMSF Phenyl methyl sulfonyl fluoride PPM Parts per million (1x10⁻¹³) QTOF Quadrupole time-of-flight

RND Resistance nodulation cell division

s Seconds

SCX Strong cation exchange SDS Sodium dodecyl sulfate

SEM Scanning electron microscopy
TCEP Tris (2-Carboxyethyl) phosphine

TE Tris EDTA

TEMED N,N,N',N'-Tetramethylethane-1,2-diamine

TFA Trifluoroacetic acid
TMCS Trimethylchlorosilane

Tris (hydroxymethyl) aminomethane TRITC Tetramethylrhodamine iso-thiocyanate

L-Trp L-Tryptophan

5-OH Trp 5-hydroxytryptophan

L-Tyr L-Tyrosine
L-Phe Phenylalanine
v/v Volume per volume

VIP Variable importance in projection

w/v Weight per volume

		List of Fig. and Table	Page no.
Tabl	e. 1:	Indoles identified from the exometabolites of L-Trp fed cultures of	57
		Rbx. benzoatilyticus.	
Tabl	e. 2:	Labeled and unlabeled exometabolites identified from $L^{-13}C_{11}Trp$ fed	65-67
		labeled and unlabeled L-Trp cultures of Rbx. benzoatilyticus.	
Tabl	e. 3:	Hydroxyindoles identified from the exometabolites of 5-OH-L-Trp fed	75
		cultures of Rbx. benzoatilyticus.	
Tabl	e. 4:	Differentially regulated proteins identified through iTRAQ analysis.	102-107
Fig.	1:	Aerobic and anaerobic catabolism of L-Tryptophan and complete	04
		mineralization through the glutaryl CoA pathways in prokaryotes	
		(Developed after: Colabroy et al., 2005; Aklujkar et al., 2014);	
		ACMS, 2-amino-3-carboxymuconate semialdehyde; ASD, 2-amino-3-	
		muconate semialdehyde. Dotted arrow and more then one arrow	
		denoted multiple step pathway.	
Fig.	2:	Pathways leading to the formation of indole-3-acetic acid from L-	07
		Tryptophan in bacteria (Source: Mujahid et at., 2011; Spaepen et al.,	
		2007). IPCD; indole-3- pyruvic acid decarboxylase, AAT; Aromatic	
		amino transferase: IAM; indole-3-acetamide, TSO; Tryptophan side	
		chain oxidase, Trp; L-Tryptophan, Dotted arrow indicates multiple	
		step pathway.	
Fig.	3:	Kynurenine pathway of L-Tryptophan catabolism in Pseudomonas	08
		aeruginosa (Bortolotti et al., 2016). Dotted arrow indicates multiple	
		step pathways.	
Fig.	4:	Common indole metabolites produced from L-Tryptophan by bacteria.	09
Fig.	5:	An overview of violacein biogenesis from L-Tryptophan by	12
		Chromobacterium violaceum (Source: Dantas et al., 2012). VioA,	
		VioB, VioC, VioD are the proteins involved in the reactions encoded	
		by VioA,B,C,D genes.	
Fig.	6:	Biologically produced melanins from the precursor L-Phe or L-Try	14
		(Singh et al., 2013). DOPA; dihydroxyphenylalanine, DHN;	
		Dihydroxynaphthaline.	

Fig.	7:	Melanogenesis of eumelanin and pheomelanin (Source: D'Orazio et al	16
		2013). DOPA; dihydroxyphenylalanine, DHI; dihydroxyindole,	
		DHICA; dihydroxyindole carboxylic acid, Trp 1; Tyrosinase.	
Fig.	8:	Protocol used for the extraction, purification and identification of	25
		exometabolites of Rbx. benzoatilyticus fed with L-Tryptophan.	
Fig.	9:	Protocol used for the purification of brown pigment produced by <i>Rbx</i> .	26
		benzoatilyticus.	
Fig.	10:	Analytical protocol used for the identification of brown pigment	27
		produced by Rbx. benzoatilyticus.	
Fig.	11:	Purification and characterization of a few colored pigment produced	28
		of Rbx. benzoatilyticus.	
Fig.	12:	Exometabolite extraction, partial purification and identification of	29
		indole derives produced from L-Trp by Rbx. benzoatilyticus.	
Fig.	13:	Hydrolysis, extraction and identification of monomers of melanin	37
		produced by Rbx. benzoatilyticus. PDCA; pyrrole-2,3- carboxylic	
		acid, PTCA; Pyrrole-2,3,4-tricarboxylic acid and PTeCA; Pyrrole-	
		2,3,4,5-tetracarbosylic acid.	
Fig.	14:	Stable isotopic exometabolite profiling (SIMP) of <i>Rbx</i> .	41
		benzoatilyticus.	
Fig.	15:	Pathway prediction based on the exometabolic profiling of Rbx.	44
		benzoatilyticus.	
Fig.	16:	Utilization of L-Tryptophan with simultaneous production of pigments	50
		by Rbx. benzoatilyticus under chemotrophic conditions. (A) Growth,	
		substrate utilization and pigment production (B) Total indoles	
		produced by Rbx. benzoatilyticus under L-Trp un-fed (control)	
		and fed conditions.	
Fig.	17:	Chromatograms of pigments eluted by TLC (A,B) and HPTLC	52
		(C,D,E) produced by Rbx. benzoatilyticus under chemotrophic L-	
		Tryptophan fed condition. TLC; Thin layer chromatography, HPLC;	
		High performance liquid chromatography; Control, L-Trp un-fed	
		condition.	

Fig.	18:	Identification of TLC eluted metabolites through HPLC.	53
Fig.	19:	m/z spectrum of purified yellow pigment and its chemical structure.	54
Fig.	20:	Comparative metabolite profiling of ethyl acetate fractions obtained	55
		from Rbx. benzoatilyticus grown under the chemotrophic condition	
		with L-Tryptophan fed and un-fed (control) conditions.	
Fig.	21:	GC-MS analysis of BSTFA derivatized exometabolites of L-	58
		Tryptophan fed Rbx. benzoatilyticus under the chemotrophic	
		condition.	
Fig.	22:	LC-MS analysis of methanolic extract of L-Tryptophan fed exo-	60
		metabolites of Rbx. benzoatilyticus under chemotrophic condition.5-	
		OH-Trp;5-hydroxytryptophan,DHIA; dihydroxyindole, aldehyde,	
		MDHICA; Methoxy- dihydroxyindole-3-carboxylic acid, HIAA;	
		hydroxy-indole-3-acetic acid, HIPy: hydroxy-indole-3-pyruvic acid,	
		HMI; hydroxy methylindole, Trp; L-Tryptophan.	
Fig.	23:	Total ion chromatograms of ethyl acetate extracted fraction from ${}^{12}C_{11}$	62
		and $^{13}\text{C}_{11}$ of L-Tryptophan fed cultures of <i>Rbx. benzoatilyticus</i> under	
		chemotrophic conditions. (A). m/z vs time plot of total labeled	
		metabolites features under chemotrophic conditions (B). Pie chart	
		illustrating the L-Tryptophan derivatives metabolites ionized under	
		Pos. and Neg. modes (C). Pos. (+ve) ionization mode; and Neg.	
		(-ve) ionization mode.	
Fig.	24:	Identification of a few exometabolites based on mass spectrum and	64
		absorption maxima as represented by stable isotope labeled indole	
		derivatives having increase in molecular mass (m/z; M) by M+16, 17,	
		+18 and M+26.	
Fig.	25:	(A) Growth, utilization of 5-hydroxytryptophan with simultaneous	69
		production of brown pigment by Rbx benzoatilyticus under	
		chemotrophic condition. (B) Photographs showing the culture flasks	
		of 5-OH-Trp un-fed (Control; bI), fed culture (bII), supernatant of	
		fed culture (bIII) and purified brown pigment (bIV).	

- **Fig. 26:** Comparative metabolite profiling of ethyl acetate fractions obtained 70 from *Rbx. benzoatilyticus* grown under chemotrophic condition with 5-hydroxytrptophan fed and un-fed (control) conditions.
- Tryptophan and 5-hydroxytryptophan fed *Rbx benzoatilyticus* grown under chemotrophic condition. (B) Quantitative differences in the brown pigment produced by *Rbx. benzoatilyticus* fed with L-Tryptophan and 5-hydroxytryptophan. (C)Hypothetical representation (based on the information from Fig. 27A,B) of the exometabolites produced by *Rbx. benzoatilyticus* from L-Trp and 5-OH Trp illustrating the larger role of 5-OH- Trp in the biogenesis of brown pigment, while L-Trp yields in addition other indole derivatives.
- **Fig. 28:** Comparative total ion chromatogram profiling of ethyl acetate 73 extracted fraction from 5-hydroxytryptophan fed cultures of *Rbx benzoatilyticus* under chemotrophic condition. (B) Time lap analysis based on m/z of metabolites. (C) Pie-chart illustration of metabolites under both +ve and –ve mode of ionization.
- Fig. 29: Photograph of culture flasks showing growth of *Rbx*. *benzoatilyticus* 76 without (A; control) and with L-Trp fed (B) cultures incubated for 48 h under chemotrophic (aerobic dark) conditions. The culture supernatants had no pigmented exometabolites in the control (C) while L-Trp fed culture showed brown pigmented exometabolites (D). The photrophic incubated (light anaerobic) L-Trp culture (E) of *Rbx*. *benzoatilyticus* did not show any pigmented exometabolites (F).
- **Fig. 30:** Physico-chemical properties of extracted brown pigment produced 77 from L-Tryptophan and 5-hydroxytryptophan fed conditions by *Rbx*. *benzoatilyticus* under chemotrophic condition.
- **Fig. 31:** Scanning Electron microscopic (SEM) images of purified brown 78 pigment. SEM image of brown pigment showing aggregated polymer (A) and typical bead like granular particles (B).

Fig.	32:	Characterization of purified brown pigment. (A) UV-Visible	79
		absorption spectra (B) Log ₁₀ absorbance linear correlation with	
		wavelength.	
Fig.	33:	Spectroscopic characterization of the brown pigment produced by	80
		Rbx. benzoatilyticus. (A) ESR spectrum (B) X-ray diffraction spectrum.	
Fig.	34:	FTIR analysis of brown pigment produced by <i>Rbx</i> . <i>benzoatilyticus</i> .	81
Fig.	35:	Solid state NMR analysis of brown pigment produced by <i>Rbx</i> .	83
		benzoatilyticus (A) ¹³ C NMR spectrum (B) ¹⁵ N NMR spectrum.	
Fig.	36:	Chromatographic analysis of hydrolyzed and un-hydrolyzed products	84
		of brown pigment. (A) Without stained. (B) Strained with TLC	
		specific reagent. 5-OH Trp; 5-hydroxytryptophan, Trp; L-Tryptophan	
Fig.	37:	Identification of oxidation products of brown pigment based on mass	85
		spectrum and absorption maxima as represented by pyrrole	
		derivatives.(A, B). PTCA and PTeCA molecular marker identified	
		brown L-Trp derivatives (C, D). PDCA, PTCA and PTeCA molecular	
		marker identified brown 5-OH Trp derivatives PDCA; pyrrole-2,3-	
		tricarboxylic acid, PTCA; pyrrole-2,3,5-tricarboxylic acid, PTeCA;	
		pyrrole-2,3,4,5- tetracarboxylic acid.	
Fig.	38:	(A) Shikimate pathways specific inhibitors (glyphosate, sulcotrion,	86
		kojic acid and quercetin) used in this study to understand the role in	
		the shikimate pathway in the biogenesis of melanins by Rbx	
		benzoatilyticus. (B) Na-azide was used as an inhibitor for the enzyme	
		monooxygenase to understand its role in melanin biogenesis by Rbx	
		benzoatilyticus. (C) The quantified yields of melanin produced by Rbx	
		benzoatilyticus in the presence of various inhibitors.	
Fig.	39:	In-vitro melanogenesis using cell free extracts of Rbx benzoatilyticus	87
		from cells growth chemotrophically for 48 h fed with L-Trp and	
		assayed in the presence of L-Trp or 5-OH-Trp. Test tubes showing the	
		supernatant after the assay in the presence of L-Trp (A), 5-OH-Trp (B)	

and the respective absorption spectra's shown in C and D.

- Fig. 40: Time-dependent *in-vitro* utilization of L-Trp or 5-OH Trp with 88 simultaneously melanin production by cell-free extract of *Rbx*.

 benzoatilyticus.

 Fig. 41: HPLC chromatogram of the ethyl acetate extract of the assay done for 89
- Fig. 41: HPLC chromatogram of the ethyl acetate extract of the assay done for 89 aromatic aminotransferase activity by cell-free extracts in the presence of L-Trp by *Rbx*. *benzoatilyticus* growth chemotrophically fed with L-Trp (A). Putative pathway of IAA biogenesis by *Rbx*. *benzoatilyticus* (B) based the metabolites identified from the chromatogram.
- Fig. 42: HPLC chromatogram of the ethyl acetate extract of the assay done for 90 aromatic aminotransferase activity by cell-free extracts in the presence of 5-OH-L-Trp by *Rbx. benzoatilyticus* growth chemotrophically fed with L-Trp (A). Putative pathway of 5-OH-IAA biogenesis by *Rbx. benzoatilyticus* (B) based the metabolites identified from the chromatogram. (Insert picture shows the testes with the supernatant after the assay).
- **Fig. 43:** Ionized chromatogram showing the differences in the masses for the 91 enzyme monooxygenase assay done with pre-denatured (Blank) and after the reaction. Mass of 190 m/z was identified as 5-OH-IAA.
- **Fig. 44:** Flow chart representing the iTRAQ based proteomic analysis used for this study.
- **Fig. 45:** SDS-PAGE separated proteins of *Rbx. benzoatilyticus* (A) as against 95 the proteins identified through iTRAQ (B).
- **Fig. 46:** (A) Hydropathy *vs* PI. (B) Map showing molecular weight *vs* PI of the 95 proteins detected through iTRAQ.
- **Fig. 47:** Fold change measured for global proteins detected through iTRAQ 96 (A). Correlation study of the identified proteins between independent biological replicates (B).
- **Fig. 48:** PCA (A) and volcano (B) plots of isobaric tags for relatives and 96 absolute quantification of identified proteins of *Rbx. benzoatilyticus*.
- **Fig. 49:** Differentially regulated proteins identified from the iTRAQ analysis 98 of *Rbx benzoatilyticus*.

- **Fig. 50:** Functional classification of differentially regulated proteins of *Rbx*. 99 benzoatilyticus Functional classification of (A) up-regulated and (B) down- regulation proteins. Data processing parameters was the same as mentioned in following Fig. 48.
- Fig. 51: Difference between the canonical and non-canonical melanogenesis. 122
- Fig. 52: Illustration of multiple L-Tryptophan catabolic pathways and its 126 differential biotransformation under photo and chemotrophic metabolism in *Rbx benzoatilyticus*. Pathways with solid arrow are predicted based on the identified labeled metabolites; dotted arrow detonated multiple steps, IPyA;indole-3-puruvic acid, IAM; Indole-3-acetamide, IAN; Indole-3-acetonitrile, 5-OH Trp; 5-hydroxytryptophan , M; Molecular ionized (m/z) mass, and +16, +18, and +26 mass increased with labeled fed L-Tryptophan.

Introduction

1.0 Introduction

Bacteria are one of the most diverse group of microorganisms which can survive in a wide range of habitats. This is primarily because they have adapted to the environmental fluctuations particularly to the extended range of substrate availability (Lakshmi et al., 2018) which is important to meet their growing demands. The extended range of substrates includes carbon as well as nitrogen sources. Aromatic hydrocarbons are the second most abundant class of organic compounds after carbohydrates and act as prevalent sources of carbon and energy for many bacteria (Arai et al., 1999; Ismail and Gescher, 2012; López Barragán et al., 2004; Teufel et al., 2010). Aromatic hydrocarbons are abundantly present in nature in the form of lignin polymers, monolignols, phenols, indoles and aromatic amino acids(Carmona et al., 2009). Besides the naturally occurring aromatic hydrocarbons, anthropogenic and xenobiotic aromatic hydrocarbons are also good sources of carbon for many bacteria (Rengarajan et al., 2015) Aromatic amino acids are one of the naturally occurring aromatic organic compounds (Carmona et al., 2009), which are originated from plants and animals primarily owing to their degradation. The other major source of aromatic amino acids is from the discharge of plant root exudates (Badri et al., 2013; Ryu and Patten, 2008), which act as metabolic magnets in attracting microorganisms and help in plant-microbial metabolite cross talk (Hassan and Mathesius, 2012; Kim et al., 1995; Lim et al., 2005) resulting in establishing a mutual association with plants (Dennis et al., 2010; Hartmann et al., 2009). The natural levels of aromatic amino acids are predicted to be significantly abundant and their absolute levels are still unknown (Phillips et al., 2004). L-Tryptophan (L-Trp), L-phenylalanine (L-Phe) and L-Tyrosine (L-Try) are generally used by bacteria as sole sources of carbon or nitrogen (Huang et al., 2012; Liu et al., 2004; Wei et al., 2013) or both as carbon and nitrogen (Bak and Widdel,

1986; Ebenau-Jehle et al., 2012; Holmes et al., 2004; Mechichi et al., 2002; Schneider et al., 1997) under aerobic and anaerobic conditions. On the other hand, aromatic amino acids are precursors of many secondary metabolites. Many of these metabolites are bio-weapons help in the chemical-warfare to defend against other organisms which compete for food, shelter, reproduction, and also provide a systemic immune response whenever attacked by pathogen or grazers (Tyc et al., 2017). Plants and microorganisms have the inherent capability of *de-novo* biosynthesis of aromatic amino acids (Less and Galili, 2008; Lim et al., 2005). While, animals have to greatly depend on plants and microorganisms for aromatic amino acids as they cannot synthesize full scale of amino acids.

The aromatic amino acids in animals act as precursors for many metabolites which participate in various physiological activities. Importantly these include those derived from L-Tyr, L-Phe or L-Trp act as precursors for the biosynthesis of pigment including melanin (Pavan et al., 2020; Solano, 2014; Toledo et al., 2017) tryptamine, serotonin, kynurenic acid and melatonin (Hardeland, 2016; Liu et al 2020). In case of bacteria aromatic amino acids act as both carbon/nitrogen source and precursor of many secondary metabolites. Many bacteria catabolize aromatic amino acids by completely degrading through a specific catabolic pathway (Aklujkar et al., 2014; Bak and Widdel, 1986; Ebenau-Jehle et al., 2012; Holmes et al., 2004; Kashefi et al., 2002; Mechichi et al., 2002; Schneider et al., 1997). On the other hand, there are many bacteria which lack the capability to break the aromatic ring but still can use the aliphatic side chain of the aromatic amino acid as sole source of carbon or nitrogen for growth (Mai and Adams, 1994; Yokooji et al., 2013). The latter results in the biotransformation of the amino acid resulting in the production of large number of secondary metabolites (Hazelwood et al., 2008; Lakshmi et al., 2012, 2018; Parthasarathy et al., 2018; Ravasio et al., 2014). Metabolism of aromatic

amino acids greatly depends on the nature of the bacteria and the condition in which the bacteria is interacting with the aromatic amino acid.

1.2. Metabolism of L-Tryptophan by prokaryotes

1.2.1. Catabolism of L-Tryptophan

Bacteria and Archaea can catabolize L-Trp as a sole source of carbon or nitrogen under both oxic and anoxic environments. Anaerobic bacteria like *Ferroglobus placidus*, *Azoarcus evansii* and sulfate-reducing bacterium; *Desulfobacterium indolicum* (Bak and Widdel, 1986) can completely mineralize L-Trp when used as a carbon and nitrogen source. This catabolism occurs through the formation of benzoyl-CoA as a central intermediate under anaerobic condition (Fig. 1; Aklujkar et al., 2014). Complete mineralization of L-Trp under strictly anaerobic conditions by an archaeon, *Ferroglobus placidus* is also well studied (Aklujkar et al., 2014). Methanogenic bacteria can also completely mineralize L-Trp into carbon dioxide and methane with the formation of intermediates; indole-3-acetate, 2-aminobenzoate and benzoate (Fig. 1; Aklujkar et al., 2014; Isaacs et al., 1994).

Aerobic and anaerobic catabolism of L-Trp catalyzed by tryptophanase (pyridoxal phosphate-dependent enzyme) lead to the formation of indole and pyruvate (Berstad et al., 2015; Cook et al., 1995; Kumar and Sperandio, 2019; Kumavath et al., 2010a). Some species belonging to Pseudomonadaceae and Bacillaceae showed oxidative mineralization of L-Trp through the anthranilate pathway (Fig. 1). The catabolism of L-Trp through kynurenine pathway (Knoten et al., 2011) is a branching point of either NAD biosynthesis or complete mineralization through the intermediate 2-amino-3-carboxymuconate semialdehyde (ACMS; Fig. 1). While the 2-amino-3-carboxymuconate semialdehyde (ACMS) either can be cyclized simultaneously converted to quinolinate

(Kumar and Sperandio, 2019) or their oxidative decarboxylation to 2-amino-3-muconate semialdehyde (ASD) and further converted to 2-aminomuconate. (Egashira et al., 1996; Parthasarathy et al., 2018; Tanabe et al., 2002). Finally channelized through the glutaryl-CoA pathway and then complete mineralizes to CO₂ and H₂O (Fig. 1).

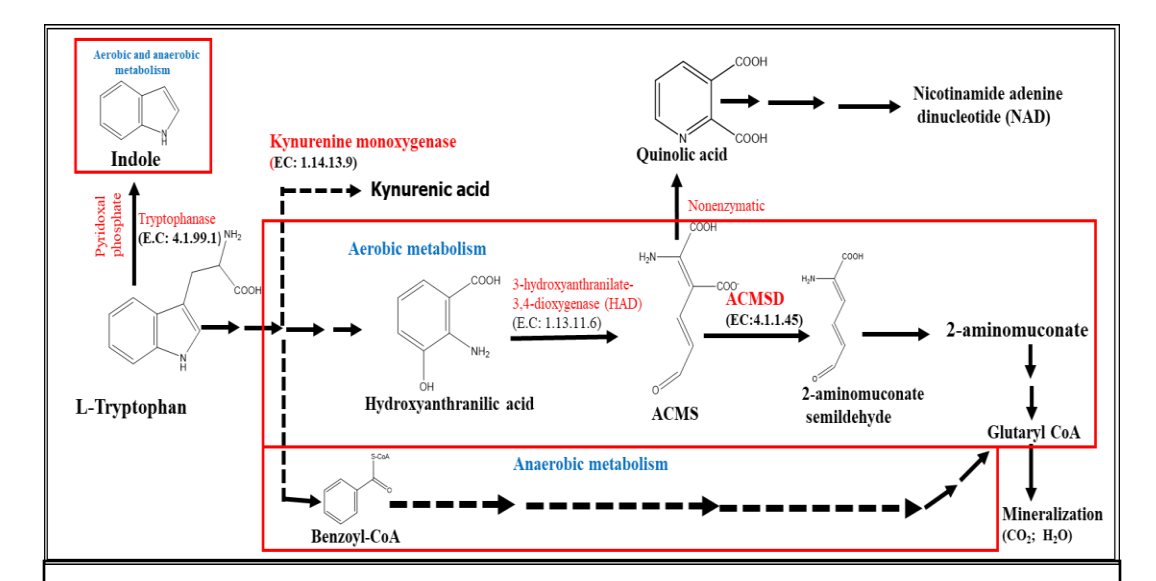


Fig. 1: Aerobic and anaerobic catabolism of L-Tryptophan and complete mineralization through the glutaryl CoA pathways in prokaryotes (Developed after: Colabroy et al., 2005; Aklujkar et al., 2014); ACMS, 2-amino-3-carboxymuconate semialdehyde; ASD, 2-amino-3-muconate semialdehyde. Dotted arrow and more then one arrow denoted multiple step pathway

1.2.2. Partial oxidation of L-Tryptophan under oxic and anoxic environments

Bacteria partially oxidize L-Trp leading to the production of indole derivatives. Biotransformation or partial oxidation of L-Trp by bacteria can occur through four different pathways (Fig. 2), among these pathways some share similarity with plants (Spaepen et al., 2007). The incomplete oxidation of L-Trp under aerobic and anaerobic conditions leads to the production of indole-3-acetic acid or indole derivatives through different pathways (Mujahid et al., 2011b). The indole-3-acetic acid production from L-Trp was commonly observed under both oxic and anoxic environments (Mujahid et al., 2011b).

1.2.2.1. Indole-3-pyruvic acid pathway [IPyA]

Indole-3-pyruvic acid [IPyA] pathway is the most common pathway among bacteria leading to the formation of indole-3-acetic acid. This pathway is commonly seen in *Azospirillum brasilense*, *Aromatoleum aromaticum*, *Pseudomonas agglomerans*, *Bradyrhizobium* spp., *Rhizobium* spp., *Enterobacter cloacae* and *Burkholderia pyrrocinia* JK-SH007 (Koga et al., 1991; Liu et al., 2019; Spaepen et al., 2007). The first step of L-Trp catabolism in many bacteria is catalyzed by an aromatic amino-transferase resulting in the formation of IPyA (Kittell et al., 1989; Koga et al., 1994) which is further converted to indole-3-acetaldehyde catalyzed by a rate-limiting enzyme indole-3-pyruvate decarboxylase (Fig. 2). Finally, Indole-3-acetaldehyde is oxidized to form indole-3-acetic acid (Koga et al., 1991; Patten and Glick, 2002) by an aldehyde oxidase (Fig. 2).

1.2.2.2. Indole-3-acetamide pathway

Some bacteria produces indole-3-acetic via indole-3-acetamide [IAM] pathway. Tryptophan 2-monooxygenase [IaaM] encoded by *iaaM* catalyzes the conversion of L-Trp to IAM which is then converted to IAA by IAM hydrolase [Isaac] encoded by *iaaH*. The genes *iaaM* and *iaaH* are well characterized in *Pseudomonas syringae*, *Pantoea agglomerans and Burkholderia pyrrocinia* JK-SH007 (Clark et al., 1993; W. H. Liu et al., 2019; Lu et al., 2009; Sekine et al., 1989; Theunis et al., 2004) *Agrobacterium tumefaciens*, *Rhizobium* spp., *Bradyrhizobium* spp. and *Pantoea agglomerans* (Clark et al., 1993; Patten and Glick, 2002; Fig. 2).

1.2.2.3. Tryptamine pathway

In bacteria like *Bacillus cereus* the tryptamine [TAM] pathway was recognized (Perley and Stowe, 1966). In this pathway, L-Trp is decarboxylated by tryptophan decarboxylase resulting in the formation of TAM which is further transformed to IAA.

While in *Azospirillum* and *Burkholderia pyrrocinia* JK-SH007 TAM is transformed by amine oxidase to IAld and finally to IAA (Hartmann et al., 1983; Liu et al., 2019; Fig. 2).

1.2.2.4. Indole-3-acetonitrile pathway

The L-Trp metabolism through the indole-3-acetonitrile (IAN) pathways is well studied in plants and bacteria. The enzymes nitrile hydratase and amidase convert L-Trp to IAN to IAA via IAM (Kobayashi et al., 1993). Nitrilases with indole-3-acetonitrile specificity were identified in bacteria (Kobayashi et al., 1993; Kobayashi et al., 1995). Nitrile hydratase and amidase activity was reported in *Agrobacterium tumefaciens*, *Burkholderia pyrrocinia* JK-SH007 and *Rhizobium* spp. (Kobayashi et al., 1993; Koga et al., 1991; Liu et al., 2019), suggesting IAN transformation to IAA *via* IAM (Fig. 2; Kobayashi et al., 1995).

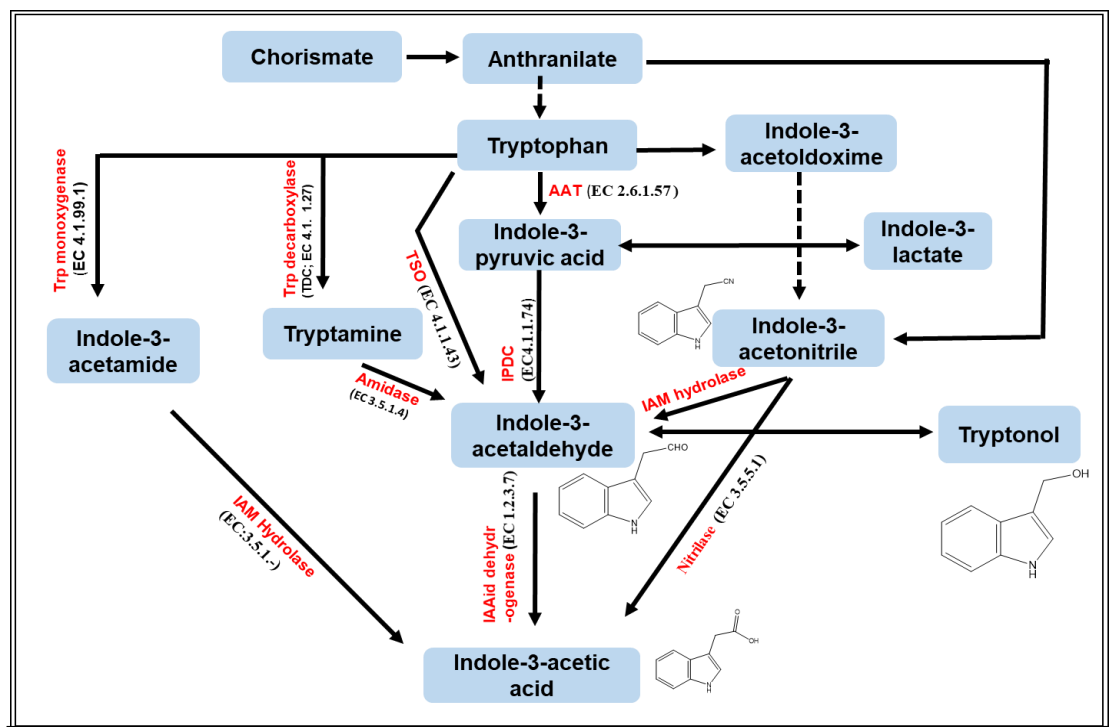


Fig. 2: Pathways leading to the formation of indole 3-acetic acid from L- Tryptophan in bacteria (Source: Mujahid et at., 2011; Spaepen et al., 2007). IPCD: indole-3- pyruvic acid decarboxylase, AAT: Aromatic amino transferase: IAM: indole-3-acetamide, TSO: Tryptophan side chain oxidase, Trp: L-Tryptophan, Dotted arrow indicates multiple step pathway.

1.3. Kynurenine pathway of L-Tryptophan metabolis

Some bacteria can catabolize L-Trp through the kynurenine pathway under aerobic conditions (Fujitani et al., 2011). *Pseudomonas aeroginosa consists of* complete set of genes of L-Trp metabolism such as Trp-2,3-dioxygenase, kynurenine formamidase and kynureninase were identified (Bortolotti et al., 2016; Fig 3). While L-Trp metabolism leads to the production of formylkynurenine, kynurenine, and anthranilate were identified in *Pseudomonas aeroginosa* (Fig. 3). L-Trp catabolism by *Pseudomonas* through the kynurenine pathway leads to the formation of kynurenic acid. On the other hand, L-Trp catabolism through kynurenine may also leads to the formation of anthranilate; quinolinine in some prokaryotes (Colabroy et al., 2005) Besides, few strains of *Pseudomonas fluorescens* possess a kynurenine monooxygenase (KMO) which is responsible for 3-OH-kynurenic acid formation (Crozier and Moran, 2007; Miller, 1953).

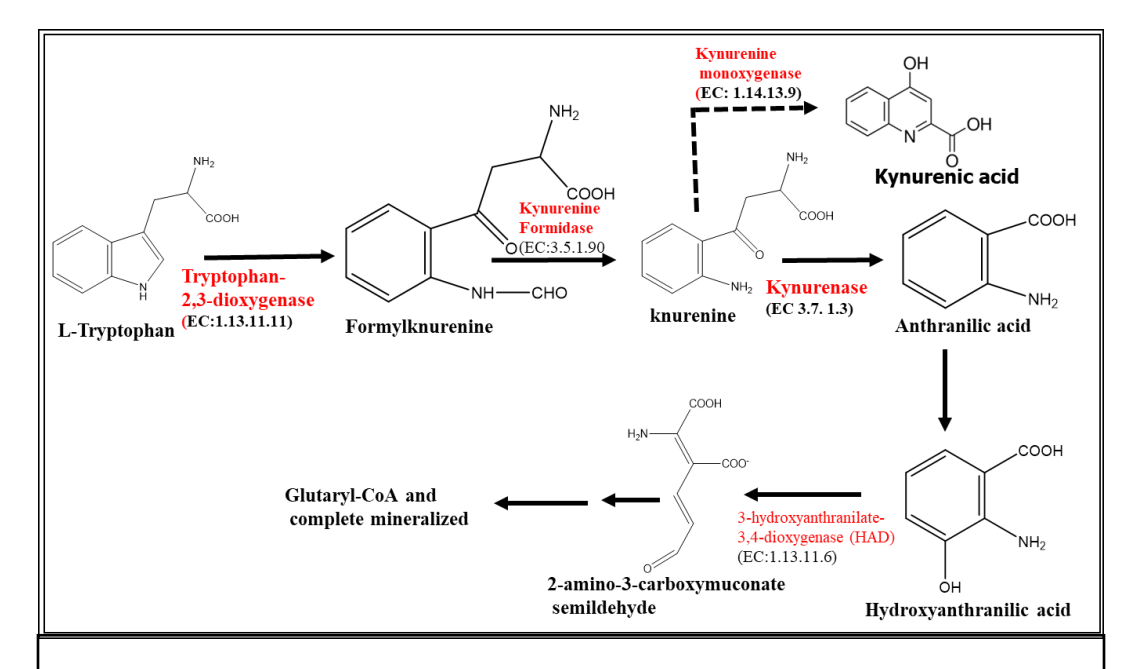


Fig. 3: Kynurenine pathway of L-Tryptophan catabolism in *Pseudomonas aeruginosa* (Bortolotti et al., 2016). Dotted arrow indicates multiple step pathways.

1.4. L-Tryptophan biotransformation

L-Trp when used as sole source of nitrogen, many bacteria transform L-Trp to indole derived acids, alcohols or other indole derivatives (Alkhalaf and Ryan, 2015; Wei et al., 2013). The alcohols or carboxylic acids thus produced have one carbon lesser than the initial carbon number of L-Trp. L-Trp transformation occurs through transamination, decarboxylation and oxidation/reduction channelized through the Ehrlich's pathway (Hazelwood et al., 2008) Many indole metabolites are commonly produced by intestinal microbiota (Henrik and Tine, 2018; Liu et al., 2020; Fig. 4) where indole derivatives act as signaling molecules in microbial communities as well as it helps in host-microbial crosstalk leading to intestinal and systemic homeostasis (Henrik and Tine, 2018; Liu et al., 2020). The human gut is a complex microbial system wherein the microorganisms use L-Trp as precursor and produce serotonin, tryptamine, kynurenine and many other indole derives which have direct impact on the human health and physiology (Alkhalaf and Ryan, 2015; Shalaby et al., 2019; Hendrikx and Schnabl, 2019; Hubbard et al., 2015; Liu et al., 2020). Bacteria like, Chromobacterium collimonas (Hakvåg et al., 2009), Janthino bacterium (Jude et al., 2012; Pantanella et al., 2007) produces indole derived pigment; violacein (Fig. 4), which help these bacteria protected from competitors.

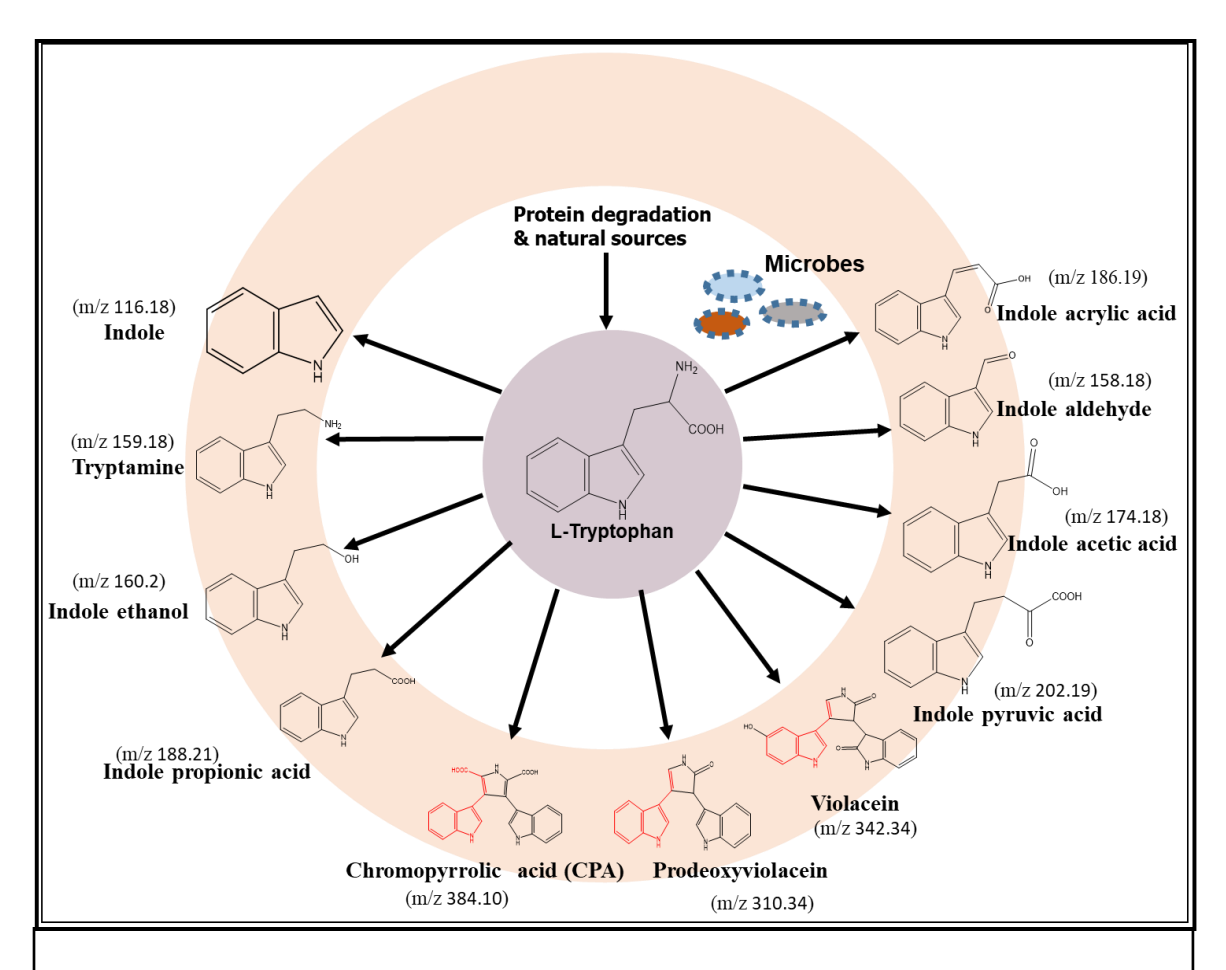


Fig. 4: Common indole metabolites produced from L-Tryptophan by bacteria.

1.5. Secondary metabolites

Metabolism of L-Trp was widely studied (Henrik and Tine, 2018) with regard to the production of secondary metabolites which display impressive pharmacological applications including pigments, alkaloids, phytohormones, neurotransmitters, toxins, inhibitors and antibiotics (Alkhalaf and Ryan, 2015; Shalaby et al., 2019; Mohammadipanah et al., 2016; Schulz and Dickschat, 2007; Tyc et al., 2017; Liu et al., 2020).

1.5.1 Indigo and violacein

The blue pigment (indigo dye or an indole dimer) metabolite was reported in some wild strains of bacteria such as, *Rhodococcus* sp. (Allen et al., 1997) *Sphingomonas* sp. (Moreno-Ruiz et al., 2003), Acinetobacter sp. (Doukyu et al., 2002; Qu et al., 2010) Comamonas sp. (Dantas et al., 2012) and engineered strains of E. coli and Pseudomonas putida (Bhushan et al., 2000; Connor et al., 1997). In addition to bacteria, indigo dye is also produced by plants like *Indigofera tinctoria*, *Polygonum tinctorium* (Bhushan et al., 2000; Connor et al., 1997) and *Isatis tinctoria* (Fabara and Fraaije, 2020). While indole dimers and trimers which are other than indigo are reported from *Pseudomonas mendocina*, Haemophilus influenzae (Stull et al., 1995), Pseudomonas aureofaciens (Hamill et al., 1967) and engineered E. coli (Kwon and Weiss, 2009). The indigo producing enzymes were generally discovered from the pink and blue colored colonies of bacteria. The enzymes such as monooxygenase and dioxygenase responsible for pigment indigo production both were discovered through the metagenome mining (Lim et al., 2005; Ma et al., 2018; Nagayama et al., 2015; Singleton et al., 2012). The enzymes (oxygenases) were also studied for indigo production from genetically engineered microorganisms (Bilsla et al., 2018; Gillam et al., 2000; Han et al., 2011; Zhang, et al., 2012; Rodrigues et al., 2013; Zhang et al., 2013). The biogenesis of indigo is well studied (Ensley et al., 1983; O'Connor et al., 1997; Qu, Shi, et al., 2012). The role of toluene 4-monooxygenase in the conversion of indole to indoxyl with spontaneous dimerization forming indigo is also well studied (Kwon and Weiss, 2009).

Violacein is a violet colored pigment of 5-hydroxyindole, 2-pyrrolidone and has 2-deoxy-indole molecules (Alkhalaf and Ryan, 2015; Rettori and Durán, 1998) This bis-indole (Dimer of indole) is produced by *Janthinobacterium* spp., *Janthinomonas svalbardensis*, *Collimonas* sp., *Duganella* sp., *Microbulbifer* sp., *Chromobacterium*

violaceum and Pseudoalteromonas luteoviolacea (Allegri et al., 2003; Hoshino, 2011; Pantanella et al., 2007; Fig. 5). Violacein has antibacterial activity against Bacillus licheniformis, Bacillus subtilis, Bacillus megaterium, Staphylococcus aureus, Mycobacterium tuberculosis and Pseudomonas aeruginosa (Durán and Menck, 2001; Nakamura et al., 2003). Violacein biosynthesis is coded by a cluster of four gene family called VioA,B,C,D (August et al., 2000; Dantas et al., 2012). The nucleotide-dependent monooxygenase is responsible for the biogenesis of violacein and indole-carbozole (Howard-Jones and Walsh, 2005) which involves the fusion of two indole rings resulting in the formation of a conjugated indole (Sánchez et al., 2006). This bioprocess occurs by the formation of 5-OH Trp from L-Trp, which is converted to violacein with the formation of intermediates; OH-indole-3-pyruvic acid (OH IPyA) and prodeoxyviolacein (Fig. 5).

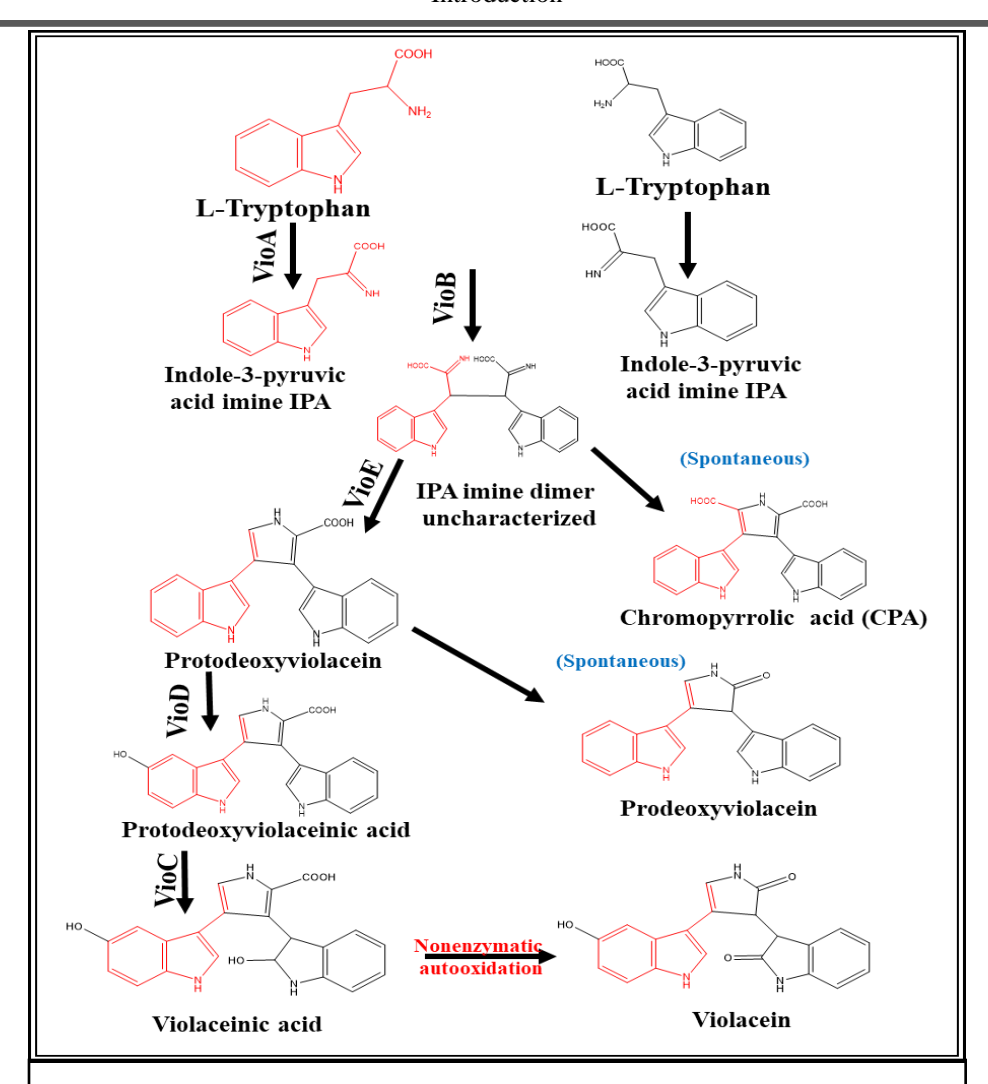


Fig. 5: An overview of violacein biogenesis from L-Tryptophan by *Chromobacterium violaceum* (Source; Dantas et al., 2012). VioA, VioB, VioC, VioD are the proteins involved in the reactions encoded by VioA,B,C,D genes.

1.5.2. *Melanins*

Melanins are enigmatic, ubiquitous, heterogeneous biopolymer brown to black colored pigment generally produced in a biological life form. Melanins typically have a wide range of distribution among the animals, plants and microorganisms (Gessler et al., 2014; Pavan et al., 2020; Solano, 2014; Toledo et al., 2017). Melanins are unorganized polymers with complex molecular structures and has pivotal role in the biological system (Solano, 2017). Majority of melanins have similar physical and chemical properties with

typical molecular composition (Marchetti and Karsili, 2016; Sugumaran, 2016). Melanin exists in different forms like amorphous or crystalline. Melanins are of three main types; 1. Eumelanins (Büngeler et al., 2017); these are brown to black pigmented and derived from L-Tyr; 2. Pheomelanins (Thody et al., 1991)are reddish colored with cysteine derivatives and commonly found in animals and 3. Allomelanins are associated with plants, fungi and bacteria (Gessler et al., 2014). Eumelanin and pheomelanin are associated pigments of human hair and skin (Piletic et al., 2010).

1.5.2.1. Melanin biosynthesis in bacteria

In bacteria, melanin biosynthesis occurs from the precursor L-Tyr or from acetyl-CoA. The acetyl-CoA dependent biogenesis is catalyzed by polyketide synthases (PKSs; Fig. 6). The most dominant melanin biosynthesis pathways in bacteria start with the precursor L-Tyr which is converted to 3,4-dihydroxyphenylalanine (DOPA) by tyrosinase or laccase. DOPA was observed as an intermediate of melanin biogenesis in Sinorhizobium meliloti (Mercado-Blanco et al., 1993), Ralstonia solanacearum (Hernández-Romero et al., 2005), Marinomonas mediterranea (López Barragán et al., 2004; F. Solano, 2014), Pseudomonas putida (McMahon et al., 2007), Vibrio tyrosinaticus (Pomerantz and Murthy, 1974), Vibrio nigripulchritudo (Goudenège et al., 2013), Saccharophagus degradans (Ekborg et al., 2005; Kelley et al., 1990), Bacillus thuringiensis (Liu et al., 2004), Bacillus megaterium (Shuster and Fishman, 2009) and Bacillus licheniformis (Shalaby et al., 2019). Tyrosinase is a bifunctional coppercontaining polyphenol oxidase and laccase is also polyphenol oxidase that can participate in melanin biosynthesis. However, laccases lack monophenol hydroxylase activity but can oxidase a variety of diphenol and polyphenolic compounds (Reiss et al., 2011; Sanchez- Amat et al., 2010). Laccases are well known in plants, fungi and bacteria. Bacterial laccase are also known as a polyphenol oxidase play an important role in melanogenesis (Chauhan et al., 2017; Singh et al., 2011; Unuofin et al., 2019). The role of laccases in melanogenesis is recorded in *Azospirillum lipoferum* (Diamantidis et al., 2000; Givaudan et al., 1993), *Sinorhizobium meliloti* (Castro-Sowinski et al., 2002), *Bacillus subtilis* (Hullo et al., 2001), and *Bacillus weihenstephanensis* (Drewnowska et al., 2015). It is also known that a few bacteria have both tyrosinase and laccases which include *Pseudomonas putida* F6 (McMahon et al., 2007), *Alteromonas* sp. (Sanchez-Amat and Solano, 1997) and *Bacillus sp*. (Dalfard et al., 2006). Melanin biogenesis through polyphenol oxidases from catechol is reported in *Azotobacter chroococcum* under nitrogen-fixing conditions in the presence of oxygen (Herter et al., 2011; Shivprasad and Page, 1989). Melanin biogenesis from the precursor L-Phe catabolized by phenylalanine hydroxylase is reported in *Rhizobium* sp. (Mercado-Blanco et al., 1993). Facultative anaerobic thermophilic bacterium *Geobacillus staerothemophilus* (Afzal, 2013) and an anoxygenic phototrophic bacterium, *Rbx. benzoatilyticus* (Lakshmi, et al., 2019) are also reported to produce melanins.

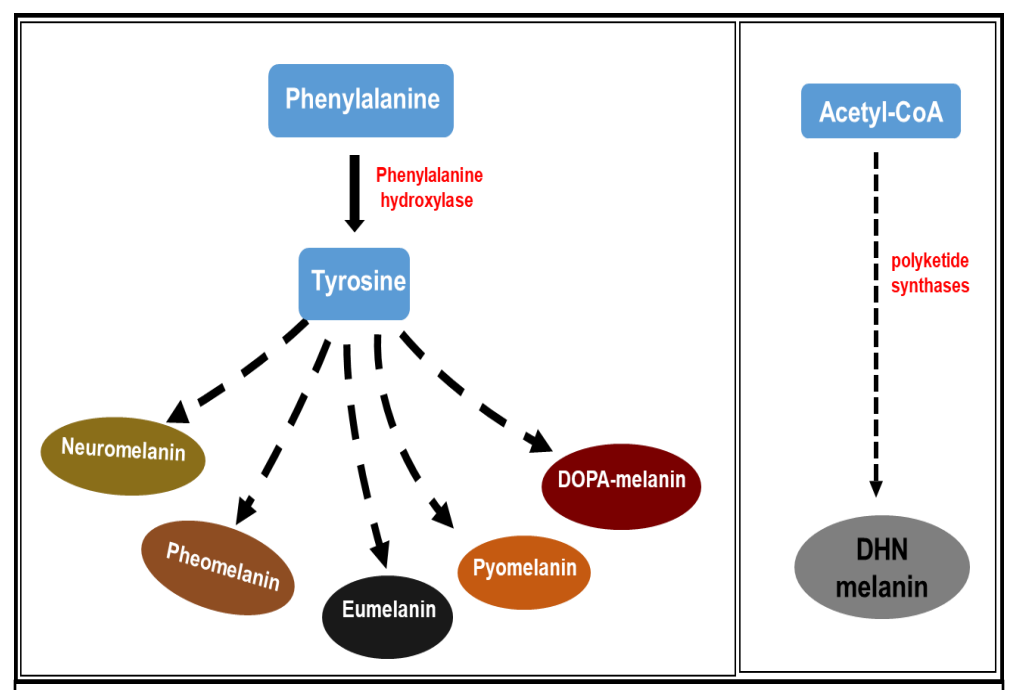


Fig. 6: Biologically produced melanins from the precursor L-Phe or L-Try (Singh et al., 2013). DOPA; dihydroxyphenylalanine, DHN; dihydroxynaphthaline.

1.5.4. Types of melanins and their biosynthesis

Different types of melanins are found in the plant, animal, fungi and bacteria namely eumelanin, pheomelanin, allomelanin, pyomelanin, DHN-melanin and neuromelanin (D'Ischia et al., 2013; Naggar and Ewasy, 2017; Plonka and Grabacka, 2006; Fig. 6). Melanins are biosynthesized by the oxidative hydroxylation of the aromatic compound resulting in the formation of free radicals (Naggar and Ewasy, 2017) which on polymerization gives heteropolymeric melanin. Our current understanding of melanin (D'Ischia et al., 2013) biosynthetic pathways for polymerization is through the Raper-Mason pathway (Mason, 1948; Raper, 1928), which was first hypothesized seventy years ago. These pathways involves a sequence of oxidative hydroxylation reactions of L-Tyr to produce dihydroxyindole (DHI) or dihydroxyindole carboxylic acid (DHICA). The monomers undergo oxidation yielding indole-5, 6-quinone-2-carboxylic acid and indole-5,6-quinone which are the immediate precursors for the polymerization (Fig. 7). Though eumelanins are multiple linkages of dispersing monomers of 5,6-dihydroxyindole (DHI) and 5,6-dihydroxyindole-2-carboxylic acid (DHICA) (Glass et al., 2012), exact proportion of the monomers remain unknown (Micillo et al., 2016; Ni et al., 2020). Pheomelanins are biosynthesized from the same precursor L-Tyr while cysteine is incorporated during the biosynthesis of pheomelanin (Napolitano et al., 2008; Fig. 7). Pheomelanin and benzothiazine are similar unit polymer and their structures contain both nitrogen and sulfur atoms (Napolitano et al., 2008; Fig. 7). Allomelanins are the most heterogeneous group of polymers biosynthesized from nitrogen-free precursors (Tarangini and Mishra, 2013) like dihydroxynaphthalene [Di-(DHN)] or tetra-hydroxynaphthalene [tetra-(DHN)] (Fig.7). Pyomelanins are generally brown to black-colored pigments biosynthesized extracellular by oxidative polymerization of homogentisic acid, an intermediate formed from L-Tyr

(Almeida-Paes et al., 2012; Coelho-Souza et al., 2013; Turick et al., 2008; Zheng et al., 2013; Fig. 7).

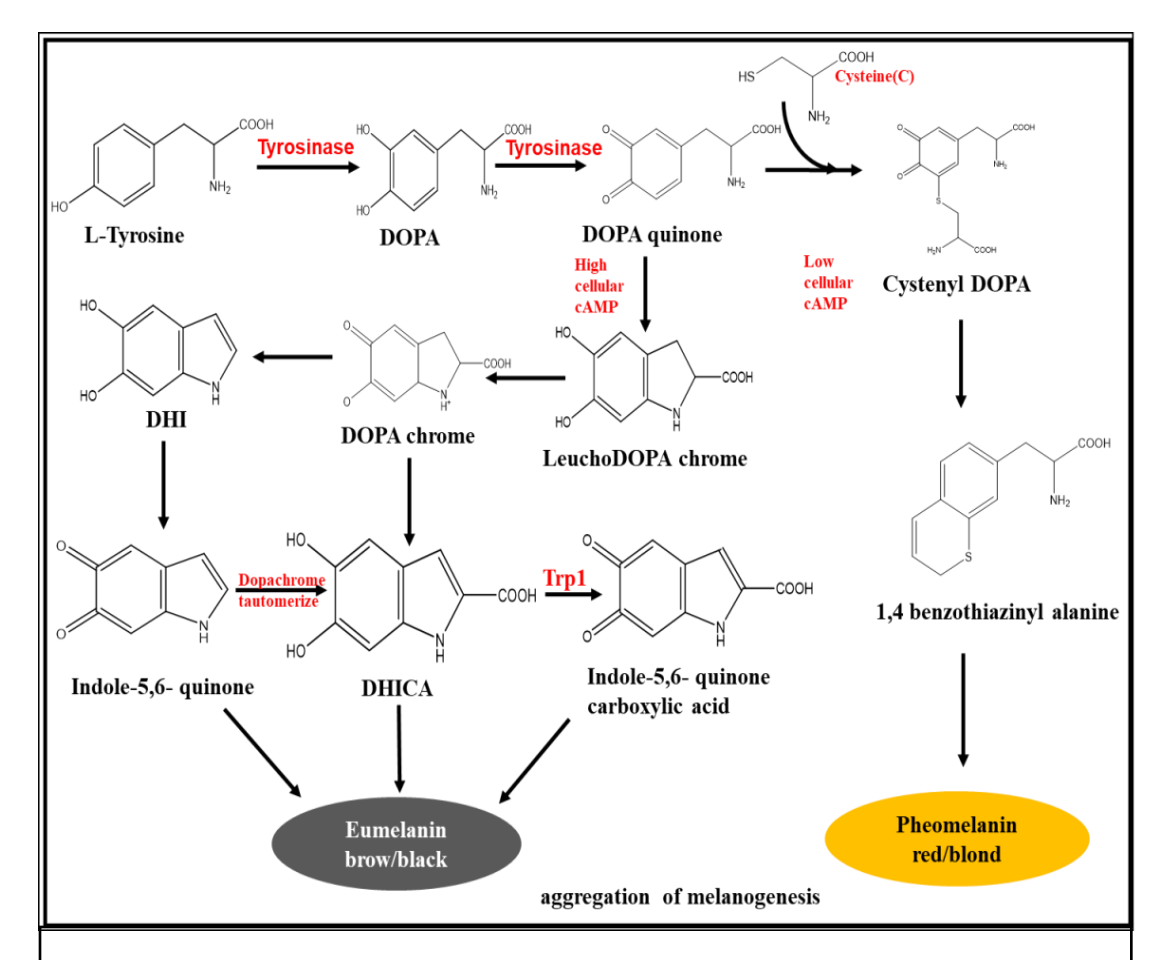


Fig. 7: Melanogenesis of eumelanin and pheomelanin (Source: D'Orazio et al 2013). DOPA; dihydroxyphenylalanine, DHI; dihydroxyindole, DHICA; dihydroxyindole carboxylic acid, Trp 1; Tyrosinase

1.6. Definition of the problem

Anoxygenic photosynthetic bacteria are a group of phototrophs capable of utilizing aromatic amino acids L-Phe, L-Trp and-Tyr for their growth under both photoheterotrophic (light anaerobic) and chemoheterotrophic (dark aerobic) conditions. *Rhodopsedomonas palusteris* can completely mineralized aromatic amino acids when used as a source of carbon and nitrogen under photoheterotrophic conditions (Larimer et al.,

2004; Oda et al., 2008). Phototrophic bacterial like *Rhodobacter spheroids* used L-Phe only as sole source of nitrogen and produces an array of phenolic compounds like caffeic acid, protocatechuic acid, gallic acid, alkyl ester of gallic acid (Ranjith et al 2007a,b), 3,4-dihydroxyphenylalanine (DOPA) and 3,4-dihydroxyphenylpuruvic acid (DOPP) (Ranjith et al., 2007b). In addition, the organism also produced many phenol esters like gallate terpenoid ester, caffeic acid ester, gentisiate ester and protocatechuate ester under photoheterotrophic conditions (Kumavath et al., 2010b).

Under photoheterotrophic conditions *Rbx. benzoatilyticus* produces a novel phenol derivative, Rubrivivaxin from the precursor L-Phe (Kumavath et al., 2010a, 2010b). *Rbx. benzoatilyticus* using the precursor L-Trp produces indole-3-acetic, indole-3-acetamide and indole-3-acetonitrile (Mujahid et al., 2011b). In addition, the organism also has the ability to photobiotransform aniline to acetanilide and can tolerated up to 30 mM aniline (Mujahid et al., 2015). In addition, the organism also photo-produced IAA and other aromatic metabolites (Mujahid et al., 2014) in response to aniline, however, stable isotope studies clearly demonstrated that these metabolites are not the photobiotransformed products of aniline (Mujahid et al., 2014). Genomics insights clearly revealed that *Rbx. benzoatilyticus* lack the genes encoding for the aromatic ring cleavage enzymes (Mujahid et al., 2011a).

In comparison with photoheterotrophic metabolism of aromatic amino acids by anoxygenic phototrophic bacteria, chemoheterotrophic metabolism is less studied and understood. This physiological group of bacteria thrive under both oxic and anoxic zones of natural habitats and contribute significantly to the carbon and nitrogen cycle (Egland et al., 1997; Merugu et al., 2012; Noh et al., 2002). Thus it becomes important to understand the chemoheterotrophic metabolism, particularly the aromatic amino acids which yields array of secondary metabolites that can help in the growth and development of plants,

particularly in flooded paddy conditions which are the true hubs for anoxygenic phototrophic bacteria. *Rbx. benzoatilyticus* is one such phototrophic bacterium isolated from a flooded paddy field and can grow under photoheterotrophic (light anaerobic) and chemoheterotrophic (dark aerobic) growth modes (Ramana et al., 2006). Under chemoheterotrophic (dark aerobic) conditions, *Rbx. benzoatilyticus* produces anthocyanin like molecules (Lakshmi et al., 2019b) and pyomelanin (Lakshmi et al., 2019a) from the precursor L-Phe. In the present thesis, I extended my work on the chemoheterotrophic (light aerobic) metabolism of L-Trp in search of novel metabolites with the following objectives.

1.7. Objectives of the study

- 1. To decipher the novel metabolic insights into chemotrophic metabolism of L-tryptophan by *Rbx*. *benzoatilyticus*.
- 2. To study the global proteomic changes occurring in the cells of *Rbx*.

 benzoatilyticus during chemotrophic metabolism of L-tryptophan.



2.0. Materials and Methods

2.1. Equipment and chemicals

2.1.1. Equipment

The equipment of glassware used in all my research work including measuring cylinders, pipettes, test tubes, round bottom flask, 500/1000 ml conical flask, reagent bottles, screw-capped tubes, Petri plates were procured from Duran borosil.

2.1.2. Water for solublization

Deionized water procured from School of Life Sciences a deionizer plant [ion exchange India Ltd. MODEL-CA20/U] was regularly used for cleaning/ wiping of glass equipment and generally media preparation. Single and double deionized water were frequently used for making the standard solutions and chemical analysis. Milli-Q water filter with 0.2 mm supor@²⁰⁰ membrane was used for metabolites filter followed to high performance liquid chromatography analysis.

2.1.3. Stock chemical and reagents

Chemicals and reagents to use in my research work were analytical grade from Sigma-Aldrich, Merck, Hi-media and Cambridge Isotope Laboratories.

2.1.4. Filtration units and equipment

Filter papers, super@ 200 membrane filters [0.2 μ m.0.45 μ m] and filtration units were from, Icon pall and PALL Life sciences, Whatman $^{@}$ paper used in this study were from Millipore.

2.1.5. Measurement of pH

pH was generally measured through a digital-pH meter [Digisun electronics, India model DI-707] and pH meter was generally normalized with standard buffer solutions of pH 4.2, 7 and pH strips.

2.1.6. Standard buffers

Deionized and autoclaved deionized Milli-Q water was normally used for making buffers solutions. Buffers were generally made according standard procedure and pH was accommodate at normal temperature unless till declared.

2.1.6.1. Normal buffers

Phosphate buffer; 50 mM sodium phosphate/potassium phosphate pH 7.5, HEPES-KOH 50mM buffer, borate buffer; 50 mM pH 10. Tris-(HCl) buffer; Citrate buffer, acidic, basic and neutral buffer; 50mM, 100 mM Tris/HCl pH 7.8 were used for this study.

2.1.7. Media and equipment sterilization

Media and equipment were sterilization was made through the autoclaving at 15 lbs, 121°C for 17 minute. Thermo labile standard chemical solution were filter sterilized by 0.22 µm (syringe filter) and membrane filter [icon pall].

2.1.8. Mineral media preparation

2.1.8.1. *Mineral medium [ingredients g.l⁻¹]*

Malate;- 3.0, KH₂PO₄;- 0.5, NaCl;- 0.4, MgSO₄.7H₂O;- 0.2, NH₄Cl;- 0.37, CaCl₂.2H₂O;- 0.05, yeast extract;- 0.2, ferric citrate 0.1% [w/v] 5 ml.l⁻¹, Trace elements SL₇ 1 ml. SL₇ [mg.ml⁻¹]; HCl [25% v/v] 1.0 ml⁻¹; ZnCl₂;- 7.0, H₃BO₃;- 60 ;MnCl₂.4H₂O;- 100; CuCl₂.H₂O;- 20; CoCl₂.6H₂O;- 200; NiCl₂.6H₂₀; -20; NaMoO₄.6H₂O;- 40]. Electron donor and ammonium chloride (NH₄Cl) [7 mM] as nitrogen source and Malate [22 mM] was used as carbon sources. All the media composition were melted in double deionized water, pH was measured to 6.8-6.9 with 5 N sodium hydroxide (NaOH). Nitrogen (NH₄Cl) source was replaced with other nitrogen sources whenever appropriate [1mM L-Trp/5-OH Trp].

2.1.8.2. Nutrient Agar [component $g.l^{-1}$]

Nutrient agar plate was prepared following component [Agar; 20.0 gm, Peptone; 10.0, sodium chloride (NaCl); 5.0, yeast; 3.50 and, pH 7.0] per liter were weighed and melted in deionized water except for agar. pH was normalized to 7.0 and agar was added to media before the autoclaving.

2.1.8.3. Standard chemical solutions

50 mM of L-Trp standard chemical solutions was made in deionized water and autoclaved sterilized, and placed at room temperature for 3-6 weeks. Stock chemical solutions were prepared, sterilized by autoclaving.

2.1.8.4. Buffers for whole cell proteome analysis

Whole cell proteome extraction buffer; 0.1% Sodium dodesyl sulphate (SDS) [w/v], 0.1% Tritan-X-100 [w/v], 50 mM HEPES-KOH, pH 7.5; 1.0 mM Ethylenediaminetetraacetic acid (EDTA), Re-suspension buffer; 50 mM Tris-HCl, pH 8.0; 100 mM sodium chloride, 2D Nano LC- SI-MS/MS; Buffer A [98% water, 2% acetonitrile, 0.2% formic acid, and 0.005% Trifluroacetic acid [v/v], Solvent B [100% acetonitrile, 0.2% formic acid, and 0.005% Trifluroacetic acid [v/v], Solvent C, and 0.5 M ammonium acetate (CH₃COONH₄), [5% acetonitrile, 0.2% formic acid [v/v].

2.1.8.5. SDS-PAGE buffers and chemicals

Stacking gel; acrylamide/bisacrylamide [w/w]; 5% polyacrylamide [30/0.8]; 125 mM Tris-HCl, pH 6.8; 0.1% [w/v] Sodium dodesyl sulphate (SDS); 0.015% [v/v] TEMED; 0.05% [w/v] Ammonium persulfate. Resolving gel; acrylamide/bisacrylamide [w/w]12.5% polyacrylamide [30/0.8]; 375 mM Tris/HCl, pH 8.8; 0.1% [w/v] TEMED; 0.05% [w/v]; SDS; 0.015% [v/v]; Ammonium persulfate. Running buffer; 25 mM Tris-HCl, pH 8.3; 0.192 M glycine; 0.1% [w/v] Sodium dodesyl sulphate. Protein loading buffer [5x concentrated]; 100 mM DTT; 2% [w/v]; 50 mM Tris/HCl, pH 6.8; Sodium dodesyl

sulphate; 0.1% bromophenol blue; 10% glycerol. Staining solution; 0.1% [w/v] Coomassie brilliant blue R-250 dissolved in 90/90/20 Methanol/ H_2O /glacial acetic acid [v/v/v]. Destaining solution; 255/115/20 isopropanol/ H_2O /glacial acetic acid [v/v/v].

2.2. Organisms and growth conditions

Rbx. benzoatilyticus strain $JA2^{T}$ (=ATCC BAA35T = JCM 13220^T = MTCC 7087^T] was used for all the experiments in the thesis.

2.2.1. Light anaerobic (phototrophic) and dark aerobic (chemotrophic) growth

Rbx. benzoatilyticus were used a model organism which was grown hotoheterotrophically [light anaerobic, $30\pm1^{\circ}$ C; illuninated 2,400 lux] on minimal edium including with (NH₄Cl) ammonium chloride [7 mM] as a sole source of nitrogen and malate [22 mM] as carbon source with full filled screw cap test tubes [10x100 mm] or reagent or glass bottles [250/500 ml] at pH 6.8- 6.9 Just before the experiment performed, the culture was streaked on a nutrient agar plate and to check the purity. The culture was growing chemotrophically on mineral medium in 500/1000 ml conical flasks containing 100/200 ml culture 190 rpm and at 30 $\pm1^{\circ}$ C. When L-Trp was supplemented as a sole source of nitrogen instead of (NH₄Cl) ammonium chloride and carbon source malate.

2.2.2. Maintenance of inoculum cultures

Inoculum cultures of *Rbx. benzoatilyticus* were maintained in a 250 ml bottle. The purity of the culture of *Rbx. benzoatilyticus* was checked on a solidified beibl pfenning medium/ nutrient plate and the culture bottle/tubes was photo illuminated [2,400 lux] and keeping at $30 \pm 1^{\circ}$ C. After incubation 2-3 days of growth was observed the pure culture. *Rbx. benzoatilyticus* culture was grown under photoheterotrophic/ light anaerobic or illuminated.

2.2.3. Determination of purity of the cultures

Purity of cultures were investigated by streaking onto nutrient browth/ nutrient agar plates and keeping light illuminated at 30 ± 1 °C. The purity of the stock culture was frequently monitored before the experiment and ending of the experiment.

2.2.4. Growth conditions

Rbx. benzoatilyticus was growing under photoheterotrophic conditions on minimal media with supplied ammonium chloride [7 mM NH₄Cl] as nitrogen sources malate [22 mM] as carbon and in filled 15 ml screw-cap test tubes [20x200 mm]/ reagent culture bottles [250/500 ml] at pH 6.8-6.9. The cultures were grown (chemotrophic) dark aerobically on 100/200 ml minimal media containing 500/1000 ml conical flasks at 30 °C, under agitation with 180 rpm [Eppendorf]. When L-Trp was used as a sole source of nitrogen, ammonium chloride [NH₄Cl] was replaced with 1mM L-Trp/5-OH Trp. The growth curve was measured turbido-metrically at O.D 660 nm.

2.2.5. L-Tryptophan feeding

Rbx. benzoatilyticus grew in photoheterotrophic condition in the nitrogen-deficient condition under illumination [2400 lux] at 30±1°C for 24 hours [early log phase culture 0.3 O.D] supplemented with L-Trp [1mM] was used as the sole source of nitrogen replaced of NH₄Cl (ammonium chloride) and malate [22 mM] as a carbon source. The cultures were then shifted to chemotrophic(dark aerobic) conditions in a conical flask to allow the shaking. Meanwhile added L-Trp [1mM] and incubated at 30±1°C with shaking for 48 hours desired period. Rbx. benzoatilyticus was also grown under aerobic conditions at 30±1°C for 24 hours with shaking condition and L-Trp [1mM] was added as a nitrogen source instead of ammonium chloride and incubated in a shaker until 48 hours.

2.2.6. Glyphosate inhibitors studies

To monitor the effect of glyphosate inhibitor to inhibit the *de-novo* aromatic amino acid biosynthesis of *Rbx. benzoatilyticus*, concentrations [1mM] of glyphosate were added to malate mineral medium and inoculated for the desired period. To monitor the does not affect of pigment production.

2.2.7. Pathway-specific inhibitors studies

Sulcotrione [0.6mM], Quercetin treatment [1mM], Ascorbate treatment [1-5mM], Kojic acid treatment [1-3 mM] and Sodium azide treatment [1-3 mM] were added to the 24 hours grown culture of *Rbx. benzoatilyticus* along with L-Trp.

2.3. Exaction of metabolites

2.3.1. Extraction of aromatic compound

The control condition and L-Trp [1mM] fed culture were grown as described in the materials methods 2.2.5 were used for the extraction of aromatic metabolites. The culture was harvested through centrifugation [10,000 rpm, 10 min 4° C] and the supernatant was taken as for ethyl acetate extraction. At first, the supernatant pH 2-2.5 was acidified by the addition of 5N HCl and the acidified supernatant was extracted three times with an equal ration (V/V) of ethyl acetate. Ethyl acetate fraction was separated through the using a separating funnel and the separated ethyl acetate fraction was dried under vacuum through the rotatory flash evaporator [Heidolp Germany] at 37°C. Finally, it was resuspended in 0.5ml HPLC grade methanol. The extracted metabolite was filtered through the membrane filter [supro@ 200 ,0.22µm], and the filtered extract was used for the HPLC analysis.

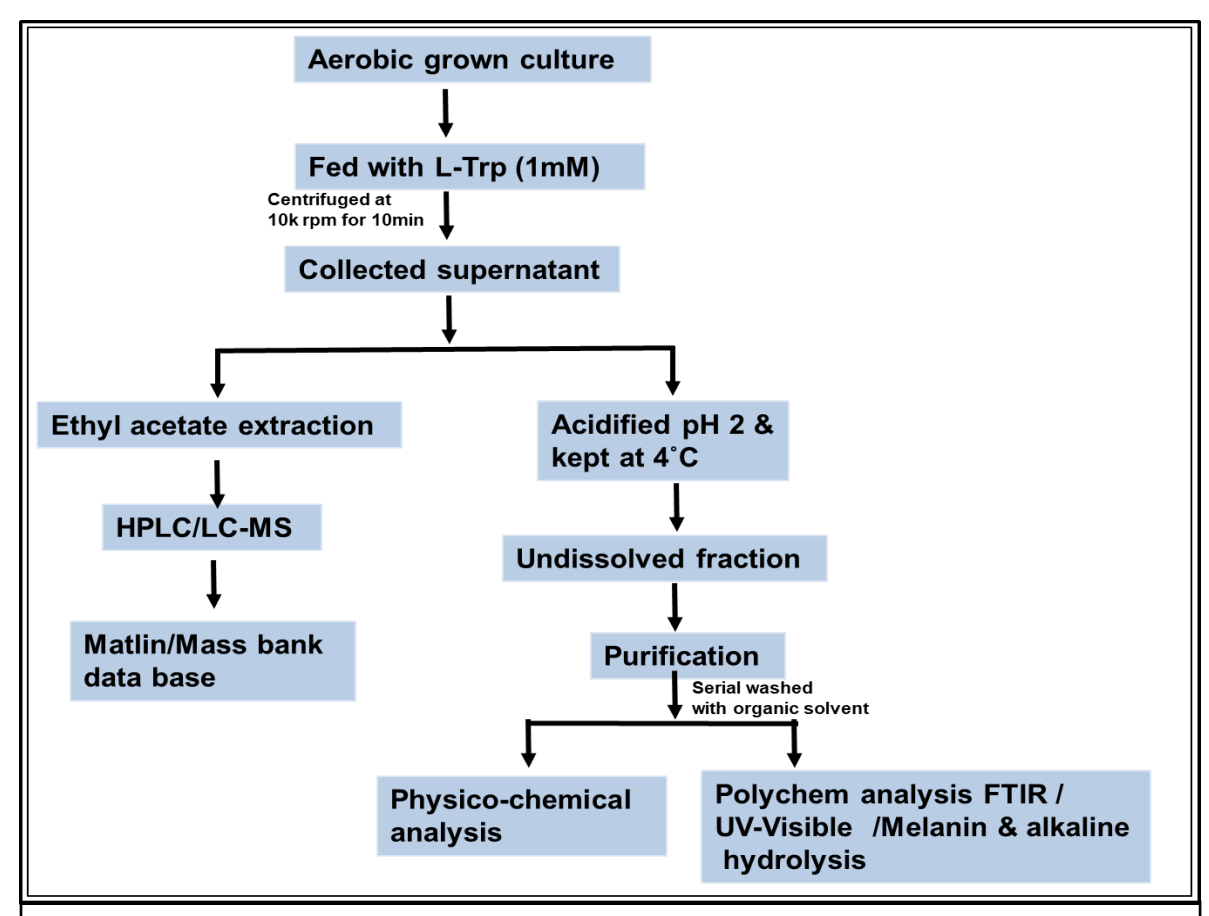


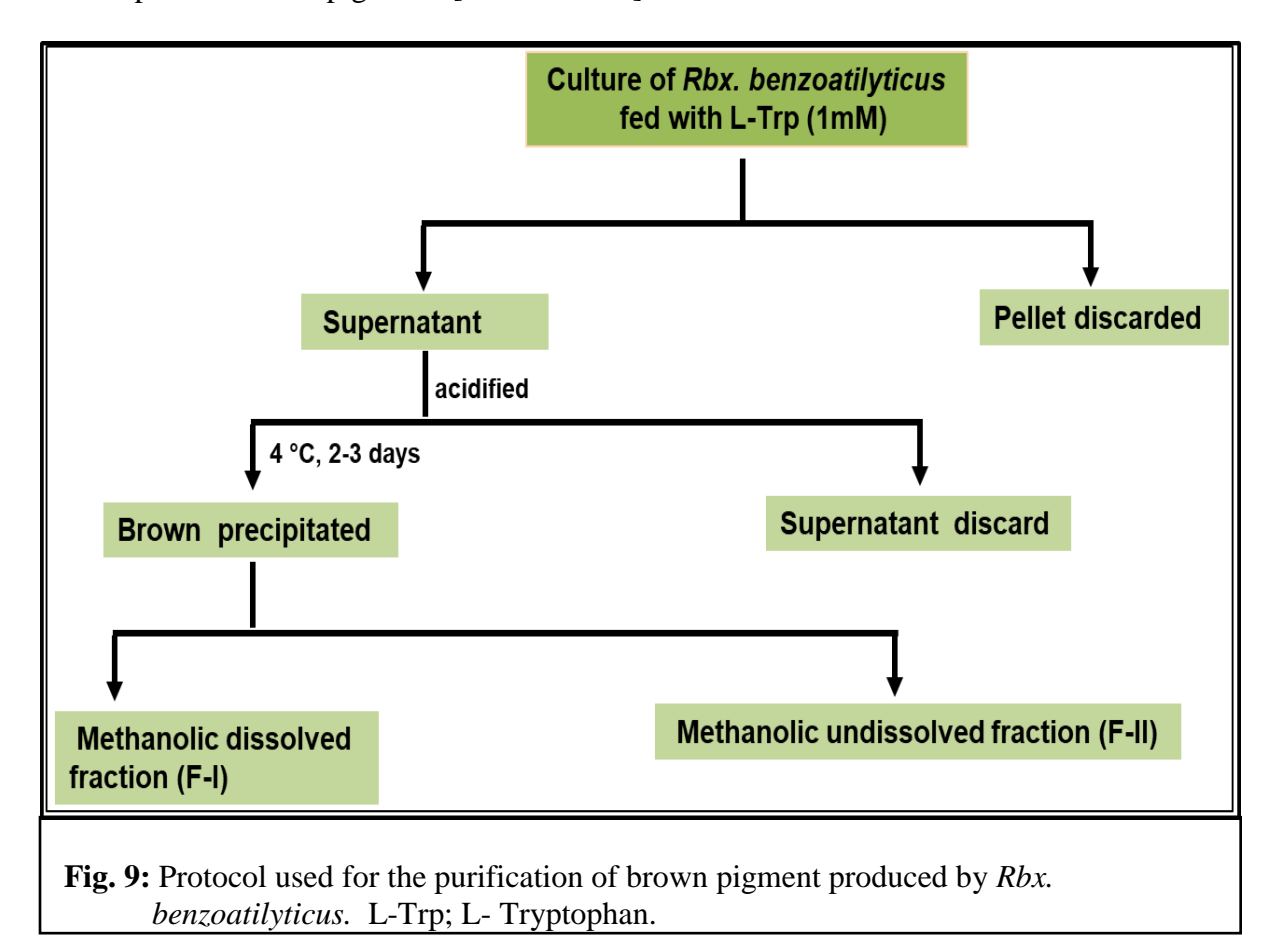
Fig. 8: Protocol used for extraction, purification and identification of exometabolites of *Rbx. benzoatilyticus* fed with L-Tryptophan. L-Trp: L- Tryptophan.

Cells grown in the presence or absence (control) of L-Trp for 48 h were used for the study. The culture supernatant was acidified and extracted into ethyl acetate and the ethyl acetate extract was concentrated to dryness and finally dissolved in MS grade methanol. The methanolic extract was used for HPLC and LC-MS analysis. Molecular ion mass, m/z; mass/charge; [M⁺] Molecular ion mass ionized in positive mode; [M⁻] molecular ion mass ionized in negative mode.

2.3.2. Extraction of brown pigments

L-Trp fed cultures of *Rbx. benzoatilyticus* were grown under the chemotrophic (dark aerobic) condition as described in section 2.2.5 and the cultures were harvested. (centrifugation at 10,000 rpm for 10 min, 4 °C), The collected supernatant was acidified to pH 1.5 to 2.0 with 5 N HCl and placed at 4°C for 48 h. Brown colored precipitated was observed to be settled at the bottom of the equipment. The brown precipitate was collected

through the centrifugation (12000 rpm, 12 min at 4°C) and the supernatant was discarded. The brown precipitate was resuspended in methanol and fractionated. Fraction-I [methanolic fraction] and Fraction-II [methanol undissolved fraction] were taken for further purification of pigments [Flow chart. 1].



2.3.2.1. Purification and characterization of brown pigment

Fraction-II was furthermore purified by frequently washings with 100 percent organic solvents [hexane, ethyl acetate, chloroform, acetonitrile, acetone, ethanol, and methanol] and later dissolved in water. Finally, the brown pigment was dissolved in 1N NaOH and then precipitated with 5 N HCl. The brown precipitate was formed with HCl precipitation characterized based on NMR, FTIR, UV-Visible and ESR/EPR spectral analysis and the characteristic features of purified brown Pigment were studied by physicochemical properties [Flow chart II].

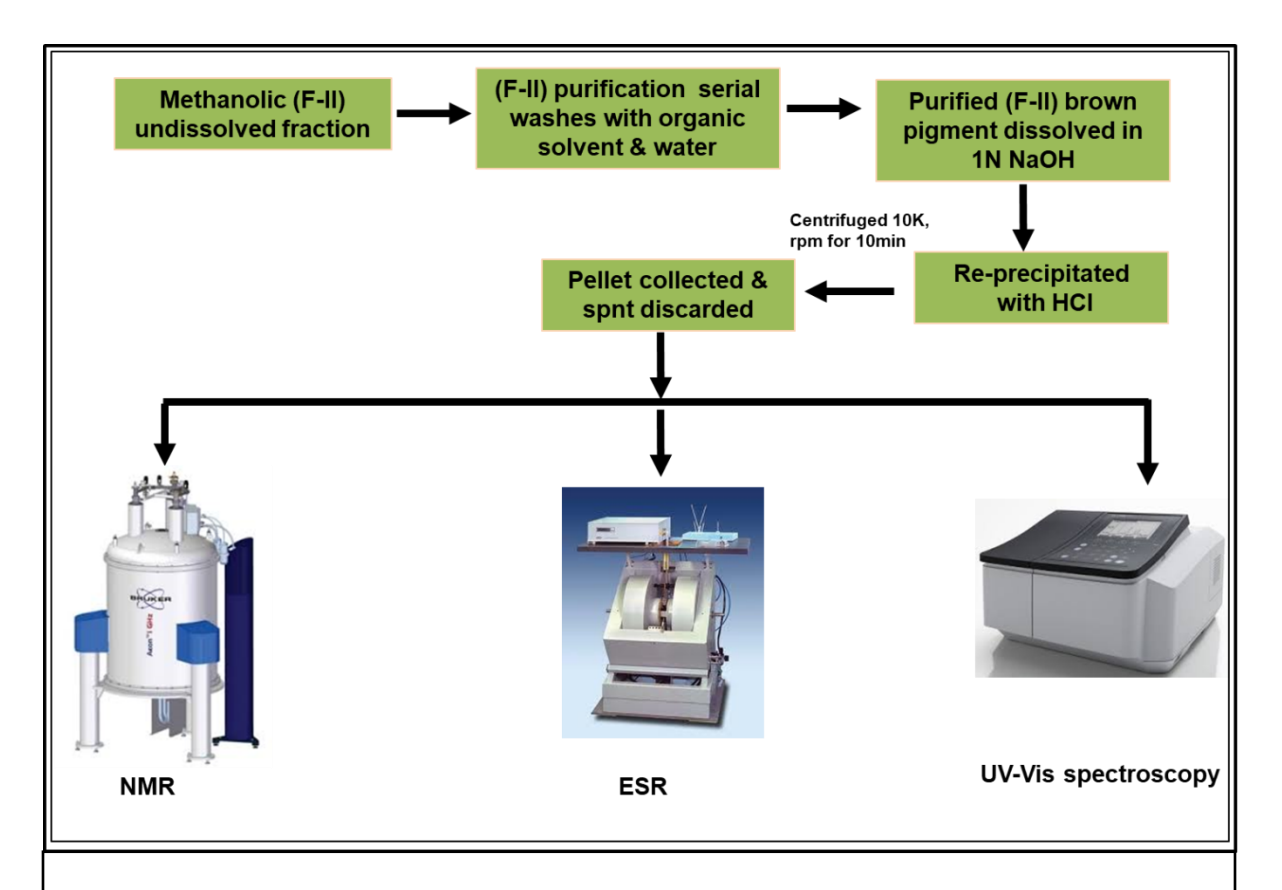


Fig. 10: Analytical protocol used for the identification of brown pigment produced by of *Rbx. benzoatilyticus*.

Fraction II was obtained from the protocol mentioned in Fig. 9. This was further purified by serially washing with organic solvents, water and finally re-precipitated with 5N HCl and collected by centrifugation. The purified brown pigment was further characterized based on poly-chem analysis using NMR, Nuclear Magnetic Resonance- spectroscopy; UV-IR, Ultra Violet-Visible-Infra-Red spectroscopy; EPR/ESR, Electron Paramagnetic Resonance/Electron Spin Resonance; min, minutes.

2.3.3. *Identification of pigments from the Fraction-I (methanolic fraction)*

The pigments were purified from the fraction-I as mentioned in the graphical Flow chart-III. The TLC analysis of fraction I (methanolic fraction) showed different blue, pink, red, orange, yellow-colored bands (Fig. 11). Each colored band was eluted into methanol and further purified by HPLC.

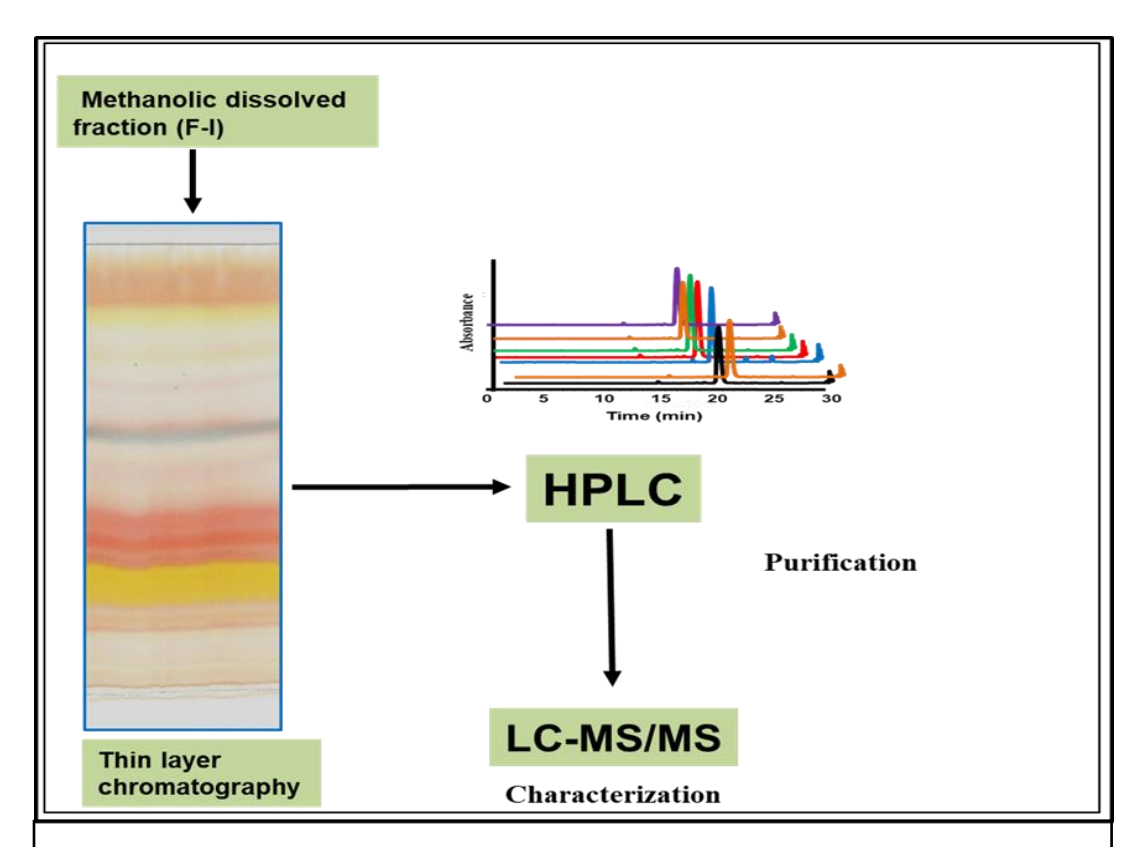


Fig. 11: Purification and characterization of a few colored pigments produced of *Rbx. benzoatilyticus*.

Colored pigments were purified from the fraction-I which obtained through the brown pigment precipitated according to the Fig. 9. Fraction-I was subjected to TLC using mobile phase chloroform: methanol: acetic acid [4:0.95:0.05 v/v]. Colored pigments were TLC eluted dissolved in MS grade methanol and were characterized by using by HPLC, GC-MS, and LC-MS/MS.

2.3.4. Extraction of extracellular metabolites [exo-metabolomics]

L-Trp fed and control cultures were grown in 500 ml flask containing 100 ml culture conical flasks incubated with agitation [180 rpm] at 30 °C under chemotrophic (dark aerobic) conditions for 48 h. Growth O.D [660 nm] were noted to normalize biomass, the cultures were pelleted through the centrifugation [12,000 rpm, 12 minutes, 4°C] and the supernatant were stored in -80°C, later supernatant were concentrated by a rotatory evaporator and dissolved in HPLC grade methanol. The samples were stored at -20°C until the GC-MS/LC-MS/HPLC analysis.

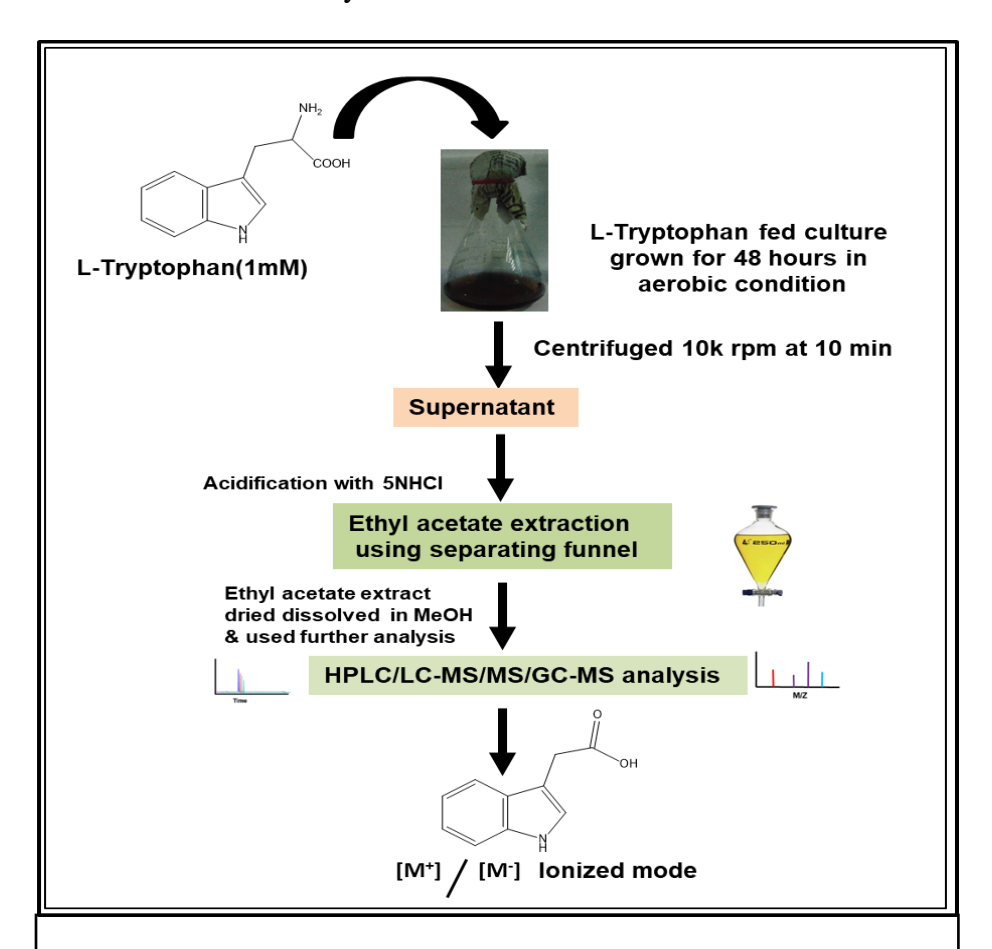


Fig. 12: Exometabolites extraction, partial purification and identification of indole derives produced from L-Tryptophan by *Rbx. benzoatilyticus*.

The culture was grown in the presence of L-Trp and control without the L-Trp Fed (unfed) under chemotrophic conditions for 48 h and the culture was harvested and the supernatants concentrated by a rotatory evaporator and dissolved in MS grade methanol.

2.4. Analytical Technique

2.4.1. Thin Layer Chromatography [TLC]

Thin Layer Chromatography [TLC] was performed using the TLC plates [Silica Gel60 F₂₅₄, Merck] to isolate and separate the pigment. The pigment was extracted into the methanol and ethyl acetate extract fraction. The methanolic dissolved extract was loaded onto to thin-layer plate and put in the container with the solvent system for metabolite separation. Thin layer chromatographic analysis was performed using the mobile phase, a mixture of chloroform: methanol: glacial acetic acid [8:1.9:0.1 v/v]. The TLC chamber was kept for solvent saturation for 30 minutes before the analysis. The sample was loaded on to the TLC plate, migrated based on the capillary force and colored [pink, yellow, and orange] bands were observed. The colored pigments were partially purified by eluting from the TLC with silica plate and further completely purified by using HPLC.

2.4.2. High-Performance Liquid Chromatography [HPLC] analysis

Shimadzu HPLC prominence was done according to Mujahid et al. 2011b. HPLC system consists of a binary pump, photodiode array of a SPD detector, and Phenomenex C-18 column [Luna, 5µm, 250 x 4.6 mm]. The gradient programmed was implemented for chromatographic partitioned and to identify the metabolites. The mobile phase solvent system used is 1% [v/v] glacial acetic acid in water and acetonitrile [100%]. Initially, the program runs with 1-55% acetonitrile for 25 min and step gradient for 3 min with 100% acetonitrile and finally ends with 1% water wash. The absorption spectrum was documented with a (PDA) photodiode array detector and metabolites concentration were determined by the peak areas using the standard known concern of their reference standards.

2.4.3. Liquid Chromatography tandem mass spectrometry (LC-MS) analysis

Mass spectrometry data were analyzed through the software Agilent technology Q-TOF [Agilent 6520] mass spectrometry coupled with HPLC prominence [Agilent Technologies1200 series] instrument with UV-Vis photodetector and auto-sampler. The injected samples metabolite was separated through the reverse phase column [Phenomenex], C-18, [Luna,5μ, 150x 4.6 mm] followed with the same gradient program as mention above 2.4.2 for HPLC analysis except for the flow rate, 0.8ml min⁻¹. The L-Trp derived metabolite was segregated and entered into the electron spray ionization [ESI] on ion source [80 °C cone voltage 15-25V] and detected by the mass detector, the absorption was recorded with UV-Visible detector. The molecular mass was detected with ESI ion sources and mass fragmentation was done through the collision energy 10-20 eV, the fragmentation pattern depends on the nature of metabolites with mass range 50-1000 Da and nitrogen gas as the collision gas. The metabolites were identified based on the mass spectrum of the authentic standard and also by comparing with mass spectra compound present in the database [http://metlin.script.edu/,http:www.massbank.jp].

2.4.4 Gas chromatography-mass spectrometry [GC-MS] analysis for indole derived metabolites

The cultures of control [absence of nitrogen] and L-Trp (L-Tryptophan) fed were harvested through the centrifugation [10000 rpm 12 mins at 4 °C] and the supernatants were stored immediately at -20 °C overnight. Supernatants were freeze-dried by using the rotatory evaporator [Heidolph Germany] and finally dissolved in 0.5 ml MS grade methanol. 20 µl samples were taken and dried by concentrator and derivatives by adding 60 µl of BSTFA Sigma Aldrich], incubated at 37 °C for 1 h, and subjected to GC-MS analysis. The gas chromatography mass spectrometry analysis was analyzed through the Pegasus HT TOF-MS [Leco, USA] system equipment with Agilent [7890 series] gas

chromatography. One microliter of the derivatized sample was injected into the HP-5 column [30 m, internal diameter 0.32 mm, thickness 0.25 μ m] with helium as carrier gas at a constant flow of 1 ml min⁻¹. Initially, the temperature was taken to 80 °C for 2 min, slowly temperature increased to 240 °C with 8 °C per min gradient and finally to 325 °C with 20 °C per min and temperature hold for 2 min. The inlet strating temperature 280 °C, transfer line temperature 225 °C, ion origin temperature 250 °C and ionization energy -70 eV. Mass spectra were documented at 40 to 1000 m/z with an acquisition rate of 10 spectra sec⁻¹. Data processing was done with 50 as the mass threshold, >700 as similarity match, library search matching with NIST, LECO-Fiehn library. The concentration of the metabolites was determined by peak areas.

2.4.5 Nuclear magnetic resonance [NMR] analysis

2.4.5.1 *Solid-state* ¹³*C NMR*

Brown pigment was purified as described in section 2.3.2 according to illustration. Flow chart III. The solid-state NMR analysis recorded through the different 5 mm probe C-13 was used to collect a Bruker AVANCE solution-state NMR spectrometer with a cryogenically cooled probe solid-state sample. The solid-state C-13 NMR spectrum was determined at room temperature on Avance III Bruker 600 MHz NMR at C -13 frequency of 100.62 MHz, 1H 600 MHz, the equipment with 5 mm double resonance probe head. Approximately twenty milligrams of lyophilized dried brown melanin powder was packed into the zirconia rotor. C-13 cross-polarization/total sideband suppression [CP/TOSS] experiment was run at a spinning speed of 7 kHz, 1H 90° pulse length was 2.83 μs and the C-13 180° pulse length was 6.52 μs. The contact time was 2000 μs, an acquisition time of 33 ms, the recycle delay was 8 s with a total of 11000 scans. The chemical shifts were referred to as CDCl3 [77.4 ppm].

2.4.5.2. *Solid-state* ¹⁵*N NMR*

The Solid-state ¹⁵N NMR spectra of lyophilized brown pigment were acquired on an Avance III Bruker Spectro spinning as 800 MHz spectrometers operating using as a triple resonance with the N-15 probe 5 mm. Lyophilized purified melanin loaded [25-35 mg] in and N¹⁵ probe Bruker operating as resonance probe with the operating conditions; spinning speed -7 kHz: 1H 90°; pulse length was 2.83 μs and the 13C 180° pulse length was 6.52 μs. The contact time -2000 μs, achievement time was 33 ms and the recycle delay 8 sec with a total of 10000 scans. The ¹³C chemical shifts were calibrated relative to tetramethylsilane [0 ppm]. The solid-state N-15 NMR CP/MAS spectra were obtained with the same instrument using N-15 probe Bruker polarization depends on the 15N—H dipole interaction.

2.4.6. Fourier Transform Infrared [FTIR] analysis

The FTIR spectra were recorded on Bruker, ALPHA FTIR/ATR spectrometer. The purified brow pigment solid lyophilized powder was used for the FTIR analysis. The purified dry powder was kept on the holder and the spectra were determined in transmittance mode with wavelength from 200 to 800 nm.

2.4.7. *UV-Visible spectral analysis*

The purified brown pigment was dissolved in [1mg/ml] [1N] NaOH/KOH and diluted 1:10 time and the UV-Visible spectrum was recorded in the wavelength from 200-800 nm on a UV-Visible spectrometer [Shimadzu] and [1N] NaOH used as a blank. The spectra were acquired for the purified brown pigments dissolved in [1N] NaOH against the NaOH blank. The UV-Vis spectrum was acquired in SHIMADZU spectrophotometer. The UV-Vis spectra were recorded at 200-800 nm.

2.4.8. Electron Spin Resonance [ESR/EPR] analysis

The precipitated brown pigment obtained from the L-Trp and 5-OH Tryptophan [5-OH Trp] added culture was used for the ESR/EPR and the experiment was done on JEOL X-band ESR spectrometry. The dried brown pigment powder was loaded into the ESR tube. The ESR spectra were acquired and analyzed.

2.4.9. X-ray Diffraction [XRD] analysis

X-ray Diffraction analysis of purified precipitated brown pigment obtained from *Rbx. benzoatilyticus* using Bruker D8 Advance, Germany X-Ray Diffractometer. The lyophilized dried powder form of brown pigment melanin was pressed onto discs of 1 cm in diameter and 1 mm thickness. The brown pigment powders were scanned through a Phillips diffractometer operating with a 1.54 A° [Angstrom] X-ray beam. The scattering intensity was acquired as a function of the scattering angle. The recorded data were converted from angle coordinates to Q scale with Q being the magnitude of the momentum change of the X-ray photon elastically scattered through an angle H. The parameter Q is related to the scattering angle by the equation: Q=4p sinðh=2p] /1, where 1 is the X-ray photon wavelength [1.54 A°]. It may be possibly useful to relate the Q peak maximum to the distance between the molecular sheets of melanin, R, where R=2p/Q. Whereas it should be borne in mind that R represents an average value for the distance, the uncertainty being related to the width of the stacking feature in Q space.

2.5. Microscopic Technique

2.5.1. Scanning electron microscopy [SEM]

Lyophilized brown pigment powder was used for SEM analysis. The brown powder was at first sonicated in HPLC grade acetonitrile then 1-2µl upper part were taken for Scanning electron microscopy according to the standardized protocol with slight modifications. The brown powder was omitted on glass pieces [0.6 x 0.6 cm] and dried by

critical point dryer according to normal procedure, dried brown pigment fraction were fixed to SEM stubs and coated with gold foil. The brown powder specimen's spots were investigation through SEM [Philips XL30 series] at desired range of magnification ranges

2.7. Melanin degradation and alkaline hydrolysis methods

2.7.1. Brown pigment degradation

The purified brown pigment molecular monomer—were identified through the hydrolysis of the brown pigment pigment as earlier reported by Ellis and Griffiths (1974) with little modifications. Six milligrams of the lyophilized dried pure brown pigment was mixed with 0.6 g of defused potassium hydroxide in a 5 ml tightly sealed screw cap tube. The reaction mixture was to boil on boiling—water bath (1.5 h) and after the dark color viscous residue thus formed was allowed to cool. To the dried viscous residue 1.5 ml, deionized water was added and acidified (pH 2.0) with 5N HCl, and metabolites were extracted with diethyl ether and dried under a rotatory evaporator (Heidolph, Germany) and were solublized MS grade methanol. To identify the indoles, the hydrolyzed fraction was run on TLC (Merk, Silica gel 60 F₂₅₄, 20x10 cm, 0.2 mm,) using a mixture of chloroform: methanol: glacial acetic acid (9: 0.95: 0.05 v/v) as a solvent system and TLC plate was developed using indole-specific TLC reagent prepared as described by Ehmann *et al.*, 1974.

2.7.2. Chemical oxidation of melanin

To identify the production of various pyrrole derivatives melanin degradation products by Alkaline H₂O₂ hydrolysis of eumelanin measure [PTCA PDCA and PTeCA] was performed as described in Wakamatsu et.al; 2012 and small modification instead of K₂CO₃ we used NaOH approximately 3 mg purified melanin specimen was taken in 5ml screw-capped tube and added 0.1ml water and 0.3g NaOH with 25% H₂O₂. The reaction mixture was heated 1-2 hour on boiling water after boiling cloudy mixture was observed

the remaining H_2O_2 decomposed by the addition of 10% Na_2CO_3 and then the mixture was acidified by addition 5N HCl and extracted with ethyl acetate three times pooled, dried by a Rotatory evaporator and dissolved in HPLC grade methanol. The melanin hydrolyzed product was used for HPLC/LCMS analysis according to Mujahid *et at.*, 2011b. In a brief description of HPLC prominence system analysis was carried out by a Phenomenex C-18 column [Luna, 5 μ m, 250 $_X$ 4.6 mm]. A linear gradient operating program was employed to separate the degradation products. A total of 1%[v/v] acetic acid in water [Solvents A] and acetonitrile [100% Solvent B] [HPLC grade Merk] was used as mobile phase with 1.5 ml/min flow rate.

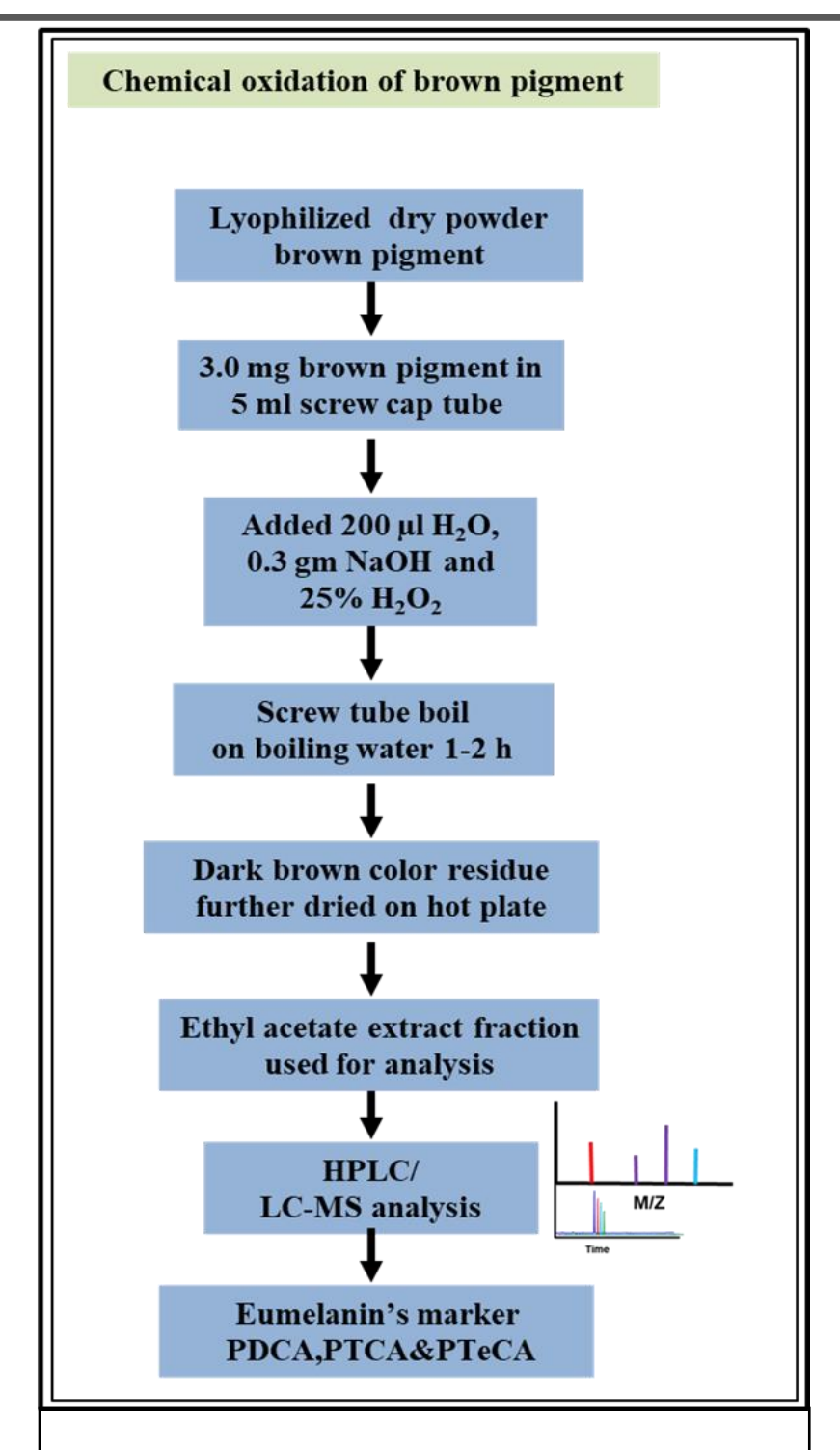


Fig. 13: Hydrolysis, extraction and identification of monomers of melanin produced by *Rbx. benzoatilyticus* of *Rbx. benzoatilyticus*. PDCA; pyrrole-2, 3-carboxylic acid, PTCA; Pyrrole-2,3,4-tricarboxylic acid and PTeCA; Pyrrole-2,3,4,5-tetracarbosylic acid

2.6. Biochemical methods

2.6.1. Spectrophotometric assays

2.6.1.1 Determination of indole concentration

Indoles concentration were monitored by Salper's method [Paleg LG and Gordon SA,1957] 0.5ml of culture supernatant was mixed with 0.5 ml of Salpers reagent and to this 1 ml of freshly prepared Salper's reagent [35% [v/v] perchloric acid in 1ml of 0.5 M FeCl₃ in 50 ml] was added and the optical density was read at 535 nm control as a reagent blank. Total indole quantification was done using known concentration as a standard.

2.6.1.2. Proteins determination

Protein concentration was determined through the Bradford's method [Bradford, 1976] which participate the staining of Coomassie brilliant blue G-250 to proteins. Solublized 100 mg of G-250 in 100 ml of 99% of pure absolute ethanol and placed on a shaker for ~ 1.0 h. One hundred milliliter of 88% Ortho-phosphoric acid was added, mixed properly and the volume was made up to 400 ml with the addition of deionized water. It was filtered by Whatman [Fluka] diluted 1:1 ration of equal volume with water and the optical density was read at 550 nm used as water blank, the reagent was stored at 4° C. $40~\mu$ l of the sample was mixed with 360 μ l of the water and to this 1600 μ l of Bradford's reagent was mixed, kept for 5 min and optical density was acquired at 595 nm against reagent blank. Bovine serum albumin [BSA] was used as a standard.

2.7. Enzyme activities

2.7.1. Preparation of cell-free extracts

Mid log phase chemotrophic (dark aerobic) cultures grown on L-Trp containing media were carried out for *in vitro* melanin production studies and cell-lysate were prepared according to Lakshmi et al., 2019. Briefly, the culture was centrifuged through

the centrifugation [at 4°C for 10 min 10,000 rpm]. The culture pellet was washed twice with 50 mM phosphate buffer and resuspended in 4 ml of 50 mM [pH 7.5] phosphate buffer. The cell-free extract were prepared by disrupting the cells using sonicator [BANDELIN, Germany 7 cycles, 60 % amplitude] and the cell lysate was centrifuged at 16,000 rpm for 25 minutes. The clear supernatant was taken generally as an enzyme source.

2.7.2. Aromatic aminotransferase /Transaminase activity

Aminotransferase/transaminase activity was carried in 4 ml volume, α -ketoglutarate [1mM] and pyridoxal phosphate [PLP; 50 μ M] as cofactors, with L-Trp/5-OH Trp [1mM] as substrate. The reaction was started with the addition of the approximate volume of the enzyme source to the reaction mixture. The reaction was placed for 1 hour at 37 °C at shaking and the reaction was terminated with 5N HCl after 1 h incubation and the blank was pre-denatured cell lysate with 5N HCl. Moreover, the reaction mixture was centrifuged at 16000 rpm, at 4° C for 20 min, the supernatant was used thrice with ethyl acetate extraction. The extracted fraction was pooled and evaporated to dryness in the rotatory flash evaporator. Finally, the extract was solubilized in 300 μ l of MS grade methanol. L-Trp consumption or indole acetic acid formation was measured with HPLC.

2.7.3. *Monooxygenase activity*

Monooxygenase enzyme activity was performed in the appropriate volume of 4 ml Tris buffer [50 mM, pH 7.4] tetrahydrobiopterin [BH₄; 50 μM] as cofactors containing substrate 1mM of L-Trp and the approximate volume of cell lysate. The reaction mixture was palced at 37°C for 60 min shaking and then the reaction was prevented by adding 300 μl of 5N HCl. The pre-denatured cell lysate was used as a blank/ control. The reaction ingredient was centrifuged [4°C for 12 min at 9,000 rpm] and the clear supernatant was used twice with metabolites extraction. Extracted ethyl acetate was pooled, evaporated to

dryness under vacuum, finally solubilized in 500 μ l of MS grade methanol, and analyzed by LC-MS.

2.7.4. *In-vitro melanogenesis*

The *in vitro* assay was carried out in 4 ml final volume consisting of 1 mM L-Trp or OH-Trp as substrate and an approximate volume of cell-free extract and reaction mixture was kept at 180 rpm, 37 °C for 1 hour in an incubator shaker [Eppendorf Innova]. The reaction was stoped by adding 300 µl of 5N HCl and Pre-denatured cell lysate (enzyme sources) [with 5N HCl] and the reaction mixture without cell-free extract was used as blanks. After the reaction was stoped, the brown pigment was purified as described in material and methods earlier. For in vitro pigment studies, the same procedure was followed as described above except, 1.0 ml sample was withdrawn periodically [at 30] mins]. Samples were centrifuged and the supernatants were analyzed for L-Trp or OH-Trp using HPLC analysis. The pigment formation was the measurement spectrophotometrically at 400 nm.

2.8 Metabolomics studies

2.8.1 Stable isotope-labeled L-Tryptophan feeding experiments

Rbx. benzoatilyticus was grown chemotrophically (dark aerobic) for 24 h [0.3 O.D₆₆₀ nm] then the culture was subjected to fed [1 mM] Tryptophan unlabeled ¹²C₁₁ as well as all carbon probing labeled ¹³C₁₁ and L-Trp[Tryptophan and all carbon-¹³C₁₁, labeled L-Trp], and separate culture was fed with unlabeled ¹²C₁₁L-Trp under chemotrophic (dark aerobic) conditions incubated simultaneously for 48 h at 30°C [180 rpm]. The cultures were harvested [centrifuge 10000 rpm 10 mins at 4°C] and the collected supernatant adjusted to pH 2.0 was extracted using ethyl acetate thrice with equal volume

pooled and dried by vacuum rotatory evaporator [Heidolph Germany] and dissolved in MS grade methanol kept -20 °C until analysis.

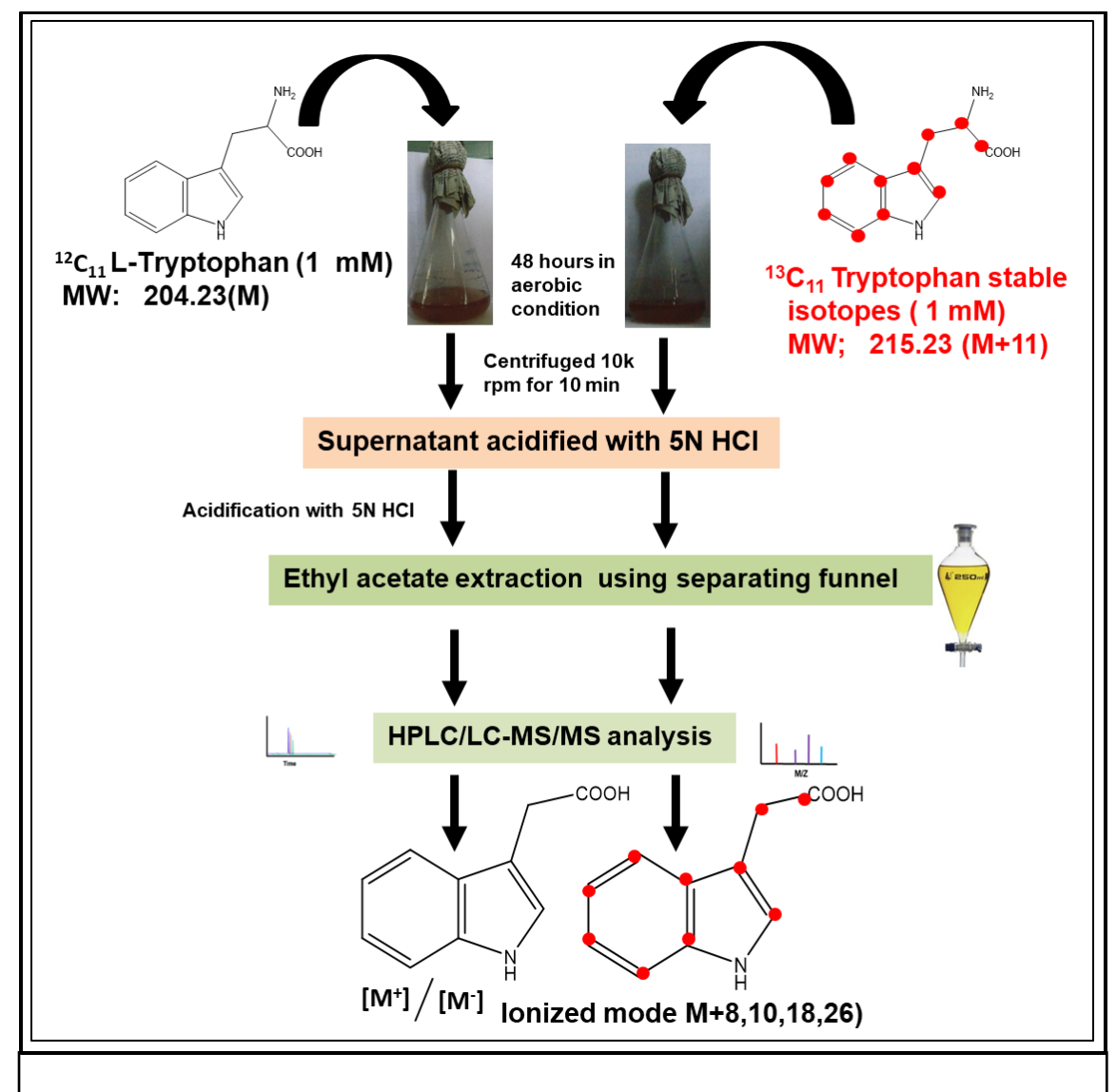


Fig. 14: Stable isotopic exometabolites profiling (SIMP) of *Rbx. benzoatilyticus*.

2.8.2. Liquid chromatography-tandem mass spectrometry (LC-MS/MS)

Ethyl acetate extracts fraction from a culture grown in the amendment of unlabeled [12 C11] or labeled [13 C11] L-Trp was separately analyzed by using Agilent series 6520 LC-MS analysis. At first, unlabeled and labeled sample was individually run on LC-MS followed by mixed [1:1] of labeled and unlabeled fraction mass and spectral analysis was implemented on 6520 accurate mass qualitative time of flight [Q-TOF] LC-MS system

[Agilent Technologies] equipment with a photodiode an array detector [PDA], and an auto-sampler was used for injecting 3 µl of the sample for the chromatographic segregated at 25 °C. The metabolites were segregation—using the—reverse phase column [Phenomenex] C-18 [Luna, 5µm, 150X4.6mm] with a constant flow rate 0.8mL/minute using 0.1% glacial acetic acid in water[v/v] [Solvent A] and acetonitrile [Solvent B]. The metabolite was eluted using a gradient operating program; initially, the mobile phase composition was 1% Solvent B followed by a linear gradient 55% within 48 min then step gradient to 100% within 65min and held for a minute.

Finally, Metabolite was recorded, and the absorption spectrum was measured using a prominence PDA detector [220-600 nm]. The metabolite was partitioned and infused into the electron spray ionization [ESI] ion source operated under full-spectrum scan mode from 50-1000 m/z. Data accomplishment was recorded under both positive[+ve] and negative[-ve] modes in separate runs. A pair of reference masses, 121.0509 m/z [C₅H₄N₄] and 922.0098 m/z [C₁₈H₁₈O₆N₃P₃F₂₄], were measured throughout the sample run for mass correction and achieve the accurate mass. Mass spectrometer condition; nitrogen as drying gas at the constant flow of 19 L/min, nebulizing at 45 psi, drying gas temperature [300°C] ion source capillary voltage [4Kv], and fragmentor voltage [144V]. Data achievement was measured using a mass hunter work software [version 6.0 Agilent Technologies].

2.8.3 Data analysis and metabolites identification

The Raw read data files were analyzed using the Agilent Mass Hunter work station Qualitative software [version 6.0, Agilent Technologies]. Data [labeled-unlabeled mix] was manually inspected for $^{12}C_{11}$ the mono-isotopically ion [M]and the corresponding $^{13}C_{11}$ ion pattern [M+N], whereas N is 8, 9, 10, 18.....26] expected for one or two and three [$^{13}C_{11}$] indole ring incorporated into the metabolites. The molecular ion masses of

isotopically labeled metabolite ring were predicted from the measured m/z value of the putative unlabeled feature [M]. The metabolite feature pairs [unlabeled vs labeled] were considered through definite criteria. Similar retention times co-eluted with the authentic standard [2] similar chromatographic peak shaped [3] identical absorption spectrum [4] a theoretical mass shift. Peak area [intensity] of ¹²C₁₁and ¹³C₁₁ metabolites features was achieved from extracted ion chromatograms [EICs]. The MAVEN (Clasquin et al., 2012) software package was also occupied to confirm the ¹²C₁₁ and ¹³C₁₁ metabolite pairs. The molecular formula generator [MFG] algorithm through using the Mass Hunter was to generate the tentative molecular formula for the metabolic feature [13C₁₁]. MFG was using the monoisotopic mass accuracy, isotopes abundance ratios, and spacing between isotopic peak to assign the molecular formula and score. Higher the MFG score [highest 100] of a candidate formula, we have taken it is likely to correctly indicate the nearest highest score. The principle to access the metabolite identity were; confirmed: m/z, abundance, predicted formula. **METLIN** [https://metlin.scripps.edu], [MassBank,www.massbank.jp], [HMDB,www.hmdb.ca] and KEGG [www.genome.jp/kegg/pathway] database through were used for metabolite identification.

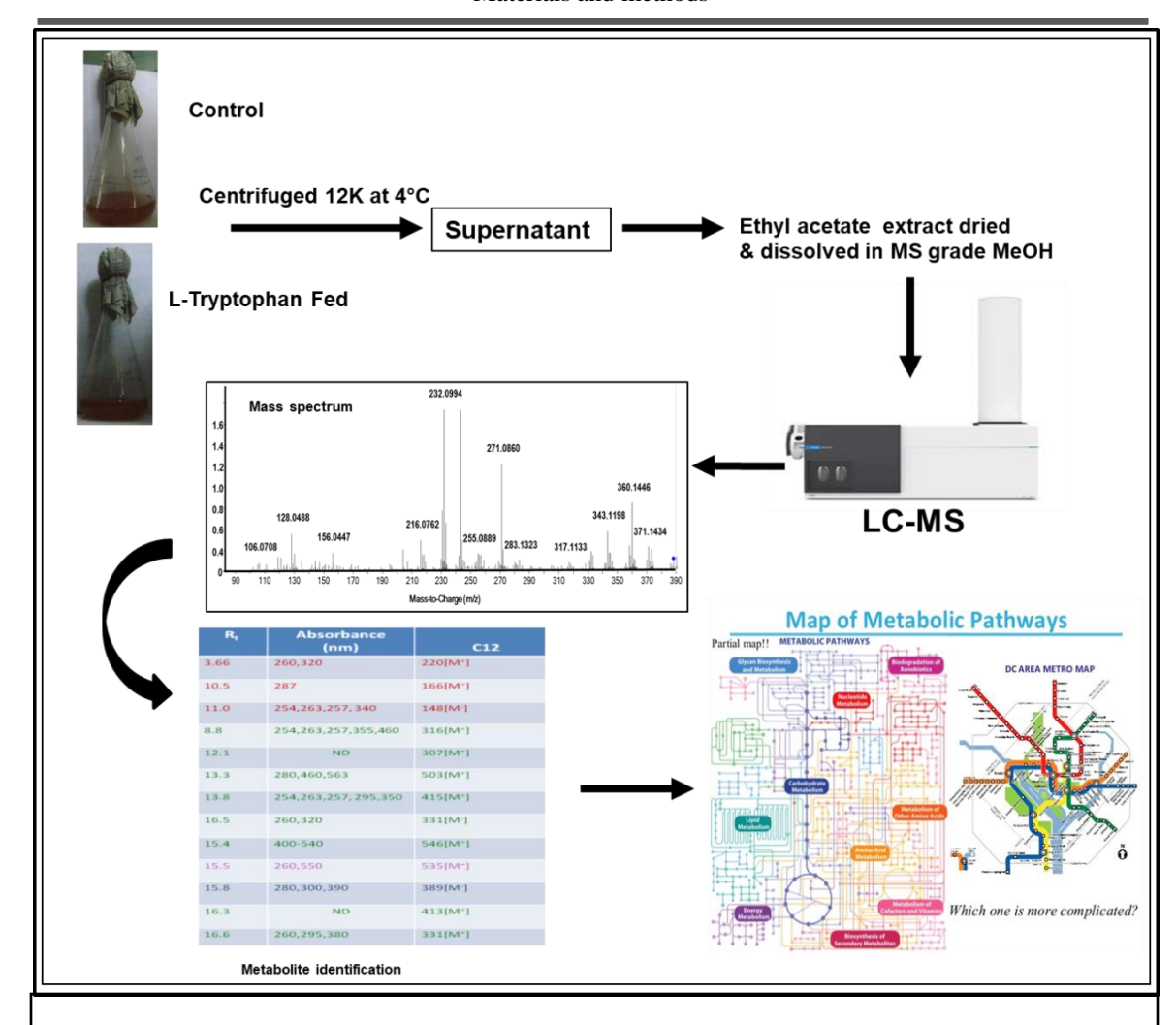


Fig. 15: Pathway prediction based on the exometabolic profiling of *Rbx. benzoatilyticus*.

2.9. Methodology used for proteomics studies

2.9.1. Isolation of total protein from cells of Rbx. benzoatilyticus

L-Trp fed and control cell [without Trp] cultures 48 hours under chemotrophic (dark aerobic) conditions were taken for global proteome [iTRAQ] analysis. The experiment design in triplicated three independent biological replicates used for the iTRAQ proteome analysis. L-Trp fed and controlled cell culture was harvested through the centrifugation at 4°C 9 000 X 12 min and the pellet was washed thrice time with 50mM HEPES-KOH buffer con pH 7.5. Finally washed pellet was re-suspended in 4 ml HEPES-

KOH containing pH 7.5; 0.1% Tritan-X-100 (w/v); 0.1% SDS (w/v). The buffer used to be sonicated [MS 70 probe, 40% power, and 7 cycles at 4°C] to prepare the cell lysate. The cell lysate was placed for 30 minutes at 4°C on the ice-cold condition and centrifuged [30 minutes at 20,000 rpmX] and then clear supernatant of cell lysate was taken as soluble proteome analysis. The total protein precipitated overnight by pre-chilled acetone with six-volume at -20 °C has centrifuged for overnight for protein precipitated protein [4 °C at 10,000 rpm for 20 minutes]. The collected protein was washed with acetone twice, the supernatant was discarded and the pellet was wash followed to lyophilization and kept at -20°C until proteome analysis.

2.9.1.1. Isobaric tags for relative and absolute quantitation [iTRAQ] labeling of proteome

Isobaric tags for relative and absolute quantification [iTRAQ] sample adapted for analysis outsources the University of California, San Diego, USA adapted the following protocol. The one hundred micrograms of each sample were resuspended in TNE buffer [50 mM Tris pH 8.0, 100 mM NaCl, 1 mM EDTA]. RapiGest SF reagent [Waters] was added to the mixed properly to a final concentration of 0.1%, samples were then boiled for 5 min at 95°C. Proteins were reduced with 1mM Tris-[2-carboxyethyl) phosphine [TCEP] for 30 min at 37°C [Pierce Chemical] and carboxy- -methylated with 0.5 mg/ml of iodoacetamide for 30 min at 37°C, the reagent iodoacetamide was used to neutralize with an additional 1 mM TCEP. The protein mixture was digested with trypsin by keeping overnight at 37°C with trypsin and protein ratio as 1:100 [trypsin: protein]. Samples were treated with 50 mM HCl at 37°C for 60 min and centrifuged at maximum speed for 30 min at 4°C to degrade and remove the RapiGest. The soluble protein was taken to a new Eppendorf tube and the pH of the solution adjusted to 3.0 addition of NH4OH.

Protein mixture was then extricated and removed the salt by using Aspire RP 30 Desalting Tips [Thermo Scientific]. Protein were re-measured through the bicinchoninic acid assay. Hungreds microgram of each sample was used to subject to labeled with a unique reagent iTRAQ₈ tag [113,114, 115, 116, 117and 118] as described in the control sample were labeled iTRAQ₈ 113, iTRAQ₈ 114, iTRAQ₈ 115 and treated sample labeled as iTRAQ₈ 116, iTRAQ₈ 117 & iTRAQ₈ 118] manufacturer's protocol [ABSCIEX]. The six samples were combined dried by speed vacuum to remove the ethanol. The sample was re-dissolved in 100 μl buffer [98% H₂O, 2% ACN and 0.2% formic acid 0.005% TFA] 5 μl sample taken as MudPIT [Multidimensional protein identification technique analysis Yun *et al*, 2011]

2.9.1.2. Two-dimensional Nano Liquid chromatography-tandem mass spectroscopy (LC- ESI-MS/MS) analysis [MudPIT]

Isobaric tag and relative absolute quantification [iTRAQ] labeled sample peptide mixture were analyzed on through the using a QSTAR-Elite hybrid mass spectrometer [AB/MDS Sciex] interfaced through the Nano-flow reverse phase high performance of liquid chromatography. The peptides mixture was separated by used Nano-flow with the high-pressure liquid chromatography coupled with tandem liquid chromatography and mass spectroscopy through the Nano-spray ionization source. The labeled sample was passed through the strong cation exchange [SCX]with fractionation was carried on BioX-SCX [5 μm particle size, 0.5 mm inner diameter x 15 mm. LC Packings P/N 161395] trap column. The protein sample mixture was loaded onto the SCX column and eluted with 7.5 μl.min⁻¹ flow rate for 10 min using gradient of buffer A and solvent C [0.5 M ammonium acetate; 5% acetonitrile, 0.2% formic acid] The SCX salt steps [first dimension] used for separation were 5%, 7.5%, 10%, 12.5%, 15%, 20%, 25%, 30%, 40%, 50%, 75% and 100%. In the second dimension [reverse phase] peptides were eluted from the Zorbax TM C-18 Column [100 x 0.18 mm, 5-μm, Agilent Technologies,

Santa Clara, CA] into the mass spectrometer using a linear gradient program of 5–80% Solvent B [100% ACN, 0.2% formic acid and 0.005% TFA] and Solvent A [98% H₂O, 2% acetonitrile, 0.2% formic acid, and 0.005% [TFA] over 60 minute at 400 nL.min⁻¹ with flow rate. Liquid chromatography-tandem mass spectroscopy data were obtained in a data-dependent fashion by collecting the 6 most high intense peaks with a random state of plus 2 to 4 that exceeds 35 counts, with the excluding of former target ions set to "60 seconds" and the mass tolerance for exclusion set to 100 part per million [ppm]. TOF [Time-of-flight] mass spectrometer was achieved at m/z 400 to 2000 Dalton atomic unit [Da] for 0.75 sec with the twelve-time bins to sum. Tandem mass spectrometer [MS/MS] data were achieve from m/z 50 to 2,000-dalton atomic unit [Da] through using enhance all and 24-time bins to sum, dynamic background subtract, automatic collision energy, and automatic tandem mass spectrometer aggregation with the fragment intensity multiplier set to 6 and maximum aggregation set to 2 sec before resuming to the survey scan. The data acquired from this was used for the identification and measurement of proteins.

2.9.1.3. Mass spectrum data analysis, protein identification

The data were conjugated into a single identification and quantification search using the Peak Studio 8.5 [ABS Sciences] version. The software was performed for peptide identification and further processed by the Pro Group algorithm against the genome project (PRJNA183033) of *Rbx. benzoatilyticus* where protein isoform-specific measurement was adopted to trace the difference among the protein isoform expressions. The fixed guideline were as followed similar: [i] Sample type, iTRAQ 6-plex [Peptide Labeled]; [ii] Cysteine alkylation, IAM; [iii] Digestion, Trypsin; [iv] Instrument, QSTAR Elite ESI; [v] Special Factors, None; [vi] Species, *Rbx. benzoatilyticus*; [vii] Specific Processing, Quantitate, Bias Correction [viii] ID Focus, Biological changes; [ix] Database, national centre for biotechnogy information (NCBI) protein sequence of *Rbx. benzoatilyticus*; [x] Search

effort, through. The measurement of peptide mixture were significantly chosen by the Pro Group algorithm on the basis that peptide was detected with an excellent assurance level and not shared with another protein, known with a greater assurance level to measure the journalist peak region, p-value. Protein met the criteria that at least two replicated protein detected peptide with minimum 2 peptides [confident level 99 %], with one unique peptide, Probability P-value <0.05, Fold chain of <0.8 [downregulated) and >1.25 [upregulated] were measured for further analysis. Protein was normally classified according to the KEGG [Kyoto Encyclopedia of Genes and Genomics].

Results

3.0 Results

3.1 Chemotrophic growth kinetics of Rbx. benzoatilyticus

Rbx. benzoatilyticus is an anoxygenic photosynthetic bacterium (APB) which is metabolically versatile due to sophisticated growth modes catering to ever-changing environmental condition. This organism has the strategy to utilize an array of organic compounds for its photoheterotrophic growth. Rbx. benzoatilyticus can metabolize aromatic amino acid as a sole source of nitrogen, but not as a sole source of carbon. This organism can bio-transform aromatic amino acid to their corresponding metabolites, namely L-Phenylalanine to phenols, L-Tryptophan to indoles, L-Tyrosine to hydroxyphenols, and 5-OH tryptophan to hydroxy-indoles. However, these studies were largely confined to anaerobic photo-metabolism and it was interesting to understand the chemotrophic (dark aerobic) aromatic amino acid metabolism since the organism can thrive under oxic/anoxic zones under natural habitats. The present study is focused on L-Trp chemotrophic metabolism by Rbx. benzoatilyticus which produces color pigment into the culture medium during its metabolism.

3.1.1. Growth, L-Tryptophan utilization and exo-metabolites production by Rbx. benzoatilyticus

Rbx. benzoatilyticus was able to grow in the presence of L-Trp (1mM) as sole sources of nitrogen under chemotrophic (dark aerobic) conditions. While L-Trp could not support growth when used as a sole carbon source. The doubling time of cells grown with L-Trp as sole source nitrogen under chemotrophic condition was 6.06 ± 0.3 h, in comparison to malate chemotrophic grown which had a doubling time of 4.6 ± 0.34 h. Growth and concomitant utilization of L-Trp by *Rbx. benzoatilyticus* (Fig. 16A). Along with growth, simultaneously brown color exo-metabolites were accumulated in the culture

supernatant along with complete utilization of L-Trp. The brown color exo-metabolites production was a maximum of 24-36 h. L-Trp was completely consumed by the organism between 12-18 h with simultaneous accumulation of colored exo-metabolites in the culture supernatant. While the exo-metabolites production was observed only under chemotrophic (dark aerobic) conditions when supplemented with L-Trp and control conditions without supplemented L-Trp and phototrophic (light anaerobic) conditions with L-Trp color exo-metabolites production was not observed. The total indole concentration was measured from L-Trp fed and control under dark aerobic conditions by Salpher's reagent (Fig. 16B).

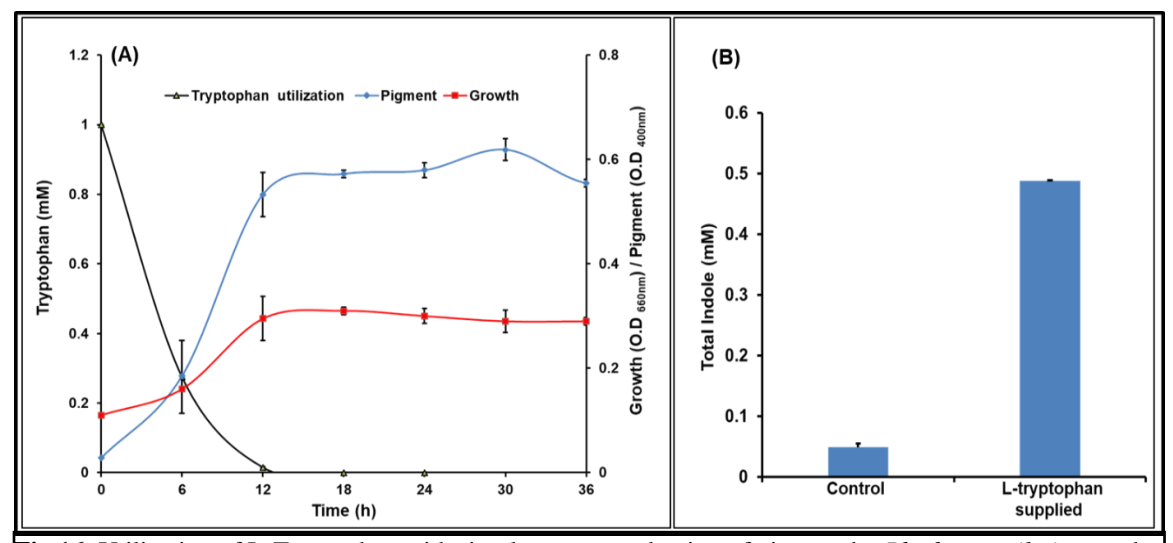


Fig.16: Utilization of L-Tryptophan with simultaneous production of pigment by *Rbx.benzoatilyticus* under chemotrophic conditions. (A) Growth, substrate utilization and pigment production.

(B) Total indoles produced under L-Tryptophan unfed (control) and fed by *Rbx. benzoatilyticus*.

of malate aroun sulture under photohetenetrophic (dark anaerobic) condition. Where mid I

Growth of malate grown culture under photoheterotrophic (dark anaerobic) condition. Where, mid-log phase culture (O.D 660 nm 0.3) was used as inoculum (10%) for the growth experiment. Growth medium was supplemented with 1mM Trp (nitrogen) and malate (carbon) sources. 2 ml of the culture was withdrawn periodically at 6 h interval and OD was recorded at 660 nm against the control (blank). Culture collected at different time point was centrifuged and the supernatant was used for pigment quantification by spectrophotometer at 400 nm. The culture supernatants of Rbx. benzoatilyticus grown with/without L-Trp at 48 h was used for the estimation of L-Trp by HPLC and total indole estimation with Salpher's reagent.

3.1.2. Identification of indole derivatives metabolites

3.1.2.1. Metabolic profiling of control and L-Tryptophan fed supernatant by using TLC and HPTLC

Culture supernatant appeared different in color between L-Trp fed and unfed (control) conditions by *Rbx*. *benzoatilyticus*. Comparative metabolite profiling of fraction-I(methanolic fraction) was subjected through the TLC (Fig. 17 A,B) and HPTLC (Fig.17 C,D,E) of both L-Trp fed and control conditions. Chromatographic analysis of fraction-I (methanolic fraction) has shown pigmented bands from L-Trp amended fraction while the same was not observed in control conditions (Fig.17 A, C). The comparative metabolite profiling analysis has shown a significant difference in metabolite profiling of L-Trp fed and control conditions. The high-performance thin-layer chromatography (HPTLC) metabolite profiling with short UV-Vis absorption has shown an array of pigmented band (Fig.17 C,D,E) compared to long UV-Vis absorption where only a few pigmented bands were observed (Fig.17E). L-Trp fed culture supernatant showed a signature of small metabolites band with short UV-Vis absorption and only a few metabolites (Fig.17E) showed long UV-Vis as shown on HPTLC profiling mainly indicating that all metabolites have indole nucleus (Fig.17 C,D,E).

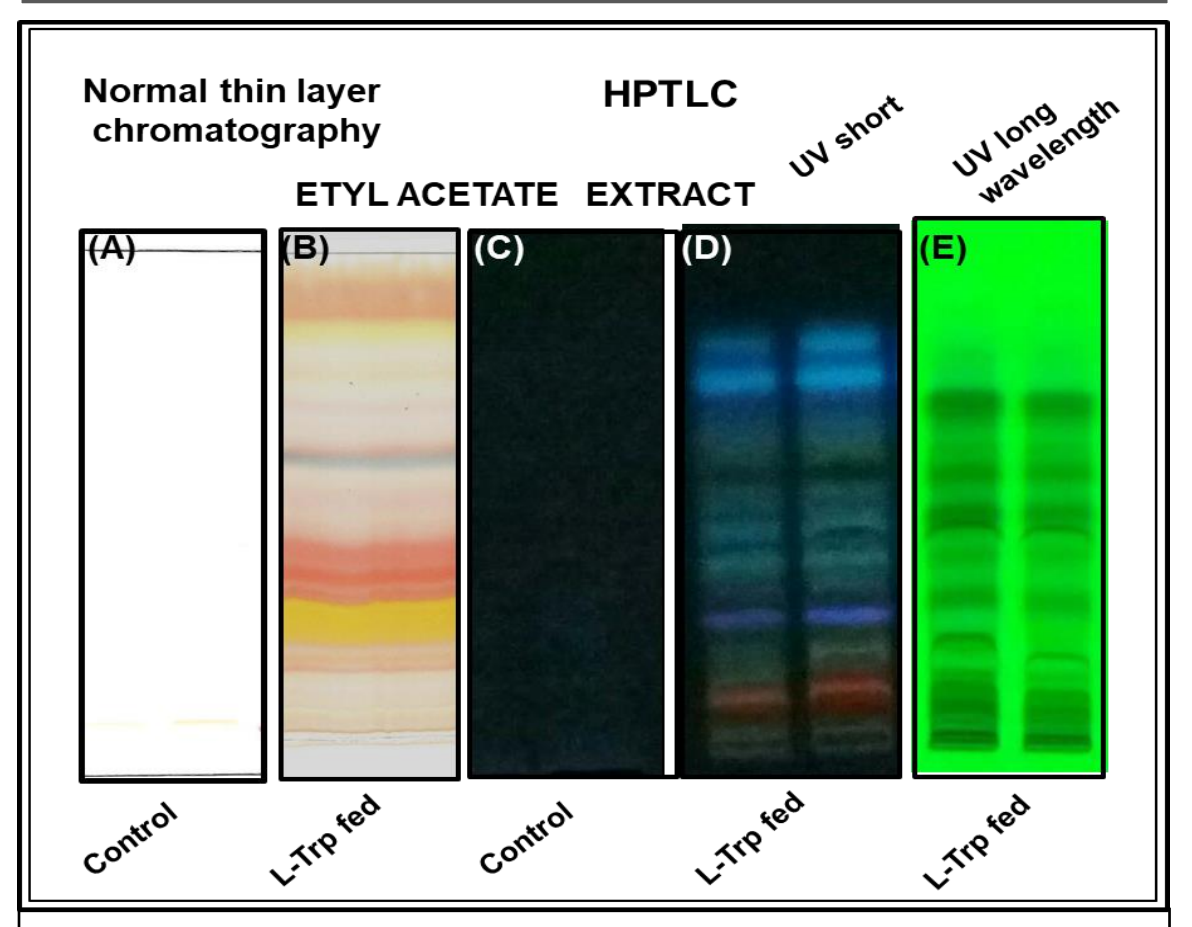


Fig. 17: Chromatogram of pigments eluted by TLC (A,B) and HPTLC (C,D,E) produced by *Rbx*. *benzoatilyticus* under chemotrophic L-Tryptophan fed and control condition. TLC; Thin layer chromatography, HPLC; High performance liquid chromatography, Control; L-Tryptophan un-fed condition.

The experimental conditions followed were same as mentioned in Fig. 16. The fraction-I (methanolic fraction) was extracted as described in section 2.3.1. Thin-layer chromatography was performed with the mobile phase chloroform: methanol: acetic acid (8:1.95:0.05 v/v) to separate the pigments in fraction-I mentioned in section 2.3.3. Purification and identification of pigments was done as per Fig. 11. The metabolite separated on TLC was exposed to the UV-Vis chamber and the image was captured.

3.1.2.2. Identification of pink and yellow pigment from a methanolic fraction

The L-Trp based pigment was purified from the fraction-1 as mention in the described (Fig. 11) as materials methods section 2.3.3. The thin layer chromatography profiling L-Trp fed metabolite analysis of fraction-I (methanolic fraction) showed an array of different color bands such as yellow, red, orange, pink-colored band (Fig.18A). Each colored band was eluted with methanol and further analysis by high-performance liquid

chromatography (HPLC). These three major pigments purified were subjected to HPLC analysis and we found a similar pattern of the absorption spectrum and retention time also not showing so significant difference (Fig. 18 B,C,D). The HPLC analysis of purified pigment might be the same molecular polarity but different chemical structures reveal similar isoforms i.e not much difference retention time as well as absorption spectrum. Two peaks were eluted, one at 20.00 min and the other at 20.9 min which had UV-Vis absorption at 270, 280, 290 and 450-550 nm respectively, as representative of pigment-1(yellow) and pink pigment-2 (Fig.18 B,C, D).

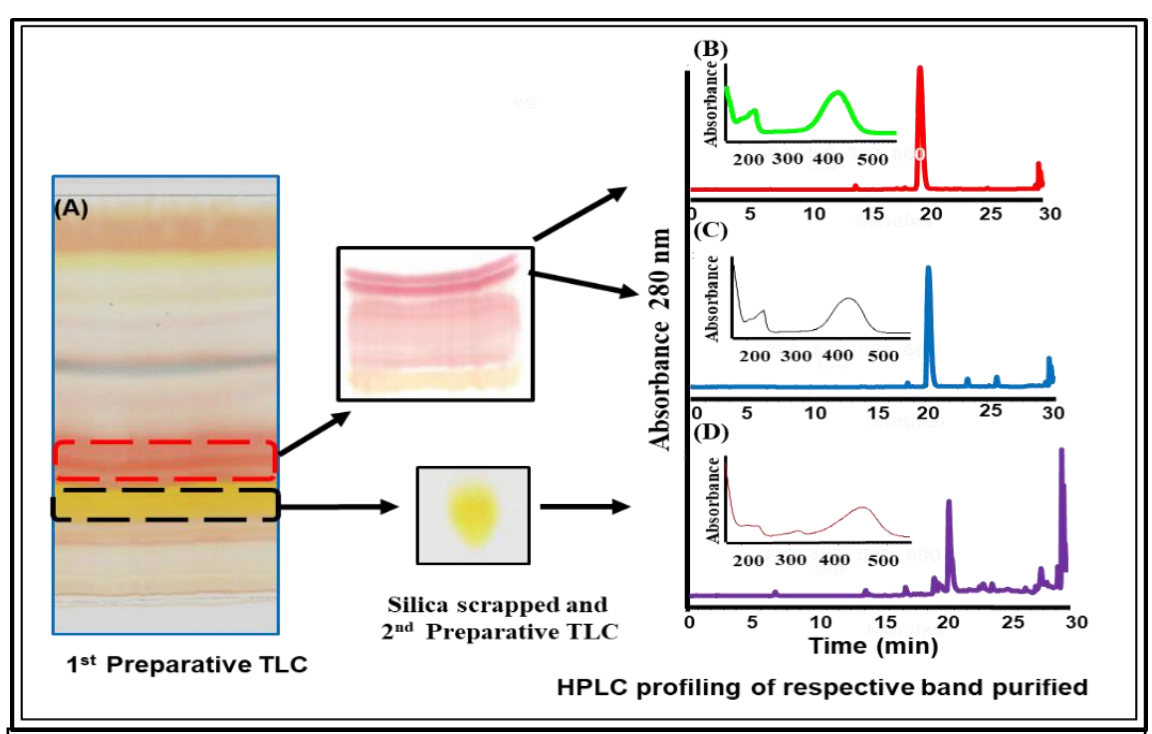


Fig. 18: Identification of TLC eluted metabolites through HPLC. TLC; Thin layer chromatography, HPLC; High performance liquid chromatography

The experimental conditions were same as mentioned in Fig. 16 and the methanolic extraction was done as described in the Fig. 9/ section 2.3.2. Thin-layer chromatography was performed through the mobile phase chloroform: methanol: acetic acid (8:1.95:0.05 v/v) to separate the pigments in fraction-I (methanolic fraction).

3.1.2.3. Mass spectral analysis of yellow pigment (yellow-1)

Furthermore, Mass spectral analysis of purified yellow pigment was performed to characterization. The purified pigments was subjected to LC-MS analysis while only yellow pigment metabolite ionized. Wherein pink color metabolites were not ionized. The purified yellow pigment was ionized under negative mode the molecular ionized mass was 358 [M⁻] having the UV-Vis absorption maxima 270, 280, 290 and 450-550 nm showed with similarity to trisindole like compound (Fig. 19).

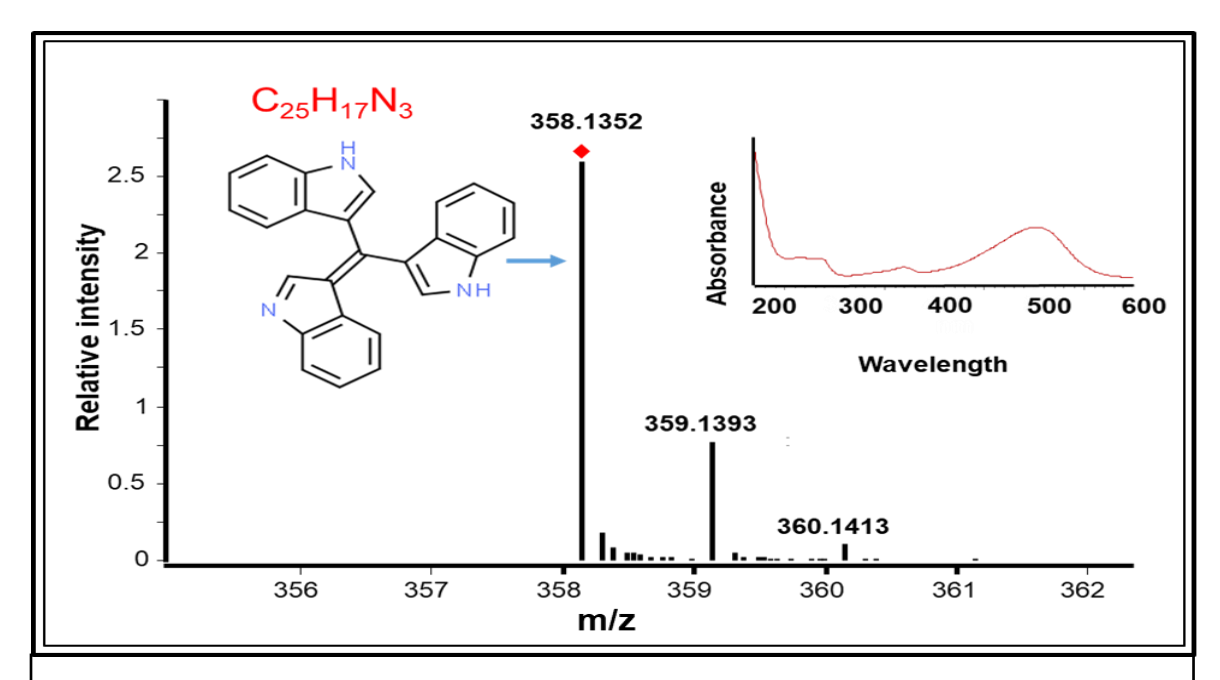


Fig. 19: m/z spectrum of purified yellow pigment and its chemical structure.

Mass spectra of pure yellow pigment. The experiment was performed as mentioned in Fig. 16. The LC-MS analysis of purified yellow pigment was done as per sections 2.4.3.

3.1.2.4. Comparative metabolite profiling of L-Tryptophan fed and control conditions by using HPLC

Chromatogram represented in green color: control (without L-Trp) and with red color: experiment (with L-Trp) peak may labeled with asteric mark was present only in L-Trp fed under chemotrophic conditions. The experimental condition parameter were as

mentioned in (Fig. 16). The metabolites were analyzed using the absorption spectrum near UV-Vis absorption at 280 nm. The 18 asteric labeled metabolites peaks were externally observed when fed with L-Trp condition compared to control (Fig. 20). The ethyl acetate fraction of L-Trp fed culture supernatant of *Rbx. benzoatilyticus* was taken further for the identification of metabolite analysis through the HPLC, LC-MS and GC-MS/MS analysis.

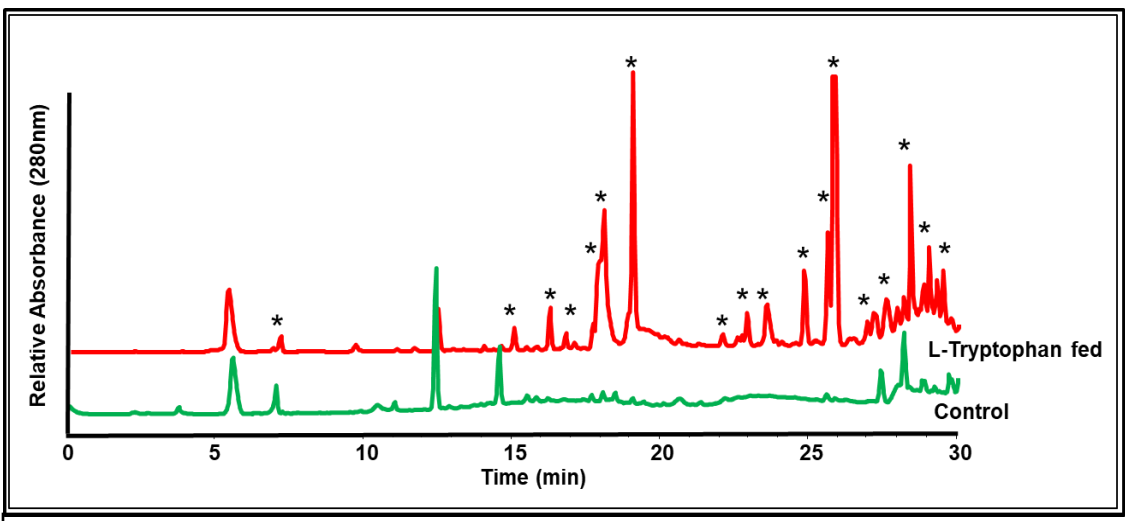


Fig. 20: Comparative metabolite profiling of ethyl acetate fractions obtained from *Rbx. benzoatilyticus* grown under the chemotrophic condition with L-Tryptophan fed and unfed (control) conditions.

HPLC profiling of ethyl acetate fractions extracted from acidified culture supernatants of control (L-Trp un-fed) and L-Trp fed cultures of Rbx. benzoatilyticus grown under chemotrophic conditions. Peaks labeled with *mark were present only in L-Trp fed condition. The materials and methods followed were as mentioned in Fig. 16 except for the ethyl acetate extraction. The ethyl acetate extracts were used for metabolites profiling. HPLC conditions were as mentioned in the materials methods section 2.4.2.

3.1.2.5. HPLC and LC-MS/MS-based metabolites identification of ethyl acetate fraction of L-Tryptophan fed culture supernatant by Rbx. benzoatilyticus

The ethyl acetate extracted fraction of L-Trp fed culture supernatant by *Rbx*. benzoatilyticus was analyzed through the using HPLC and LC-MS/MS to identify the targeted and untargeted exo-metabolites. The targeted metabolites were identified through the HPLC analysis of photodiode an array of detectors based on the retention time and absorption spectrum. Whereas, the LC-MS analysis was performed to identify the metabolites based on the mass spectrum and fragmentation pattern concerning the authentic

standard obtained from the Database like such as Metlin (http://metlin.scrips.edu). Mass bank (http://www.massbank.jp), Human Metabolome Database (http://www.hmdb.ca). The identified metabolite was further validated by co-eluting with authentic reference standards.

The peak at retention time [R_{t.}] 15 min has a molecular ion mass of 137[M⁻] with absorption spectrum at 254 nm (Table. 1) it was identified as 4-hydroxybenzoic acid (4-HBA). Similarly, metabolites eluted at R_t.17.75 min molecular ionized mass 188 [M⁻] with absorption 260, 310 nm. It was identified as kynurenine based on databased (Table. 1) and co-eluted with an authentic standard. The peak at R_{t.} 22.4 min the molecular ionized mass 190[M⁻] having absorption with a maximum of 260, 300 nm. It was putatively identified as methoxy-indole-3-carboxaldehyde /5-hydroxy-indole acetic acid [5-OHIAA] (Table. 1). Metabolite eluted at R_{t.} 21.4 min molecular ionized mass 190[M⁻] having absorbance maxima at 290 nm which was identified as hydroxy-indole-3-acetic acid coeluted with an authentic standard. The peak at R_t 26.4 min molecular ionized mass 160 [M⁻] having absorbance maxima at 280 nm was identified as indole-3-carboxylic acid. The signal R_t at 28.4 min molecular ionized mass 144 [M⁻] having the absorption spectrum at 280 nm which was identified as indole-3-carboxaldehyde and co-eluted with an authentic standard. A total of 16 metabolites have been identified from the ethyl acetate fraction of L-Trp fed culture supernatant by using LC-MS based profiling when compared to control condition whereas the majority of metabolites were L-Trp derivatives (Table. 1).

Table. 1: Indoles identified from the exometabolites of L-Trp fed cultures of *Rbx. benzoatilyticus*.

S.no	R _{t.} (min)	Generated Formula	Exact mass	Ionized m/z	Mass accuracy (ppm)	Absorbance [y]	Name of the metabolites
1	17.75	$C_{10}H_7NO_3$	189	188	-4.43	260,310	Kynurenine
2	18.3	$C_{10}H_9NO_2$	175	174	-1.21	270,278,288	UN
3	22.4	$C_{10}H_9NO_3$	191	190	- 0.41	260 310	Methoxy indole-3- carboldehde
4	22.1	$C_{10}H_{10}N_2O$	174	173	-1.7	270, 278,287	Indole-3-acetamide
5	21.4	$C_{10}H_9NO_3$	191	190	-1.82	275	OH indole-3-acetic acid
6	24.8	C ₁₀ H ₉ NO ₂	175	174	- 1.99	240, 260 300	methoxy3methyl carboxldehde tentative
7	25.38	$C_{15}H_{15}N_3O_4S$	333	332	-0.5	270,278,285	UN
8	25.79	$C_{18}H_{12}N_2O_2$	288	287	1.34	280 ,288	2,2'-bis[1H-indole-3- carbaldehyde
9	26.5	$C_9H_7NO_2$	161	160	1.5	280	Indole-3-carboxylic acid/3 formyl 6 OH indole
10	26.7	$C_{10}H_8N_2O_2$	188	187	2.0	300, 325,274	UN
11	28.4	C ₉ H ₇ NO	145	144	-1.2	240,260,290	Indole-3-carboxyldehyde
12	29.3	$C_{10}H_{10}NO_2$	175	174	-0.69	270,278	Indole-3-acetic acid
13	35.5	$C_{11}H_9NO_3$	203	202	-0.3	260,268,320	2-indole-3-oxopropinic acid (tent)
14	40.3	$C_{11}H_{11}NO_2$	189	188	-0.07	280,288	Indole-3-propionic acid
15	40.9	$C_{17}H_{12}N_2O$	260	259	-3.0	288,279,272	Di-indole-2-ylmethanone indole
16	21.9	$C_{10}H_{10}N_2O$	174	173	-1.2	270,278,287	Indole-3-acetaldehyde oxime

Metabolites italicized are confirmed by using authentic standards—retention—time, fragmentation pattern and compared with available databases. The metabolites identified putatively are based on certain parameters, such as generated molecular formula, absorption spectrum of metabolites and ionized molecular mass compared with databases. Metabolites, UN; unidentified; R_t retention time. Neg.;(-ve) ionization mode, Pos.; (+ve) ionization mode.

3.1.2.6. GC-MS analysis of L-Tryptophan fed culture supernatant by Rbx.benzoatilyticus

The culture supernatant was obtained from the L-Trp fed by *Rbx*. *benzoatilyticus* under chemotrophic (dark aerobic) conditions was dried by using the rotatory evaporator and extracted in methanol. The methanolic extracted fraction derivatized with BSTFA (Sigma Aldrich) reagent was subjected to gas chromatographymass spectrometric (GC-MS) analysis to identify the volatile aromatic intermediary biotransformed of L-Trp derivatives metabolites. The metabolites were identified by comparing the mass spectra of the authentic standard obtained from the National Institute of Standard and Technology [NIST] Library. Gas chromatography fragmented mass chromatogram was represented by the peak at R_t. 9.0 min with a mass of 191 m/z identified as 5-hydroxyindole-3-acetic acid (Fig. 21B) and another peak at R_t. 8 min with mass 220[M⁻] identified as 5-hydroxytryptophan (Fig. 21A) derivatized mass respectively and metabolites were identified as respectively.

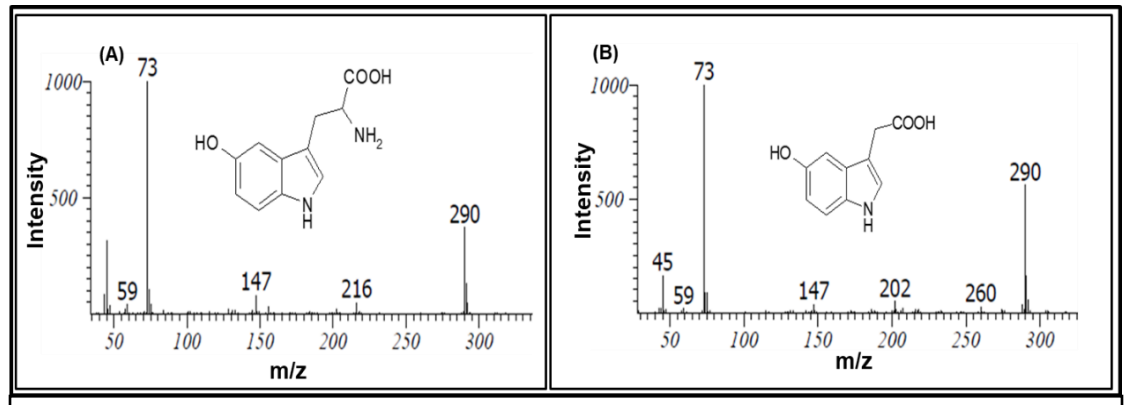


Fig. 21: GC-MS analysis of BSTFA derivatized exometabolites of L-Tryptophan fed *Rbx*. *benzoatilyticus* under the chemotrophic condition.

The experiment was performed as mentioned in Fig. 16 except for the GC-MS analysis. Samples were derivatized with BSTFA; TMCS and subjected to GC-MS analysis as mentioned section 2.4.4. Metabolites were identified by comparing the mass spectra with NIST library 5-hydroxytryptophan (5-OH Trp), 5-hydroxyindole-3-acetic acid (5-OHIAA).

3.1.2.7. LC-MS based exo-metabolite profiling of L-Tryptophan fed chemotrophic cultures

LC-MS based exo-metabolite profiling was carried out to identify the L-Trp derivatives metabolites of chemotrophic (dark aerobic) condition L-Trp metabolism and potential immediate precursor/intermediates of pigment biosynthesis. Typical total ion chromatogram of methanolic extracts of chemotrophic L-Trp fed culture supernatants represented here showing the elution profile of the L-Trp derived metabolites (Fig. 22A). LC-MS analysis of a methanolic extract of chemotrophic L-Trp fed culture supernatants revealed metabolite showing identical UV-Visible profile, peak at R_t7.9 mins having a molecular ion mass of 219.0778 [M⁻] corresponding to 5-hydroxytryptophan (5-OH Trp) (Fig. 22A). Metabolite with R_t 14.3 min also showed identical UV-Visible spectrum and molecular ion of the mass of 190.0509 [M⁻] corresponds to 5-hydroxyindole-3-acetic acid (Fig. 22A). Subsequently, metabolites with R_t 7.9 min and 14.3 min were confirmed as 5-OH Trp and 5-hydroxyindole-3-acetic acid by co-eluting with authentic standards. Metabolites with R_{t.} 10.9, 15.5, and 16.3 mins having molecular ion masses of 206.04 [M⁻], 218.04[M⁻], and 147.06[M⁻], were putatively identified as 5,6-dihydroxyindole-3acetic acid (DHIAA), 5-hydroxyindole-3-pyruvate (HIPy), and 5-hydroxy-methyl-indole (HMI) (Fig. 22A) respectively based on mass spectra search against database hit, and UV-Visible profiles.

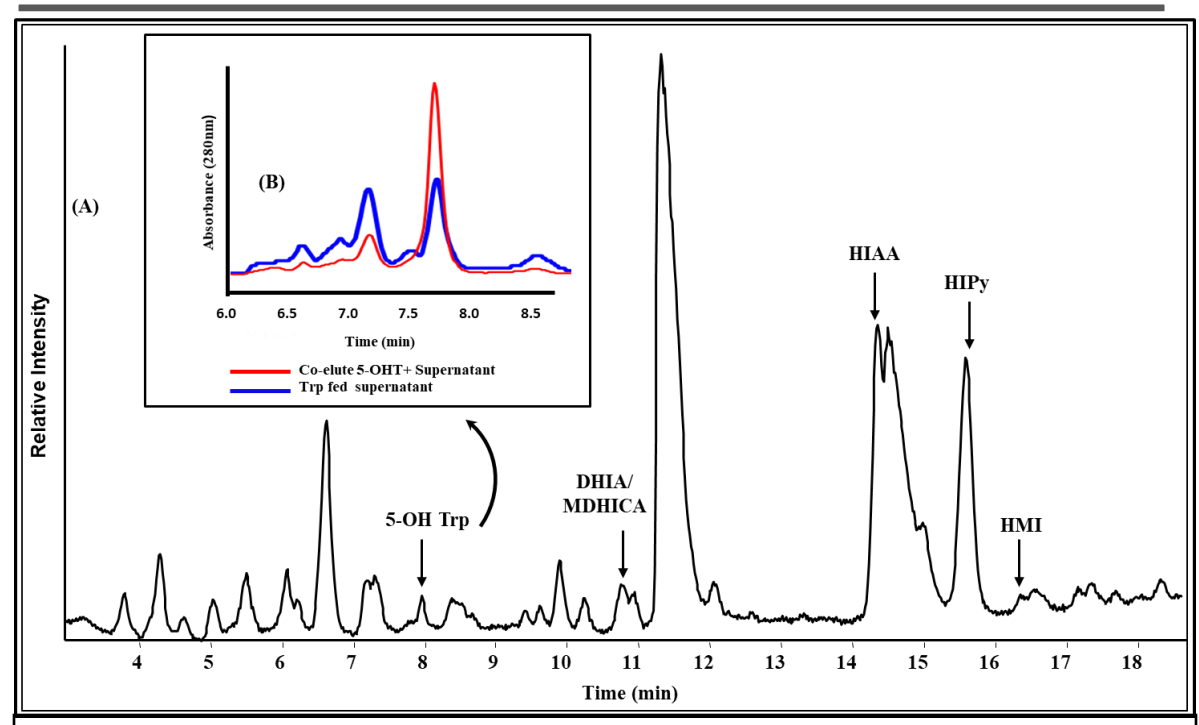


Fig. 22:LC-MS analysis of methanolic extract of L-Tryptophan fed exometabolites of *Rbx.benzoatilyticus* under chemotrophic condition. 5-OH-Trp; 5-hydroxytryptophan, DHIA; dihydroxyindole aldehyde, DHICA; Methoxy- dihydroxyindole-3-carboxylic acid, HIAA; hydroxy-indole-3-acetic acid, HIPy; hydroxy-indole-3-pyruvic acid, HMI; hydroxymethy-indole, Trp; L-Tryptophan (Inserted chromatogram of co-eluted sample with standard 5-OH Trp.

Experimental conditions followed were similar as mentioned in Fig. 16 and the methanolic extract was obtained as described in section 2.3.4. The liquid chromatography and mass spectrometry was performed by using mobile phase Pump A: water with 0.1% acetic acid and Pump B 100% acetonitrile.

3.2. Stable isotope metabolite profiling (SIMP) of L-Tryptophan fed chemotrophic cultures of *Rbx. benzoatilyticus*

3.2.1. SIMP analysis of $[^{13}C_{11}]$ L-Tryptophan fed cultures of Rbx. benzoatilyticus

Stable isotope analysis helps in differentiating metabolites produced by cells from the externally fed processor to those of *de novo* generated. For these studies, labeled L-Trp ¹³C₁₁ feeding experiments were performed with *Rbx. benzoatilyticus* followed by stable isotope metabolite profiling using LC-MS. Cells were grown separately under dark aerobic (chemoheterotrophic) conditions fed with unlabeled [¹²C₁₁] and labeled [¹³C₁₁] L-Trp [1mM] for the desired period. The total ionization chromatogram [TICs] (Fig. 23A) of L-Trp derived metabolites were identified based on mass shift between unlabeled *vs* labeled with a mass difference of [M+N], whereas N is +8, +9, +10, +11, +16, +17, +18, +19, +26 units as isotopologues. The raw data files were analyzed for stable isotopes by comparing the unlabeled and labeled metabolites that have similar R_t and the peak intensity between unlabeled *vs* labeled was equal or with a difference of not less than fifty percent.

Through SIMP metabolite profiling, we could detect seventy metabolites from L-Trp fed cultures of *Rbx. benzoatilyticus* when cultivated under chemotrophic (dark aerobic) conditions. The metabolites had an increment in mass units by [M+N], whereas N is +8, +9, +10, +11, +16, +17, +18, +19, +26 compared to unlabeled L-Trp (Table. 2). The higher number of metabolites were detected under negative ionization mode compare to positive ionization mode, while a few metabolites were ionized under both ionization modes (Fig. 23C). Further, the mass distribution profiles of the majority of the metabolites indicate that these are middle polar (Fig. 23B). Twenty-six metabolites were identified with +10 m/z mass increment [M+10], nine with +16 m/z [M+16] and eight with +18 m/z

[M+18] unit mass (Table. 2) which could represent as indole dimers. Similarly, metabolites with a mass increment by +26 m/z [M+26] represent indole trimers. Among the seventy metabolites detected through SIMP, some of these were confirmed with co-elution using standards, some of which were putatively annotated based on the mass fragmentation pattern and the remaining were unidentified (Table. 2).

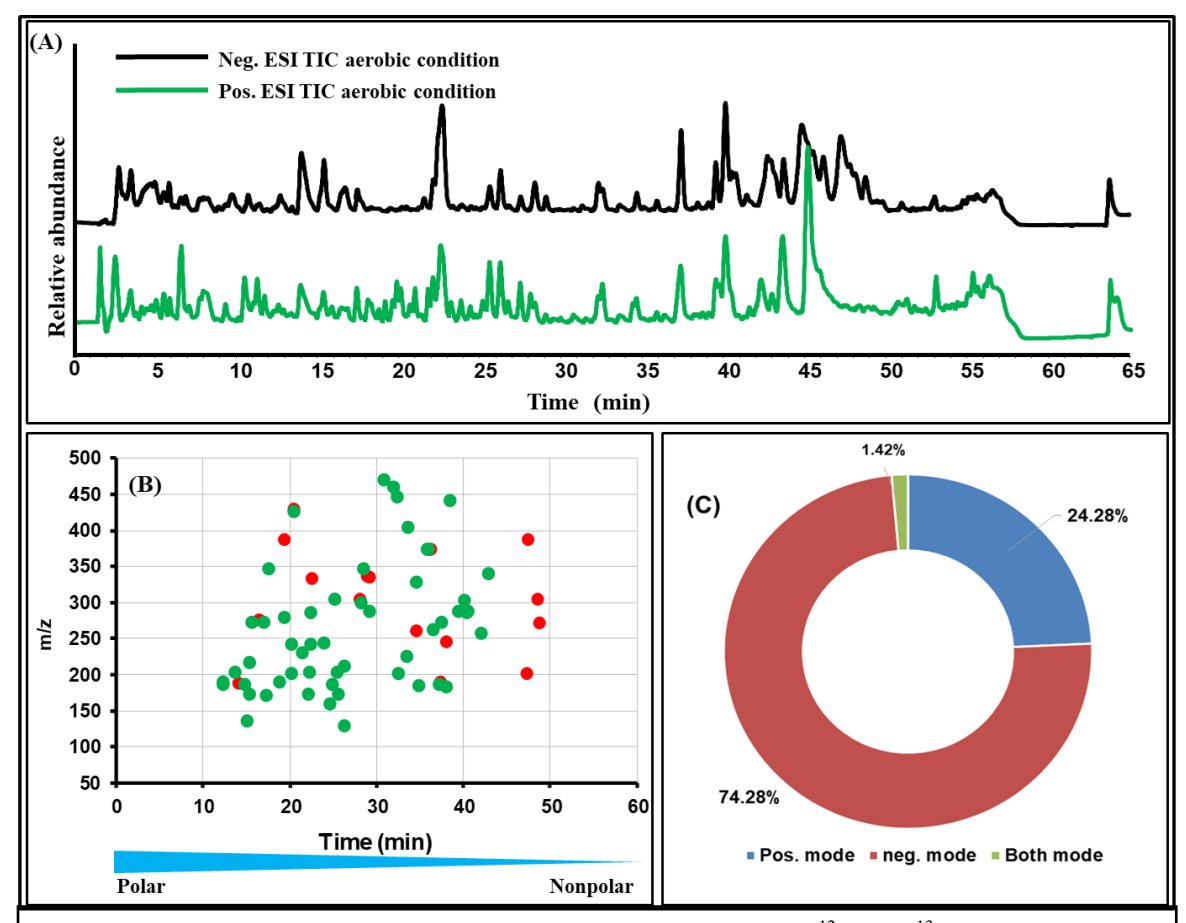


Fig. 23: Total ion chromatograms of ethyl acetate extracted fraction from ¹²C₁₁ and ¹³C₁₁ of L-Tryptophan fed culture of *Rbx. benzoatilyticus* under chemotrophic condition (A). m/z vs time plot of total labeled metabolites features under chemotrophic conditions (B). Pie chart illustrating the L-Tryptophan derivatives metabolites ionized under Pos. and Neg. modes (C). Pos. (+ve) ionization mode; and Neg. (-ve) ionization mode.

3.2.2. Identification of indole footprints of $[^{13}C_{11}]$ L-Tryptophan fed cultures of Rbx. benzoatilyticus

Peak eluted at R_t 12.29 min under negative mode [M⁻] has a molecular ionized mass of 190 m/z for unlabeled and 200 m/z for labeled having an increment of 10 m/z units [M⁻+10] with absorption maxima at 275,300 nm and is identified as 5-hydroxyindole acetic acid (5-OH IAA) (Table. 2). Whereas peak at R_t, 14.77 min for unlabeled had a mass of $188 \text{ m/z} [\text{M}^-]$, labeled $198 \text{ m/z} [\text{M}^-]$ with $+10 \text{ m/z} [\text{M}^-+10]$ absorption spectrum at 265, 395 nm, it was identified as kynurenic acid (Table. 2). The peak at R_t 15.3 min had a mass unlabeled of 174 m/z [M⁻] vs labeled 184 m/z [M⁻] with +10 m/z [M⁻+10] increment and absorption maxima at 272, 278, 290 nm was identified as 5-hydroxyindole-3-acetaldehyde (Table. 2). A peak at R_{t.} 20 min had a molecular ionized mass of 137 m/z [M+0] with an absorption maximum at 254 nm and the metabolite was identified as 4-hydroxybenzoic acid (4-HBA) (Table. 2). Peak eluted at R_{t.} 22.3 min with molecular ion mass under positive mode for unlabeled was 287 m/z [M⁺], while the labeled had an ionized mass of 305 m/z [M⁺] with an increase of +18 m/z [M⁺+18] and absorption maxima 270, 280, 290 nm was identified as diindole ethane dione [Fig. 24C]. Peak eluted at R_{t.} 26.3 min for unlabeled had a molecular ionized mass of 130 m/z [M⁻] and for a labeled molecular ion mass of 139 m/z [M⁻] showing an increase of +9 m/z [M⁻+9] with absorption maxima at 270, 280, 290 nm is similar to skatole (Table. 2). A peak at R_t. 28 min under negative mode had molecular ionized mass for unlabeled 174 m/z [M+0] and labeled 184 m/z [M+10] with absorption maxima at 270, 280 and 290 nm was identified as a indole-3-acetic acid (Table. 2).

Peak at R_t . 28 min under positive ionized mode for unlabeled had a mass of 301 m/z [M⁺] and labeled had a mass of 317 m/z [M⁺] showing +16 units mass increase [M⁺+16],

absorption maxima at 270, 290, 310 and 430-530 nm with symmetrical chromatographic spectrum was identified as an indole dimer [Fig. 24D]. Peak at R_t. 38 min for unlabeled had an ionized mass of 245 m/z [M⁺] and for labeled 261 m/z [M⁺] showing with +16 m/z increment [M⁺+16], absorption maximum at 270, 280, 290 and 320 nm [Fig. 24A] was identified as 3,3-diindolylmethane. Peak at R_t. 47.29 min unlabeled had a mass of 388 m/z [M⁺] vs labeled 414 m/z [M⁺] with an increment of +26 m/z [M⁺+26], absorption maxima at 270, 280, 290 and 450-550 along with symmetric chromatographic spectra was identified as trisindolate (Fig. 24D).

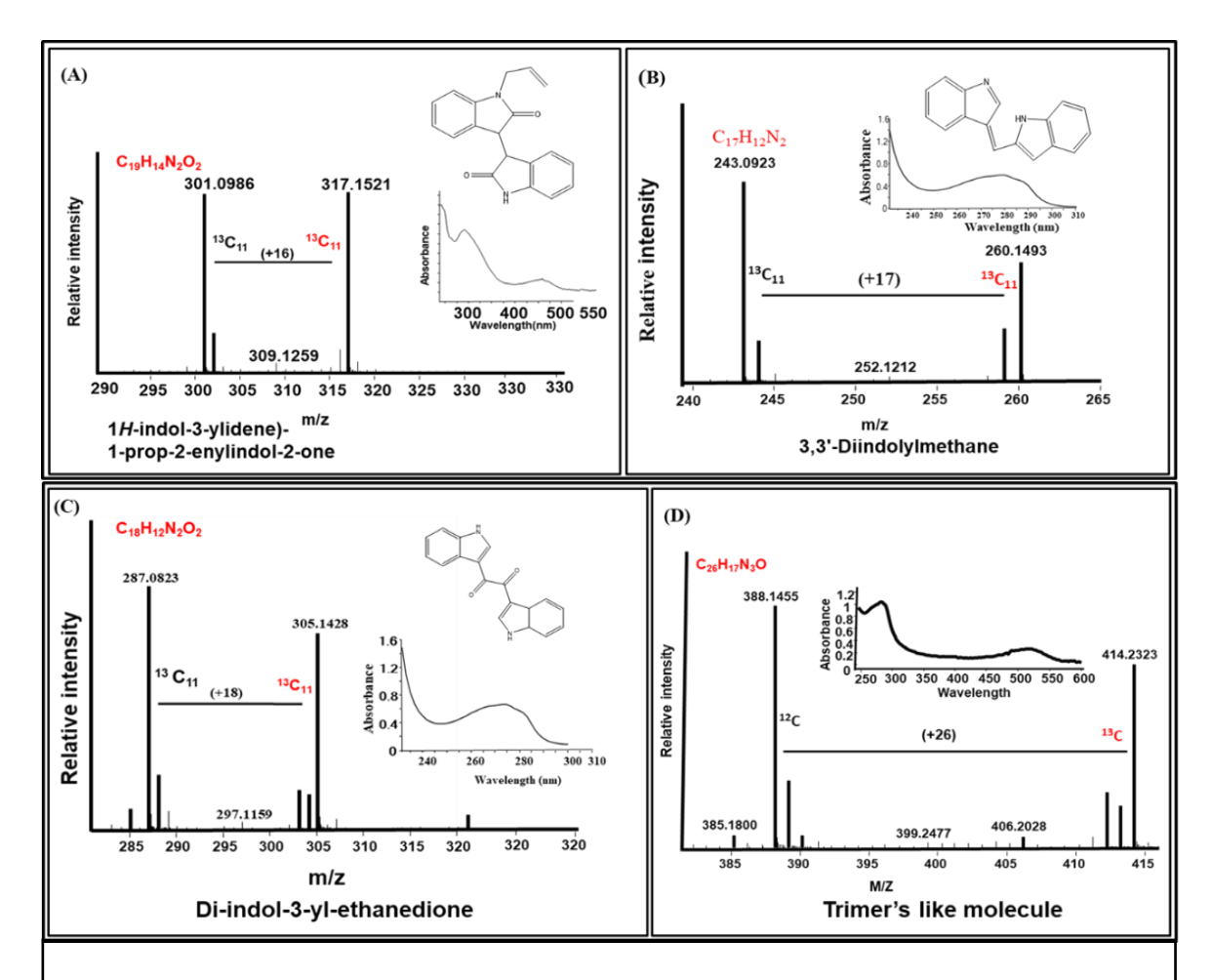


Fig. 24: Identification of a few exo-metabolites based on mass spectrum and absorption maxima as represented by stable isotope labeled indole derivatives having increase in molecular mass (m/z; M) by M+16, 17, +18 and M+26.

Table. 2: Labeled and unlabeled exometabolites identified from L- 13 C₁₁Trp fed cultures of *Rbx. benzoatilyticus*.

6		Generated Mol. Formula	Exact mass	m/z		UV- visible	Management	
S.no	$\mathbf{R}_{t.}$ (min)			Neg. [M-]	Pos. [M ⁺]	spectrum[y]	Mass Accuracy (ppm)	Identification of metabolites
1	12.26	C ₁₀ H ₇ NO ₃	189	188 198 (+ 10)		245,330,350	0.83	UN
2	12.29	C ₁₀ H ₉ NO ₃	191	190 200 (+ 10)		260,280	UN	UN
3	13.6	C ₁₀ H ₇ NO ₄	205	204 214 (+ 10)		265,310	-1.54	Xenthurenic acid/OH- KYN
4	14.06	$C_{12}H_3N_3$	189	188 198 (+ 10)	188 198 (+ 10)	260,305	-6.26	UN
5	14.77	$C_{10}H_7NO_3$	189	188 198(+10)		265,305	0.72	Kynurenic acid
6	15	C ₇ H ₉ O ₃	138	137 137 (+ 0)		254	2.47	Hydroxy benzoic acid
7	15.3	$C_{10}H_8NO_2$	175	174 184(+10)		272,278,290	3.17	5-OHindole-3- acetaldehyde
8	15.3	$C_{11}H_9NO_4$	219	218 229(+11)		272,278,290	4.14	OH-IPyA
9	15.6	$C_{14}H_{14}N_2O_4$	274	273 284(+11)		280,290	-2.45	1xi,3S)-1,2,3,4-Tetrahydro- 1-methyl-beta-carboline- 1,3-dicarboxylic acid
10	16.4	C ₁₀ H ₁₃ NO ₈	275		276 284 (+ 8)	280,290	-3.53	UN
11	16.9	C ₁₄ H ₁₃ NO ₅	275	274 282 (+ 8)		270,280,288	7.54	UN
12	17.2	C ₈ H ₁₄ NO ₃	173	172 189 (+ 7)		270,280,290	0.24	UN
13	17.5	C ₁₈ H ₁₁ N ₃ O ₅	349	348 358 (+ 10)		270,280,288	-4.5	UN
14	18.74	$C_{10}H_9NO_3$	191	190 200 (+1 0)		260,280	4.3	OH IAA
15	19.29	C ₁₀ H ₁₉ NO ₈	281	280 289 (+ 9)		270,280,290	9.9	UN
16	19.38	C ₂₄ H ₉ N ₃ O ₃	387		388 398 (+ 10)	270,320	4.91	UN
17	20.1	$C_{13}H_{12}N_2O_3$	244	243 251(+11)		280,290	4.96	UN
18	20.14	$C_{11}H_{12}N_2O_2$	204	203 214 (+ 11)		280,290	7	3-Amino-3-(1H-indol-3- yl)propanoic acid
19	20.4	C ₁₈ H ₂₃ NO ₁₁	429	428 438 (+ 10)		270,280,290	1.49	UN
20	20.48	C ₂₃ H ₁₅ N ₃ O ₆	429		430 440 (+ 10)	280,280,350-450	-0.91	UN
21	21.33	C ₁₂ H ₁₂ N ₂ O ₃	232	231 231(+ 0)		275	2.34	UN
22	22.2	$C_{II}H_{II}NO_3$	205	204 215(+11)		272,280,290	-1.2	Indole-3-lactate
23	22.3	C ₁₈ H ₁₂ N ₂ O ₂	288	287 305 (+ 18)		272,278,290	2.32	Di-indol-3-yl-ethanedione
24	22.4	$C_{17}H_{12}N_2$	244	243 260(+17)		272,278,290	-0.93	T 3-(3H-Indol-3-ylidenemethyl)-1H-indole
25	22.04	$C_{10}H_9NO_2$	175	174 184(+10)		260,290,300	-0.05	5-OH indole aldehyde
26	22.55	$C_{21}H_7N_3O_2$	333		334 344 (+ 10)	270,280,290	-1.42	UN

Results

27	24.5	C ₉ H ₇ NO2	161	160 169 (+ 9)		285	2.5	Indole-3-carboxylic acid
28	24.8	$C_{10}H_8N_2O_2$	188	187 197(+10)		270,320	4	3-Indoleglyoxamide
29	25.06	$C_{18}H_{28}N_2O_2$	306	305 323 (+ 10)		260,400	-7.26	UN
30	25.4	C ₁₁ H ₁₁ NO ₃	205	204 214 (+ 10)		260,300	5	5-Me-O-Indole lactate
31	25.49	C_9H_7NO	145	144 153(+9)	146 155(+9)	245,260,300	-0.85	Indole carboxyldehyde/formyl indole
32	26.2	$C_{10}H_9NO_2$	175	174 184 (+ 10)		272,278,290	1.33	Indole-3-acetic acid
33	26.23	C ₉ H ₉ N	131	130 139 (+ 9)		272,280,290	1	Skatole
34	26.23	C ₁₃ H ₁₁ NO ₂	213	212 220 (+ 8)		272,278,290	1.5	1-Phthalimido-4-pentyne
35	28.06	$C_{15}H_{14}N_2O_5$	304		303 319(+16)	270,288,290	5.25	UN
36	28.18	$C_{19}H_{14}N_2O_2$	302	301 317 (+ 16)		270,290,310,430- 530	1.47	Isotein dimer
37	28.4	C ₂₃ H ₁₁ NO ₃	349	348 358 (+ 10)		260,270,,320	1.57	UN
38	28.9	$C_{22}H_{10}N_2O_2$	335		335 354(+19)	280,290,300	-1.77	UN
39	29.1	$C_{18}H_{14}N_2O_2$	290	289 307 (+ 18)		275,290,305	1.27	3-(2-Phthalimidoethyl) indole
40	29.12	$C_{21}H_{10}N_4O$	334		335 354 (+ 19)	280,290,300	5.75	UN
41	30.8	C ₂₂ H ₂₃ N ₃ O ₉	473		474 492 (+ 18)	272,278,290	5.25	UN
42	31.88	$C_{25}H_{22}N_2O_7$	462	461 477 (+ 10)	, , , ,	270,280,285,305		UN
43	32.27	$C_{19}H_{20}N_4O_9$	448	447 465 (+ 18)		270,280,290	4.68	UN
44	32.5	$C_{11}H_9NO_3$	203	202 212(+10)		208,272,288	1.35	Indole-3-pyruvic acid
45	33.4	C ₁₃ H ₉ NO ₃	227	226 236 (+ 10)		280,285,310	2.23	UN
46	33.56	C ₂₃ H ₂₂ N ₂ O ₅	406	405 421 (+ 16)		284,290,310	-1.35	UN
47	34.5	$C_{21}H_{18}N_2O_2$	330	329 345 (+ 16)		272,278,290	0.35	UN
48	34.57	C ₁₆ H ₇ N ₃ O	259		260 266 (+ 8)	270,280,290	-10.3	UN
49	34.8	C ₁₁ H ₉ NO ₂	187	186 197 (+ 11)		272,278,280,290	4.5	Indole-3-acrylic acid
50	35.8	C ₂₂ H ₂₀ N ₂ O ₄	376	375 391 (+ 16)		272,278,280,290	4.95	1H-Isoindole-1,3(2H)- dione,2,2'-(1,6- hexanediyl)bis
51	35.9	$C_{22}H_{20}N_2O_6$	376	375 391 (+ 16)		270,280,290	-1.56	UN
52	36.28	$C_{20}H_{11}N_3O_5$	373		374 593 (+ 19)	270,288,290	-5.9	UN
53	36.5	C ₁₉ H ₇ NO	265	264 272 (+ 8)		270,280,290	2.37	UN
54	37.2	$C_{11}H_{10}NO_2$	189	188 198 (+ 10)		272,280,290	5.8	3-(1H-Indol-6-yl)prop-2- enoic acid
55	37.29	C ₁₄ H ₇ N	189		190 200 (+ 10)	270,280,290	2.57	UN
56	37.4	C ₂₂ H ₁₈ N ₂ O ₄	374	373 389 (+ 10)		270,280,290	-0.58	UN
57	37.5	C ₂₂ H ₁₈ N ₂ O ₄	374	373 389 (+ 16)		272,278,282,290	-0.58	UN
58	38.015	C ₁₂ H ₁₁ NO	185	184 192 (+ 8)		280,290	1.55	3-Buten-2-one, 4-(1H- indol-4-yl)-
59	38.019	$C_{17}H_{12}N_2$	244		245	270,280,290,330	4.83	3,3'-Diindolylmethane

Results

					261(+17)			
60	38.4	$C_{25}H_{20}N_2O_6$	445	443 459 (+ 16)		270,280,290	0.43	UN
61	39.4	C ₁₈ H ₁₄ N ₂ O ₂	290	289 307 (+ 18)		272,288,290	0.01	1H-Isoindole-1,3(2H)- dione,2-[2-(1H-indol-3- yl)ethyl]
62	40.04	$C_{19}H_{16}N_2O_2$	304	303 319 (+ 16)		270,280,290	-0.53	UN
63	40.39	$C_{18}H_{12}N_2O_2$	288	287 297 (+ 10)		270,280,290,330	0.45	UN
64	40.47	$C_{18}H_{12}N_2O_2$	290	289 307 (+ 18)		270,280,290	-3.93	UN
65	41.96	C ₁₇ H ₁₂ N ₂ O	260	259 276 (+ 17)		270,280,290	1.99	H-Indol-2-one,1,3- dihydro-3-(1H-indol-3- ylmethylene)
66	42.4	$C_{21}H_{14}N_2O_3$	342	341 359(+18)		270,285,350	-1.03	UN
67	42.82	C ₁₂ H ₁₁ NO	201		202 210 (+ 8)	270,280,290	4.31	UN
68	47.29	C ₂₆ H ₁₇ N ₃ O	387		388 414 (+ 26)	270,280,290,450- 550	-5.43	Trisindole
69	47.5	$C_{19}H_{16}N_2O_2$	304		305 321 (+ 16)	278,282,290 450- 550	-1.54	UN
70	48.7	$C_{18}H_{12}N_2O$	272		273 291 (+ 18)	270,290	-3.61	UN

Metabolites italicized are confirmed by using authentic standards retention time, fragmentation pattern and compared with available databases. The metabolites identified putatively are based on certain parameters, such as generated formula, absorption maxima, and molecular ionized masses compared with databases. Metabolites UN; unidentified; not found suitable structure in databased, R_L retention time. Bold entries are the molecular ionized mass of labeled metabolites, Neg.; (-ve) ionization mode; Pos.; (+ve) ionization mode, UN; Unidentified, OHIAA; hydroxy-indole-3-acetic acid, Labeled metabolites are represented in bold

3.3. Chemotrophic metabolism of 5-hydroxytryptophan by Rbx. benzoatilyticus

While working on the chemotrophic (dark aerobic) metabolism of L-Trp, it was observed that 5-OH Trp was one of the major intermediate identified which might be the precursor for other hydroxylated indole derivatives. *Rbx. benzoatilyticus* was grown chemotrophic (dark aerobic) condition in 500 ml flask having 100 ml minimal media, supplemented with 5-OH Trp as the sole source of nitrogen. We observed that the pigment production increased to a larger extent as compare to Trp fed condition (Fig. 25 bII, III). The result revealed that 5-OH Trp chemotrophic metabolism initiated to enhance the pigment production by *Rbx. benzoatilyticus*. The brown color pigment production was only observed when *Rbx. benzoatilyticus* was grown under the chemotrophic (dark aerobic) condition when supplemented with 5-OH Trp, while under control condition, without supplemented 5-OH Trp the organism did not produce any pigment. On the other hand, the organism also did not produce any pigment under the phototrophic (light anaerobic) condition with 5-OH Trp as also observed with L-Trp.

3.3.1. Growth, 5-hydroxytryptophan consumption and pigment production by Rbx. benzoatilyticus

Rbx. benzoatilyticus was fed with 5-OH Trp and grown for 48 h under chemotrophic (dark aerobic) conditions. 5-OH Trp was completely consumed by 24 -30 h of growth and simultaneously pigment production was observed with the time period (Fig. 25A). 5-OH Trp fed culture supernatant becomes intense brown color as compared with control conditions implicating the production of exo-metabolites with simultaneous consumption of 5-OH Trp (Fig. 25A). The pigment produced in the presence of 5-OH Trp was radially precipitated on acidification followed by storage at 4°C for 2-3 days (Fig. 25bIII). The precipitated intense brown color pigment is insoluble in water as well as an

organic solvent which is predicted to be melanin like pigment (Fig. 25bIV) produced by *Rbx. benzoatilyticus* under the chemotrophic condition when fed with 5-OH Trp.

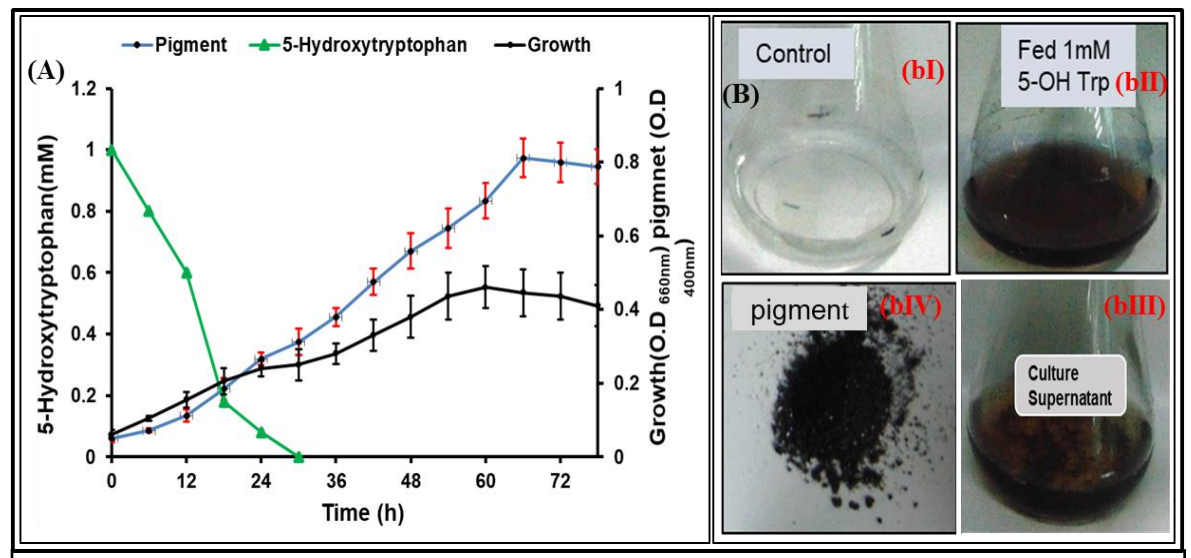


Fig. 25: (A) Growth, utilization of 5-hydroxytryptophan with simultaneous production of brown pigment by *Rbx benzoatilyticus* under chemotrophic condition. (B) Photographs showing the culture flasks of 5-OH-Trp un-fed (Control; bI), fed culture (bII), supernatant of fed culture (bIII) and purified brown pigment (bIV).

The experimental conditions followed were same as mention in Fig. 16. Cultures were grown chemotropically (dark aerobically) with nitrogen sources (ImM 5-OH Trp) and malate (carbon source). 2 ml culture was withdrawn periodically with a gap of 6 h time interval and OD was recorded at 660 nm against the control (blank). Culture collected at different time point was centrifuged and the supernatant was used for pigment quantification by spectrophotometer at 400 nm.

3.3.1.1 Exo-metabolite profiling of 5-hydroxytryptophan fed culture supernatant

Metabolites profiling of 5-OH Trp (5-hydroxytryptophan) fed culture supernatant of *Rbx. benzoatilyticus* was compared with the control (without 5-OH Trp) assayed after 48 h of from chemotropically grown cultures. The comparative metabolomics profiling of ethyl acetate fraction of both 5-OH Trp fed and control condition was done at 280 nm in HPLC. The HPLC chromatogram of ethyl acetate fraction was overlaid (red color 5-OH Trp fed and green color control) and the peak of specific to 5-OH Trp fed supernatant extract condition was asterisk marked (Fig. 26). Nearly sixteen peaks were identified from 5-OH Trp fed conditions compared to that of control (Fig. 26). The ethyl

acetate fraction of 5-OH Trp fed culture supernatant of *Rbx. benzoatilyticus* was taken further for the identification of metabolites analysis through the HPLC and LC-MS analysis.

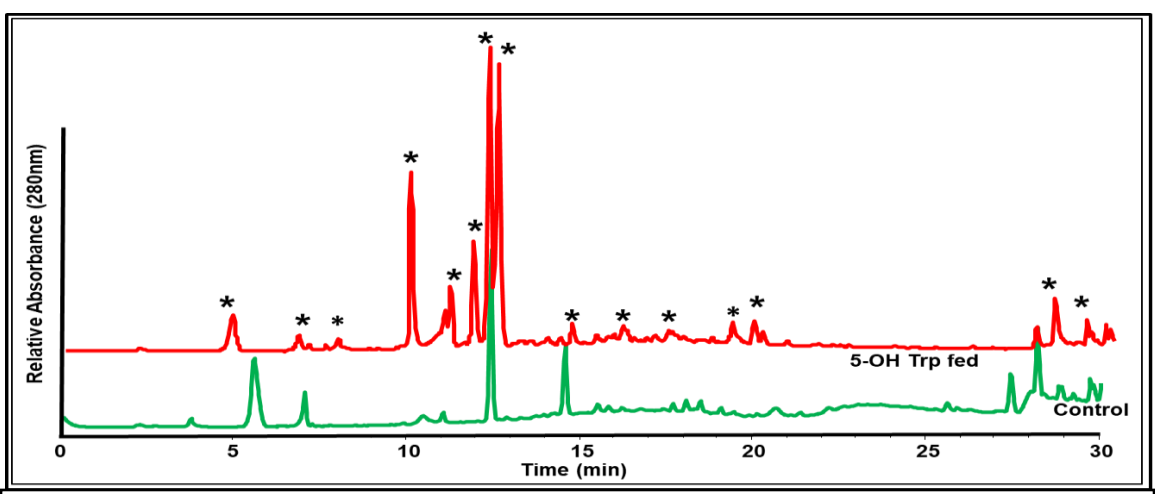


Fig. 26: Comparative metabolite profiling of ethyl acetate fractions obtained from *Rbx. benzoatilyticus* grown under chemotrophic condition with 5-hydroxytrptophan fed and un-fed (control) conditions.

HPLC spectrum of ethyl acetate fraction from acidified culture supernatants of control (without 5-OH Trp) and 5-OH Trp fed (1mM) cultures of Rbx. benzoatilyticus has grown under chemotrophic condition. Chromatograms represented in green color; control (without 5-OH Trp), red color with 5-OH Trp fed. Peaks labeled with '*' mark were present only in 5-OH Trp fed condition. Experimental condition were similar as mentioned in Fig. 16. The ethyl acetate extracts were used for metabolites profiling. HPLC conditions were as mentioned in the materials methods section 2.4.2.

3.3.1.2 Comparative exo-metabolite profiling of L-Tryptophan and 5-hydroxytryptophan fed Rbx. benzoatilyticus

The brown pigmented exo-metabolites were observed from the culture supernatants of both L-Trp and 5-OH Trp fed culture supernatants of *Rbx. benzoatilyticus* assayed under chemotrophic (dark aerobic) conditions. The comparative metabolite profiling was found the significant difference from the methanolic fraction-I (Fig. 26B) of 5-OH Trp or L-Trp derived metabolite. The methanolic fraction from L-Trp derived was observed might be the small indole containing molecule separated with the mobile phase. Whereas 5-OH Trp derived fraction might be some polymer not moving along with the solvent system it remained at the TLC on origin positions (Fig. 27B). The comparative

analysis of pigment formation in the presence of L-Trp and 5-OH Trp fed culture revealed that the brown pigment production was major quantity of yield through the 5-OH Trp (Fig. 27A and C). Whereas the L-Trp derived metabolites [indolic metabolites] could be the major fluxed L-Trp to indole derivatives metabolites and only minor quantity of yield from L-Trp possibly converted to 5-OH Trp finally transformed to brown pigment (Fig. 27C). The result suggested that might be precursor for a brown pigment in *Rbx. benzoatilyticus*.

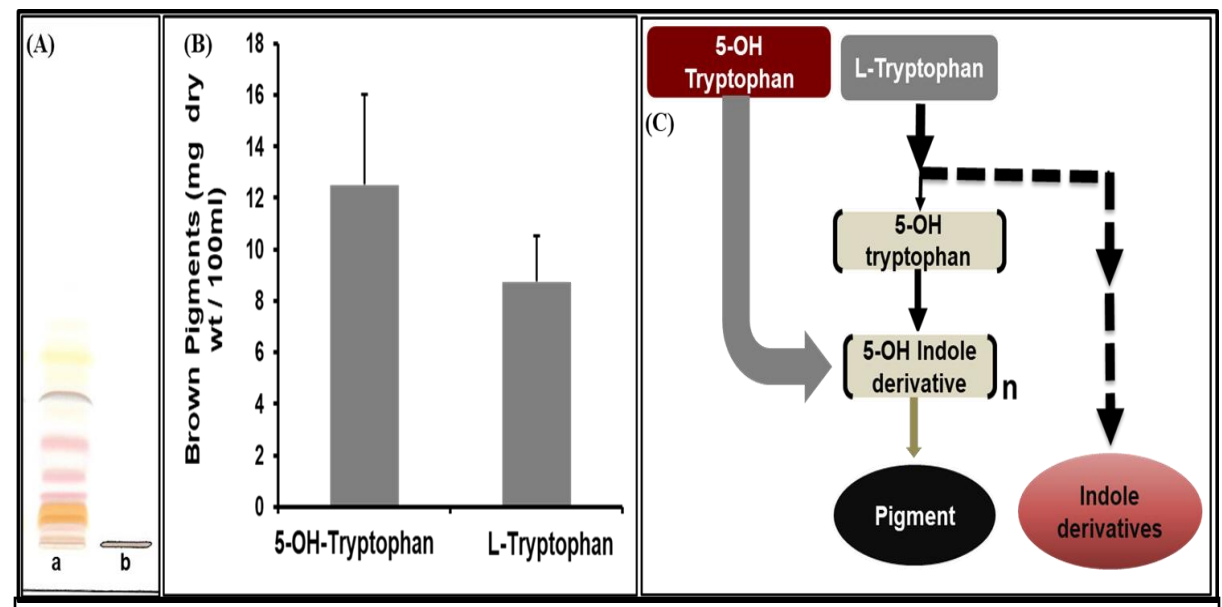


Fig. 27: (A) Chromatogram showing differences in the exometabolites of L-Tryptophan and 5-hydroxytryptophan fed *Rbx benzoatilyticus* grown under chemotrophic condition.(B) Quantitative differences in the brown pigment produced by *Rbx. benzoatilyticus* fed with L-Tryptophan and 5-hydroxytryptophan. (C) Hypothetical representation (based on the information from Fig. 27A,B) of the exometabolites produced by *Rbx. benzoatilyticus* from L-Trp and 5-OH Trp illustrating the larger role of 5-OH- Trp in the biogenesis of brown pigment, while L-Trp yields in addition other indole derivatives. Lane a, b; exometabolites of L-Trp and 5-OH Trp derivatives.

Cell cultures of Rbx. benzoatilyticus were grown chemotrophically with nitrogen (1mM 5-OH Trp or L-Trp) and malate (carbon) sources. Exo-metabolites was separated through the mobile phase chloroform: methanol: acetic acid (8:1.95:0.05 v/v) from fraction-I (methanolic fraction).

3.3.1.3. LC-MS based metabolite identification of ethyl acetate fraction of 5-hydroxytryptoptophan fed culture supernatant

The ethyl acetate extract fraction from the 5-OH Trp fed culture supernatant was analyzed by using LC-MS/MS analysis. The LC-MS analysis was done to identify the metabolites based on the mass fragmentation with the reference of authentic standard obtained from the database like Matlin (http://metlin.scripps.edu) Mass Bank (http://www.massbank.jp) Human Metabolome Database (http://www.hmdb.ca). The detected peak of 5-OH Trp derivatives metabolite further confirmed by co-eluting with an authentic standard and the majority of the metabolites were putatively identified based on the databased. The peak at retention time [R_L] 11.78 min having the absorption maxima 254 nm and the molecular ion of mass 137[M⁻] was identified as 4-hydroxybenzoic acid [Table. 2]. The peak at R_L 15.8 min having the absorption maxima 275, 300 nm and ionized mass 190 [M⁻] was identified as 5-hydroxylindole acetic acid [Table. 3]. The metabolite eluted at R_L 13.6 min having the absorption maxima 275, 300 nm with the molecular ionized mass 220[M⁻] identified as 5-hydroxylindole lactate [Table. 3].

Metabolite eluted R_{t.} at 9.88 min have absorption at 275, 300 nm represented molecular ion mass 204[M⁻] identified as hydroxy-kynurenic acid [Table. 3]. Metabolite eluted with R_{t.} at 13.5 min having an absorption maxima with 280 nm showed the molecular mass ion 219 [M⁻] identified as N-acetyl-5-hydroxytryptophan [Table. 3]. The metabolites have the R_{t.} 17 min having an absorption spectra 275, 290 nm represented the molecular ionized mass [M⁻] identified as 5-hydroxyanthranilic acid [Table. 3]. Liquid chromatography-mass spectrometric analysis of exo-metabolites of 5-OH Trp revealed thirty-seven derivatives of 5-OH Trp metabolites (Table. 3). Out of thirty-seven metabolites, only six metabolites were confirmed through standards, five metabolites

putatively/ tentatively while the twenty six remain identified metabolites were based on the database search (Table. 3).

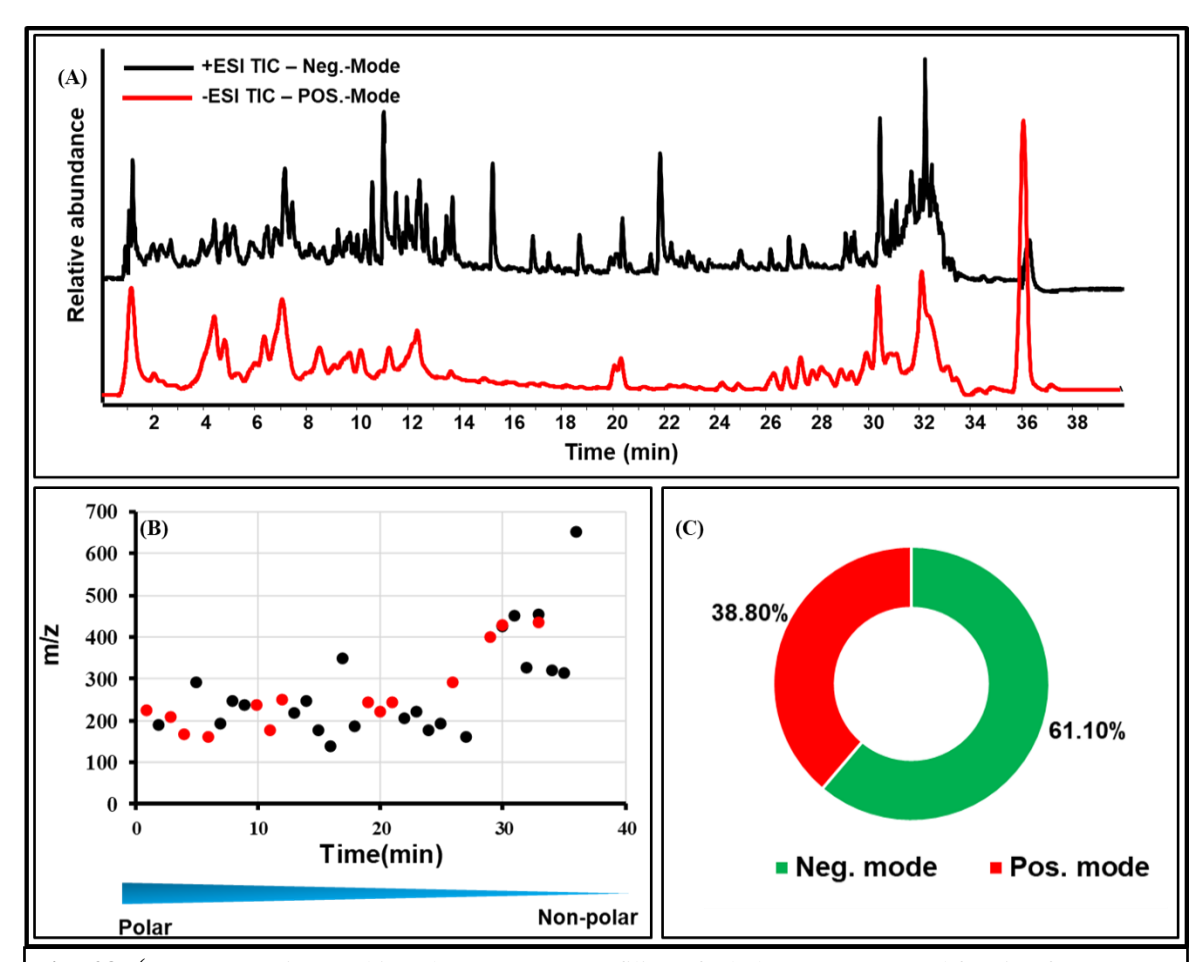


Fig. 28: (A) Comparative total ion chromatogram profiling of ethyl acetate extracted fraction from 5-hydroxytryptophan fed cultures of *Rbx. benzoatilyticus* under chemotrophic condition. (B) Time lap analysis based on m/z of metabolites (C) Pie-chart illustration of metabolites under both +ve and -ve mode of ionization. Pos.; (+ve) mode; and Neg.; (-ve) ionization mode.

Table. 3: Hydrox**y**indoles derivatives identified from the exometabolites of 5-OH-L-Trp fed cultures of *Rbx. benzoatilyticus*.

		Generated	Exact	m/z		UV- visible		
S.no	R _{t.}	Mol. Formula	mass	Neg. [M-]	Pos. [M ⁺]	spectrum[y]	Mass Accuracy (ppm)	Identification of metabolites
1	3.58	$C_{12}H_{17}NO_8$	225		224	270,280	-6.31	UN
2	4.2	$C_{10}H_7NO_3$	190	189		272,282	-5.62	UN
3	4.68	$C_{10}H_7NO_4$	205		206	272,260,305	1.86	Xenthurenic acid
4	5.96	C ₈ H ₅ NO ₃	163		164	260,280,305	3	N-Hydroxyphthalimide/ 5-Hydroxyisoindoline- 1,3-dione
5	6.22	$C_{10}H_{16}N_2O_8$	292	291		270,300	2.51	UN
6	6.26	C ₇ H ₁₁ NO ₃	157		158	270,305	5.96	UN
7	6.3	$C_{10}H_9NO_3$	191	190		270,310	2.82	UN
8	8.08	$C_{13}H_{13}NO_4$	247	246		270,300	5.15	UN
9	8.57	C ₁₁ H ₉ NO ₅	235	234		270,290,300	2.01	3-(1,3-Dioxoisoindol-2- yl)oxypropanoic acid
10	8.6	C ₁₄ H ₅ NO ₃	235		236	270,300,360	-1.88	UN
11	9.22	$C_{10}H_{11}N_3$	173		174	275,300	2.49	UN
12	9.55	C ₁₂ H ₁₃ N ₃ O ₃	247		248	230,315	2.37	N-carbomyl tryptophan
13	10.24	$C_{II}H_9NO_4$	219	218		240,340	-1.15	OH indole pyruvate
14	10.32	$C_{11}H_8N_2O_2$	244	245		280,330	5.94	UN
15	10.52	$C_{10}H_9NO_2$	175	174		270,280,300	5.3	UN
16	11.78	$C_7H_6O_3$	138	137		254	0.53	Hydroxyl benzoic acid
17	11.9	$C_{12}H_{18}N_2O_7$	348	347		280,300	-4.72	UN
18	12.11	$C_9H_{17}NO_3$	187	186		280,290,310	-5.81	UN
19	12.7	$C_{13}H_{10}N_2O_3$	242		243	270,305	4.01	UN
20	13.5	$C_{12}H_{14}N_2O_2$	220		219	280,310	2.96	N-acetyl Hydroxy tryptophan
21	13.54	$C_{14}H_{12}N_2O_2$	240		241	270,305	4.01	UN
22	9.88	$C_{10}H_7NO_3$	205	204		275 300,308	-2.5	5-Hydroxy Kynurenic acid
23	13.6	$C_{II}H_{I0}NO_4$	221	220		275,300	-5.2	5-OH indole lactate
24	14	$C_{10}H_9NO_2$	176	175		205,270	0.32	UN
	15.33	$C_{11}H_{12}N_2O_2$	204		205	275,300	-3.34	Trp
25	15.8	$C_{10}N_9NO_3$	191	190		270,290,300	-3.6	OHIAA
26	15.37	$C_{15}H_{18}N_2O_4$	290		291	270,380	-6.62	UN
27	15.9	$C_9H_7NO_2$	161	160		275,289,300	6.2	Indole 3 carboxylic acid
28	17	$C_7H_7NO_3$	153	152	200	275,289,300	-1.2	OH anthranilic acid
29	18.78	C ₂₁ H ₂₂ N ₂ O ₆	398	12.1	399	270,280,310	-2.74	UN
30	25.78	C ₂₁ H ₃₅ N ₃ O ₆	425	424	426	270,350-450	2.22	UN
31 32	27.72 29.09	C ₂₃ H ₃₇ N ₃ O ₆ C ₄₃ H ₃₄ N ₂ O ₆	451 326	450 325		280,300 280,290	0.1/98.6 -7.91	UN UN
33	29.09	C ₄₃ H ₃₄ N ₂ O ₆ C ₂₃ H ₃₉ N ₃ O ₆	453	452	434	275.282.295	-0.01	UN
34	29.8	C ₁₉ H ₂₀ N ₄ O	320	319	.51	260,280	-1.3	UN
35	30.86	C ₁₆ H ₂₈ N ₂ O ₄	312	311		260,270,280	-7.71	UN
36	31.	C ₃₄ H ₅₇ N ₃ O ₉	651	650		260,270,282	1.02	UN

Metabolites italicized are confirmed by using authentic standards retention time, fragmentation pattern and compared with available databases. The metabolites identified putatively are based on certain parameters, such as generated formula, absorption maxima, and molecular ionized masses compared with databases. Metabolites. UN; unidentified; not found suitable structure in databased, R_t ; retention time. UN; unidentified; not found in database; R_t ; retention time, Neg. (-ve) ionization mode; Pos. (+ve) ionization

3.4. Characterization of brown pigment produced from L-Tryptophan/ 5-hydroxytryptophan fed cultures

3.4.1. Brown pigment production by Rbx. benzoatilyticus fed with L-Tryptophan/5-hydroxytryptophan

Rbx. benzoatilyticus has grown for 48 h with or without L-Trp/5-OH-Trp (1mM) for the production of brown pigment either under chemotrophic (dark aerobic) or light anaerobic conditions. Brown pigment production was observed only from the cultures fed with L-Trp or 5-OH-Trp incubated under chemotrophic (dark aerobic) conditions while either the phototrophic (light anaerobic) incubated cultures with L-Trp/5-OH Trp or without fed cultures did not yield any pigment production (Fig. 29 E,F). Further, the intensity of brown pigment was about three-fold higher for 5-OH Trp fed cultures compared to L-Trp fed cultures. The brown pigment isolated from L-Trp or 5-OH Trp culture supernatants (Fig. 29B) precipitated on acidification followed by storage at 4°C for 2-3 days (Fig. 29D). Both of these brown pigments were insoluble in organic solvents or in water and the purified brown pigments (as described as similar in materials and methods section 2.3.2 and flow chart II) isolated from L-Trp and 5-OH Trp fed conditions was used characterization.

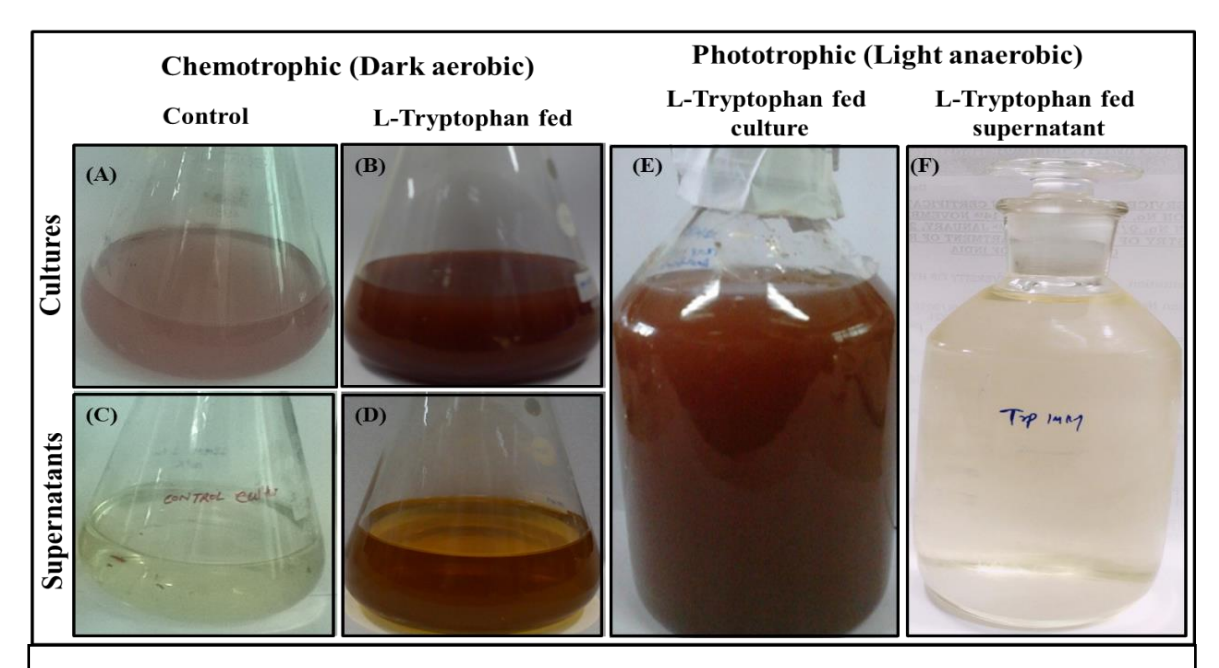


Fig. 29: Photograph of culture flasks showing growth of *Rbx. benzoatilyticus* unfed (A; control) and fed with L-Tryptophan (B) cultures incubated for 48 h under chemotrophic (dark aerobic) conditions. The culture supernatant had no pigmented exometabolites in the control (C) while L-Tryptophan fed culture showed the brown pigmented exometabolites (D). The phototrophic incubated (light anaerobic) L-Tryptophan culture (E) of *Rbx. benzoatilyticus* did not show any pigmented exometabolites (F).

Experimental conditions were similar as mentioned in Fig 16, except for the 24 h grown culture in nitrogen-deficient condition. Malate grown culture under phototrophic condition with O.D _{660 nm} 0.3 was used as inoculum (10%) for the experiment. Cultures were grown under phototrophic (light anaerobic) condition in nitrogen-deficient (without NH₄Cl) malate (carbon source) medium for 24 h and then fed with L-Trp (1mM) as the nitrogen source, followed by growth in chemotrophic (dark aerobic) conditions. After 48 hours of incubation, the culture was centrifuged and supernatant of the culture was used for the pigment precipitation.

3.4.2. Physico-chemical properties of purified brown pigment

The purified brown pigment powder was soluble only in alkaline solution [1N NaOH/KOH] and insoluble in water as well as in organic solvents [hexane, chloroform, acetone, ethyl acetate, ethanol, benzene] (Fig. 30). Both brown pigments (extracted from L-Trp and 5-OH Trp fed cultures) readily precipitated in acidic conditions (5N HCl), bleached when treated with oxidizing agents like (100%) H₂O₂ and NaOCl (Fig. 30). Both brown pigments gave a positive reaction with the polyphenol test by producing flocculent brown precipitate reacting with (500 mM) FeCl₃. Both pigments gave a positive test for ammonical

silver nitrate. The addition of Na₂S₂O₄ solution decolorized the pigment and upon adding (1%) potassium ferricyanide the colorless pigment turned brown (Fig. 30). The physicochemical properties revealed that the purified brown pigment produced by *Rbx*. *benzoatilyticus* either feed with L-Trp or 5-OH Trp showed close similarity to melanin (Fig. 30).

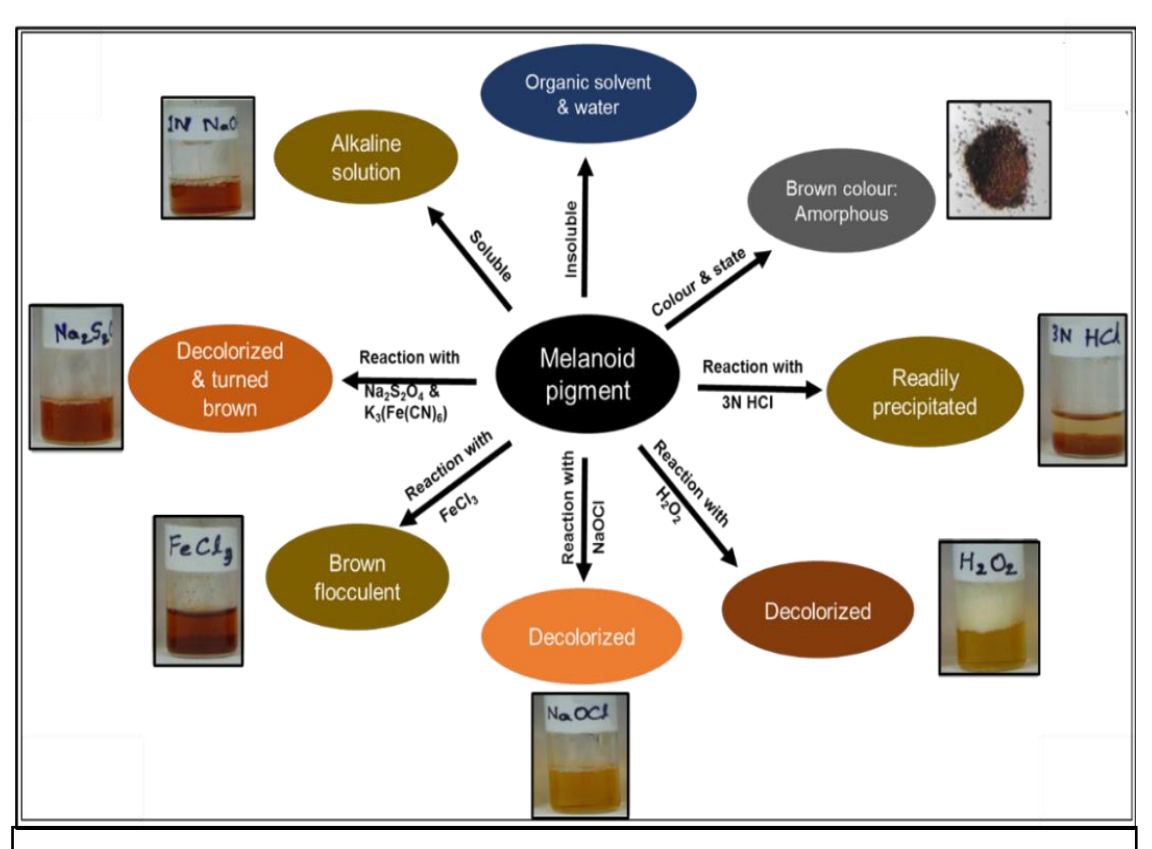


Fig. 30: Physico-chemical properties of extracted brown pigment produced from L-Tryptophan and 5-hydroxytryptophan fed conditions by *Rbx. benzoatilyticus* under chemotrophic condition

The experimental conditions were same as mentioned in Fig. 16, except for the precipitation of brown pigment and its purification. It was purified by dissolving with 1N NaOH and followed precipitated with 5 N HCl. The brown pigment was used for biochemical analysis [materials and methods Fig. 10 as section 2.3.2.].

3.4.3. Structural characterization of purified brown pigment

3.4.3.1. Scanning electron microscope (SEM) analysis

The ultrastructure feature of both the brown pigment powder showed a homogenous smooth surface, size typical bead-like partials. These sample were examined using SEM (Philips- XL30 series) at 8 to 12 different random locations under different magnifications. At higher magnification, both brown powders showed an unorganized aggregated polymer (Fig. 31A) with a randomly unite bead-like appearance similar to that of melanin's which appear as chunks of typical bead-like structure. At higher (60x) magnification, the bead surface of both brown powders appeared smooth (Fig. 31A). The isolated melanosomes appeared as granular with spherical to ellipsoidal shape for both the brown powders (Fig.31B)

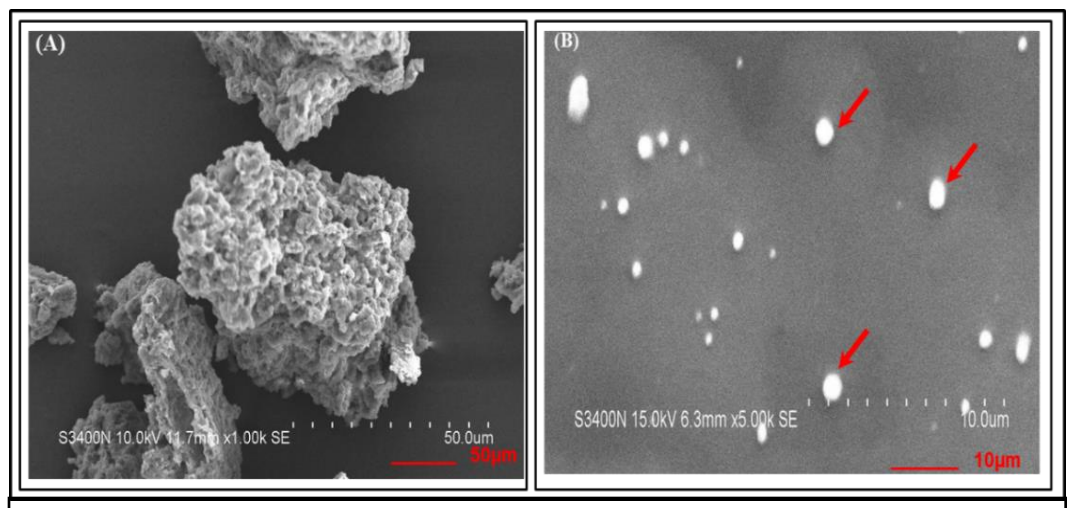


Fig. 31: Scanning electron microscopic (SEM) image of purified brown pigment. SEM image of brown pigment aggregated polymer (A) and typical bead like granular particles (B).

The experiment conditions followed are described in Fig. 8, except for the SEM analysis. For SEM visualization of brown pigment it was dried and the powder was mounted on stab for gold sputtering.

3.4.3.2. UV-Visible spectroscopic analysis

The purified brown pigments extracted from L-Trp and 5-OH-Trp fed cultures were used for spectroscopic analysis. Spectrum was recorded from 200-800 nm in a UV-Visible spectrometer [Shimadzu] against 1N NaOH. Brown pigment isolated from L-Trp fed cultures had an absorption maxima at 240 nm (Fig. 32), while the pigment isolated from 5-OH Trp fed cultures showed maxima at 250 nm. Both pigments showed a linear absorption correlation in the UV region which decreased in the visible region (Fig. 32B). The UV-Vis absorption spectroscopy of purified brown pigments extracted from L-Trp and 5-OH-Trp fed cultures revealed a linear correlation with absorbance and wavelength (Fig. 32B).

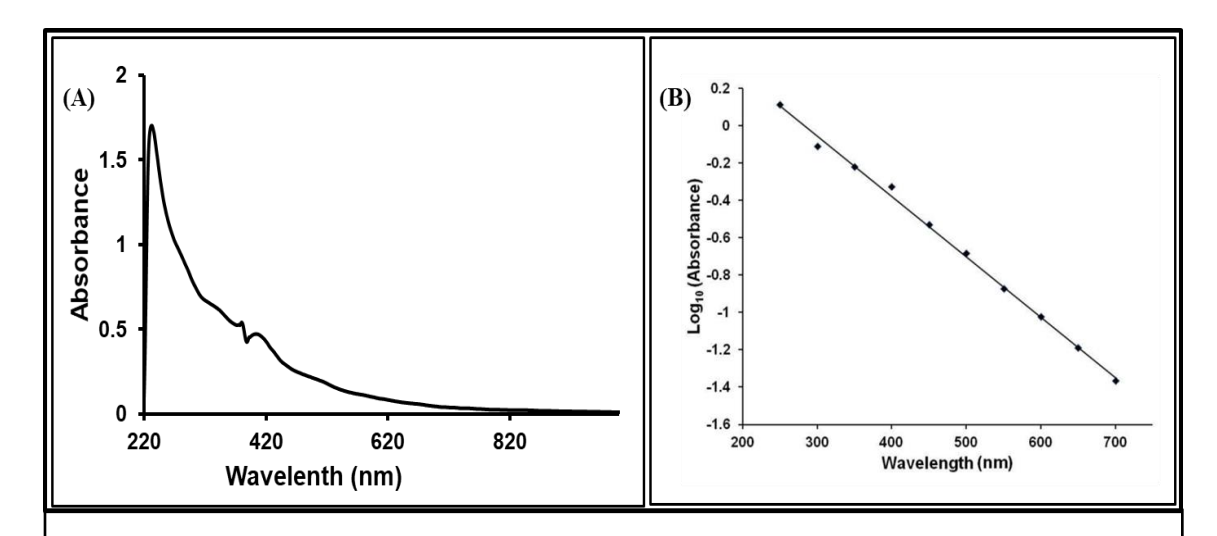


Fig. 32: Characterization of purified brown pigment. (A) UV-Visible absorption maxima (B) Log₁₀ absorbance linear correlation with wavelength.

The experimental conditions used for pigment purification were same as mentioned in material methods section 2.3.1. The purified pigment was subjected for UV-Visible spectrophotometry against blank.

3.4.3.3 ESR/EPR spectroscopic analysis

Both the brown pigments exhibited characteristics asymmetry, 4-G wide single line EPR spectra with a G value (Fig. 33A). Electron spin resonance [ESR] spectra of the brown pigment extracted from the L-Trp fed culture showed a signal at 336.46 mT. While

brown pigment from 5-OH Trp fed cultures had a signal at 340 mT corresponding to a value of 2.00643 (Fig. 33A). The ESR spectrum observed for both the brown pigments assigned the presence of stable free radicals [paramagnetic], which is a salient characteristic of melanin.

3.4.3.4. X-ray Diffraction (XRD) analysis

X-ray Diffraction analysis of brown pigment obtained from L-Trp and 5-OH-Trp fed cultures was performed using Bruker D8 (Advance Germany) X-ray Diffractometer.

The purified brown pigments were amorphous powder of homogenous polymer (Fig. 33B).

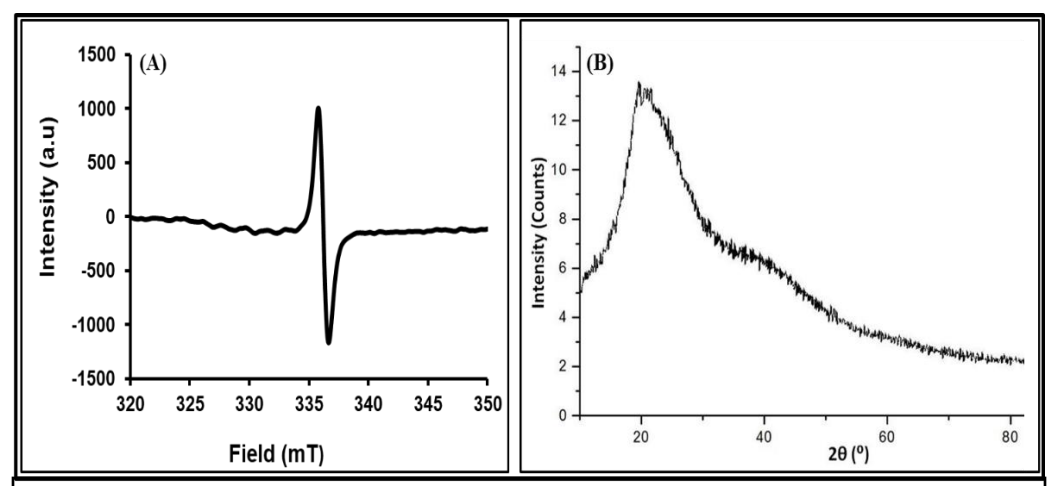


Fig. 33: Spectroscopic characterization of brown pigment produced by *Rbx. benzoatilyticus*. (A) ESR spectrum and (B) X-ray Diffraction spectrum.

Experimental conditions used are described in Fig. 8, Fig. 10 and section 2.3.2. The purified brown pigment was used for ESR and XRD analysis.

3.4.3.5 Fourier-transform infrared spectroscopy (FTIR) analysis

The FTIR spectrum (Fig. 34) of both brown pigments showed stretching vibration at 3275 cm⁻¹ which indicates the presence of –OH and –NH functional groups. The band at 2928 to 2902cm⁻¹ indicates -CH₃, -CH₂- aliphatic group. The peak assigned at 3600-2800 cm⁻¹ is the stretching vibration [-OH and-NH] of the amine carboxylic acid, a phenolic aromatic amino acid of indole and pyrrole system. The vibration peak at 1723

cm⁻¹ assigned to C=O/C=C, C=N/N-H groups from carbonyl, carboxyl, ketone or quinones/ indole having strong absorption at 1626 cm⁻¹ can be assigned to C=C stretching vibration of aromatic/pyrrole moiety (Fig. 34). The peak at 1526 cm⁻¹ can be designated as –N-H-bending along with the band at 1414 cm⁻¹ [C-N stretching] suggests the presence of indole and pyrrole functional groups. Absorption at 1220 cm⁻¹, indicative of the presence of – CH₂OH group of the [Fig. 34] phenolic and the indole moiety. The bending vibration peak at 1048 cm⁻¹ can be ascribed to -CH- plane or CH out of plane deformation and abruption 700 cm⁻¹ to out of plane carbon-hydrogen bending of the aromatic moiety (Fig. 34).

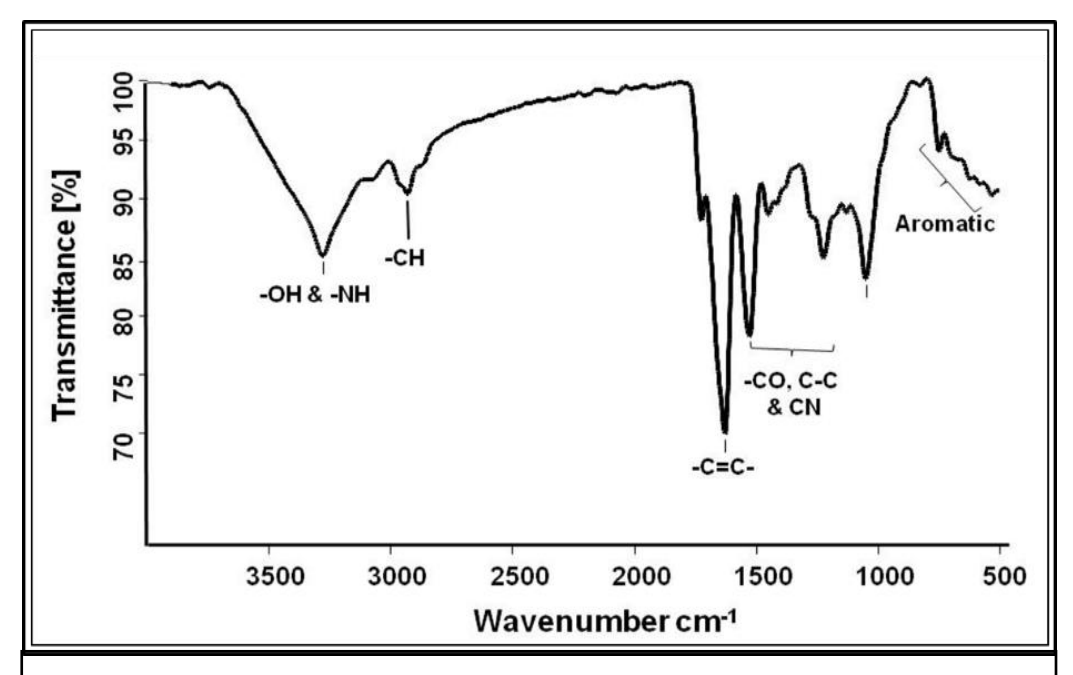


Fig. 34: FTIR analysis of brown pigment produced by *Rbx. benzoatilyticus*.

Experimental conditions were same as mentioned in Fig. 16, and section 2.3.2. The purified brown pigment was used for FTIR analysis.

3.4.3.6. Solid-state C-13 NMR spectroscopy

¹³C Solid-state NMR of purified brown pigment obtained from L-Trp fed cultures showed an intense signal at 160-180 ppm corresponding to the carbonyl region; usually assigned as carbonyl carbon of amide, carboxylate or quinones (Fig. 35A). The signal at 110-150 ppm corresponds to aromatic carbon associated with aromatic moiety and 100-134 ppm with a broad and weak signal at 126-110 ppm is assigned to the aromatic part of indole/ pyrrole moiety. The intense signal at 10-45 ppm is due to the side chain of aliphatic carbon which corresponds to the methylene and methane group. The signal at 45-60 ppm can be designated to the backboneα, β- carbon (Fig. 35A).

3.4.3.7. *Solid State N-15 NMR spectroscopy*

The solid-state ¹⁵N NMR (CP/MAS) spectra of the brown pigment designate an intense broad chemical shift ranging between 115-140 ppm. This is assigned to the chemical shift of molecular nitrogen atom from indole/pyrrole aromatic ring (Fig. 35B).

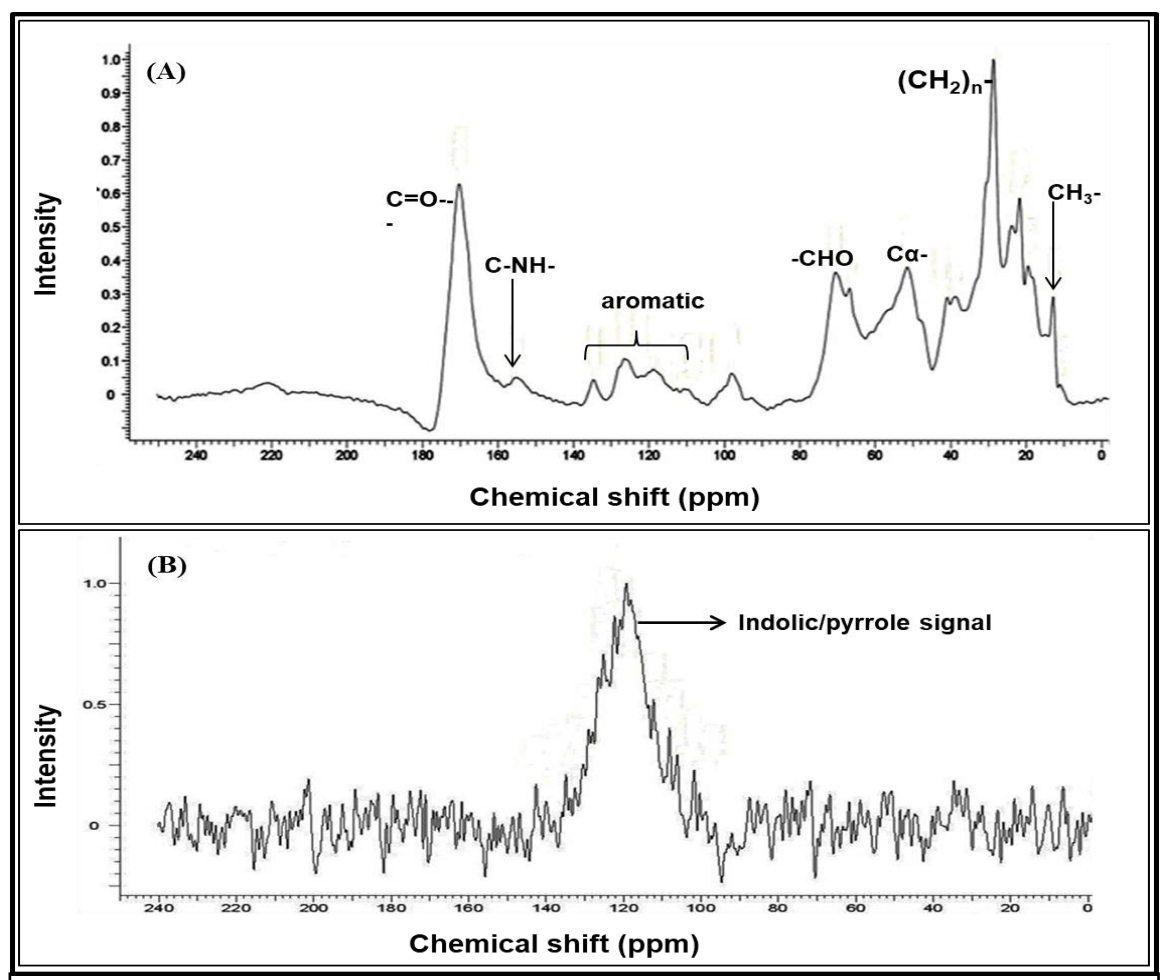


Fig. 35: Solid state NMR analysis of brown pigment by *Rbx. benzoatilyticus* (A) ¹³C NMR spectrum (B) ¹⁵N NMR spectrum.

The experimental conditions for extraction and purification of brown pigment were as mentioned in Fig. 8. The ¹³C and ¹⁵N NMR, Nuclear Magnetic Resonance analysis was carried out at the School of Chemistry, Hyderabad University.

3.4.3.8. Identification of monomers of brown pigment

To identify the monomers of the polymeric purified brown pigment obtained from L-Trp and 5-OH Trp fed cultures, the polymer was hydrolyzed with diffused KOH (Section 2.7.1 as materials and methods for details). The monomers were extracted into ethyl acetate and run on TLC to identify the hydrolyzed products by staining with indole specific reagent. Identical staining patterns were observed for both brown pigments compared with that of control (Fig. 36 A and B). Both brown pigments were alkaline (H₂O₂) oxidation according to Wakamatsu and Ito et al., 2012 and the oxidized products were

measured using LC-MS/MS analysis. The peak at R_t. 8 min under negative mode has an ionized mass of 198.235[M⁻] with absorption spectrum at 270 nm it was identified as pyrrole-2,3,4-dicarboxylic acid (PTCA) (Fig. 37 A and C). Similarly, peak at R_t. 1.9 min under negative mode had a molecular ionized mass of 241.685 [M⁻] with absorption maxima at 270 nm is similar to pyrrole-2,3,4,5-tetracarboxylic acid (PTeCA) (Fig. 37 B and D). Both of these pyrrole derivatives were common to both brown pigments. Furthermore, the brown pigment obtained from 5-OH Trp fed culture had a peak at R_t. 12.0 min under negative mode with an ionized mass of 154.443 (M⁻] with absorption maxima at 270 nm is similar to pyrrole-2,3-dicarboxylic acid (PDCA) (Fig. 37C). PTCA, PDCA was confirmed using authentic standards while PTeCA was putatively identified based on the mass fragmentation and absorption spectrum.

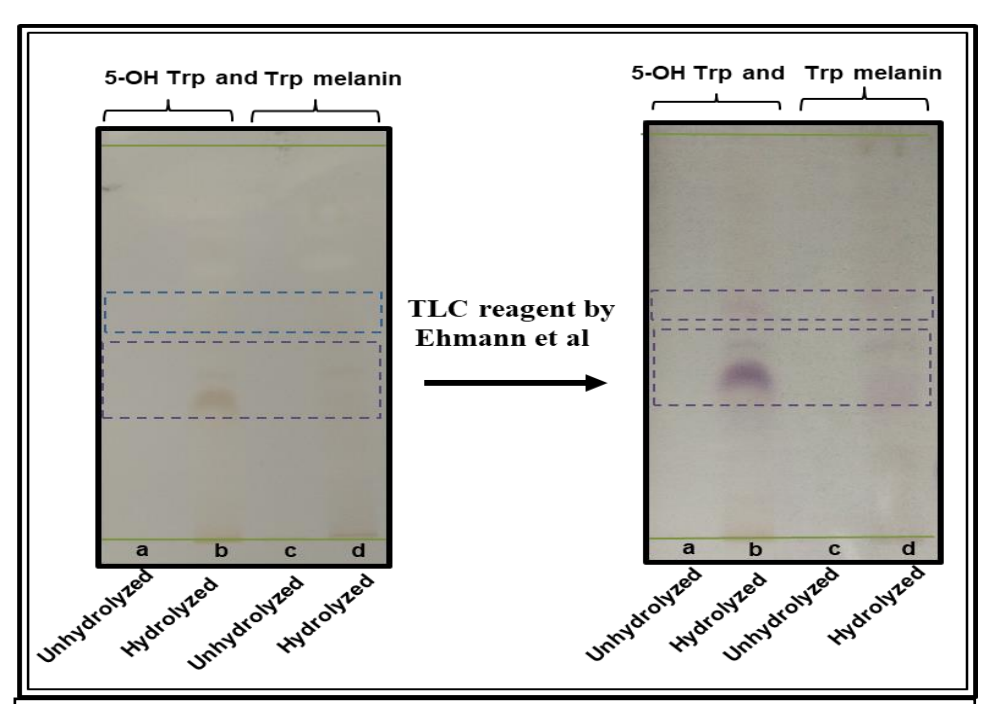


Fig. 36: Chromatographic analysis of hydrolyzed and un-hydrolyzed products of brown pigment of (A) Without stained. (B) Strained with TLC specific reagent, 5-OH Trp; 5-hydroxytryptophan, Trp; L-Tryptophan

The experimental conditions for pigment extraction and purification were similar to as described in section 2.3.1. Completely dried and purified brown pigment was used for analysis. Degradation of the brown pigment was studied according to Ellis and Griffiths, (1974) with slight modifications in protocol as described in section 2.7.1.

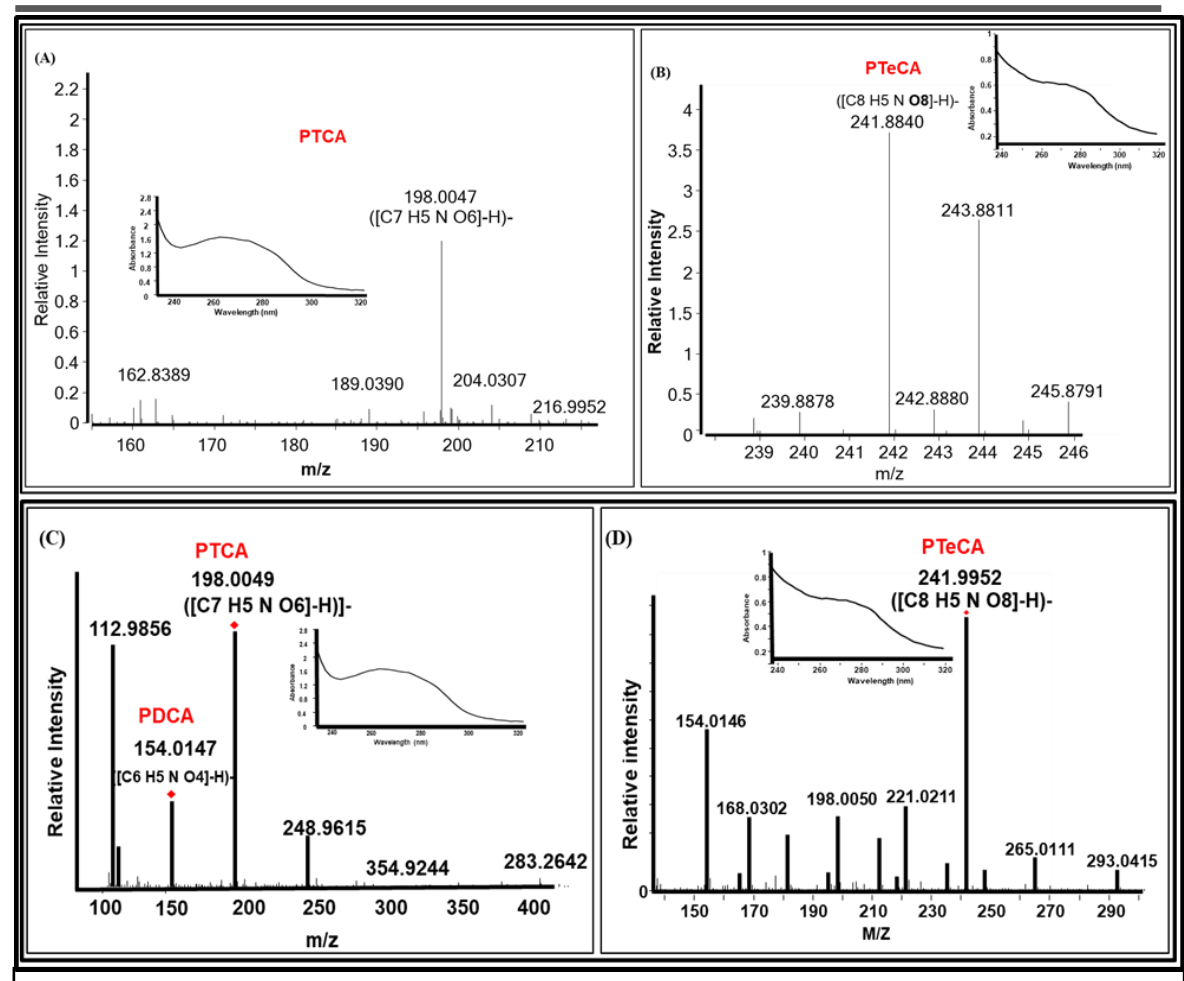


Fig. 37: Identification of oxidation product of brown pigment based on mass spectrum and absorption maxima as represented by pyrrole derivatives. (A, B) PTCA and PTeCA molecular marker identified brown pigment of L-Tryptophan derivatives. (C,D) PDCA, PTCA and PTeCA molecular marker identified brown pigment of 5-hydroxytryptophan derivatives. PDCA; pyrrole-2,3- tricarboxylic acid, PTCA; pyrrole-2,3,5-tricarboxylic acid, PTeCA; pyrrole-2,3,4,5-tetracarboxylic acid

PDCA, PTCA, and PTeCA represents molecular ion mass of 154.014[M⁻], 198[M⁻], 241 [M⁻] respectively, with their corresponding UV-Vis spectrum. Alkaline oxidation of the brown pigment is described in section 2.7.2 according to Wakamatsu and Ito et al., 2012.

3.5. Melanogenesis in *Rbx. benzoatilyticus*

3.5.1. Brown pigment production

The brown pigment formation in the presence of L-Trp as well as 5-OH Trp fed *Rbx. benzoatilyticus* was investigated along with different inhibitors as known as melanin synthetic pathways. Whereas the glyphosate inhibits tyrosine dependent melanin synthesis as well as quercetin and kojic acid was a eumelanin inhibitor does not affect pigment

production. Similarly, pigment formation remained unaffected in the presence of sulcotrion a pyomelanin specific inhibitor (Fig. 38 A and C). Interestingly, brown pigment production from L-Trp fed culture in presence of sodium-azide, a laccase/ monooxygenase specific inhibitor was significantly affected leading to decrease pigment production (Fig. 38B). While brown pigment production was from 5-OH Trp fed culture neither effect known melanin biosynthesis pathways inhibitor and nor sodium-azide.

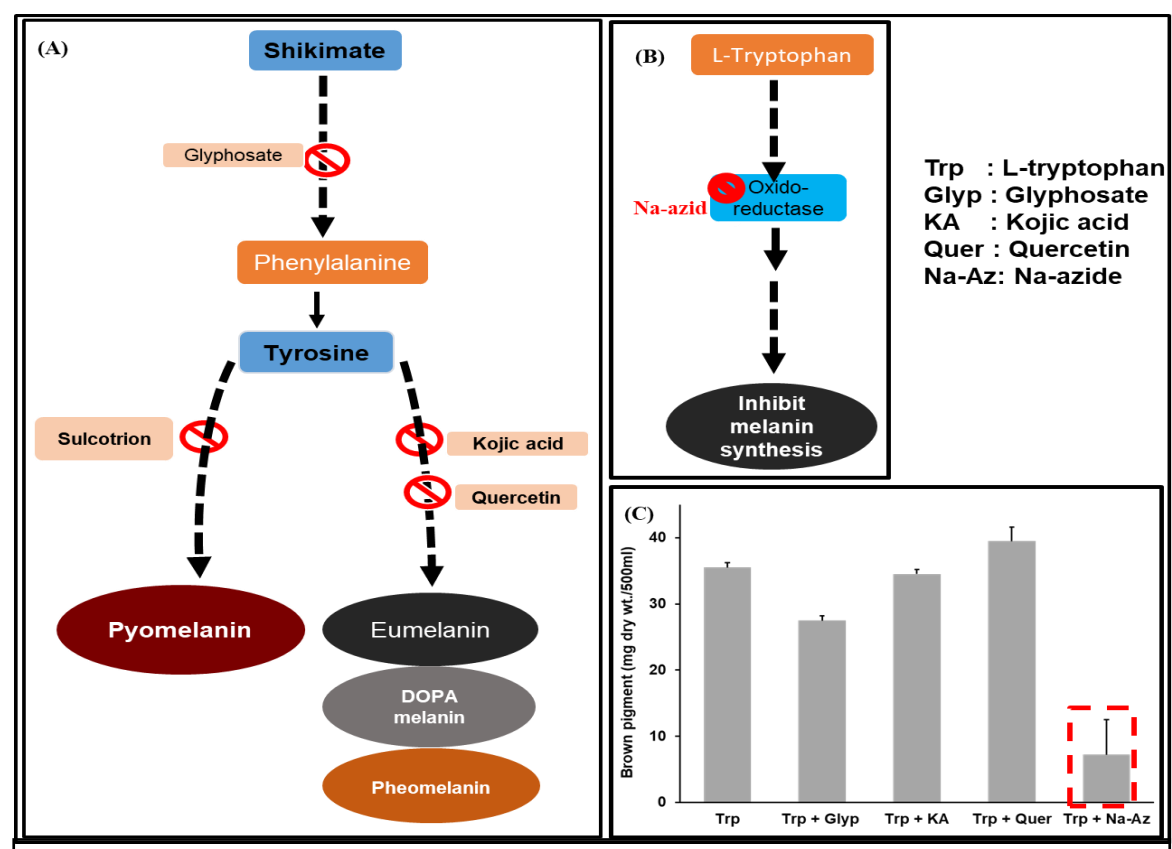


Fig. 38: (A) Shikimate pathway specific inhibitor (glyphosate, sulcotrion, kojic acid and quercetin) used in this study to understand the role in the shikimate pathway in the biogenesis of melanins by *Rbx*. benzoatilyticus. (B) Na-azide was used as an inhibitor for monooxygenase to understand its role melanin biogenesis by *Rbx*. benzoatilyticus. (C) The quantified yield of melanin produced by *Rbx*. benzoatilyticus in persence of various inhibitors.

The experimental conditions used, were as mention in section 2.3.1. Here, cultures were grown under light anaerobic condition in nitrogen-deficient (without NH₄Cl) malate (carbon source) medium for 24 h and then fed with L-Trp (1mM) as nitrogen source with the specific inhibitor of pathway. The culture was shifted to chemotropic condition and incubated for 48 h at 30 °C. After 48 hours the culture was centrifuged and supernatant of the culture was used for the pigment precipitation followed by its quantification.

3.5.2. In-vitro melanogenesis

Cell lysates of *Rbx. benzoatilyticus* grown chemotrophic (dark aerobic) or light anaerobic conditions were used for *in vitro* melanogenesis assay. Melanin production was observed only from cell lysates which were obtained from cells grown chemotrophic condition fed with L-Trp compared to under L-Trp fed phototrophic(light anaerobic) conditions (Fig. 39A). Further, the intense brown color melanin production was observed from 5-OH Trp cells compared to L-Trp fed cultures (Fig. 39B). The *in vitro* studies and purified *in vitro* brown pigment displayed similar UV-Visible profiles (Fig. 39 C and D). Time-dependent melanin formation with simultaneous utilization of the precursors (L-Trp or 5-OH Trp) is shown in Fig. 40 A,B (cell lysate obtained from (light anaerobic) photo and chemotropically or dark aerobic condition).

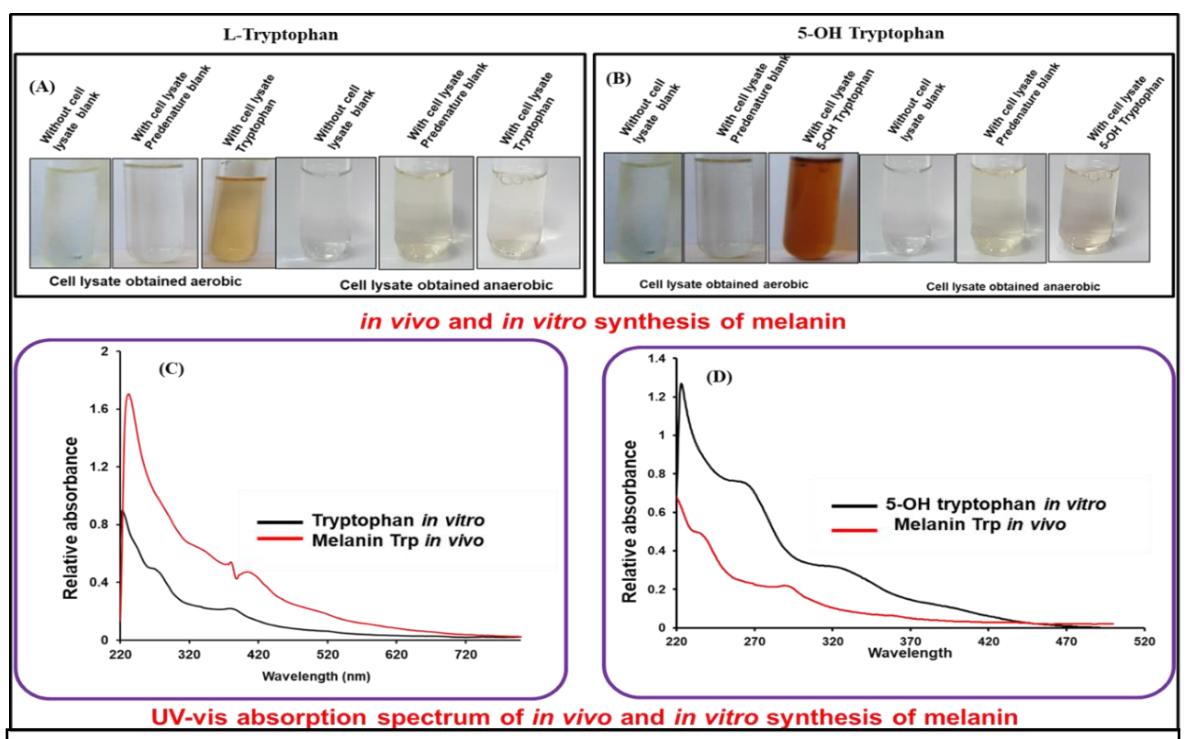


Fig. 39: *In-vitro* melanogenesis using cell free extracts of *Rbx. benzoatilyticus* from cells grown chemotrophically for 48 h fed with L-Tryptophan and assayed in the presence of L-Tryptophan or 5-hydroxytryptophan. Test tube showing the supernatant after the assay in the presence of L-Tryptophan (A), 5-hydroxytryptophan (B) and the respective absorption spectra shown in C and D.

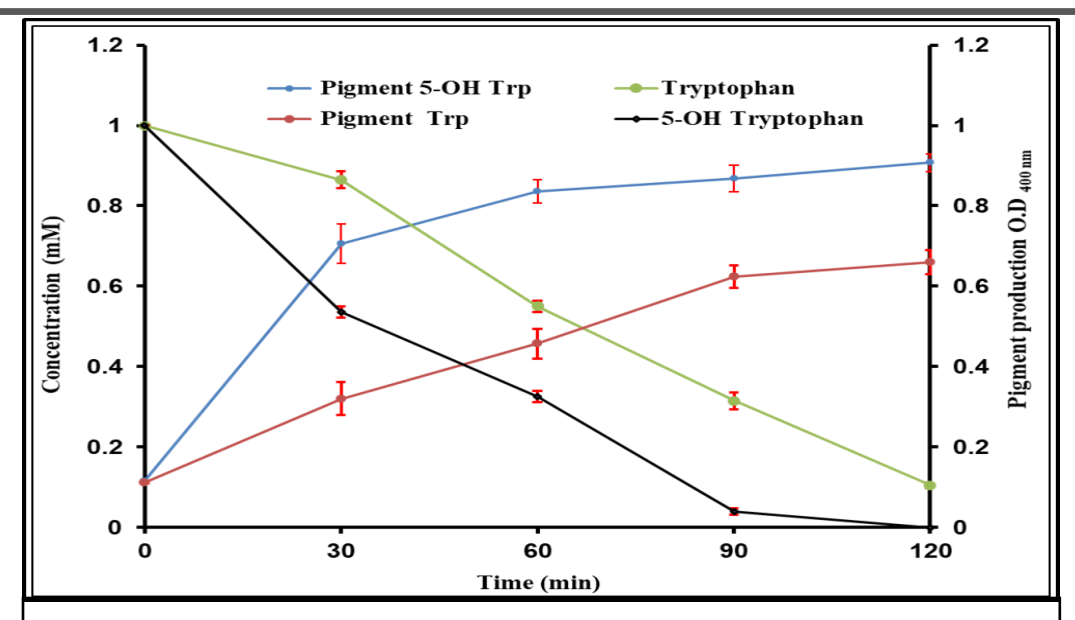


Fig. 40: Time-dependent *in-vitro* utilization of L-Tryptophan or 5- hydroxytryptophan with simultaneously melanin production by cell-free extract of *Rbx. benzoatilyticus* grown under chemotrophic condition

Cell-free extracts were prepared as mentioned in the materials and methods section 2.7.1. Invitro melanogenesis assay was performed with cell lysate as enzyme source and it contained L-Trp/5-OH Trp (1mM) as substrate. The blank was pre-denatured cell lysate and negative control was without cell lysate. The reaction was stopped by adding 5N HCl. In vitro pigment production was measured by spectrophotometer and L-Trp and 5-OH Trp consumption by HPLC at desired time period.

3.5.3. Enzyme studies

3.5.3.1. Aromatic aminotransferase

The enzyme assay was documented as mention similar as in materials and methods (section 2.7.2) from cell-free extracts obtained from L-Trp fed culture of *Rbx*. *benzoatilyticus*. The reaction mixture was placed at 37 °C for 60 min and then the reaction was stopped using 5N HCl. Pre-denatured cell-free extract served as control. Since indole-3-pyruvic acid or 5-hydroxyindole-3-pyruvic acid is unstable products of the assay, the spontaneously converted products indole-3-acetic acid or 5-hydroxyindole-3-acetic acid, respectively were measured using HPLC [Fig. 41, 42]. Trace amounts of 5-hydroxyindole-3-pyruvic acid and 5-hydroxyindole-3-lactic acid were also detected in the assay (Fig. 42).

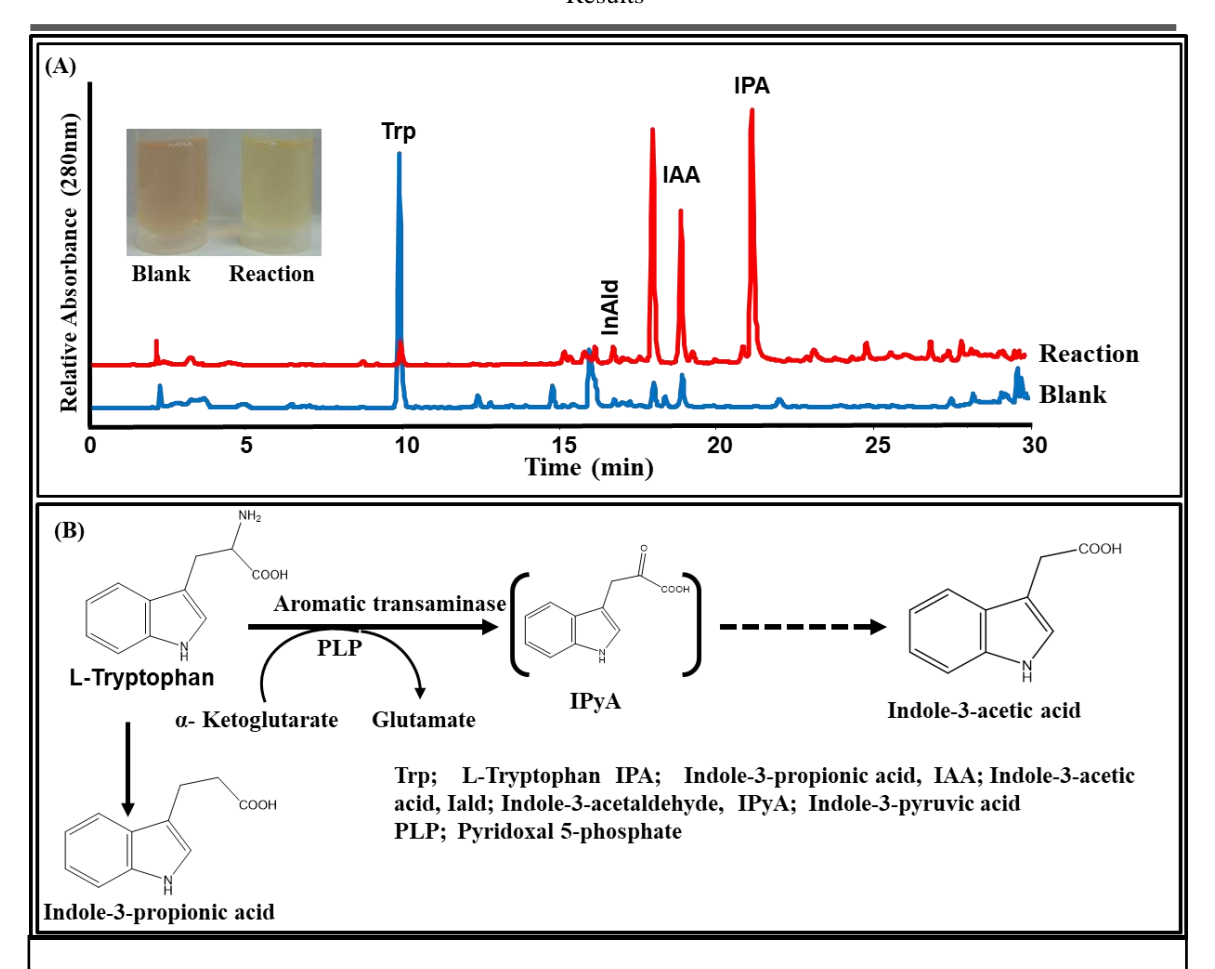


Fig. 41: HPLC chromatogram of the ethyl extract of the assay done for the aromatic amino activity of cell-free extract in the presence of L-Tryptophan by *Rbx. benzoatilyticus* grown under chemotropically fed with L-Tryptophan (A). Putative pathway of indole-3-acetic acid formation by *Rbx. benzoatilyticus* (B) based the metabolites identified from the chromatogram.(Insert picture shows the test tube with the supernatant after the assay).

Enzyme assay of aminotransferase/transaminase, which converts L-Trp to indole-3-pyruvic acid (IPyA) (A). Product of indole-3-acetic acid (IAA) was observed at R_t . 18 min. (B) HPLC analysis of aminotransferase/transaminase activity in the pre-denatured (blank; blue chromatogram) in comparison to the reaction mixture after 60 min incubation (red chromatogram). Analysis was done through HPLC.

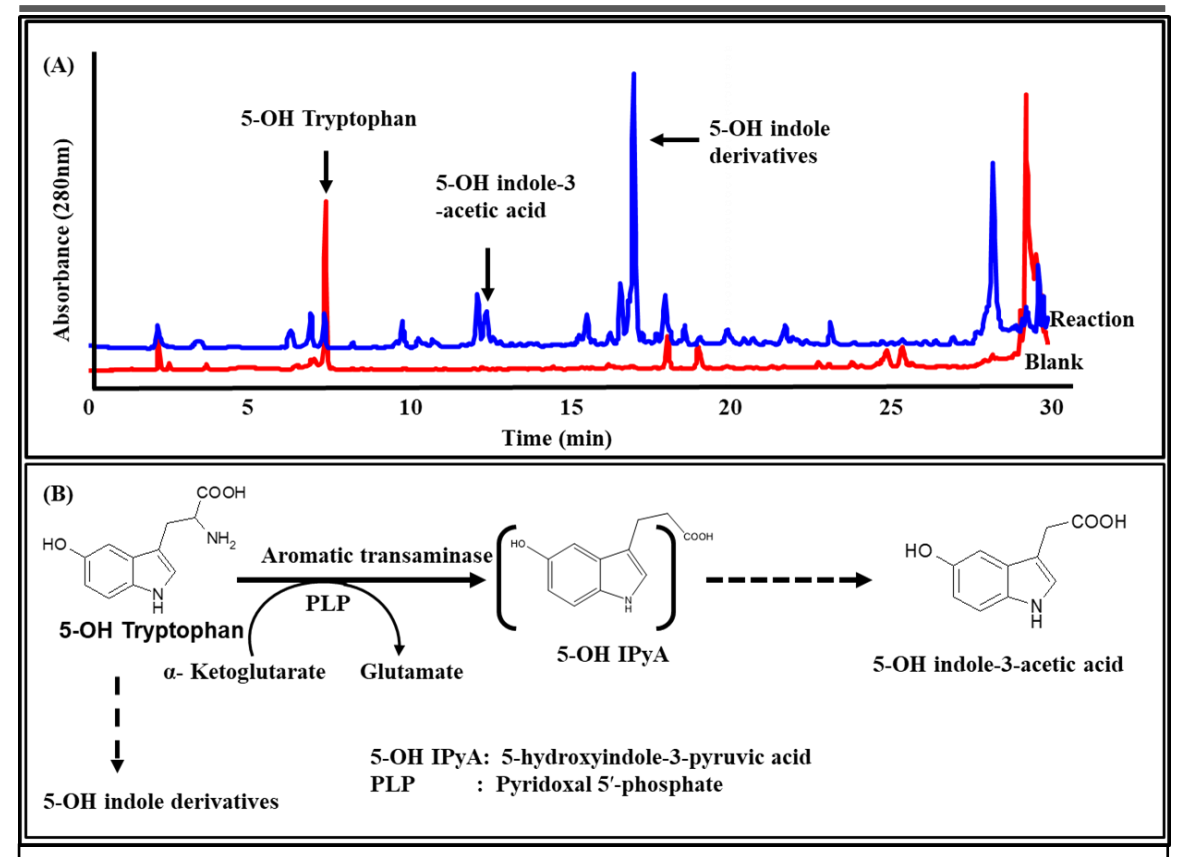


Fig. 42: HPLC chromatogram of the ethyl extract of the assay done for the aromatic amino activity of cell-free extract in the presence of 5-hydroxytryptophan by *Rbx. benzoatilyticus* grown under chemotropically fed with L-Tryptophan(A). Putative pathway of hydroxyindole-3-acetic acid formation by *Rbx. benzoatilyticus* (B) based the metabolites identified from the chromatogram.

Enzyme assay of aromatic aminotransferase/transaminase, which converts 5-OH Trp to 5-OH indole-3-pyruvic acid (5-OHIPyA). (A) Product 5-OH indole-3-acetic acid (OHIAA) was observed at $R_{\rm L}$ 12.5 min. Specific activities of aromatic aminotransferase/transaminase in Rbx. benzoatilyticus. (B) HPLC analysis of aromatic aminotransferase/transaminase activity in the pre-denatured (blank: red chromatogram) in comparison to the reaction mixture after 1 h incubation (reaction: red chromatogram).

3.5.3.2. Monooxygenase

Monooxygenase enzyme activity was carried out as described in materials and methods (section 2.7.3) and the product was measured using LC-MS (Fig. 43). The reaction mixture was placed at 37 °C for 60 min and then the reaction was stopped using 5N HCl. Pre-denatured cell-free extract served as blank. Since the 5-hydroxytryptophan not able to detect it might be simultaneously converted to 5-hydroxyindole-3-acetic acid the product was measured using LC-MS analysis.

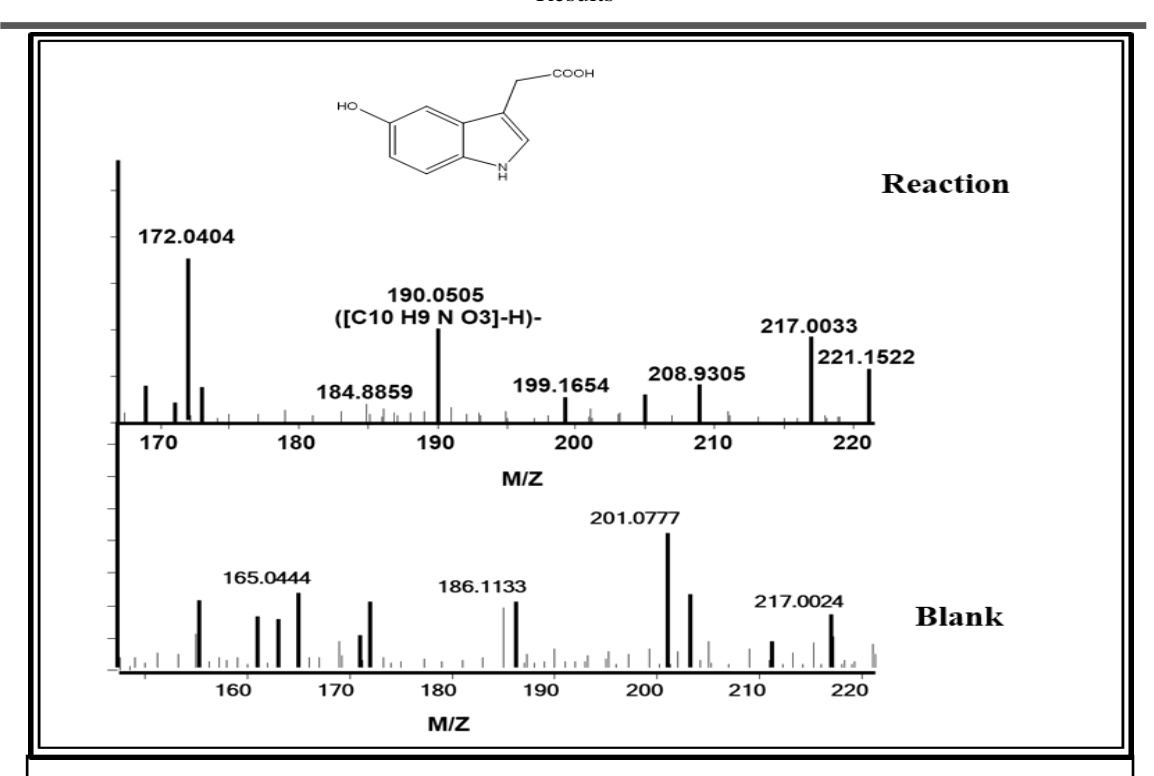


Fig. 43: Ionized chromatogram showing the difference in the masses for the enzyme monooxygenase assay done with pre-denatured (blank) an after the reaction. Mass of 190 m/z was identified as 5-hydroxyindole-3-acetic acid (5-OH IAA).

3.6. Global proteome analysis of L-Tryptophan fed cells of *Rbx. benzoatilyticus* cultivated under chemotrophic conditions

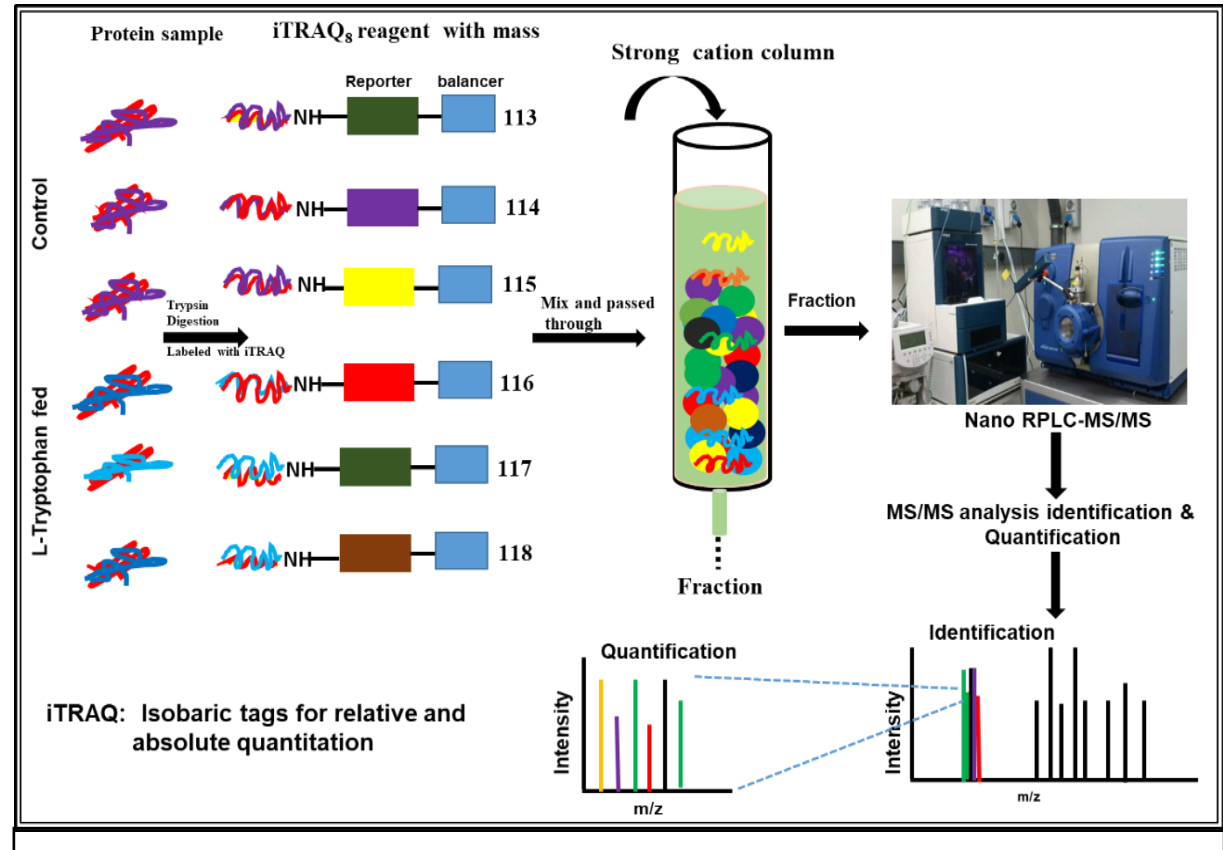
3.6.1 Proteomic inventory

Comparative proteomics analysis were performed to elucidate the molecular responses of *Rbx. benzoatilyticus* when fed with L-Trp and cultivated under chemotrophic (dark aerobic) conditions. This helps in understanding the functional molecular responses of the organism as influenced by the processor L-Trp. Proteomics approaches has emerged as a powerful robust technique for gaining insights into the physiological variations at the molecular and biochemical level, allowing the function and regulation of an organism which is under the influence of specific conditions. Proteomic analysis was done in this study using the Isobaric tag for relative and absolute Quantification [iTRAQ] technique, which was outsourced with M/S. California University, USA. Whole-cell protein was isolated from three independent experiments done in triplicates of L-Trp fed and unfed (control) cells and protein integrity was checked on SDS-PAGE evaluation (12.5%) before the iTRAQ analysis (Fig. 45).

Proteins were digested with trypsin and each sample protein was pooled and were labeled through the isobaric tag [Control iTRAQ₈-113, iTRAQ₈-114, iTRAQ₈-115, and L-Trp fed iTRAQ₈-116, iTRAQ₈-117, and iTRAQ₈-118] (Fig. 44). The labeled peptides of an equal amount from each sample were pooled in equal ratio and were mixed with all the six samples of labeled peptides. Samples were passed through a strong cation exchange chromatography (SCX) and the collected fractions were separated and analyzed using reverse-phase Nano liquid chromatography integrated to mass spectroscopy (RP Nano LC-MS/MS). The peptide mass fingerprint was subjected to the identification of proteins in a one-step process against the genome project of *Rbx. benzoatilyticus* and quantification were based on the reporter

ion intensity against iTRAQ reagent. The snapshot of the methodology used for iTRAQ analysis is illustrated in Fig. 44.

Two thousand four hundred and twenty-one proteins were detected through iTRAQ analysis. This corresponds to 64.5% coverage (Fig. 45B) of total theoretical proteins (3,898 protein-coding genes) according to the protein-coding genes of Rbx. benzoatilyticus (PRJNA63127) The differentially regulated proteins were subjected to insilico investigation of theoretical molecular weight, isoelectric point (PI) map, and hydropathy investigation (www.expasy.org). Molecular weight versus isoelectric point map was showed two clusters of protein with isoelectric point (pI) of 4.0 to 8.0 and 8.4 to 11.9 respectively (Fig. 46B). About 62% of proteins were hydrophilic and the remaining were hydrophobic according to grand average hydropathy (GRAVY) investigation (Fig. 46A). Fold change investigation of total proteins showed that the levels majority of proteins were remain unchanged (Fig. 47A). Linear regression analysis between two independent biological replicates (1 and 3, 3 and 2) has a correlation coefficient value (R, R2) of R= 0.0.785, R2=0.659 it suggested that the data was highly reproducible (Fig. 47B). The majority of the proteins which are differentially regulated showed P < 0.05 for multiple testing correlation in at least two replicates out of three replicate experiment suggesting that fold change is statistically significant. All the 2421 proteins were implied to volcano plot analysis which identify the up and downregulated proteins. A protein was reflected differentially regulated if the ratio of L-Trp fed to control was less than 0.8 fold it was considered as up and downregulated proteins. Fold change greater than 1.25 was considered as upregulated in at least two biologicals replicates out of three experiments with a p-value less than 0.05 (peptide score above the 20). Two hundred and ten proteins were identified as differentially regulated of which, eighty-three proteins were upregulated and one hundred and twenty-seven proteins as down-regulated (Table. 4).



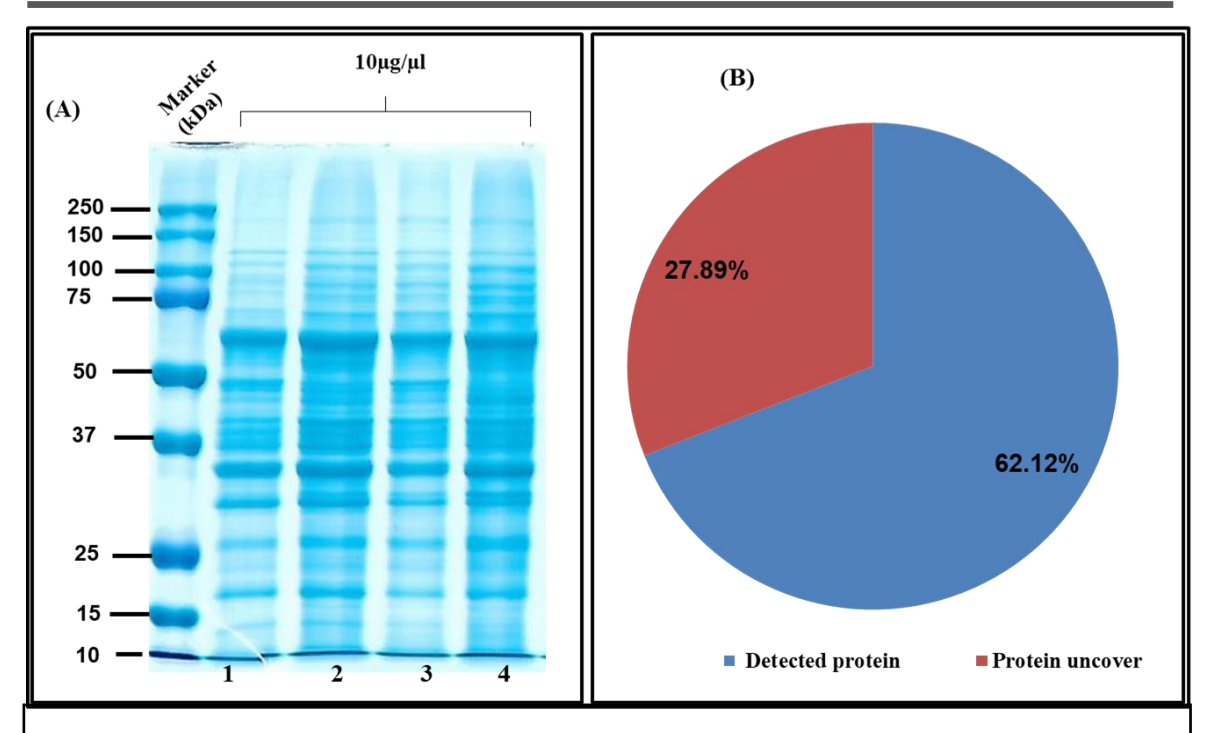


Fig. 45: SDS-PAGE separated protein of *Rbx. benzoatilyticus* (A) as against the proteins identified through iTRAQ (B). Lane 1,3 L-Tryptophan unfed (control) and 2,4 L-Tryptophan fed sample.

Whole cell proteins from control (unfed L-Trp) and L-Trp fed cells proteins were subjected to 12.5% SDS-PAGE analysis. The experimental parameter as similar mentioned in Fig. 16/excluding for the culture was centrifuged and whole cell proteins was isolated (materials and methods section 2.9.1), lyophilized, and analyzed through the iTRAQ (isobaric for tags relative and absolute quantitation). Proteins were differentiated and quantified through the Peak studio 8.5 [ABS Sciences] version data represent three independent experiments.

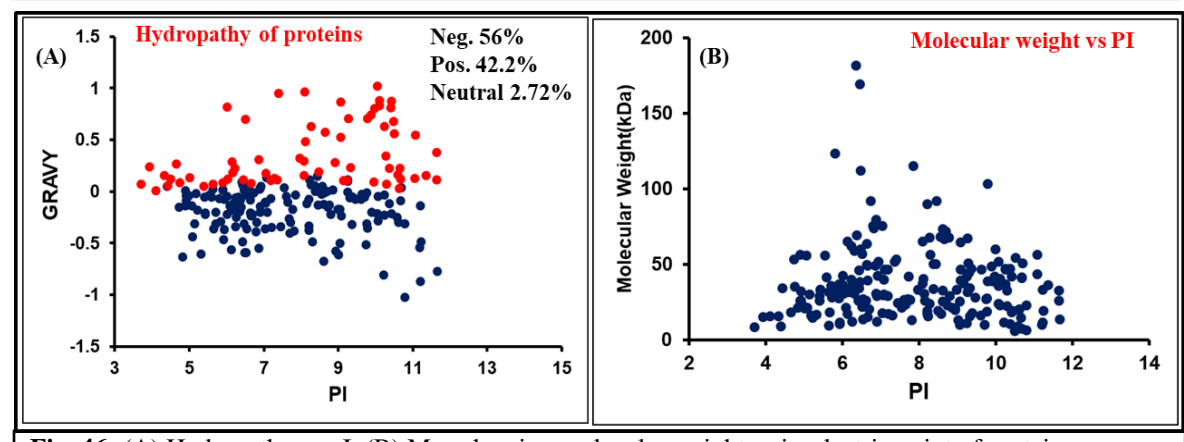


Fig. 46: (A) Hydropathy *vs* pI. (B) Map showing molecular weight *vs* isoelectric point of proteins detected through the iTRAQ.

Proteins detected through the iTRAQ analysis as similar in Fig. 44 were investigation to molecular weight, pI analysis by ExPASy tool (www.expasy.org), and GRAVY (grand average of hydropathy) by Sequence Manipulation Suite (www.bioinformatics.org/sms2/protein_gravy). Red circles indicate hydrophobic (positive GRAVY) and blue circles hydrophilic (negative GRAVY).

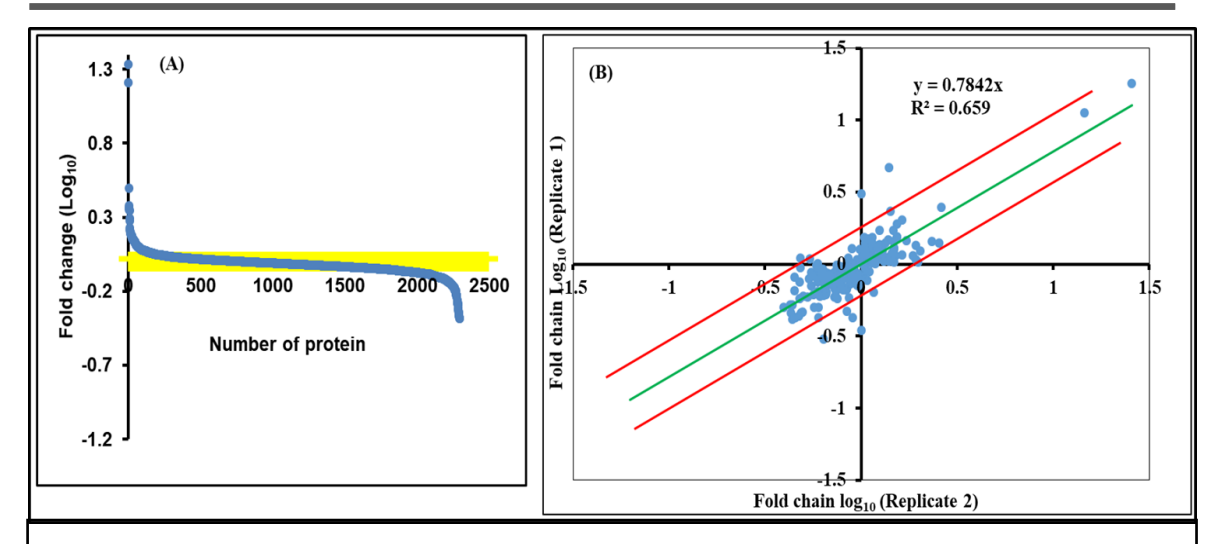


Fig. 47: Fold change measured for global proteins detected by iTRAQ analysis (A). Correlation study of the identified protein through iTRAQ proteins of between independent biological replicates (B).

Proteins identified by iTRAQ analysis as mention in Fig. 44 were used for linear regression analysis. Fold change corresponding protein ratio (L-Trp fed/ unfed; control) from iTRAQ analyzed value were log-transformed (log10) and graph drown by Xcel stat.

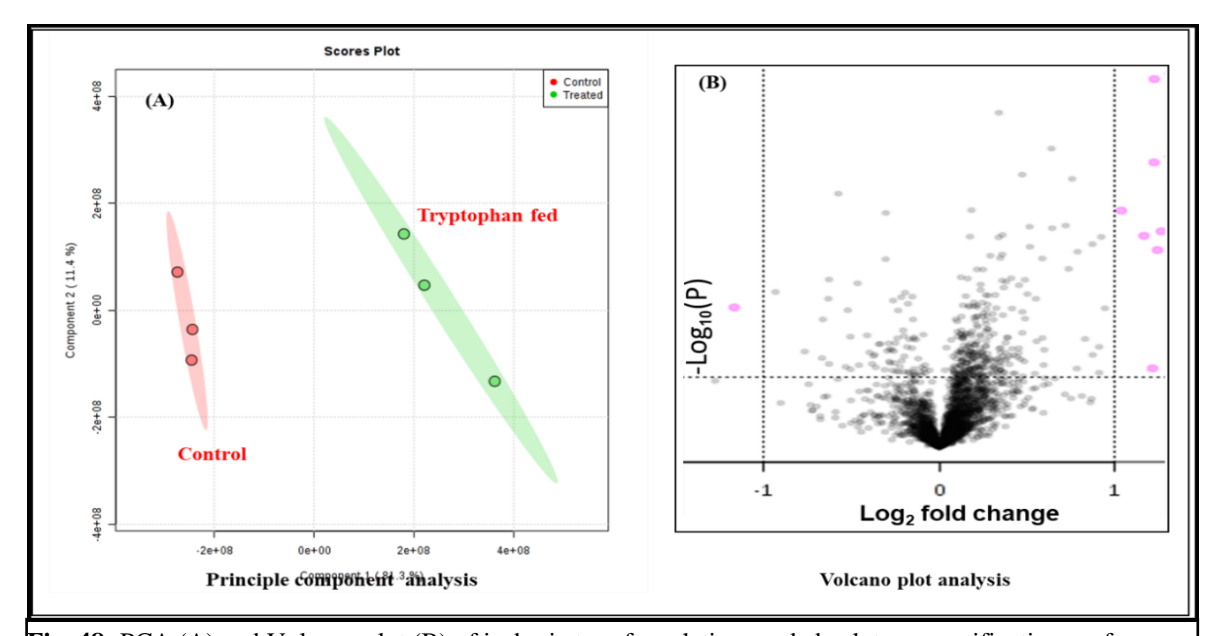


Fig. 48: PCA (A) and Volcano plot (B) of isobaric tags for relatives and absolute quantification of identified proteins of *Rbx. benzoatilyticus*.

Round spot indicate proteins with statistically significant p-value (<0.05/<20 peptide score), on X-axis values indicate up-regulation and negative values down-regulation fold change respective to the protein ratio of L-Trp/control condition cells. Log₁₀ >0.08 was considered upregulated (ratio > 1.25) and log₁₀ < -0.1 was considered downregulated (ratio < 0.8)

3.6.2. Functional classification of proteins

The two-hundred and ten differentially regulated proteins were classified into nineteen different functional classifications according to the KEGG pathways database (http://www.genome.jp/kegg/). Majority of the differentially regulated proteins belonging to cellular metabolism, transcription, translation, membrane transport, signal transduction, stress, replication, energy-related protein, and DNA repair system, cell wall-related proteins, hypothetical proteins, metabolism of vitamins-cofactor, amino acids, and nucleotide metabolism-related proteins (Fig. 49).

Among the upregulated proteins, 25.3% were hypothetical proteins. Proteins related to metabolism (3.44%), energy (6.9%), DNA repair system (2.29%), membrane proteins (11.5%), stress (5.74%), transmembrane (3.44%), lipid metabolism (5.74%), carbohydrate metabolism (6.9%), vitamin and cofactor (4.6%), transcription (6.9%), translation (3.44%), signal transduction (10.44%), and amino acid metabolism (3.4%) were upregulated (Fig. 50A). Proteins related to indole metabolism and other aromatic amino acid metabolism were also differentially regulated. Aromatic aminotransferase, deaminase, and phenylalanine-4-monooxygenase are upregulated.

Among the down-regulated proteins, 18.7% were hypothetical proteins. The other down-regulated proteins are related to those which was involved in membrane transport (8.1%), carbohydrate metabolism and cell wall-related (5.7%), shikimate pathway (0.8%), stress (1.6%), membrane proteins (8.1%), photo-electric system related (8.1%), translation (5.7%), transcription (8.1%), metabolism-related (7.3%), amino acid metabolism (5.7%), nucleotide metabolism (1.7%), lipid metabolism (1.6%), antioxidant related proteins (4%) and fatty acid metabolism (6.5%)(Fig. 50B).

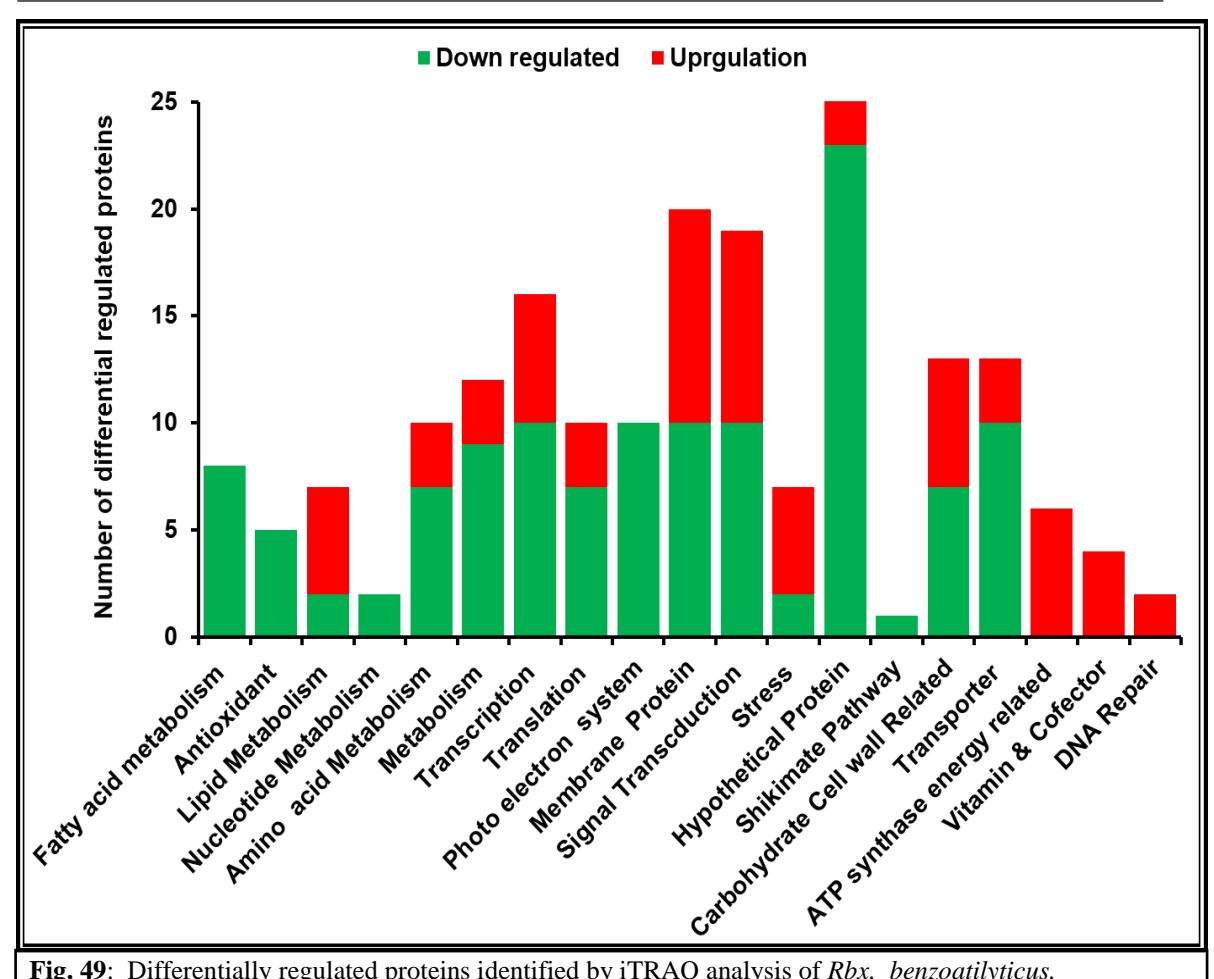


Fig. 49: Differentially regulated proteins identified by iTRAQ analysis of Rbx. benzoatilyticus.

Differentially regulated protein classification was done through the KEGG (Kyoto Encyclopedia of Genes and Genomes pathways database, (www.genome.jp/kegg/). Differentially regulated detected proteins subjected to volcano plot analysis as similar mention in Fig. 47B were functionally showed.

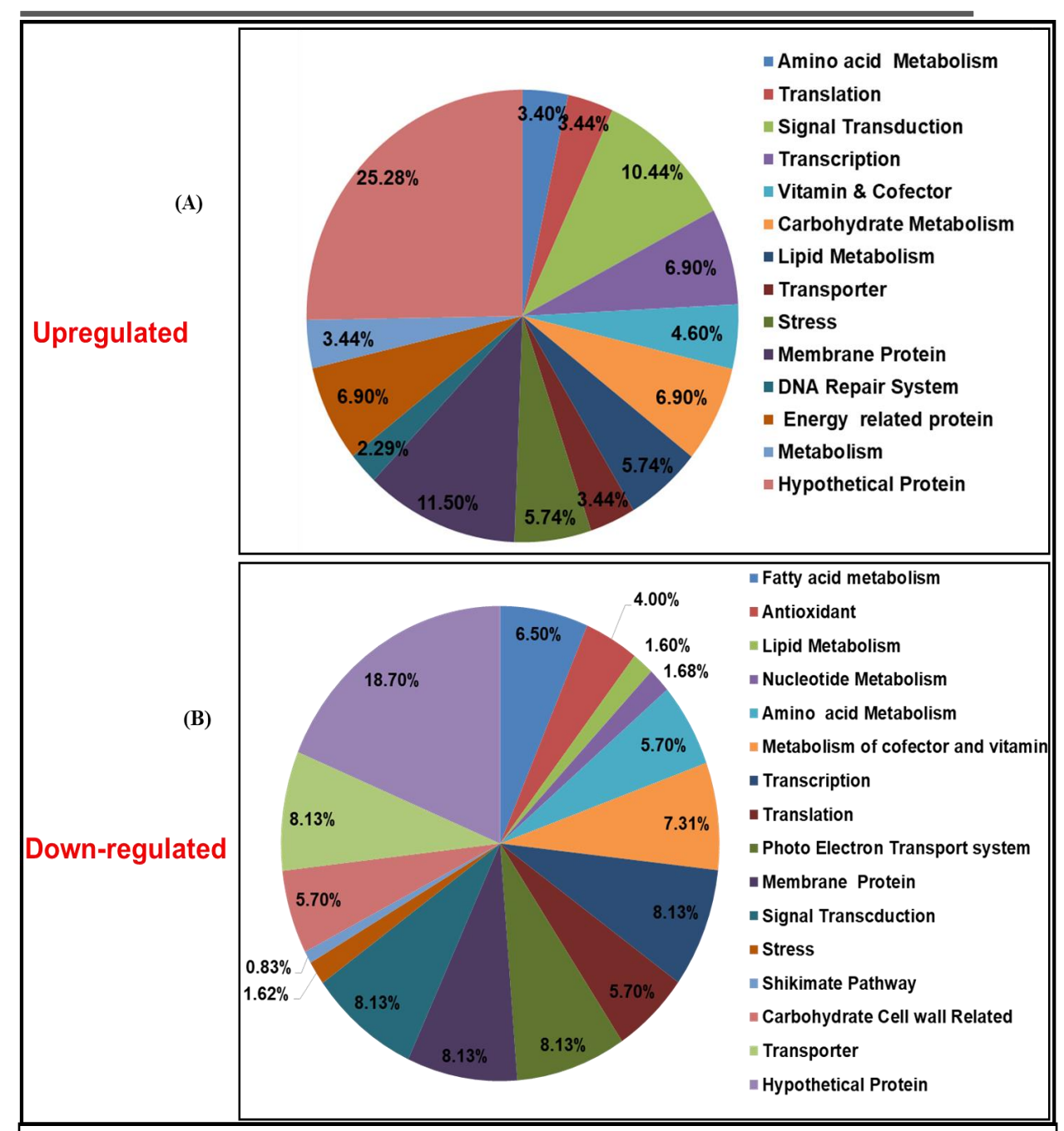


Fig. 50: Functional classification of differentially regulated proteins of *Rbx. benzoatilyticus*. Functional classification of (A) up-regulated and (B) down-regulation protein. Data processing parameters was the same as mentioned in following (Fig. 48).

3.6.3. Cellular response of L-Tryptophan fed by of *Rbx. benzoatilyticus* under chemotrophic conditions

3.6.3.1. *Membrane related proteins*

Proteins related to membrane trafficking were differentially regulated to L-Trp fed conditions. The efflux pumps related protein and putative efflux proteins such as resistance nodulation-cell division (RND) were upregulated (Table. 4). While putative ABC transporter, ABC transporter, TRAP dicarboxylate transporter subunit, translocation protein (TonB), phosphate-binding proteins, polar amino acid transporter, ABC transporter permease, putative ABC transporter for ATP-binding protein, putative transporter efflux transmembrane protein was upregulated. Vitamin B_{12} transporter, transcriptional regulator NifA, zinc-binding alcohol dehydrogenase, succinyl-CoA synthetase β -subunit, methylmalonyl-CoA (Mut-CoA) mutase maltoporin and many extracellular solute-binding proteins were down-regulated (Table. 4).

3.6.3.2 Signal transduction related proteins

Signal transduction related proteins like histidine kinase, putative high potential iron-sulfur (hipip) signal peptide protein, diguanylate cyclase/phosphodiesterase, response regulator protein (RR), YidE/YbjL duplication protein, signal recognition particle protein, PAS/PAC hybrid histidine kinase, signal transduction histidine kinase-like protein, diguanylate cyclase/phosphodiesterase were up-regulated. While, the response regulator receiver protein, signal transduction histidine kinase, twitching motility protein, multisensor hybrid histidine kinase and methyl-accepting chemotaxis sensory transducer were down-regulated in L-Trp fed cells when grown chemotrophically (Table. 4).

3.6.3.3 Transcription and translation-related proteins

Transcription factor-like radical SAM family proteins, two-component PAS/PAC sensor hybrid histidine kinase were upregulated while transcriptional regulator NifA, zinc-binding alcohol dehydrogenase, saccharopine dehydrogenase were downregulated protein. Nitrogen regulatory protein two-component transcriptional regulator, silent information regulation (Sir2), putative transmembrane sensor histidine kinase transcription regulator protein and TetR family transcriptional regulator have also upregulated in L-Trp fed conditions (Table. 4). Translation related protein such as the 50S and 30S subunits, sigma 54 modulation protein/ribosomal proteins S30EA and GTP-binding protein, and some chaperon associated protein ES was also upregulated in L-Trp fed conditions (Table. 4).

3.6.3.4. Proteins related to metabolism

De-novo aromatic amino acid biosynthesis i.e Shikamate pathway-related proteins except for iso-chorismate synthase which was downregulated, others *viz.*, tryptophan synthase α, β subunits, 3-dehydroquinate dehydratase and anthranilate synthase, were remained unaffected in L-Trp fed cultures of *Rbx. benzoatilyticus* cultivated under aerobic conditions. Proteins related to aromatic amino acid catabolism like tryptophan, phenylalanine-4-monooxygenase, and aromatic aminotransferase were upregulated in L-Trp fed conditions (Table. 4). Proteins that are related to citric acid metabolisms like pyruvate flavodoxin/ferredoxin oxidoreductase, oxidoreductase, and NADH dehydrogenase were up-regulated (Table. 4). Proteins related to sulfur-containing amino acids, glycine cleavage system H protein, isovaleryl-CoA dehydrogenase, S-adenosyl-L-homocysteine hydrolase, cysteine, and methionine related protein were down-regulated (Table. 4).

Proteins related to lipid metabolism, β-oxidation related proteins, methyl-malonyl-CoA mutase (Mut-A), putative phospholipase-A as well as lipid oxidation proteins were all upregulated. Lipid-A biosynthesis acyltransferase, enoyl-CoA hydratase/isomerase, hydroxymethylglutaryl-CoA lyase, and lipoprotein YaeC family proteins were down regulated under L-Trp fed conditions (Table. 4). Carbohydrate metabolism-related proteins; gluycosyl transferase group1, galactosamine-containing minor teichoic acid biosynthesis, polyhydroxyalkanoate, depolymerase, intracellular, poly-beta-hydroxybutyrate polymerase-like protein, inositol monophosphatase were upregulated (Table. 4).

3.6.3.5. Proteins involved in replication and repair mechanism

Proteins involved to replication and repair mechanism such as DNA-directed DNA polymerase, holliday junction DNA helicase RuvA were upregulated under L-Trp fed conditions (Table. 4).

3.6.3.6. Proteins related to stress

Putative transport system ATP-binding protein, putative lipoprotein, putative transmembrane sensor histidine kinase, transcription regulator protein, RND family efflux transporter MFP subunit and phos family proteins PHA granule biosynthesis were upregulated (Table. 4).

3.6.3.7. *Molecular chaperones protein*

Molecular chaperon proteins are a family of proteins belong to protein sorting degradation, folding, miss folded proteins. Class I heat-inducible transcription repressor, cysteine proteinase, transthyretin, and NmrA-like protein were up-regulated in L-Trp fed

cells (Table. 4). Proteins related to urease accessory protein (Ure-D) and co-chaperonin GroES and YceI family proteins were downregulated (Table. 4).

3.6.3.8. Proteins related to antioxidant

Antioxidant related proteins like alkyl hydro-peroxide reductase, thiol specific antioxidant, Mal allergen, alkyl hydro-peroxide reductase, multiple antibiotic resistance (MarC)-like proteins, glyoxalase/bleomycin resistance proteins, dioxygenase, cytochrome ubiquinol oxidase subunit II and benzoate transporter were down-regulated (Table. 4).

Table. 4: Differentially regulated proteins identified through iTRAQ analysis

Accession	Description	Coverage (%)	Avg_Log ₁₀ _Fc	SD
	Protein synthesis			
332109861	50S ribosomal protein L33	48	0.04084	0.551598
332108000	sigma 54 modulation protein/ribosomal protein S30EA	13	0.102664	0.047306
332111487	GTP-binding protein	11	0.154735	0.214125
332109180	selenocysteine-specific translation elongation factor	19	0.0722	0.097365
332109232	50S ribosomal protein L34	16	0.360307	0.616053
332107870	30S ribosomal protein S19	30	-0.17808	0.184761
332107880	30S ribosomal protein S14	21	-0.11481	0.096944
332112450	ribosome recycling factor	9	-0.11663	0.09991
332108097	ribosomal protein 111	25	-0.10547	0.048772
332108090	30S ribosomal protein S12	35	-0.119	0.172108
332112098	ABC transporter-like protein	11	-0.10215	0.070808
	Signal related protein			
332110811	Signal Recognition Particle protein	4	0.098885	0.113059
332107759	kinase-like protein	2	0.071746	0.179213
332108264	cyclic glucan phosphoglycerol modification protein	3	0.085447	0.030267
332112187	PAS/PAC sensor hybrid histidine kinase	10	0.18859	0.060059
332109370	putative high potential iron-sulfur (hipip) signal peptide protein	65	0.1301	0.044504
332109371	diguanylate cyclase/phosphodiesterase	2	0.119413	0.262764
332108263	Crp/FNR family transcriptional regulator	32	0.092187	0.013171
332107914	TetR family transcriptional regulator	5	0.495177	0.552208
332110811	Signal Recognition Particle protein	4	0.098885	0.113059
332111446	methyl-accepting chemotaxis sensory transducer	2	-0.31964	0.240615
332110825	CheW protein	10	-0.37516	0.065022
332111479	response regulator receiver protein	15	-0.35593	0.067809

332111651	osmosensitive K+ channel signal transduction histidine kinase	5	-0.35258	0.0189
332111971	bifunctional 3-demethylubiquinone-9 3- methyltransferase/ 2-octaprenyl-6-hydroxy phenol methylase	38	-0.1088	0.011096
332111476	methyl-accepting chemotaxis sensory transducer	1	-0.38102	0.654661
	DNA replication and repair			
332112171	DNA-directed DNA polymerase	3	0.115652	0.150143
332111924	Holliday junction DNA helicase RuvA	17	0.057922	0.273658
332107903	restriction endonuclease S subunits-like protein	2	0.069152	0.163931
332112572	DNA-directed RNA polymerase subunit omega	15	0.011194	0.351083
	Lipid metabolism			
332110872	acyltransferase WS/DGAT/MGAT	2	0.079363	0.056543
332109922	hydroxyneurosporene synthase	39	0.087351	0.169613
332109204	pullanase-associated protein	63	0.091964	0.006892
332109908	geranyltranstransferase	22	0.144747	0.218178
332111746	diacylglycerol O-acyltransferase	4	0.107592	0.276839
332110050	putative phospholipase A1	2	0.151268	0.042938
332112215	lipid A biosynthesis acyltransferase	3	0.145317	0.250501
332108133	lipoprotein YaeC family	39	0.189666	0.039473
332108566	esterase/lipase/thioesterase family protein	6	0.05022	0.198624
332108038	acetyl-CoA acetyltransferase	42	-0.21714	0.006328
332108563	modular polyketide synthase	1	-0.10136	0.051645
332109100	acyltransferase	3	-0.12577	0.075156
332108035	isovaleryl-CoA dehydrogenase	34	-0.36922	0.023989
332111406	acyl carrier protein ACP	14	-0.13844	0.096934
332108046	enoyl-CoA hydratase/isomerase	18	-0.27939	0.067127
332108044	propionyl-CoA carboxylase	32	-0.38447	0.102906
332108049	hydroxymethylglutaryl-CoA lyase	47	-0.10229	0.027697
332108049	hydroxymethylglutaryl-CoA lyase	47	-0.10229	0.027697
332108116	propionyl-CoA carboxylase subunit alpha	45	-0.22891	0.0419
332109504	butyryl-CoA dehydrogenase	1	-0.32884	0.338557
222111210	Amino acid metabolism and Shikimate pathway	0	0.140020	0.20004
332111318	putative amidase	9	0.140939	0.30094
332107776	phenylalanine 4-monooxygenase	7	0.202764	0.095197
332112186	tryptophanase/L-cysteine desulfhydrase PLP-dependent	69	1.332674	0.077444
332108048	carbamoyl-phosphate synthase L chain ATP- binding protein	29	-0.36947	0.048883
332109992	carboxyl transferase	45	-0.22271	0.075871
332108280	urease accessory protein UreD	6	-0.1222	0.034407
332111194	glycine cleavage system H protein	22	-0.22268	0.252108
332109142	FAD linked oxidase domain-containing protein	10	-0.10996	0.0845
332112222	S-adenosyl-L-homocysteine hydrolase	39	-0.28002	0.078485
332109176	aminotransferase class-III	10	-0.19396	0.012225
	Shikimate pathway and DNA synthesis			
332108691	phosphoribosylaminoimidazole carboxylase ATPase subunit	6	-0.14283	0.114038

332110436	anaerobic ribonucleoside triphosphate reductase	2	-0.13466	0.217804
332110749	chromosome segregation and condensation protein ScpA	3	-0.14727	0.100932
332109290	isochorismate synthase	3	-0.13749	0.053732
332111459	Transporter and membrane protein putative monovalent cation/H+ antiporter subunit	1	-0.05802	0.420715
	A			
332108253	Outer membrane autotransporter barrel	0	0.068139	0.196659
332107761	integral membrane sensor signal transduction histidine kinase	5	0.076886	0.384529
332109251	RND family efflux transporter MFP subunit	31	0.117063	0.059969
332107915	efflux transporter RND family MFP subunit [38	0.13989	0.048904
332112091	putative ABC transporter ATP-binding protein	6	0.111175	0.222226
332109313	ferrous iron transport protein B	1	0.098245	0.109868
332111809	putative composite ATP-binding transmembrane ABC transporter protein	1	0.138235	0.388913
332107916	RND efflux system outer membrane lipoprotein	8	0.185638	0.149292
332109840	periplasmic solute binding protein	9	0.071161	0.134452
332107651	Toluene transport system ATP-binding protein	27	0.084401	0.044122
332108220	pirin domain-containing protein	31	0.155951	0.035126
332112675	putative transport/efflux transmembrane protein	19	0.082792	0.053814
332107661	fimbrial assembly protein	33	-0.10484	0.110642
332107926	periplasmic protein thiol	45	-0.15162	0.044629
332110893	twitching motility protein	26	-0.15815	0.271268
332111814	putative polar amino acid transport system ATP- binding protein	32	-0.13394	0.176881
332107951	TonB-dependent siderophore receptor family protein 13	21	-0.16554	0.06996
332108054	acetate permease	5	-0.11278	0.079658
332110494	putative transmembrane protein	3	-0.14081	0.072124
332110561	potassium transporter	4	-0.11468	0.042608
332107546	anaerobic c4-dicarboxylate membrane transporter family protein	2	-0.13614	0.103902
332108262	molybdenum cofactor sulfurylase	3	-0.17466	0.173397
332109185	formate dehydrogenase subunit alpha	2	-0.17561	0.104479
332109907	cytochrome c-552 precourser	8	-0.17582	0.052807
332111853	putative molybdenum transport protein	14	-0.0929	0.021991
332109844	transcriptional regulatory protein	6	-0.17283	0.167103
332111449	putative two-component response-regulatory protein YehT	19	-0.1277	0.080353
332108330	transcriptional regulator NifA	1	-0.14688	0.088084
332109946	zinc-binding alcohol dehydrogenase	17	-0.11676	0.133698
332107887	preprotein translocase subunit SecY	7	-0.13029	0.124596
332109483	integration host factor alpha-subunit	24	-0.11619	0.034022
332107589	LysR family transcriptional regulator	14	-0.10051	0.083997
332111850	heavy metal translocating P-type ATPase	15	-0.12095	0.081188
332110560	benzoate transporter	11	-0.1877	0.076029
332107543	nucleoid protein Hbs	61	-0.15722	0.282477
332109092	putative N utilization substance B	12	-0.12442	0.161277
	Stress protein			

332107928	CcmE/CycJ protein	15	-0.15134	0.131878
332109993	membrane ATPase/protein kinase	33	-0.17719	0.0347
332108331	co-chaperonin GroES	83	-0.15371	0.19239
332110848	alkyl hydroperoxide reductase/ Thiol specific antioxidant/ Mal allergen	60	-0.19266	0.010722
332110906	alkyl hydroperoxide reductase/ Thiol specific antioxidant/ Mal allergen	18	-0.17158	0.144799
332111629	multiple antibiotic resistance (MarC)-like protein	6	-0.13695	0.254592
332108118	glyoxalase/bleomycin resistance protein/dioxygenase	42	-0.19508	0.142838
332111669	cytochrome d ubiquinol oxidase subunit II	2	-0.12017	0.159393
332109995	GntR family transcriptional regulator	5	-0.15548	0.02108
	Vitamin cofactor			
332108336	TMAO/DMSO reductase	15	-0.14844	0.032776
332110824	biotin carboxyl carrier protein	42	-0.19579	0.182103
332108117	biotin synthase	6	-0.10906	0.063372
332112748	adenosylcobinamide-phosphate synthase	3	-0.1891	0.313741
332112223	5 10-methylenetetrahydrofolate reductase	18	-0.14677	0.009864
332109937	coenzyme B12-binding aerobic repressor	14	-0.10784	0.066481
332107698	Metabolism protein radical SAM family protein	11	0.154951	0.158851
332107098		18	0.364764	0.138831
	blue (type 1) copper domain protein			
332108733	methyltransferase FkbM family protein	5	0.226199	0.145732
332112236	dihydroneopterin aldolase	15	0.130216	0.149005
332109196	glutaconyl-CoA decarboxylase	7	0.053243	0.19207
332109093	6 7-dimethyl-8-ribityllumazine synthase	53	0.079186	0.063707
332108628	precorrin-2 C20-methyltransferase	3	0.150192	0.493323
332108584	glycosyl transferase group 1	3	0.097229	0.273457
332108769	group 1 glycosyl transferase	3	0.143037	0.163735
332108575	galactosamine-containing minor teichoic acid biosynthesis	1	0.169162	0.127898
332111130	polyhydroxyalkanoate depolymerase intracellular	32	0.068569	0.219222
332110443	poly-beta-hydroxybutyrate polymerase-like protein	1	-0.07346	0.722681
332108738	inositol monophosphatase	46	0.173587	0.024237
	Cell wall protein			
332109978	metallophosphoesterase	3	-0.09871	0.037705
332107758	peptidyl-dipeptidase Dcp	16	-0.10792	0.089857
332109465	hydrolase	5	-0.34223	0.165655
332107618	acetylpolyamine aminohydrolase	23	-0.09649	0.067847
332111736	peptidoglycan-binding domain-containing protein	10	-0.10069	0.096295
332111521	phospho-N-acetylmuramoyl-pentapeptide- transferase	2	-0.11161	0.108067
332109122	putative HtrA-like serine protease signal peptide protein	7	-0.11227	0.158704
332108581	polysaccharide deacetylase	3	-0.26709	0.114778
332108759	mannose-1-phosphate guanylyltransferase/mannose-6-phosphate	12	-0.1016	0.071808
332110816	isomerase N-acetyl-anhydromuranmyl-L-alanine amidase	19	-0.13796	0.040107
332112579	HAD-superfamily hydrolase subfamily IA	18	-0.11876	0.040375
	variant 3			

332108541	alpha/beta hydrolase fold protein	24	-0.12101	0.079825
	Hypothetic proteins			
332108504	hypothetical protein RBXJA2T_05333	3	0.190241	0.246682
332111444	hypothetical protein RBXJA2T_13904	3	0.181876	0.227014
332111907	hypothetical protein RBXJA2T_16222	3	0.19531	0.123126

Protein ratios of L-Tryptophan fed and control condition identified under chemotrophically were \log_{10} transformed, and values are mean \pm standard deviation of three independent biological replicates experiments. Proteins discovered in at least two out of three replicates with two peptide and one unique peptide, fold change of >1.25, and P-value \leq 0.05 (peptide score 20 >) were presented in the table. Proteins shaded in gray and dark indicate upregulated, and unshaded are down-regulated



4.0 Discussion

Bacteria have adapted remarkable strategies to survive under a wide range of environmental conditions through their extended range of carbon as well as nitrogen sources utilization (Berkhout et al., 2013; Carbonero et al., 2014; Chubukov et al., 2014; Mosier et al., 2013; Lakshmi et al., 2018). Bacteria meet their energy and carbon demands from aliphatic and aromatic hydrocarbons (Brzeszcz and Kaszycki, 2018; Das and Chandran, 2011). Compared to the aliphatic hydrocarbon metabolism, which is widespread among bacteria, aromatic hydrocarbon metabolism is restricted to a few bacteria (Carmona et al., 2009) since many of these are xenobiotic (Carmona et al., 2009; Teufel et al., 2010) and anthropogenic (Johnson et al., 2012; Ramos et al., 2002).

Besides anthropogenic aromatic hydrocarbons, naturally occurring aromatic hydrocarbons(Fuch and boll, 2011) are the major sources of carbon pool mainly derived from the lignin degradation (p-coumaryl alcohol, coniferyl alcohol, sinapyl alcohol) and decay of plant and animal biomass (aromatic amino acids, nitrogen-containing heterocyclic aromatic compounds) (Larimer et al., 2004) are some of the natural sources of aromatic compounds and the aromatic ring serves as a source of carbon/nitrogen for many aerobic and anaerobic bacteria (Gorontzy et al., 1993; Liang et al., 2005). On the other hand, some bacteria cannot degrade the aromatic ring but can use the aromatic substituted aliphatic chain as a source of carbon or nitrogen resulting in biotransformation (Vangnai and Petchkroh, 2007). Bacterial transformation of aromatic hydrocarbons is extensively studied particularly aromatic amino acids, resulting in the formation of several novel bioactive biomolecules (Lakshmi et al., 2018, 2019a,b; Damla et al., 2019; Shuhei and Konda, 2017; Fengli et al., 2018; Ramesh et al., 2016; Bongaerts et al., 2001; Lee et al 2012; Wang et al., 2018; Ranjith et al., 2007a,b; Sáez et al., 1999). Although many groups bacteria

biotransform aromatic amino acids, photo-biotransformation of aromatic amino acids by anoxygenic group of photosynthetic bacteria is an upcoming and interesting area since these organisms use light as a source of energy resulting in high efficiency in the biotransformed product formation in addition to producing novel metabolites (Kumavath et al., 2010b; Mujahid et al., 2011b; Mujahid et al., 2014; Ranjith et al., 2007). Most of the phototrophic purple non-sulfur bacteria are facultative aerobes that can oxidize many aromatic compounds both anaerobically and aerobically *via* two completely different pathways, with the aerobic pathways requiring oxygen (Lakshmi et al., 2018; Gibson et al., 2002; Harwood et al., 1998).

Previous studies with *Rbx. benzoatilyticus* clearly showed that the dynamics of metabolite footprints greatly depend on the physiological lifestyle of the organism together with the substrate availability for transformation (Lakshmi et al., 2018, 2019a,b: Kumavath et al., 2010a,b; Lakshmi et al., 2012; Mujahid et al., 2011b). In this study a phototrophic bacterium, *Rbx. benzoatilyticus* was fed with L-Trp was used as sole sources of nitrogen under the chemotrophic (dark aerobic) conditions to explore oxidative L-Trp metabolic potential. L-Trp utilization by *Rbx. benzoatilyticus* under chemotrophic conditions was similar to that of phototrophic (light anaerobic) condition (Mujahid et al., 2011b). However, under chemotrophic condition L-Trp is completely utilized within 18-24 h (Fig. 16) while in phototrophic condition it is not completely utilized (0.2 mM remained unutilized at 48 h) (Mujahid et al., 2011b).

This result indicates that the presence of oxygen might have an influence on the L-Trp utilization or biotransformation by *Rbx*. *benzoatilyticus*. It was observed that generation time of 6.0 ± 0.5 h of *Rbx*. *benzoatilyticus* under chemotrophic conditions

represent its slow growth as compared to phototrophic conditions (Mujahid et al., 2011b). These results explain the preferred growth mode of *Rbx. benzoatilyticus* is phototrophic condition (Mujahid et al., 2011b) despite the organism has also adapted to chemotrophic condition. However, in an either of the case, the substrate, L-Trp was used as a sole source of nitrogen and not as carbon or carbon and nitrogen source and it correlated well with previous report (Mujahid et al., 2011b). Earlier study revealed production of indole or indole derivatives by *Rbx. benzoatilyticus* by utilization of L-Trp as sole sources of nitrogen under phototrophic conditions(Mujahid et al., 2011b). Similarly in the present study, chemotrophic conditions also lead to the secondary metabolites production by *Rbx. benzoatilyticus* in the presence of L-Trp as compared to the control. The change in the color of culture supernatant observed under chemotrophic condition (dark brown color) (Fig. 29 B,D) compared to the phototrophic incubations (Fig. 29E,F) is possibly due to the accumulation of colored metabolites formed as a result of chemotrophic incubation.

L-Tryptophan metabolism under chemotrophic incubations by Rbx. benzoatilyticus

The enzyme tryptophanse (EC: 4.1.99.1) which catalyzes the formation of indole and pyruvate is predicted from the genome of *Rbx. benzoatilyticus* and its activity is demonstrated in an earlier study (Mujahid et al., 2011b) as well as current study. The indole ring of L-Trp remained unutilized by *Rbx. benzoatilyticus* either as carbon or nitrogen source which could be because of the absence of genes coding for ring cleavage enzymes such as aromatic dioxygenase (under aerobic conditions) and benzoyl-CoA thioesterase (under anaerobic conditions) in the genome of *Rbx. benzoatilyticus* (Mujahid et al., 2011a). Similar results were reported with other phototrophic bacteria; *Rhodobacter sphaeroides* (Ranjit et al., 2007b) and *Rhodobacter capsulatus* (Sáez et al., 1999) which

could not utilizes other aromatic amino acid as sole source of carbon (Lakshmi et al., 2018). Similarly, *Rbx. benzoatilyticus* utilizes other aromatic amino acid (L-Phe, L-Tyr) only as a sole source of nitrogen (Lakshmi et al., 2018). The present study provides a comprehensive understanding of L-Trp biotransformation under chemotrophic conditions and the same was discussed in greater detail.

L-Tryptophan/5-hydroxytryptophan catabolism under chemotrophic conditions by Rbx. benzoatilyticus

The central pathway of amino acid catabolism is known as Ehrlich's pathway, which leads to the production of alcohol and carboxylic acid-containing aromatic organic compounds which have one carbon atom less than the precursor amino acid (Ravasio et al., 2014). Aromatic aminotransferases, decarboxylases (EC: 1.2.7.1) and dehydrogenases (EC: 1.2.4.1) are directly involve in aromatic amino acid biotransformation via Ehrlich's pathway (Ranjit et al., 2007b; Mujahid et al., 2011b; Lakshmi et al., 2018). Rbx. benzoatilyticus genome has gene encoding for putative aromatic amino transferase (EC: 2.6.1.27), which help in the conversion of L-Trp to indole-3-pyruvic acid. Furthermore, genome analysis of Rbx. benzoatilyticus also indicated the presence of genes encoding for decarboxylases (EC: 1.2.7.1) and dehydrogenases (EC: 1.2.4.1), which are involved in the conversion of indole-3-pyruvic acid to indole-3-acetic acid thus indicating the possible existence of Ehrlich's pathway even in Rbx. benzoatilyticus (Fig. 41 and 52). It is well documented that Rbx. benzoatilyticus under phototrophic conditions produces indole-3acetic acid through the IPyA (Kumavath et al., 2010), indole-3-acetamide and indole-3acetonitrile pathways (Mujahid et al., 2011b), while similar pathways responsible for indole-3-acetic acid production were observed in chemotrophic conditions in this study (Fig. 52). These results suggest that the formation of indole-3-acetic acid by *via* these pathways is independent of the physiological life style of the organism.

Although Ehrlich pathway metabolites were identified in both phototrophic (Mujahid et al., 2011b) and chemotrophic conditions (Fig. 52), however the range of metabolites varied. Under chemotrophic incubation of Rbx. benzoatilyticus with L-Trp as sole source of nitrogen produces an array of indole derivatives as a result of the downstream process of L-Trp metabolism (Fig. 52), which were not observed under phototrophic incubations (Mujahid et al., 2011b). Some of these were identified as kynurenic acid, indole-3-propionic acid and many hydroxy-indole derivatives (Table.1 and 2). Kynurenic acid is a product of oxidative metabolism of L-Tryptophan in microorganisms (Kurnasov et al., 2003; Liu et al., 2020; Mona et al., 2019) and this is the first report of kynurenic acid production by a phototrophic bacterium under chemotrophic conditions but not under phototrophic incubations. Kynurenic acid is a neurologically active molecule considered as a neuromodulator to release of neurotransmitters as glutamate, dopamine and acetylcholine. The detection of kynurenic acid supports the existence of the kynurenine pathway of L-Trp catabolism in *Rbx. benzoatilyticus* (Fig. 52). However, genome mining of Rbx. benzoatilyticus did not show the presence of kynurenine monooxygenase (KMO) or its homologs enzyme encoding genes probably suggest the formation of kynurenic acid is due to the non-specific activity of other monooxygenase (s). The existence of kynurenine pathway in Rbx. benzoatilyticus is also supported by the detection of hydroxy-kynurenic acid (Table. 1, 2 and 3) when 5-OH Trp was used as precursor. Finally, the kynurenine pathway in Rbx. benzoatilyticus was confirmed through the stable isotope (¹³C₁₁-Trp) metabolic profiling wherein kynurenic acid and hydroxykynurenic acids were identified based on increase in molecular ion mass (M+0) to 10 units (M+10) (Table. 2).

Stable isotope metabolic profiling of ¹³C₁₁-Trp fed cultures indicated the abundance of mono-indoles (compounds with single indole nucleus) with increase in mass by +8, +9, +10 and +11 (Table. 2). Some of these were confirmed as skatole, indole-3-acrylic acid, indole-3-acetic acid, indole-3-propionic acid, 5-hydroxyindole-3-acetic acid, 5-hydroxyindole-3-acetic acid, 5-hydroxyindole-3-acetic acid acid acid and 3-amino-3-(1H-indol-3-yl) propanoic acid (Table. 2). As expected, large number of indoles produced under chemotrophic conditions were hydroxyindole derivatives (Table. 2), which are not observed under phototrophic metabolism by *Rbx. benzoatilyticus* (Mujahid et al., 2011b).

Genome analysis of *Rbx. benzoatilyticus* showed the presence of phenylalanine 4-monooxygenase (EGJ09000) and other monooxygenase which may have role in L-Trp hydroxylation. Similarly, the utilization 5-OH Trp as a sole source of nitrogen by *Rbx. benzoatilyticus* was studied under both phototrophic (data not shown) and chemotrophic conditions. The metabolic profiling of 5-OH Trp fed culture supernatants revealed production of 5-hydroxy-indole-3-acetic acid (5-OH IAA) and 5-hydroxyindole derivatives suggesting 5-OH Trp metabolism through the Ehrlich's pathway (Table. 3). The 5-OH Trp catabolism in *Rbx. benzoatilyticus* revealed some unidentified 5-hydroxyindole derivative metabolites (Table. 3) possibly indicating the other unknown catabolic pathway(s). These results suggests that *Rbx. benzoatilyticus* a just like L-Trp catabolism has remarkable 5-OH Trp biotransformation ability under chemotrophic conditions.

L-Tryptophan dependent pigment biosynthesis by Rbx. benzoatilyticus

Few bacteria are capable of producing pigments such as indigo (Guang et al., 2015) and violacein (Hoshino et al., 2011) as a result of L-Trp biotransformation under varying conditions. Similarly, Rbx. benzoatilyticus uses L-Trp as the sole source of nitrogen and produces pigmented metabolites under chemotrophic condition but not phototrophic conditions. This was evident from accumulation of the colored metabolite in the supernatant of L-Trp fed cultures formed possibly due to L-Trp biotransformation (Fig. 29 B,D). This is further supported by the differences in the metabolite profiling observed in culture supernatants of L-Trp fed and control conditions using TLC (Fig. 17A, B) and HPTLC (Fig. 17 C, D,E) analysis. Different colored metabolites such as yellow, pink, orange, and red were observed on thin layer chromatography analysis under chemotrophic incubated culture supernatant (Fig. 29B,D and 17B). Further, these metabolite displayed both UV-Vis absorption range (280 nm aromatic nucleus; >400 nm visible) thus suggesting the presence of the aromatic nucleus in the metabolites. Ethyl acetate and methanolic fractions obtained from L-Trp fed under chemotropic conditions also displayed the absorption maxima at 270,280,290 nm indicating the presence of the indole nucleus in the metabolites (Fig. 20). Unlike chemotrophic incubations (Fig. 29 B,D) Rbx. benzoatilyticus did not show any pigment metabolites under phototrophic incubations (Mujahid et al., 2011b; Fig. 29E,F)). This indicates that pigmented metabolite production is an oxygendependent mechanism in Rbx. benzoatilyticus. Further, mass spectrometric characterization revealed major pigmented metabolite; The yellow pigmented metabolite with a molecular mass 358 [M] was identified as an indole trimer (Fig. 19) with characteristic similarity to indoxyl red (Kevin McClay et al., 2015). In addition, we have identified a few conjugated indole ring containing metabolites under chemotrophic

conditions which display increase in mass by +16, +17, +18, +19, +26 units in stable isotope studies suggests (Table. 2), the possible of role of oxygen and oxygenases in coupling of hydroxy-indole into dimer and trimers. Similarly, the coupling and conjugation of indole into indole dimer or trimers in the presence of laccase and monooxygenase/indole monooxygenases/ styrene monooxygenase / toluene-4-monooxygenase (Heine et al., 2019) were well studied in wild types and engineered bacteria (Kevin McClay et al., 2015).

Mining of *Rbx. benzoatilyticus* genome for oxygenases revealed putative laccase (EGJ10298) and phenylalanine 4-monooxygenase (EGJ09000) and other non-specific monoxygenase and we speculate that these enzymes might be participating in the coupling and dimerization of indole during the chemotrophic L-Trp metabolism. Bacteria such as *Pseudomonas mendocina* KR1, *Haemophilus influenzae* (Stull et al., 1995), *Pseudomonas aureofaciens* (Hamill et al., 1967), engineered *E. coli* (Kevin-McClay et al., 2013), *Janthinobacterium*, and *Collimonas* produced conjugated indoles metabolites such as indigo dye and violacein from L-Trp biotransformation. Although *Rbx. benzoatilyticus* formed indole conjugates these indole derived pigments were neither indigo nor violacein (Fig. 18).

Characterization of melanin produced by Rbx. benzoatilyticus

Many bacteria naturally produce different types of pigments such as melanins (Coelho-Souza et al., 2014; Sajjan et al., 2010; Youngchim et al., 2013) as a result of biotransformation of L-Tyr/L-Phe or Acetyl-CoA under aerobic conditions. Similarly, chemotrophic (dark aerobic) incubation of *Rbx. benzoatilyticus* feeding with L-Trp or 5-OH Trp produced brown pigment which is not a product of photometabolism (Fig. 29 E,F). Further the brown pigment produced by *Rbx. benzoatilyticus* was insoluble in organic

solvent suggests its melanoid nature and the physicochemical properties of melanin was characterized according to Ellis and Griffith 1974 (Fig. 30).

The SEM analysis of brown pigment showed unorganized aggregates while dispersed form showed homogenous smooth surfaced/typical bead-like granule(Fig. 31 A and B), a characteristic feature of melanins (Saini and Melo 2015). The UV-Visible spectrum of brown pigment showed a higher absorption in UV region compared to visible region similar to that of previously reported melanins (Saini and Melo 2015; Goncalves et al., 2012; Fig. 32) while the IR spectrum of the brown pigment indicates the presence of – OH or -NH,-CH, -C=C-,-CO and -CN typical functional group (Fig. 34) as similar to eumelanin (Banerjee et al., 2014; Glass et al., 2012; Centeno and Shamir 2008). Further, the singlet ESR signal showed by the brown pigment indicates stable free-radicals (paramagnetic) in nature of the pigment (Fig. 33A) which is as a characteristic melanins (Lakshmi et al., 2019). X-ray diffraction analysis of the brown pigment showed a broad diffraction peak, which indicated on its amorphous in nature (Fig. 33B) as similar observation was found for other melanins (Lakshmi et al., 2019).

The high C/H (8.9%) ratio of pigment suggests that the brown pigment has conjugated aromatic rings which is also characteristics feature of melanins (Saini and Melo 2015; Hu et al., 2019). The presence of high (9%) nitrogen content and absence of sulfur moiety further indicates that brown pigment is possibly a nitrogen-containing eumelanin. The ¹³C solid-state NMR of the brown pigment has peak at 160 ppm in the carboxyl region which indicates the presence of carbonyl carbon atoms of amides, carboxylates, and quinones which are associated with the pigment (Fig. 35A) as also usually observed with eumelanin (Glass et al., 2012; Banerjee et al., 2014; Centeno and Shamir 2008). The ¹⁵N NMR spectrum has an intense broad chemical shift of the nitrogen atom of indole/pyrrole

moiety (Fig. 35B) which is also a characteristic feature of heterocyclic aromatic moiety of the eumelanins (Adhyaru et al 2003; Chatterjee *et al.*, 2014). The solid-state ¹³C NMR (Fig. 35A) and ¹⁵N NMR (Fig. 35B) data reveals that the brown pigment showed the presence of both aliphatic and aromatic molecules and this is very close to human hair melanin (Ghiani et al., 2008). The ¹⁵N NMR spectrum of brown pigment is also similar to ¹⁵N spectrum of indole-type sepia and human hair melanin (Centeno and Shamir, 2008) which was evident from characteristics signals shown by brown pigment.

Further, brown pigment degradation and chromatographic (TLC) analysis showed a similar pattern of two purple color bands after staining with indole specific TLC reagent (Ellis and Griffith, 1974), which indicates indole derivatives (Fig. 36). Detection of pyrrole derivatives, marker of eumelanin in chemical oxidation studies of brown pigment confirms it as an indole polymer; as pyrrole units are formed as result of chemical oxidation of indoles (Saini and Melo, 2015), Although the both brown pigments L-Trp and 5-OH Trp fed by Rbx. benzoatilyticus were showed the marker of eumelanin, Trpmelanin DHICA (Dihydroxy indole carboxylic acid) based eumelanin while (brown pigment) OH Trp-melanin is a DHI (Dihydroxyindole) and DHICA based eumelanin (Fig. 37C). The quantification of brown pigment from L-Trp and 5-OH Trp fed by Rbx. benzoatilyticus has revealed that higher yields of brown pigment production in the case of 5-OH Trp fed cultures compared to L-Trp fed conditions (Fig. 27B), which indicates 5-OH Trp may be an immediate precursor to brown pigment formation (Fig. 27C). Although, the chromatographic analysis showed some indole derived metabolites in the case of L-Trp fed condition no such indole found in case of 5-OH Trp fed condition only brown pigment (Fig. 27A).

Our result suggested that in L-Trp fed conditions most of the L-Trp was channelized toward indole derivatives while only minor amount of L-Trp was biotransformed to 5-OH Trp leading to brown pigment formation (Fig. 27C). This was further supported by the metabolomics analysis wherein the detection of 5-OH Trp and 5-hydroxyindole-3-acetic acid L-Trp fed cultures under chemotrophic condition. Genome analysis of *Rbx. benzoatilyticus* has shown the presence of monooxygenase enzymes which involve in hydroxylation of aromatic rings. Proteome analysis of L-Trp fed under chemotrophic cultures revealed upregulation of phenylalanine-4-monooxygense which involves in conversion of L-Phe to tyrosine specifically or hydroxylation of other aromatic non-specifically (Liu et al., 2020; Roberts and Fetzpatrick, 2013; Arias et al., 2004; Daubner et al., 2011; Lakshmi et al., 2019). Thus we speculate that the upregulated the phenylalanine 4-monooxygense possibly the playing the crucial role in conversion of L-Trp to 5-OH Trp and 5-hydroxyindole derivatives. These intermediates of 5-hydroxyindole derivatives are precursor to the brown pigment (Fig. 27C).

In Raper Mason Pathway (Raper, 1928; Mason, 1948), L-Tyr/L-Phe act as a precursor for the 5,6-dihydroxyindole (DHI) and 5,6-dihydroxyindole carboxylic acid (DHICA) which are further copolymerizes to form eumelanin, while pyomelanin formation was observed from homogenasitic acid (Lakshmi et al., 2018; Turick et al 2008; Zheng et al., 2013; Chai et al., 2012). Melanin bio-production from the precursor of L-Trp is not reported to date. Recently, it was reported that tryptophan hydroxylase is required eye melanogenesis (pigment production) in planarian larva (Lambrus et al., 2015) enzyme converts L-Trp to 5-OH Trp, and their derivatives of 5-hydroxytryptamine can involve melanin production (Vogliardi et al., 2002). Consistently with this scenario, in the present study, L-Trp may have converted to 5-OH Trp or its immediate hydroxy-indoles

derivatives which act as precursors of melanin. Furthermore, well-known eumelanin pathways specific inhibitor kojic acid (Drewnowska et al., 2015) did not affect pigment production in Rbx. benzoatilyticus and this hinted the existence of non-canonical melanin biosynthesis in Rbx. benzoatilyticus. These result suggests that DOPA or homogentisic acids independent melanin biosynthesis pathway from L-Trp in Rbx. benzoatilyticus (Fig. 38A). Furthermore, sodium-azide, a monooxygenase inhibitor, inhibited of Trp-melanin (Fig. 38B) biosynthesis while 5-OH Trp-melanin remained unaffected. This result can be explained that monooxygenase enzyme interferes with L-Trp hydroxylation thereby 5-OH Trp formation and subsequent pigment production (Fig. 38B). These results strongly suggests that OH-indoles roles in pigment synthesis in Rbx. benzoatilyticus. This scenario corroborated with hydroxy-indole derivatives being immediate precursor to CYP-melanin biosynthesis (Park et al., 2020). CYP-melanin was produced from OH indole which was formed in the presence of cytochrome P450 monooxygenase (CYP102G4) dependent hydroxylation of indole ring (Nambung et al., 2019). *In vitro* melanogenesis from L-Trp or 5-OH Trp only by chemotrophic cell-free extract (Fig. 39 A, B) revealed that the enzymatic system required for melanin biosynthesis in Rbx. benzoatilyticus occur only in aerobically grown (Fig. 39 A, B).

Melanins are an enigmatic pigments of biological life forms and their biogenesis is through the canonical precursors (Fig 51), L-Tyr or Acetyl–CoA (Lambrus et al 2015; Vogliardi et al., 2002; Allegri et al., 2003). Our present work discusses melanin biosynthesis by *Rbx. benzoatilyticus* (Fig. 51) from L-Trp or its derivatives OH-Trp/hydroxy-indole derivatives. However, the high yield of melanin in the presence of OH-Trp possibly (Fig. 27 B, C) because of the availability of high levels of hydroxy-indoles derived from OH-Trp and their subsequent polymerization leads to melanin biosynthesis.

Similarly, we propose Trp-melanin biosynthesis (Fig. 51) wherein during the chemotrophic metabolism of L-Trp possibly biotransformed to OH-Trp and then OH-Trp or hydroxy-indole derivatives subsequently polymerized to eumelanin. Our study on Trp-melanin biosynthesis indicated a possible Trp based non-canonical pathway of melanogensis in *Rbx. benzoatilyticus*.

Molecular response of Rbx. benzoatilyticus grown under chemotrophic L-Tryptophan fed conditions

The omics approaches like metabolomics and proteomics help to understand the sequential event in a biological system. Proteomic and metabolomics are used to understand the molecular response of Rbx. benzoatilyticus under the L-Trp fed conditions. The global proteome of whole-cell L-Trp fed and control cultures were analyzed through the isobaric tags for relative and absolute quantitation (iTRAQ) (Fig. 44). Bacteria respond to environmental conditions and bring the adaptive response at all levels of cellular and molecular processes. The systematic response of protein histidine kinase, PAS/PAC involves modulation of gene expression resulting in protein up-regulation in response to the environmental conditions for survival (Mascher et al., 2006). The result revealed that the global transcription machinery respond to the dynamics of ever-changing environmental conditions in bacteria. The transcriptional machinery was modulated under L-Trp fed condition such as Crp/FNR family transcriptional regulator, kinase-like protein, TetR family of transcription regulator, and sigma 54 modulation protein/ribosomal protein S30EA were up-regulated (Table. 4). This result suggests active transcription and the selective gene expression by *Rbx. benzoatilyticus* to adapt the under L-Trp fed conditions. The organisms possibly require more energy under L-Trp fed conditions, which was

Indicated by upregulated ATP synthase which will be further aid to generate more energy. The proteins related to aliphatic amino acids biosynthesis such as cysteine and methionine which are highly reducible were down-regulated. Our result revealed the downregulation of amino acid, fatty acid, lipid biosynthesis while acetyl-CoA acetyltransferase and lipolysis gene were upregulated. The result revealed high yields of acetyl CoA, possibly involved polyhydroxyalkanoates (PHAs) synthesis required for cell survival under stress as reported earlier (York *et al.*, 2001; Trautwein *et al.*, 2008). Moreover, the accumulation of PHAs granule was observed under the L-Trp fed conditions and it is consistence similar findings in bacteria under stress (Susana et al., 2010).

Aromatic amino acid metabolism in bacteria are stringently regulated. These are normally biosynthesized via shikimate pathway which operate in bacteria, fungi and plants but absent in animals. Bacteria regulates the shikimate pathway both at transcriptional and post-translation levels (Bentley, 1990; Maeda and Dudareva, 2012). While formation of DHAP (2-dehydro-3-deoxyphosphoheptonate aldolase) is a first committed, rate limiting enzyme in shikimate pathway (Maeda and Dudareva, 2012). This enzyme is feedback inhibited either by L-Phe, L-Try or L-Trp and thus regulates the shikimate pathway (Bohlmann et al., 1996; Knochel et al., 1999; Romero et al 1995) when organism is exposed aromatic amino acid the de-novo shikimate biosynthesis was inhibited by either of aromatic amino acids (Maeda and Dudareva, 2012). However, in our study when Rbx. benzoatilyticus was fed with L-Trp under chemotrophic conditions shikimate pathways remained unaffected. L-Trp metabolism-related protein tryptophanse, amidase and phenylalanine-4-monooxygense were up-regulated under chemotrophic conditions, indicating L-Trp bio-transformation to indole metabolites (Fig. 52). Upregulation of phenylalanine-4-monooxygense was corroborated the production of 5-OH Trp and 5hydroxyindole-3-acetic acid and their derivatives from L-Trp metabolism (Fig. 52). The 5-hydroxyindole derivatives were probably toxic to bacteria, therefore the organism must effluxes to survive using efflux transporter pump, this is evident from the up-regulation of RND efflux pump and ABC transporter (Table. 4) which are implicated in the efflux of toxic compounds (Segura et al., 2012). The organism adapt to the exogenously supplemented L-Trp and this requires different proteins to modulate the metabolic function to survive. We found translational machinery highly up-regulated to modulate the protein synthesis under L-Trp fed conditions which might be occurring to meet the demand of new proteins to regulate metabolism under L-Trp fed conditions (Table. 4).

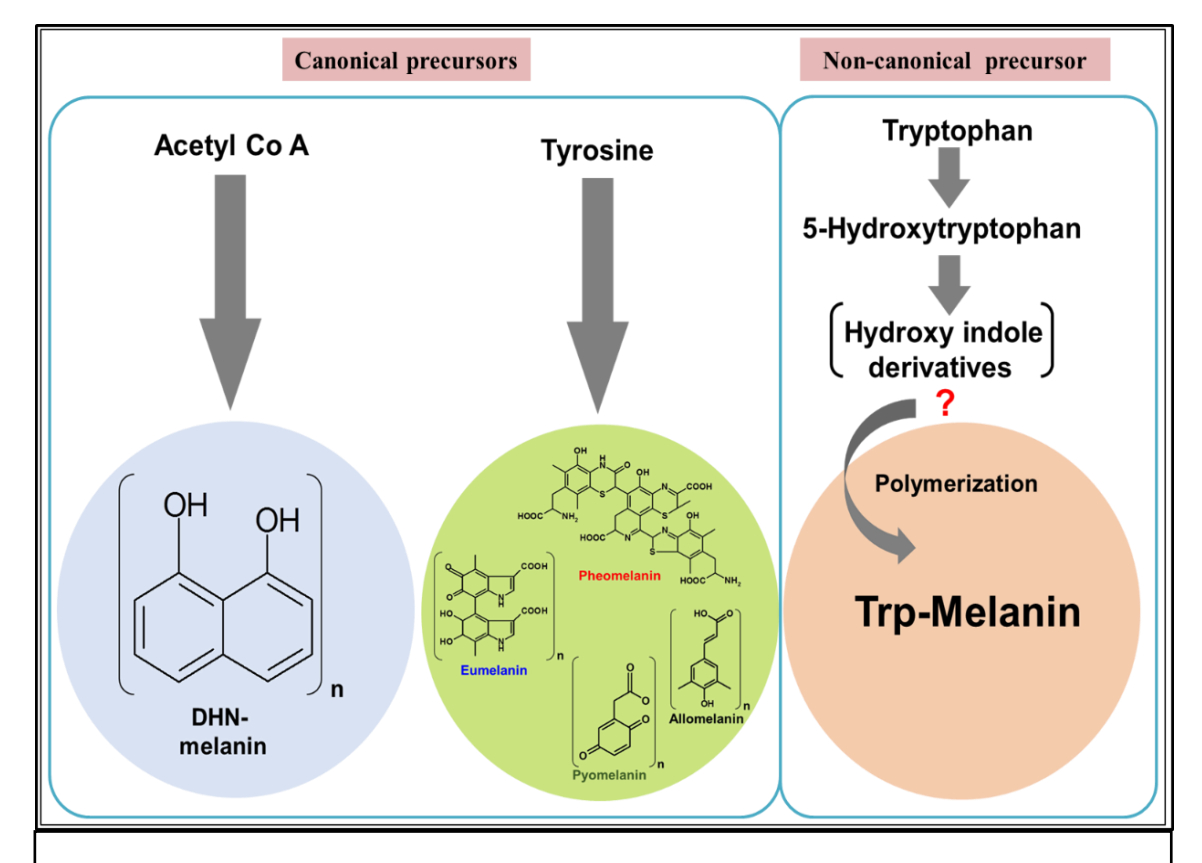


Fig. 51: Difference between the canonical and non- canonical L-Tryptophan based melanogenesis.

Summary

5.0 Summary

Aromatic compound are the most abundant groups of organic compounds found in the natural environments. Bacteria utilize aromatic compound for their growth under aerobic and anaerobic conditions. One such metabolically versatile bacterium is *Rbx*. *benzoatilyticus* which is commonly found in the oxic and anoxic zones of flooded paddy soils. This organism can thrive under both photo and chemotrophic mode of metabolism. *Rbx. benzoatilyticus* is metabolically versatile and has inherent strategy to respond to the ever-changing environmental conditions to an extended range of utilizing different carbon and nitrogen sources, including aromatic hydrocarbons.

Rbx. benzoatilyticus utilize L-Trp as sole source of nitrogen under chemo and phototrophic growth conditions. This organism is metabolically active and capable of biotransforming L-Trp to indole and 5-hydroxyindole derivatives under phototrophic and chemotrophic conditions. Metabolic profiling of L-Trp or 5-OH Trp fed chemotrophic cultures revealed the catabolic diversity of L-Trp/5-OH Trp in Rbx. benzoatilyticus. Stable isotopes studies and enzyme activity suggests that the organism has multitasking biochemical pathways of L-Trp biotransformation. Pathways like Ehrlich's; indole 3-acetonitrile, indole 3-acetamide pathway for producing indole 3-acetic acid operated independent of physiological life style of Rbx. benzoatilyticus, while kynurenine pathway was dependent on the chemotrophic life style of the organism (Fig. 52). Rbx. benzoatilyticus has the capability of biotransforming L-Trp to 5-hydroxytryptophan, 5-hydroxyindole derivatives which are involved Trp-melanin formation under chemotrophic conditions while same is not found phototrophic conditions. Existence of multiple catabolic pathways of L-Trp under chemotrophic conditions indicated the catabolic multitasking in

Rbx. benzoatilyticus (Fig. 52). Under chemotrophic of L-Trp metabolism of Rbx. benzoatilyticus also produced pink and yellow colored pigment via some unidentified pathways to indole dimer (s) and trimer (s) which are the products of oxidative metabolism of L-Trp (Fig. 52). Thus, the discovery of oxidative metabolism of L-Trp by Rbx. benzoatilyticus leads to the discovery of novel metabolites.

The proteomics study revealed the up-regulation of signal transduction, transcription and translation machinery suggest their possible role the environmental changes and in orchestrating gene expression, protein synthesis to thrive under chemotrophic conditions when exposed to L-Trp. The downregulation of lipid and amino acid biosynthesis-related protein and up-regulation of L-Trp catabolism, energy-related, PHAs granule biosynthesis which support the organism survival. While up-regulation of proteins related to energy metabolism under L-Trp fed condition indicates increased energy demand during stress adaptation when exposed of L-Trp under chemotrophic conditions. Up-regulation of L-Trp metabolism related protein such as phenylalanine 4-monooxygenase which was corroborated the hydroxylation L-Trp to formation of hydroxyl-tryptophan and subsequent formation of hydroxyl-indole derivatives. The current study indicates oxidative detoxification of indole by *Rbx. benzoatilyticus* under chemotrophic incubations with added L-Trp.

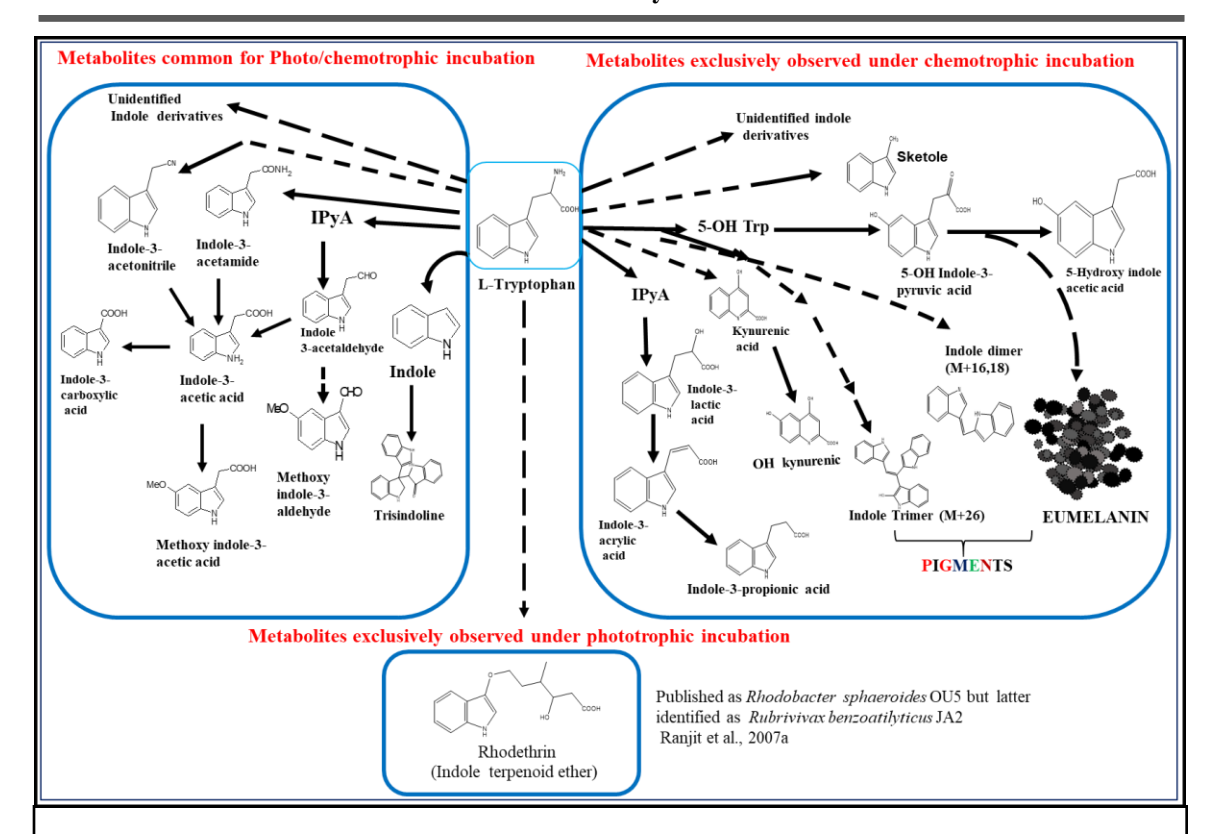


Fig. 52: Illustration of multiple L-Tryptophan catabolic pathways and its differential biotransformation under photo and chemotrophic metabolism in *Rbx. benzoatilyticus*. Pathways with solid arrow are predicted based on the identified labeled metabolites; dotted arrow detonated multiple steps, IPyA; indole-3-puruvic acid, IAM; Indole-3-acetamide, IAN; Indole-3-acetonitrile, 5-OH Trp; 5-hydroxytryptophan, M; Molecular ionized (m/z) mass, and +16, +18, and +26 mass increased with labeled fed L-Tryptophan.

Major findings

Major findings

- ➤ L-Tryptophan chemotrophic metabolism by *Rbx. benzoatilyticus* is multi-tasking.
- Major pathways are kynurenine pathways, indole-3-pyruvic acid pathway (IPyA), indole-3-acetamide pathway (IAM), and indole-3-acetonitrile (IAN) pathway.
- ➤ Indole dimers, trimers and polymers (eumelanin) are produced by *Rbx*.

 benzoatilyticus from L-Trp or 5-OH Trp under chemotrophic incubation.
- ➤ Non-canonical melanogenesis was demonstrated in *Rbx*. *benzoatilyticus*.
- ➤ iTRAQ proteome analysis revealed that the L-Trp metabolism-related protein were highly upregulated.
- ➤ Oxidative detoxification of indole by *Rbx. benzoatilyticus* was observed in this study as a result of chemotrophic incubation which is different from conjugative and reductive detoxification observed under phototrophic incubations in previous studies.

References

7.0 References

- Afzal, M. (2013) L-Phenylalanine and L-Tyrosine Catabolism by *Thermophilic Geobacillus* stearothermophilus. *Br. Biotechnol. J.* **3**:581-591.
- Aklujkar, Muktak, Risso, Carla Smith, Jessica Beaulieu, Derek Dubay, Ryan Giloteaux, Ludovic DiBurro and Kristin Holmes Dawn (2014) Anaerobic degradation of aromatic amino acids by the hyperthermophilic archaeon *Ferroglobus placidus*. *Microbiol.* **160**: 2694-2709.
- Alkhalaf, L. M. and Ryan, K. S. (2015) Biosynthetic manipulation of tryptophan in bacteria: Pathways and mechanisms. *Chemistry and Biology* **22**: 317-328.
- Allegri, Graziella Vogliardi, Susanna Bertazzo, Antonella Costa, Carlo V.L. Seraglia, and Roberta Traldi, Pietro (2003) Involvement of 5-hydroxytryptophan in melanogenesis. in *Advances in Experimental Medicine and Biology*. **527**: 723-730.
- Allen, C. C.R. Boyd, D. R. Larkin, M. J. Reid, Karen A. Sharma and N. D. Wilson, K. (1997) Metabolism of naphthalene, 1-naphthol, indene, and indole by Rhodococcus sp. strain NCIMB 12038. *Appl. Environ. Microbiol.* **63**: 151-155.
- Almeida-Paes, Rodrigo Frases, Susana de Sousa Araújo, Glauber Evangelista de Oliveira, Manoel Marques Gerfen, Gary J. Nosanchuk, Joshua D. Zancopé-Oliveira and Rosely Maria (2012) Biosynthesis and functions of a melanoid pigment produced by species of the sporothrix complex in the presence of L-Tyrosine. *Appl. Environ. Microbiol.* **78**: 8623-8630.
- Arai, H., Akahira, S., Ohishi, T. and Kudo, T. (1999) Adaptation of Comamonas testosteroni TA441 to utilization of phenol by spontaneous mutation of the gene for a trans-acting factor. *Mol. Microbiol.* **33**: 1132-1140.
- August, P. R. Grossman, T. H. Minor, C. Draper, M. P. MacNeil, I. A. Pemberton, J. M. Call, K. M. Holt and D. Osburne, M. S. (2000) Sequence analysis and functional characterization of the violacein biosynthetic pathway from *Chromobacterium violaceum*. J. Mol. Microbiol. Biotechnol. 2:513-519.

- Badri, D. V., Chaparro, J. M., Zhang, R., Shen, Q. and Vivanco, J. M. (2013) Application of natural blends of phytochemicals derived from the root exudates of arabidopsis to the soil reveal that phenolic-related compounds predominantly modulate the soil microbiome. *J. Biol. Chem.* **288**: 4502-4512.
- Banerjee, A., Supakar, S. and Banerjee, R. (2014) Melanin from the nitrogen-fixing bacterium *Azotobacter chroococcum*: A spectroscopic characterization. *PLoS One* **9**.
- Bak, F. and Widdel, F. (1986) Anaerobic degradation of phenol and phenol derivatives by Desulfobacterium phenolicum sp. nov. *Arch. Microbiol.* **146**:177-180.
- Bentley, D. L. (2005)Rules of engagement: Co-transcriptional recruitment of pre-mRNA processing factors. *Current Opinion in Cell Biology*. **17**: 251-256.
- Bohlmann, J., Lins, T., Martin and W. Eilert, U.(1996) Anthranilate synthase from Ruta graveolens: Duplicated ASα genes encode tryptophan-sensitive and tryptophan-insensitive isoenzymes specific to amino acid and alkaloid biosynthesis. *Plant Physiol.* **111**: 507-514.
- Berkhout, J., Teusink, B. and Bruggeman, F. J. (2013) Gene network requirements for regulation of metabolic gene expression to a desired state. *Sci. Rep.* **3**.
- Berstad, A., Raa, J. and Valeur, J. (2015) Indole the scent of a healthy 'inner soil'. *Microb. Ecol. Heal. Dis.* **26**.
- Bhushan, B., Samanta, S. K. and Jain, R. K. (2000) Indigo production by naphthalene-degrading bacteria. *Lett. Appl. Microbiol.* **31**: 5-9.
- Bortolotti, Perrine Hennart, Benjamin Thieffry, Camille Jausions, Guillaume Faure, Emmanuel Grandjean, Teddy Thepaut, Marion Dessein, Rodrigue Allorge, Delphine Guery, Benoit P. Faure, Karine Kipnis, Eric Toussaint and Bertrand Le Gouellec, Audrey (2016) Tryptophan catabolism in *Pseudomonas aeruginosa* and potential for inter-kingdom relationship. *BMC Microbiol.* **16**: 1-10.
- Bouknight, R. R. and Sadoff, H. L. (1975) Tryptophan catabolism in Bacillus megaterium.

- J. Bacteriol. 121:70-76.
- Brzeszcz, J. and Kaszycki, P. (2018) Aerobic bacteria degrading both n-alkanes and aromatic hydrocarbons: an undervalued strategy for metabolic diversity and flexibility. *Biodegradation*. **29**:359-407.
- Büngeler, A., Hämisch, B. and Strube, O. I. (2017) The supramolecular buildup of eumelanin: Structures, mechanisms, controllability. *International Journal of Molecular Sciences*. **18**.
- Castro-Sowinski, S., Burdman, S., Matan, O. and Okon, Y. (2010) Natural Functions of Bacterial Polyhydroxyalkanoates. in. doi:10.1007/978-3-642-03287-5_3.
- Centeno, S. A. and Shamir, J. (2008) Surface enhanced Raman scattering (SERS) and FTIR characterization of the sepia melanin pigment used in works of art. *J. Mol. Struct.* **873**: 149-159.
- Carbonero, F., Oakley, B. B. and Purdy K. J. (2014) Metabolic flexibility as a major predictor of spatial distribution in microbial communities. *PLoS One* **9**.
- Carmona, Manuel Zamarro, María Teresa Blázquez, Blas Durante-Rodríguez, Gonzalo Juárez, Javier F. Valderrama, J. Andrés Barragán, María J. L. García and José Luis Díaz, Eduardo (2009) Anaerobic Catabolism of Aromatic Compounds: a Genetic and Genomic View. *Microbiol. Mol. Biol. Rev.* **73**:71-133.
- Castro-Sowinski, S., Martinez-Drets, G. and Okon, Y. (2002) Laccase activity in melanin-producing strains of *Sinorhizobium meliloti*. *FEMS Microbiol*. *Lett.* **209**: 119-125.
- Chai, B., Wang, H. and Chen, X. (2012) Draft genome sequence of high-melanin-yielding Aeromonas media strain WS. *Journal of Bacteriology*. **194**: 6693-6694.
- Chatterjee, Subhasish Prados-Rosales, Rafael Tan, Sindy Itin, Boris Casadevall, Arturo Stark, Ruth E. (2014) Demonstration of a common indole-based aromatic core in natural and synthetic eumelanins by solid-state NMR. *Org. Biomol. Chem.* **12**: 6730-6736.
- Chauhan, P. S., Goradia, B. and Saxena, A. (2017) Bacterial laccase: recent update on production, properties and industrial applications. *3 Biotech.* **7**.

- Chubukov, V., Gerosa, L., Kochanowski, K. and Sauer, U. (2014) Coordination of microbial metabolism. *Nature Reviews Microbiology*. 12: 327-340.
- Clark, E., Manulis, S., Ophir, Y., Barash, I. and Gafni, Y. (1993) Cloning and Characterization of iaaM and iaaH from Erwinia herbicola pathovar gypsophilae. *Phytopathology.* **83**: 234-240.
- Clasquin, M. F.; Melamud, E.; Rabinowitz, J. D. (2012) LC-MS data processing with MAVEN: a metabolomic analysis and visualization engine. *Curr. Protoc Bioinformatics*.37. **11**.
- Coelho-Souza, Talita Martins, Natacha Maia, Fernanda Frases, Susana Bonelli, Raquel Regina Riley, Lee W. Moreira and Beatriz Meurer (2013) Pyomelanin production: A rare phenotype in *Acinetobacter baumannii*. *Journal of Medical Microbiology*. **63**:152-154.
- Colabroy, K. L., and T. P. B. N (2005) The pyridine ring of NAD is formedby a nonenzymatic pericyclic reaction. *J. Am. Chem. Soc* **127**.
- Crozier, K. R. and Moran, G. R. (2007) Heterologous expression and purification of kynurenine-3-monooxygenase from *Pseudomonas fluorescens* strain 17400. *Protein Expr. Purif.* **51**: 324-333.
- D'Ischia, Marco Wakamatsu, Kazumasa Napolitano, Alessandra Briganti, Stefania Garcia-Borron, José Carlos Kovacs, Daniela Meredith, Paul Pezzella, Alessandro Picardo, Mauro Sarna, Tadeusz Simon and John D. Ito, Shosuke (2013) Melanins and melanogenesis: Methods, standards, protocols. *Pigment Cell and Melanoma Research.* **26.**
- Dalfard, Arastoo Badoei Khajeh, Khosro Soudi, Mohammad Reza Naderi-Manesh, Hossein Ranjbar, Bijan and Sajedi Reza Hassan (2006) Isolation and biochemical characterization of laccase and tyrosinase activities in a novel melanogenic soil bacterium. *Enzyme Microb. Technol.* **39**: 1409-1416.
- Dantas, C., Volpe, P. L. O., Durán, N. and Ferreira, M. M. C. (2012) The violacein biosynthesis monitored by multi-wavelength fluorescence spectroscopy and by the PARAFAC method. *J. Braz. Chem. Soc.* **23**: 2054-2064.

- Das, N. and Chandran, P. Microbial (2011) Degradation of Petroleum Hydrocarbon Contaminants: An Overview. *Biotechnol. Res. Int.* **2011**.
- Dennis, P. G., Miller, A. J. and Hirsch, P. R. (2010) Are root exudates more important than other sources of rhizodeposits in structuring rhizosphere bacterial communities? *FEMS Microbiology Ecology.* **72**: 313-327.
- Diamantidis, G., Effosse, A., Potier, P. and Bally, R. (2000) Purification and characterization of the first bacterial laccase in the rhizospheric bacterium *Azospirillum lipoferum*. *Soil Biol. Biochem.* **32**: 919-927.
- Doukyu, N., Nakano, T., Okuyama, Y. and Aono, R. (2002) Isolation of Anacinetobacter sp. ST-550 which produces a high level of indigo in a water-organic solvent two-phase system containing high levels of indole. *Appl. Microbiol. Biotechnol.* **58**: 543-546.
- Drewnowska, J. M., Zambrzycka, M., Kalska-Szostko, B., Fiedoruk, K. and Swiecicka, I. (2015) Melanin-like pigment synthesis by soil *bacillus weihenstephanensis* isolates from Northeastern Poland. *PLoS One* **10**.
- Durán, N. and Menck, C. F. M. (2001) Chromobacterium violaceum: A review of harmacological and industiral perspectives. *Critical Reviews in Microbiology* vol. **27**: 201-222.
- Ebenau-Jehle, Christa Thomas, Markus Scharf, Gernot Kockelkorn, Daniel Knapp, Bettina Schühle, Karola Heider, Johann and Fuchs, Georg (2012) Anaerobic metabolism of indoleacetate. *J. Bacteriol.* **194**: 2894-2903.
- Egashira, Y., Kouhashi, H., Ohta, T. and Sanada, H. (1996) Purification and properties of α-amino-β-carboxymuconate-ε-semialdehyde decarboxylase (ACMSD), key enzyme of niacin synthesis from tryptophan, from hog kidney. *J. Nutr. Sci. Vitaminol.* (*Tokyo*). **42**: 173-183.
- Egland, P. G., Pelletier, D. A., Dispensa, M., Gibson, J. and Harwood, C. S. (1997) A cluster of bacterial genes for anaerobic benzene ring biodegradation. *Proc. Natl. Acad. Sci. U. S. A.* **94**: 6484-6489.

- Ekborg, Nathan A. Gonzalez, Jose M. Howard, Michael B. Taylor, Larry E. Hutcheson, Steven W. and Weiner, Ronald M. (2005) Saccharophagus degradans gen. nov., sp. nov., a versatile marine degrader of complex polysaccharides. *Int. J. Syst. Evol. Microbiol.* **55**: 1545-1549.
- Ellis, D. H. and Griffith, D. A. (1974) The location and analysis of melanins in the cell walls of some soil fungi. *Can. J. Microbiol.* **20**.
- El-Naggar, N. E. A. and El-Ewasy, S. M. (2017) Bioproduction, characterization, anticancer and antioxidant activities of extracellular melanin pigment produced by newly isolated microbial cell factories *Streptomyces glaucescens* NEAE-H. *Sci. Rep.* 7.
- Ensley, Burt D. Ratzkin, Barry J. Osslund, Timothy D. Simon, Mary J. Wackett, Lawrence P. Gibson, David T. (1983) Expression of Naphthalene Oxidation Genes in Escherichia coli Results in the Biosynthesis of Indigo. *Science*. **222**: 167-169.
- Fabara, A. N. and Fraaije, M. W. (2020) An overview of microbial indigo-forming enzymes. *Applied Microbiology and Biotechnology*. **104**: 925-933.
- Fujitani, S., Sun, H. Y., Yu, V. L. and Weingarten, J. A. (2011) Pneumonia due to *pseudomonas aeruginosa*: Part I: Epidemiology, clinical diagnosis, and source. *Chest* vol. **139**: 909-919.
- Gamal Shalaby, A. S., Ragab, T. I. M., Helal, M. M. I. and Esawy, M. A. (2019) Optimization of *Bacillus licheniformis* MAL tyrosinase: in vitro anticancer activity for brown and black eumelanin. *Heliyon* 5.
- Gessler, N. N., Egorova, A. S. and Belozerskaya, T. A. (2014) Melanin pigments of fungi under extreme environmental conditions. *Applied Biochemistry and Microbiology*. **50:** 105-113.
- Ghiani, Simona Baroni, Simona Burgio, Daniela Digilio, Giuseppe Fukuhara, Masaki Martino, Paola Monda, Keiji Nervi, Carlo Kiyomine and Akira Aime, Silvio (2008) Characterization of human hair melanin and its degradation products by means of magnetic resonance techniques. *Magn. Reson. Chem.* **46**: 471-479.

- Gómez-Romero, M., Segura-Carretero, A. and Fernández-Gutiérrez, A. (2010) Metabolite profiling and quantification of phenolic compounds in methanol extracts of tomato fruit. *Phytochemistry*. **71**: 1848-1864.
- Gonçalves, R. C. R., Lisboa, H. C. F. and Pombeiro-Sponchiado, S. R. (2012) Characterization of melanin pigment produced by *Aspergillus nidulans*. *World J. Microbiol. Biotechnol.* **28**: 1467-1474.
- Gillam, E. M. J., Notley, L. M., Cai, H., De Voss, J. J. and Guengerich, F. P. (2000) Oxidation of indole by cytochrome P450 enzymes. *Biochemistry* **39**: 13817-13824.
- Givaudan, Alain Effosse, Aline Faure, Denis Potier, Patrick Bouillant, Marie Louise Bally, René (1993) Polyphenol oxidase in *Azospirillum lipoferum* isolated from rice rhizosphere: Evidence for laccase activity in non-motile strains of Azospirillum lipoferum. *FEMS Microbiol. Lett.* **108**: 205-210.
- Glass, Keely Ito, Shosuke Wilby, Philip R. Sota, Takayuki Nakamura, Atsushi Bowers, C. Russell Vinther, Jakob Dutta, Suryendu Summons, Roger Briggs, Derek E.G. Wakamatsu, Kazumasa Simon, John D. (2012) Direct chemical evidence for eumelanin pigment from the Jurassic period. *Proc. Natl. Acad. Sci.* **109**: 10218-10223.
- Gorontzy, T., Kuver, J. and Blotevogel, K. H. (1993) Microbial transformation of nitroaromatic compounds under anaerobic conditions. *J. Gen. Microbiol.* **139**: 1331-1336.
- Goudenège, David Labreuche, Yannick Krin, Evelyne Ansquer, Dominique Mangenot, Sophie Calteau, Alexandra Médigue, Claudine Mazel, Didier Polz and Martin F. Le Roux, Frédérique (2013) Comparative genomics of pathogenic lineages of *Vibrio nigripulchritudo* identifies virulence-associated traits. *ISME J.* 7: 1985-1996.
- Hakvåg, Sigrid Fjærvik, Espen Klinkenberg, Geir Borgos, Sven Even F. Josefsen, Kjell D. Ellingsen, Trond E. Zotchev, Sergey B. (2009) Violacein-producing Collimonas sp. from the sea surface microlayer of costal waters in Trøndelag, Norway. *Mar. Drugs* 7: 576-588.

- Heine, T., Großmann, C., Hofmann, S. and Tischler, D. (2019) Indigoid dyes by group e monooxygenases: Mechanism and biocatalysis. *Biol. Chem.* **400**: 939-950.
- Hamill, R., Elander, R., Mabe, J. and Gorman, M. (1967) Metabolism of tryptophans by *Pseudomonas aureofaciens*. V. Conversion of tryptophan to pyrrolnitrin. *Antimicrob. Agents Chemother*. **7**: 388-396.
- Han, Gui Hwan Bang, Seong Eun Babu, Bandamaravuri Kishore Chang, Man Shin and Hyun Jae Kim, Si Wouk (2011) Bio-indigo production in two different fermentation systems using recombinant *Escherichia coli* cells harboring a flavin-containing monooxygenase gene (fmo). *Process Biochem.* **46**: 788-791.
- Hardeland, R. (2016) Melatonin in plants Diversity of levels and multiplicity of functions. *Front. Plant Sci.* **7**.
- Hartmann, A., Singh, M. and Klingmüller, W. (1983) Isolation and characterization of Azospirillum mutants excreting high amounts of indoleacetic acid. *Can. J. Microbiol.* **29**: 916-923.
- Harwood, C. S., Burchhardt, G., Herrmann, H. and Fuchs, G. (1998) Anaerobic metabolism of aromatic compounds via the benzoyl-CoA pathway. *FEMS Microbiol. Rev.* **22**, 6484-6489.
- Hassan, S. and Mathesius, U. (2012) The role of flavonoids in root-rhizosphere signalling: Opportunities and challenges for improving plant-microbe interactions. *Journal of Experimental Botany*. **63:** 3429-3444.
- Hazelwood, L. A., Daran, J. M., Van Maris, A. J. A., Pronk, J. T. and Dickinson, J. R. (2008) The Ehrlich pathway for fusel alcohol production: A century of research on *Saccharomyces cerevisiae* metabolism. *Applied and Environmental Microbiology*.
 74: 2259-2266.
- Hendrikx, T. and Schnabl, B. (2019) Indoles: metabolites produced by intestinal bacteria capable of controlling liver disease manifestation. *Journal of Internal Medicine*. **286**:32-40.

- Henrik M. Roager1, 2 and Tine R. Licht. (2018) Microbial tryptophan catabolites in health and disease. *Nat. Commun*..
- Hernández-Romero, D., Solano, F. and Sanchez-Amat, A. (2005) Polyphenol oxidase activity expression in *Ralstonia solanacearum*. *Appl. Environ. Microbiol.* **71**: 6808-6815.
- Herter, S., Schmidt, M., Thompson, M. L., Mikolasch, A. and Schauer, F. (2011) A new phenol oxidase produced during melanogenesis and encystment stage in the nitrogen-fixing soil bacterium *Azotobacter chroococcum*. *Appl. Microbiol*. *Biotechnol.* **90**: 1037-1049.
- Holmes, D. E., Nevin, K. P. and Lovley, D. R. (2004) In situ expression of nifD in Geobacteraceae in subsurface sediments. *Appl. Environ. Microbiol.* **70**: 7251-7259.
- Hoshino, T. (2011) Violacein and related tryptophan metabolites produced by Chromobacterium violaceum: Biosynthetic mechanism and pathway for construction of violacein core. *Applied Microbiology and Biotechnology* . **91**: 1463-1475.
- Howard-Jones, A. R. and Walsh, C. T. (2005) Enzymatic generation of the chromopyrrolic acid scaffold of rebeccamycin by the tandem action of RebO and RebD. *Biochemistry* **44**:15652-15663.
- Huang, T., Rehak, L. and Jander, G. (2012) Meta-Tyrosine in Festuca rubra ssp. commutata (Chewings fescue) is synthesized by hydroxylation of phenylalanine. *Phytochemistry* **75**: 60-66.
- Hubbard, T. D., Murray, I. A. and Perdew, G. H. (2015) Indole and Tryptophan Metabolism: Endogenous and Dietary Routes to Ah Receptor Activation. *Drug Metab. Dispos.* 43: 1522-1535.
- Hullo, M. F., Moszer, I., Danchin, A. and Martin-Verstraete, I. (2001) CotA of *Bacillus subtilis* is a copper-dependent laccase. *J. Bacteriol.* **183**. 5426-5430.
- Hu, Xun Nango, Keigo Bao, Lei Li, Tingting Mahmudul Hasan, M. D. Li and Chun Zhu

- (2019) High yields of solid carbonaceous materials from biomass. *Green Chem.* **21**: 1128-1140.
- Huccetogullari, D., Luo, Z. W. and Lee, S. Y. (2019) Metabolic engineering of microorganisms for production of aromatic compounds. *Microb. Cell Fact.* **18**.
- Isaacs, H., Chao, D., Yanofsky, C. and Saier, M. H. (1994) Mechanism of catabolite repression of tryptophanase synthesis in *Escherichia coli*. *Microbiology* **140**: 2125-2134.
- Ismail, wael and Gescher, J. (2012) Epoxy coenzyme a thioester pathways for degradation of aromatic compounds. *Applied and Environmental Microbiology*. **78**: 5043-5051.
- Johnson, C. H., Patterson, A. D., Idle, J. R. and Gonzalez, F. J. (2012) Xenobiotic metabolomics: Major impact on the metabolome. *Annu. Rev. Pharmacol. Toxicol.* 52: 37-56.
- Jude, B. A., Tanner, J., KoKo, T. and McLaughlin, E. C. (2012) Analysis, characterization, and synthesis of violacein from Janthinobacterium isolate extracts. 19-23.
- Kashefi, Kazem Tor, Jason M. Holmes, Dawn E. Gaw Van Praagh, Catherine ,Anna Louise Lovley and Derek R. (2002) *Geoglobus ahangari* gen. nov., sp. nov., a novel hyperthermophilic archaeon capable of oxidizing organic acids and growing autotrophically on hydrogen with Fe(III) serving as the sole electron acceptor. *Int. J. Syst. Evol. Microbiol.* **52**: 719-728.
- Kelley, S. K., Coyne, V. E., Sledjeski, D. D., Claiborne Fuqua, W. and Weiner, R. M. (1990) Identification of a tyrosinasse from a periphytic marine bacterium. *FEMS Microbiol. Lett.* 67: 275-279.
- Cook, R. James Thomashow, Linda S. Weller, David M. Fujimoto, Debbie Mazzola, Mark Bangera, Gita Kim and Dal Soo (1995) Molecular mechanisms of defense by rhizobacteria against root disease. *Proc. Natl. Acad. Sci. U. S. A.* **92**: 4197-4201.
- Kittell, B. L., Helinski, D. R. and Ditta, G. S. (1989) Aromatic aminotransferase activity and indoleacetic acid production in *Rhizobium meliloti*. *J. Bacteriol*. **171**: 5458-5466.

- Knoten, C. A., Hudson, L. L., Coleman, J. P., Farrow, J. M. and Pesci, E. C. KynR, (2011) a Lrp/AsnC-type transcriptional regulator, directly controls the kynurenine pathway in *Pseudomonas aeruginosa*. *J. Bacteriol.* **193**:6567-6575.
- Kobayashi, M., Izui, H., Nagasawa, T. and Yamada, H. (1993) Nitrilase in biosynthesis of the plant hormone indole-3-acetic acid from indole-3-acetonitrile: Cloning of the Alcaligenes gene and site-directed mutagenesis of cysteine residues. *Proc. Natl. Acad. Sci. U. S. A.* **90**: 247-251.
- Kobayashi, M., Suzuki, T., Fujita, T., Masuda, M. and Shimizu, S. (1995) Occurrence of enzymes involved in biosynthesis of indole-3-acetic acid from indole-3-acetonitrile in plant-associated bacteria, Agrobacterium and Rhizobium. *Proc. Natl. Acad. Sci. U. S. A.* **92**: 714-718.
- Koga, J., Syoono, K., Ichikawa, T. and Adachi, T. (1994) Involvement of 1-tryptophan aminotransferase in indole-3-acetic acid biosynthesis in *Enterobacter cloacae*. *Biochim. Biophys. Acta (BBA)/Protein Struct. Mol.* **1209**: 241-247.
- Kumar, A. and Sperandio, V. (2019) Indole signaling at the host-microbiota-pathogen interface. *MBio* **10**.
- Kumavath, R. N., Ramana, C. V. and Sasikala, C. (2010b) L-Tryptophan catabolism by *Rubrivivax benzoatilyticus* JA2 occurs through indole-3-pyruvic acid pathway. *Biodegradation* **21**: 825-832.
- Kumavath, R. N., Ramana, C. V. and Sasikala, C. (2010a) Production of phenols and alkyl gallate esters by Rhodobacter sphaeroides OU5. Curr. Microbiol. **60**. 107-111.
- Kurnasov, Oleg Jablonski, Lynn Polanuyer, Boris Dorrestein, Pieter Begley,

 TadhgOsterman, Andrei (2003) Aerobic tryptophan degradation pathway in bacteria: Novel kynurenine formamidase. *FEMS Microbiol. Lett.* **227**: 219–227.
- Kwon, Y. M. and Weiss, B. (2009) Production of 3-nitrosoindole derivatives by *Escherichia coli* during anaerobic growth. *J. Bacteriol.* **191**: 5369-5376.
- Lambrus, Bramwell G. Cochet-Escartin, Olivier Gao, Jiarong Newmark, Phillip A.

- collins, Eva Maria S. and Collins, James J. (2015) Tryptophan hydroxylase is required for eye melanogenesis in the planarian *schmidtea mediterranea*. *PLoS One* **10**.
- Lakshmi Prasuna, M., Mujahid, M., Sasikala, C. and Ramana, C. V. (2012) L-Phenylalanine catabolism and l-phenyllactic acid production by a phototrophic bacterium, *Rubrivivax benzoatilyticus* JA2. *Microbiol. Res.* **167**: 526-531.
- Larimer, Frank W. Chain, Patrick Hauser, Loren Lamerdin, Jane Malfatti, Stephanie Do, Long Land, Miriam L. Pelletier, Dale A. Beatty, J. Thomas Lang, Andrew S. Tabita, F. Robert Gibson, Janet L. Hanson, Thomas E. Bobst, Cedric Torres Y Torres, Janelle L. Peres, Caroline Harrison, Faith H. Gibson, Jane Harwood and Caroline S. (2004) Complete genome quence of the metabolically versatile photosynthetic bacterium *Rhodopseudomonas palustris*. *Nat. Biotechnol.* 22.
- Less, H. and Galili, G. (2008) Principal transcriptional programs regulating plant amino acid metabolism in response to abiotic stresses. *Plant Physiol.* **147**: 55-61.
- Liang Q, Takeo M, Chen M, Zhang W, X. Y. (2005) Chromosomeencoded gene cluster for the metabolic pathway that converts aniline to TCA cycle intermediates in *Delftia tsuruhatensis* AD9. *Microbiology*.
- Lim, He Kyoung Chung, Eu Jin Kim, Jin Cheol Choi, Gyung Ja Jang, Kyoung Soo Chung, Young. (2005) Characterization of a forest soil metagenome clone that confers indirubin and indigo production on *Escherichia coli*. *Appl. Environ*. *Microbiol*. **71**: 7768-7777.
- Ryun Cho, Kwang Yun Lee, Seon Woo (2005) Characterization of a forest soil metagenome clone that confers indirubin and indigo production on *Escherichia coli. Appl. Environ. Microbiol.* **71**: 7768-7777.
- Lin, G. H., Chen, H. P. and Shu, H. Y. (2015) Detoxification of indole by an indole-induced flavoprotein oxygenase from *acinetobacter baumannii*. *PLoS One* **10**.
- Liu, N. Zhang, T. Wang, Y. J. Huang, Y. P. Ou, J. H. Shen, Ping (2004) A heat inducible tyrosinase with distinct properties from *Bacillus thuringiensis*. *Lett. Appl. Microbiol.* 39: 407-412.

- Liu, Wan Hui Chen, Fei Fei Wang, Chao En Fu, Huan Huan Fang, Xue Qi Ye, Jian Ren Shi, JiYuan (2019) Indole-3-Acetic Acid in *Burkholderia pyrrocinia* JK-SH007: Enzymatic Identification of the Indole-3-Acetamide Synthesis Pathway. *Front. Microbiol.* **10**.
- Liu, Y., Hou, Y., Wang, G., Zheng, X. and Hao, H. (2020) Gut Microbial Metabolites of

 Aromatic Amino Acids as Signals in Host–Microbe Interplay. *Trends in Endocrinology and Metabolism* vol. **31**: 818-834.
- López Barragán, María J. Carmona, Manuel Zamarro, María T. Thiele, Bärbel Boll,

 Matthias Fuchs, Georg García, José L. and Díaz, Eduardo (2004) The bzd gene
 cluster, coding for anaerobic benzoate catabolism, in Azoarcus sp. strain CIB. *J. Bacteriol.* **186**: 179-187.
- Liu, Wan Hui Chen, Fei Fei Wang, Chao En Fu, Huan Huan Fang, Xue Qi Ye and Jian Ren Shi, Ji Yuan (2009) Production of violet pigment by a newly isolated psychrotrophic bacterium from a glacier in Xinjiang, China. *Biochem. Eng. J.* **43**: 71-133.
- Ma, Q., Zhang, X. and Qu, Y. (2018) Biodegradation and biotransformation of indole: Advances and perspectives. *Frontiers in Microbiology*. 9.
- Mai, X. and Adams, M. W. (1994) Indolepyruvate ferredoxin oxidoreductase from the hyperthermophilic archaeon *Pyrococcus furiosus*. A new enzyme involved in peptide fermentation. *J. Biol. Chem.* **269**: 16726-16732.
- Maeda, H. and Dudareva, N. (2012) The shikimate pathway and aromatic amino acid biosynthesis in plants. *Annual Review of Plant Biology*. **63**: 73-105.
- Mascher, T., Helmann, J. D. and Unden, G. (2006) Stimulus Perception in Bacterial Signal-Transducing Histidine Kinases. *Microbiol. Mol. Biol. Rev.* **70**: 910-938.
- Marchetti, B. and Karsili, T. N. V. (2016) Theoretical insights into the photo-protective

- mechanisms of natural biological sunscreens: Building blocks of eumelanin and pheomelanin. *Phys. Chem. Chem. Phys.* **18**: 3644-3658.
- MASON, H. S. (1948) The chemistry of melanin; mechanism of the oxidation of dihydroxyphenylalanine by tyrosinase. *J. Biol. Chem.* **172**: 235-247.
- McMahon, A. M., Doyle, E. M., Brooks, S. and O'Connor, K. E. (2007) Biochemical characterisation of the coexisting tyrosinase and laccase in the soil bacterium Pseudomonas putida F6. *Enzyme Microb. Technol.* **40**: 1435-1441.
- McClay, Kevin Mehboob, Shahila Yu, Jerry Santarsiero, Bernard D. Deng, Jiangping

 Cook, James L. Jeong, Hyunyoung Johnson, Michael E. Steffan, Robert J. (2015)

 Indole trimers with antibacterial activity against Gram-positive organisms produced using combinatorial biocatalysis. *AMB Express.* 5.
- McClay, Kevin Wan, Baojie Wang, Yuehong Cho, Sanghyun Yu, Jerry Santarsiero, Bernard Mehboob, Shahila Johnson, Michael Franzblau, Scott Steffan, Robert (2013) A novel combinatorial biocatalytic approach for producing antibacterial compounds effective against *Mycobacterium tuberculosis* (TB). *Appl. Microbiol. Biotechnol.* 97: 7151-7163.
- Mechichi, T., Stackebrandt, E., Gad'on, N. and Fuchs, G. (2002) Phylogenetic and metabolic diversity of bacteria degrading aromatic compounds under denitrifying conditions, and description of *Thauera phenylacetica* sp. nov., *Thauera aminoaromatica* sp. nov., and Azoarcus buckelii sp. nov. *Arch. Microbiol.* **178**: 26-35.
- Mekala, Lakshmi. P., Mohammed, M., Chintalapati, S. and Chintalapati, V. R. (2018) Stable Isotope-Assisted Metabolic Profiling Reveals Growth Mode Dependent Differential Metabolism and Multiple Catabolic Pathways of 1 -Phenylalanine in *Rubrivivax benzoatilyticus* JA2. *J. Proteome Res.* 17: 189-202.
- Mekala, Lakshmi. P., Mohammed, M., Chintalapati, S. and Chintalapati, V. R. (2019b) Precursor-feeding and altered-growth conditions reveal novel blue pigment production by *Rubrivivax benzoatilyticus* JA2. *Biotechnol. Lett.* **41**: 813-822.

- Mekala, Lakshmi. P., Mohammed, M., Chinthalapati, S. and Chinthalapati, V. R. (2019a) Pyomelanin production: Insights into the incomplete aerobic L-phenylalanine catabolism of a photosynthetic bacterium, *Rubrivivax benzoatilyticus* JA2. *Int. J. Biol. Macromol.* **126**: 755-764.
- Mercado-Blanco, J., Garcia, F., Fernandez-Lopez, M. and Olivares, J. (1993) Melanin production by *Rhizobium meliloti* GR4 is linked to nonsymbiotic plasmid pRmeGR4b: Cloning, sequencing, and expression of the tyrosinase gene mepA. *J. Bacteriol.* **175**: 5403-5410.
- Merugu, R., Rudra, M. P. P., Girisham, S. and Reddy, S. M. (2012) Biotechnological applications of purple non sulphur phototrophic bacteria: A minireview. *Int. J. Appl. Biol. Pharm. Technol.* **3**: 376-384.
- Micillo, Raffaella Panzella, Lucia Koike, Kenzo Monfrecola, Giuseppe Napolitano, Alessandra D'Ischia, Marco (2016). "Fifty shades" of black and red or how carboxyl groups fine tune eumelanin and pheomelanin properties. *International Journal of Molecular Sciences* vol. 17.
- Miller, S. L. (1953) A production of amino acids under possible primitive earth conditions. *Science* (80-.). **117**.
- Mohammadipanah, F., Kazemi Shariat Panahi, H., Imanparast, F. and Hamedi, J. (2016) Development of a Reversed-Phase Liquid Chromatographic Assay for the Quantification of Total Persipeptides in Fermentation Broth. *Chromatographia*. **79**: 1325-1332.
- Mohammed, Mujahid Isukapatla, Arvind Mekala, Lakshmi Prasuna Venkata, Rama prasad Eedara Veera Chintalapati, Sasikala Chintalapati, Venkata Ramana (2011a) Genome sequence of the phototrophic betaproteobacterium *Rubrivivax benzoatilyticus* strain JA2 T. *Journal of Bacteriology*. **193**: 2898-2899.
- Moreno-Ruiz, E., José Hernáez, M., Martínez-Pérez, O. and Santero, E. (2003) Identification and functional characterization of *Sphingomonas macrogolitabida* strain TFA genes involved in the first two steps of the tetralin catabolic pathway. *J. Bacteriol.* **185**: 2026-2030.

- Mosier, Annika C. Justice, Nicholas B. Bowen, Benjamin P. Baran, Richard Thomas, Brian C. Northen, Trent R. Banfield, and Jillian F. (2013) Metabolites associated with adaptation of microorganisms to an acidophilic, metal-rich environment identified by stable-isotope-enabled metabolomics. *MBio* 4.
- Mujahid, M., Prasuna, M. L., Sasikala, C. and Ramana, C. V. (2015) Integrated metabolomic and proteomic analysis reveals systemic responses of *Rubrivivax benzoatilyticus* JA2 to aniline stress. *J. Proteome Res.* **14**: 711-727.
- Mujahid, M., Sasikala, C. and Ramana, C. V. (2011b) Production of indole-3-acetic acid and related indole derivatives from L-tryptophan by *Rubrivivax benzoatilyticus* JA2. *Appl. Microbiol. Biotechnol.* **89**: 1001-1008.
- Mujahid, M., Sasikala, C. and Ramana, V. C. (2014) Aniline is an inducer, and not a precursor, for indole derivatives in *Rubrivivax benzoatilyticus* JA2. *PLoS One* **9**.
- Nagayama, Hirofumi Sugawara, Tomonori Endo, Ryo Ono, Akira Kato, Hiromi Ohtsubo, and Yoshiyuki Nagata, Yuji (2015) Isolation of oxygenase genes for indigo-forming activity from an artificially polluted soil metagenome by functional screening using *Pseudomonas putida* strains as hosts. *Appl. Microbiol. Biotechnol.* **99**: 4453-4470.
- Nakamura, Y., Asada, C. and Sawada, T. (2003) Production of antibacterial violet pigment by psychrotropic bacterium RT102 strain. *Biotechnol. Bioprocess Eng.* **8**.
- Namgung, Seyun Park, Hyun A. Kim, Joonwon Lee, Pyung Gang Kim, Byung Gee Yang, Yung Hun Choi and Kwon Young (2019) Ecofriendly one-pot biosynthesis of indigo derivative dyes using CYP102G4 and PrnA halogenase. *Dye. Pigment.* **162**: 37-40.
- Napolitano, A., De Lucia, M., Panzella, L. and D'Ischia, M. (2008) The 'benzothiazine' chromophore of pheomelanins: A reassessment. *Photochem. Photobiol.* **84**: 593-599.
- Ni, Q. Z., Sierra, B. N., La Clair, J. J. and Burkart, M. D. (2020) Chemoenzymatic elaboration of the Raper-Mason pathway unravels the structural diversity within eumelanin pigments. *Chem. Sci.* **11**: 7836-7841.

- Noda, S. and Kondo, (2017) A. Recent Advances in Microbial Production of Aromatic Chemicals and Derivatives. *Trends in Biotechnology* vol. **35**: 785-796.
- Noh, U., Heck, S., Giffhorn, F. and Kohring, G. W. (2002) Phototrophic transformation of phenol to 4-hydroxyphenylacetate by *Rhodopseudomonas palustris*. *Appl. Microbiol. Biotechnol.* **58**: 830-835.
- O'Connor, K. E., Dobson, A. D. W. and Hartmans, S. (1997) Indigo formation by microorganisms expressing styrene monooxygenase activity. *Appl. Environ. Microbiol.* **63**: 4287-4291.
- Oda, Yasuhiro Larimer, Frank W. Chain, Patrick S.G. Malfatti, Stephanie Shin, Maria V. Vergez, Lisa M. Hauser, Loren Land, Miriam L. Braatsch, Stephan Beatty, J. Thomas Pelletier, Dale A. Schaefer, Amy L. Harwood, Caroline S. (2008) Multiple genome sequences reveal adaptations of a phototrophic bacterium to sediment microenvironments. *Proc. Natl. Acad. Sci. U. S. A.* **105**: 18543-18548.
- Pantanella, F. Berlutti, F. Passariello, C. Sarli, S. Morea, C. and Schippa, S. (2007) Violacein and biofilm production in *Janthinobacterium lividum*. *J. Appl. Microbiol*. **102**: 992-999.
- Pandey, R. P., Parajuli, P., Koffas, M. A. G. and Sohng, J. K. (2016) Microbial production of natural and non-natural flavonoids: Pathway engineering, directed evolution and systems/synthetic biology. *Biotechnology Advances* vol. **34**: 634-662.
- Parthasarathy, Anutthaman Cross, Penelope J. Dobson, Renwick C.J. Adams, Lily E. Savka and Michael A. Hudson, André O. (2018) A Three-Ring circus: Metabolism of the three proteogenic aromatic amino acids and their role in the health of plants and animals. *Frontiers in Molecular Biosciences* 5.
- Park, Hyun A. Yang, Inchan Choi, Mira Jang, Kyoung Soon Jung, Ji Chul Choi and Kwon Young (2020) Engineering of melanin biopolymer by co-expression of MelC tyrosinase with CYP102G4 monooxygenase: Structural composition understanding by 15 tesla FT-ICR MS analysis. *Biochem. Eng. J.* **157**.
- Patten, C. L. and Glick, B. R. (2002) Role of *Pseudomonas putida* indoleacetic acid in

- development of the host plant root system. Appl. Environ. Microbiol. 68: 3795-3801.
- Pavan, M. E., López, N. I. & Pettinari, M. J. (2020) Melanin biosynthesis in bacteria, regulation and production perspectives. *Applied Microbiology and Biotechnology*. **104**: 1357-1370.
- Perley, J. E. and Stowe, B. B. (1966) On the ability of Taphrina deformans to produce indoleacetic acid from tryptophan by way of tryptamine. *Plant Physiol.* **41**: 234-237.
- Phillips, D. A., Fox, T. C., King, M. D., Bhuvaneswari, T. V. and Teuber, L. R. (2004) Microbial products trigger amino acid exudation from plant roots. *Plant Physiol.* **136**: 2887-2894.
- Piletic, I. R., Matthews, T. E. and Warren, W. S. (2010) Probing near-infrared photorelaxation pathways in eumelanins and pheomelanins. *J. Phys. Chem. A* **114**: 11483-11491.
- Plonka, P. M. and Grabacka, M. (2006) Melanin synthesis in microorganisms Biotechnological and medical aspects. *Acta Biochimica Polonica* vol. **53**: 429-443.
- Pomerantz, S. H. and Murthy, V. V. (1974) Purification and properties of tyrosinases from *Vibrio tyrosinaticus*. *Arch. Biochem. Biophys.* **160**: 73-82.
- Qu, Y., Pi, W., Ma, F., Zhou, J. and Zhang, X. (2010) Influence and optimization of growth substrates on indigo formation by a novel isolate Acinetobacter sp. PP-2. *Bioresour. Technol.* **101**: 1848-1864.
- Qu, Yuanyuan Zhang, Xuwang Ma, Qiao Ma, Fang Zhang, Qiang Li, Xinliang Zhou and Hao Zhou, Jiti (2012) Indigo biosynthesis by Comamonas sp. MQ. *Biotechnol. Lett.* **34**: 353-357.
- Qu, Yuanyuan Shi, Shengnan Zhou, Hao Ma, Qiao Li, Xinliang Zhang and Xuwang Zhou, Jiti (2012) Characterization of a Novel Phenol Hydroxylase in Indoles Biotranformation from a Strain Arthrobacter sp. W1. PLoS One 7.
- Ramana Ch, V.; Sasikala, C.; Arunasri, K.; Anil Kumar, P.; Srinivas, T. N.; Shivaji, S.; Gupta, P.; Suling, J.; Imhoff, J. F. (2006) *Rubrivivax benzoatilyticus* sp. nov., an aromatic, hydrocarbon-degrading purple betaproteobacterium. *Int. J. Syst. Evol*

Microbio 56.

- Ramos, Juan L. Duque, Estrella Gallegos, María Trinidad Godoy, Patricia Ramos-González, María Isabel Rojas, Antonia Terán and Wilson Segura, Ana (2002) Mechanisms of solvent tolerance in gram-negative bacteria. *Annual Review of Microbiology* vol. **56**: 743-768.
- Ranjith, N.K., Ramana, C.V., and Sasikala, C. (2007a). Rhodethrin: a novel indole terpenoid ether produced by *Rhodobacter sphaeroides* has cytotoxic and phytohormonal activities. *Biotechnol. Lett.* **29**.
- Ranjith, N.K., Sasikala, C., and Ramana Ch, V. (2007b) Catabolism of L-phenylalanine and Ltyrosine by *Rhodobacter sphaeroides* OU5 occurs through 3,4-dihydroxyphenylalanine. *Res. Microbiol.* **156**.
- Raper, H. S. (1928) The aerobic oxidases. *Physiol. Rev.* 8: 245-282.
- Ravasio, D., Walther, A., Trost, K., Vrhovsek, U. and Wendland, J. (2014) An indirect assay for volatile compound production in yeast strains. *Sci. Rep.* **4**.
- Reiss, R., Ihssen, J. and Thöny-Meyer, L. (2011) *Bacillus pumilus* laccase: A heat stable enzyme with a wide substrate spectrum. *BMC Biotechnol.* **11**.
- Rengarajan, Thamaraiselvan Rajendran, Peramaiyan Nandakumar, Natarajan Lokeshkumar, Boopathy Rajendran and Palaniswami Nishigaki, Ikuo (2015) Exposure to polycyclic aromatic hydrocarbons with special focus on cancer. *Asian Pacific Journal of Tropical Biomedicine* vol. **5**: 182-189.
- Rettori, D. and Durán, N. (1998) Production, extraction and purification of violacein: An antibiotic pigment produced by *Chromobacterium violaceum*. *World J. Microbiol*. *Biotechnol*. **14**; 685-688.
- Rodrigues, André L. Trachtmann, Nathalie Becker, Judith Lohanatha, Ananta F. Blotenberg, Jana Bolten, Christoph J. Korneli, Claudia de Souza Lima, André O. Porto, Luismar M. Sprenger, Georg A. and Wittmann, Christoph (2013) Systems metabolic engineering of *Escherichia coli* for production of the antitumor drugs violacein and deoxyviolacein. *Metab. Eng.* 20: 29-41.

- Ryu, R. J. and Patten, C. L. (2008) Aromatic amino acid-dependent expression of indole-3-pyruvate decarboxylase is regulated by tyrr in *Enterobacter cloacae* UW5. *J. Bacteriol.* **190**: 7200-7208.
- Sáez, L. P., Castillo, F. and Caballero, F. J. (1999) Metabolism of L-Phenylalanine and L-tyrosine by the phototrophic bacterium *Rhodobacter capsulatus*. *Curr. Microbiol.* 38: 51-56.
- Sanchez-Amat, A. and Solano, F. (1997) A pluripotent polyphenol oxidase from the melanogenic marine Alteromonas sp shares catalytic capabilities of tyrosinases and laccases. *Biochem. Biophys. Res. Commun.* **240**: 787-792.
- Sanchez-Amat, A., Solano, F. and Lucas-Elío, P. (2010) Finding new enzymes from bacterial physiology: A successful approach illustrated by the detection of novel oxidases in *Marinomonas mediterranea*. *Marine Drugs* 8: 519-541.
- Sánchez, C., Braña, A. F., Méndez, C. and Salas, J. A. (2006) Reevaluation of the violacein biosynthetic pathway and its relationship to indolocarbazole biosynthesis. *ChemBioChem* **7**: 1231-1240.
- Saini, A. S. and Melo, J. S. (2015). One-pot green synthesis of eumelanin: Process optimization and its characterization. *RSC Adv.* **5**: 47671-47680.
- Sajjan, S., Kulkarni, G., Yaligara, V., Kyoung, L. and Karegoudar, T. B. (2010) Purification and physiochemical characterization of melanin pigment from klebsiella sp. GSK. *J. Microbiol. Biotechnol.* **20**: 1513-1520..
- Schneider, S., Mohamed, M. E. S. and Fuchs, G. (1997) Anaerobic metabolism of L-phenylalanine via benzoyl-CoA in the denitrifying bacterium *Thauera aromatica*. *Arch. Microbiol.* **168**: 310-320.
- Schulz, S. and Dickschat, J. S. (2007) Bacterial volatiles: The smell of small organisms. *Natural Product Reports.* **24**: 814-842.
- Sekine, M., Watanabe, K. and Syono, K. (1989) Molecular cloning of a gene for indole-3-acetamide hydrolase from *Bradyrhizobium japonicum*. *J. Bacteriol.* **171**: 1718-

- Shivprasad, S. and Page, W. J. (1989) Catechol formation and melanization by Na+-dependent *Azotobacter chroococcum*: A protective mechanism for aeroadaptation? *Appl. Environ. Microbiol.* **55**: 1811-1817.
- Shuster, V. and Fishman, A. (2009) Isolation, cloning and characterization of a tyrosinase with improved activity in organic solvents from *bacillus megaterium*. *J. Mol. Microbiol. Biotechnol.* **17**: 188-200.
- Singh, G., Bhalla, A., Kaur, P., Capalash, N. and Sharma, P. (2011) Laccase from prokaryotes: A new source for an old enzyme. *Reviews in Environmental Science and Biotechnology*. **10**: 309-326.
- Singleton, D. R., Hu, J. and Aitken, M. D. (2012) Heterologous expression of polycyclic aromatic hydrocarbon ring-hydroxylating dioxygenase genes from a novel pyrenedegrading betaproteobacterium. *Appl. Environ. Microbiol.* **78**: 3552-3559.
- Solano, F. (2014) Melanins: Skin Pigments and Much More-Types, Structural Models, Biological Functions, and Formation Routes. *New J. Sci.* **2014**.
- Solano, F. (2017) Melanin and melanin-related polymers as materials with biomedical and biotechnological applications— Cuttlefish ink and mussel foot proteins as inspired biomolecules. *International Journal of Molecular Sciences*. **18**.
- Spaepen, S., Vanderleyden, J. and Remans, R. (2007) Indole-3-acetic acid in microbial and microorganism-plant signaling. *FEMS Microbiology Reviews*. **31**: 425-448.
- Stull, T. L. Hyun, L. Sharetzsky, C. Wooten, J. McCauley, J. P. and Smith, A. B. (1995) Production and oxidation of indole by *Haemophilus influenzae*. *J. Biol. Chem.* **270**.
- Sugumaran, M. (2016) Reactivities of quinone methides versus o-Quinones in catecholamine metabolism and eumelanin biosynthesis. *International Journal of Molecular Sciences*. **17**.
- Tanabe, A., Egashira, Y., Fukuoka, S. I., Shibata, K. and Sanada, H. (2002) Purification and molecular cloning of rat 2-amino-3-carboxymuconate-6-semialdehyde

- decarboxylase. Biochem. J. 361.
- Tarangini, K. and Mishra, S. (2013) Production, Characterization and Analysis of Melanin from Isolated Marine Pseudomonas sp. using Vegetable waste. *Res. J. Eng. Sci.* _ *ISSN Res. J. Eng. Sci* **2**: 2278-9472.
- Trautwein, K. et al. (2008) Solvent stress response of the denitrifying bacterium 'Aromatoleum aromaticum' strain EbN1. Appl. Environ. Microbiol. 74: 2267-2274.
- Teufel, R. Mascaraque, V. Ismail, W. Voss, M. Perera, J. Eisenreich, W. Haehnel, and W. Fuchs, G. (2010) Bacterial phenylalanine and phenylacetate catabolic pathway revealed. *Proc. Natl. Acad. Sci. U. S. A.* 107: 14390-14395.
- Theunis, M., Kobayashi, H., Broughton, W. J. and Prinsen, E. (2004) Flavonoids, NodD1, NodD2, and Nod-Box NB15 modulate expression of the y4wEFG locus that is required for indole-3-acetic acid synthesis in Rhizobium sp. strain NGR234. *Mol. Plant-Microbe Interact.* **17**: 1153-1161.
- Thody, Anthony J. Higgins, Elisabeth M. Wakamatsu, Kazumasa Ito, Shosuke Burchill, Susan A.and Marks, Janet M. (1991) Pheomelanin as well as eumelanin is present in human epidermis. *J. Invest. Dermatol.* **97**: 340-344.
- Toledo, Andrea Vanesa Franco, Mario Emilio Ernesto Yanil Lopez, Silvina Marianela Troncozo, María Inés Saparrat, Mario Carlos Nazareno Balatti and Pedro Alberto (2017) Melanins in fungi: Types, localization and putative biological roles. *Physiological and Molecular Plant Pathology.* **99**.
- Turick, C. E., Caccavo, F. and Tisa, L. S. (2008) Pyomelanin is produced by Shewanella algae BrY and affected by exogenous iron. *Can. J. Microbiol.* **54**: 334-339.
- Tyc, O., Song, C., Dickschat, J. S., Vos, M. and Garbeva, P. (2017) The Ecological Role of Volatile and Soluble Secondary Metabolites Produced by Soil Bacteria. *Trends in Microbiology*, **25**: 280-292.
- Unuofin, J. O., Okoh, A. I. and Nwodo, U. U. (2019) Aptitude of oxidative enzymes for treatment of wastewater pollutants: A laccase perspective. *Molecules* vol. 24.

- Vangnai, A. S. and Petchkroh, W. (2007) Biodegradation of 4-chloroaniline by bacteria enriched from soil. *FEMS Microbiol. Lett.* **268**: 209-216.
- Vogliardi, Susanna Allegri, Graziella Bertazzo, Antonella Costa, Carlo V.L. Seraglia, Roberta and Traldi, Pietro (2002) An investigation on the role of 5-hydroxytryptophan in the biosynthesis of melanins. *Journal of Mass Spectrometry*, **37**: 1292-1296.
- Wei, J., Timler, J. G., Knutson, C. M. and Barney, B. M. (2013) Branched-chain 2-keto acid decarboxylases derived from Psychrobacter. *FEMS Microbiol. Lett.* **346**: 105-112.
- Wu, F., Cao, P., Song, G., Chen, W. and Wang, Q. (2018) Expanding the repertoire of aromatic chemicals by microbial production. *Journal of Chemical Technology and Biotechnology*, **93**: 2804-2816.
- Yokooji, Y., Sato, T., Fujiwar, S., Imanak, T. and Atomi, H. (2013) Genetic examination of initial amino acid oxidation and glutamate catabolism in the hyperthermophilic archaeon *Thermococcus kodakarensis*. *J. Bacteriol.* **195**: 1940-1948.
- York, G. M., Junker, B. H., Stubbe, J. and Sinskey, A. J. (2001) Accumulation of the PhaP phasin of Ralstonia eutropha is dependent on production of polyhydroxybutyrate in cells. *J. Bacteriol.* **183**: 4217-4226.
- Youngchim, S., Nosanchuk, J. D., Pornsuwan, S., Kajiwara, S. and Vanittanakom, N. (2013) The Role of L-DOPA on Melanization and Mycelial Production in Malassezia Furfur. *PLoS One* **8**.
- Yun, S. H.; Park, G. W.; Kim, J. Y.; Kwon, S. O.; Choi, C. W.; Leem, S. H.; Kwon, K. H.; Yoo, J. S.; Lee, C.; Kim, S.; Kim, S. I.(2011) Proteomic characterization of the *Pseudomonas putida* KT2440 global response to a monocyclic aromatic compound by iTRAQ analysis and 1DE-MudPIT. J. *Proteomics*. 74: 909-919.
- Badri, Dayakar V. Chaparro, Jacqueline M. Zhang, Ruifu Shen, Qirong and Vivanco,Jorge M. (2013) Cloning and expression of naphthalene dioxygenase genes fromComamonas sp. MQ for indigoids production. *Process Biochem.* 48: 581-587.

Zheng, H., Chatfield, C. H., Liles, M. R. and Cianciotto, N. P. (2013) Secreted pyomelanin of legionella pneumophila promotes bacterial iron uptake and growth under iron-limiting conditions. *Infect. Immun.* **81**: 4182-4191.

Publications

8.0. Publications

- 1. **Shabbir Ahmad**, Mujahid Mohammed, Lakshmi Prasuna Mekala, Sasikala Ch and Ramana Ch.V. (2020) Tryptophan, a non-canonical melanin precursor: new L-tryptophan based melanin production by *Rubrivivax benzoatilyticus* JA2. *Sci Rep.* 10:8925. doi: 10.1038/s41598-020-65803-6.
- 2. Indu B., Kumar G., Smita N., <u>Shabbir A</u>., Sasikala Ch., and Ramana Ch. V. (2020). *Chryseobacterium candidae* sp. nov., isolated from a yeast (*Candida tropicalis*). *Int J Syst Evol Microbiol*. 70:93-99. doi.org.10.1099/ijsem.0.003716.
- 3. Dhanesh Kumar, Kumar Gaurav, Sreya PK, <u>Shabbir A.</u>, Jagadeeshwari Uppada, Sasikala Ch., and Ramana Ch.V. (2020) *Gimesia chilikensis* sp. nov., a haloalkalitolerant planctomycete isolated from Chilika lagoon and emended description of the genus *Gimesia*. *Int J Syst Evol Microbiol*. 70:3647-3655 doi.org.10.1099/ijsem.0.004211.
- 4. Anusha Rai, Smita N, Suresh G, <u>Shabbir A</u>, Deepshikha G, Sasikala Ch, and Ramana Ch.V (2020) *Paracoccus aeridis* sp. nov., an indole-producing bacterium isolated from the rhizosphere of an orchid, *Aerides maculosa*. *Int J Syst Evol Microbiol*. 70:1720-1728. doi.org. 10.1099/ijsem.0.003962.
- 5. Rishabh Kaushik, Meesha Sharma, Kumar Gaurav, Jagadeeshwari U., **Shabbir A**, Sasikala Ch., Ramana Ch.V. and Maharaj K Pandit (2020) *Paludisphaera soli* sp. nov., a new member of the family *Isosphaeraceae* isolated from high altitude soil in the Western Himalaya. *Ant van Leev Microbiol*. 113:1663-1674. https://doi.org/10.1007/s10482-020-01471-w
- 6. Dhanesh Kumar., Gaurav, K., <u>Shabbir, A</u>, Jagadeeshwari, U., Sasikala, Ch. and Ramana, Ch.V. (2020). Descriptions of *Roseiconus nitratireducens* gen. nov. sp. nov., *Roseiconus lacunae*. sp. nov. isolated from Chilika lagoon. *Arch. Microbiol*. https://doi.org/10.1007/s00203-020-02078-5
- 7. Anusha Rai., Smita N., **Shabbir A**., Jagadeeshwari U., Keertana T., Sasikala Ch. and Ramana Ch.V. (2020) *Mesobacillus aurantiibacter* sp. nov., isolated from an orange pond near a solar saltern. Arch. Microbiol. (Accepted AOMI-D-20-00565R2)
- 8. Kumar Gaurav, Dhanesh Kumar, Jagadeeshwari U, Sreya PK, <u>Shabbir A</u>, Sasikala Ch. and Ramana ChV. (2020). *Crateriforma spongiae* sp. nov., isolated from a marine sponge. Ant van Leev Microbiol. (Under revision).
- 9. Kumar Gaurav, Dhanesh Kumar, Jagadeeshwari U, **Shabbir A**, Sasikala Ch. and Ramana ChV. (2020) Phylo-taxogenomics of the genus *Tautonia* with descriptions of *Tautonia marina* sp. nov., *Tautonia rosea* sp. nov., and emended description of the genus. Syst. Appl. Microbiol. (Communicated).

A. Presented in the following conferences and award:

- **1.** Poster presentation Title "Novel melaniod-like pigment production by a Betaproteobacteria *Rubrivivax benzoatilyticus* JA2 " Md. Shabbir Ahmad, M.Lakshmi Prasuna, M. Mujahid ,Ch. Sasikala Ch. V. Ramana 56th Annual Conference of Association of Microbiologists of India (AMI) Dec 07-10 2015.
- **2.** Poster presentation Title" Characterization of 5-hydroxytryptophan-based melanin and it's hydrolysis products in the photosynthetic bacterium *Rubrivivax benzoatilyticus* JA2^T" **Shabbir Ahmad**, Lakshmi Prasuna, M, Mujahid.Muhammed and Ramana Ch.V. 59th Annual Conference of Association of Microbiologists of India (AMI) Dec 09-12, 2018.
- **3.** Oral presentation Title "Characterization of novel L-Tryptophan based melanin from *Rubrivivax benzoatilyticus* JA2." **Shabbir Ahmad** and Prof. Ch. Venkata Ramana, Department of Plant Science, School Life Science University of Hyderabad Telangana 500046. In 8th International Conference "Photosynthesis and Hydrogen Energy Research for Sustainability-2017" Oct 30- 03 Nov 2017.

AWARDED BEST ORAL PRESENTATION



natureresearch



OPEN

Tryptophan, a non-canonical melanin precursor: New L-tryptophan based melanin production by *Rubrivivax* benzoatilyticus JA2

Shabbir Ahmad¹, Mujahid Mohammed¹,³, Lakshmi Prasuna Mekala¹,⁴, Sasikala Chintalapati² & Venkata Ramana Chintalapati¹ ⊠

Melanins are chemically diverse ubiquitous pigments found across the life forms synthesized via different biochemical pathways mainly from L-tyrosine or acetyl CoA. Though few reports suggest the possibility of tryptophan-based melanin synthesis, however, such tryptophan-based melanin and its biosynthesis remained a biochemical riddle. Here we report tryptophan-based melanin production by bacterium, Rubrivivax benzoatilyticus JA2. Aerobic cultures of strain JA2 produced brown pigment when grown on L-tryptophan-containing media. Purified pigment showed typical physico-chemical properties of melanin. Further, extensive spectroscopic studies revealed that pigment is an amorphous, indole-type polymer with stable free radical centers. Further, hydrolysis of the brown pigment revealed the presence of indole moiety, confirming the indolic nature of the pigment. Demonstration of in vitro and in vivo pigment synthesis directly from L-tryptophan or hydroxytryptophan confirms tryptophanbased melanin synthesis in strain JA2. Interestingly, canonical melanin biosynthetic inhibitors did not affect the pigment synthesis indicating possible non-canonical tryptophan-based melanin biosynthesis in strain JA2. Further, the exometabolite profiling and precursor feeding studies suggests that L-tryptophan converted to hydroxytryptophan/hydroxyindoles and their subsequent polymerization lead to the formation of melanin. The current study sheds light on biosynthetic diversity of melanins and L-tryptophan can be a potential precursor for melanin synthesis in life forms.

Microorganisms are prolific producers of a diverse array of pigments and these pigments are produced under different physiological conditions. The pigments are structurally diverse ranging from simple low molecular organic compound to complex macromolecules such as melanins¹. Melanins are structurally complex, ubiquitous heterogenous polymeric pigments found in all biological systems^{2–5}. Melanins are enigmatic biopolymers formed by oxidative polymerization of phenolic and hydroxyindole derivatives^{3,6}. Melanins display different colors such as black, brown to yellow and are highly hydrophobic amorphous polymers^{2,3,6}. Melanins are negatively charged³ and contain stable free radicals, a characteristic feature of melanins and are highly resistant to degradation^{4,5,7}.

Melanins display remarkable chemical diversity and are classified as eumelanin, pheomelanin, pyomelanin, allomelanin, neuromelanin and DHN melanin based on the color and chemical composition of the melanin^{3,8,9}. Eumelanin, pheomelanin, pyomelanin, and neuromelanin are synthesized from L-tyrosine^{3,8} whereas, DHN melanins are synthesized from acetyl CoA or malonyl CoA as a precursor⁷. Eumelanins contain nitrogen, pheomelanin contains both nitrogen and sulfur while allomelanin or DHN melanin contains neither of them^{3,8}. Diverse life forms synthesize different melanins, for example, several groups of fungi produce mainly nitrogen-free DHN melanin as well as nitrogenous DOPA melanin^{6,7,10}. Eumelanins are mainly found in all animals imparting

¹Department of Plant Sciences, School of Life Sciences, University of Hyderabad, Hyderabad, 500046, India. ²Centre for Environment, IST, JNT University, Hyderabad, 500 085, India. ³Present address: Department of Botany, Bharathidasan Government College for Women, Puducherry, U.T. − 605003, India. ⁴Present address: Department of Plant Sciences, Avvaiyar Government College for Women, Karaikal, Puducherry, U.T 609602, India. [∞]e-mail: cvramana449@gmail.com

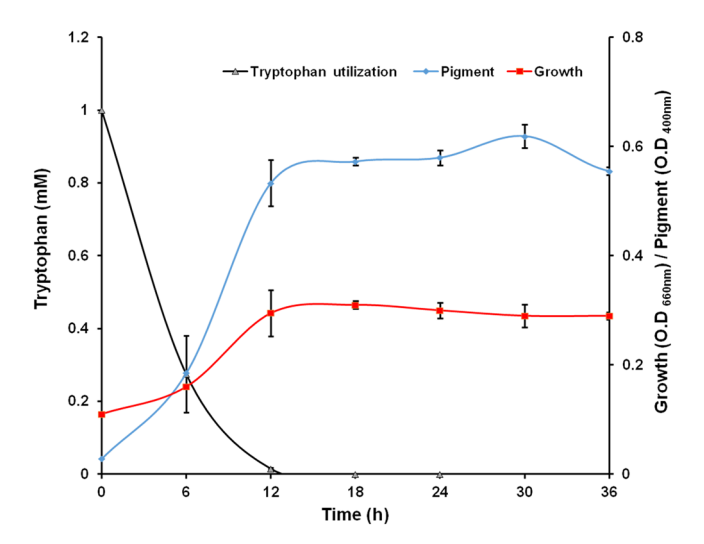


Figure 1. Growth, tryptophan utilization and brown pigment production by *Rubrivivax benzoatilyticus* JA2 under aerobic conditions. Values are the mean \pm standard deviation of two biological replicates.

different colors and few microorganisms also produce eumelanin^{2,3,8}. Except for the DHN melanin, all other types of melanins are synthesized from, tyrosine/phenylalanine. On the other hand, DHN melanins are synthesized mainly from acetyl CoA/malonyl CoA using the polyketide synthase enzyme system^{7,8,10}. Though melanins are chemically diverse their biosynthetic origin is fairly simple starts from tyrosine or acetyl CoA as a precursor^{8,11}. However, a recent study revealed a non-canonical Asp-melanin biosynthesis in *Aspergillus terreus* indicating melanin biosynthetic diversity in life forms¹². Similarly, few *in vivo* studies in animal models^{13,14} and *in vitro* oxidation studies suggested tryptophan can be a potential precursor for melanin synthesis^{14,15}. However, tryptophan-based (named as Trp-melanin) melanins are neither characterized nor their biosynthetic pathway is identified and more so there are no reports of Trp-melanins in microorganisms.

Anoxygenic photosynthetic bacteria are metabolically versatile yet less explored group of bacteria capable of producing different biomolecules such as carotenoid pigments^{16,17} and melanin using aromatic amino acids as precursors¹⁸. *Rubrivivax benzoatilyticus* JA2 is one such a photosynthetic bacterium with remarkable aromatic compound biotransformation abililty¹⁹⁻²². Studies on aromatic compound metabolism by strain JA2 revealed the production of several value-added compounds^{22,23} and multiple catabolic pathways^{22,24}. Recently we reported pyomelanin production by aerobic cultures of strain JA2 and genomic and metabolic insights revealed pyomelanin biosynthetic pathway in strain JA2¹⁸ Employing the newly developed metabolite-centric approach we identified anthocyanin-like pigment production in phenylalanine-amended aerobic cultures of strain JA2¹⁹. Our recent studies on aerobic aromatic metabolism of strain JA2 revealed new biomolecules and metabolic pathways^{18,19,24}. Similarly, while working on aerobic L-tryptophan metabolism in strain JA2 surprisingly we found melanin-like pigment synthesis in aerobic tryptophan amended cultures. In the present study, we report a tryptophan-based melanin production for the first time in a microorganism and characterized the novel melanin produced by strain JA2. The study also suggests a possible non-canonical route of tryptophan-based melanin (Trp-melanin) synthesis.

Results

Growth, L-Tryptophan utilization, and pigment production. Strain JA2 could grow on L-tryptophan as a nitrogen source under aerobic conditions and utilized 90% of L-tryptophan within 12h of incubation (Fig. 1). Strain JA2 produced brown pigment with concomitant utilization of L-tryptophan and pigment production was higher at 12h wherein the maximum amount of tryptophan was utilized (Fig. 1). The pigment was produced only in tryptophan-containing aerobic cultures while no pigment was observed in L-tryptophan-amended anaerobic as well as control (without tryptophan) aerobic cultures (Fig. S1). The pigment produced only in L-tryptophan-containing media inoculated with strain JA2 and pigment was not formed in un-inoculated tryptophan-containing media. The pigment produced by strain JA2 was purified from acidified culture supernatants of L-tryptophan-amended aerobic cultures and upon acidification, the pigment settled as a brown precipitate (Fig. 2A). The dried pure pigment appeared as dark brown (Fig. 2B) and the yield of the pigment was 33 ± 3 mg dry weight per 0.5 liters.

Physicochemical properties of purified brown pigment. The purified pigment was soluble only in alkaline solution (1 M NaOH) and insoluble in organic solvents (hexane, chloroform, acetone, ethyl acetate, ethanol, benzene) as well as water. Pigment is insoluble in neutral buffers and sparingly soluble in alkaline buffers (pH:10–12) (Table S1). The pigment readily precipitated in acidic conditions (5 M HCl), bleached when treated with oxidizing agents like $\rm H_2O_2$ and NaOCl (Table S1). The pigment gave a positive reaction to the polyphenol test by forming flocculent brown precipitate reacting with FeCl₃ (Table S1). Pigment gave positive to ammonical silver nitrate test and $\rm Na_2S_2O_4$ addition decolorized the pigment, upon adding potassium ferricyanide colorless

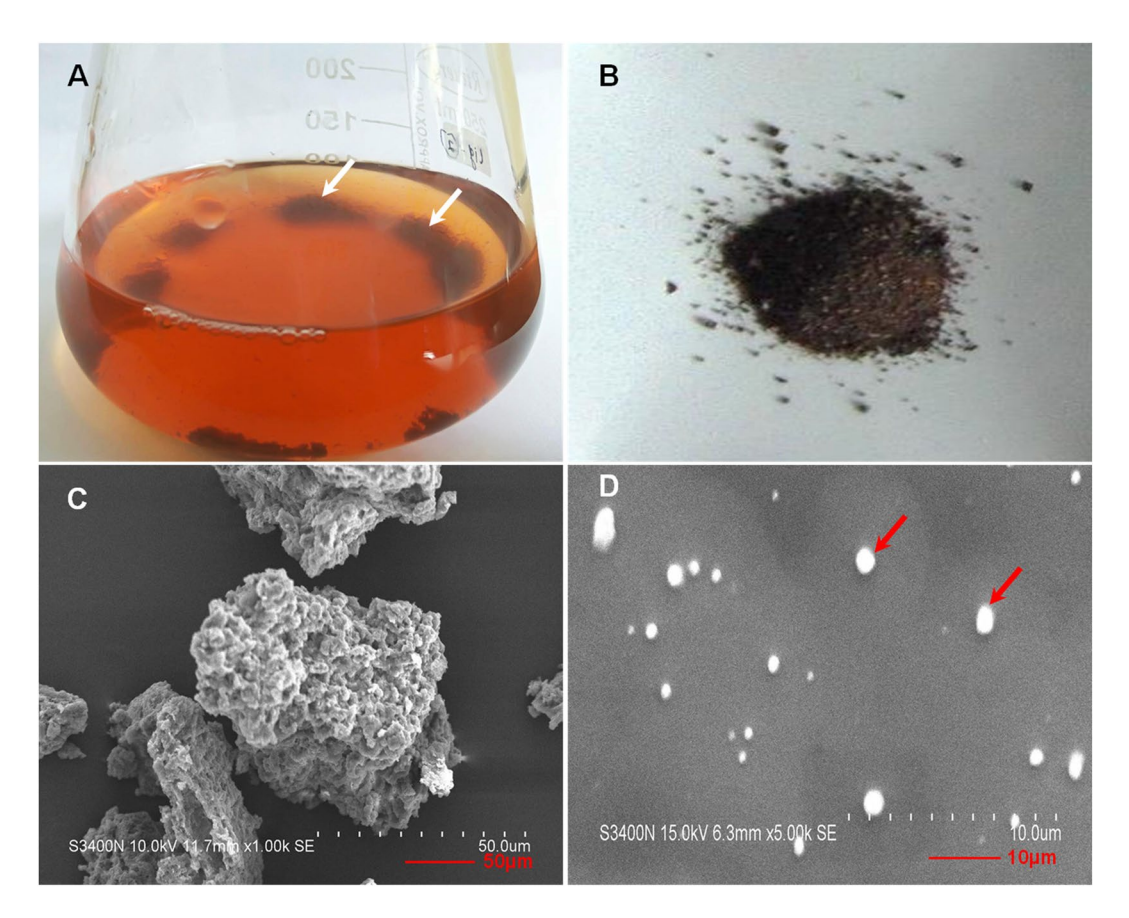


Figure 2. Image showing the brown pigment in acidified culture supernatant obtained from tryptophanamended aerobic culture of strain JA2 (**A**), Dry purified pigment (**B**), SEM micrograph showing aggregated granules of pigments (**C**) and dispersed individual spherical granules of pigment (**D**).

pigment turned brown. The purified brown pigment was positive to all the characteristic chemical tests used to identify melanins²⁵ (Table S1).

Characterization of brown pigment revealed that the pigment is melanin. Scanning electron micrographs of the purified brown pigment revealed unorganized aggregated spherical granules of pigment (Fig. 2C) while the SEM micrograph of the sonicated sample showed dispersed typical sphere-like structures with the homogenous smooth surface characteristic of typical melanin²⁶ (Fig. 2D). The UV-Visible spectrum of purified pigment showed a broad absorption spectrum from UV to the visible region and the absorption was higher in the UV compared to visible region (Fig. 3A). Absorption of brown pigment decreased progressively with increasing wavelength showing a linear correlation between absorption and wavelength (Fig. S2), a characteristic feature of melanins^{26,27}. Elemental analysis of purified brown pigment revealed the presence of C, H, N, O, and no sulfur was detected. Pigment consisted of carbon-46.73%-, hydrogen-5.26%, nitrogen-9.16% and oxygen-38.38% and high C/H ratio (8.9%) of brown pigment indicates the presence of many fused aromatic structures in the pigment^{26,28}. Presence of high nitrogen content (9%) and absence of sulfur moiety indicates that brown pigment is a nitrogen-containing pigment.

FTIR spectrum of the purified pigment exhibited the absorption bands typical to a functional moiety of melanin. The broad band at $3276\,\mathrm{cm^{-1}}$ can be assigned to the –OH and –NH stretching vibrations and the bands at $2928-2802\,\mathrm{cm^{-1}}$ ascribed to CH₃, -CH₂ stretching (Fig. 3B). The band at $1723\,\mathrm{cm^{-1}}$ assigned to C=O stretching vibrations from carbonyl, carboxyl, ketone or quinone groups present in the pigment²⁹. Strong absorption at $1626\,\mathrm{cm^{-1}}$ can be assigned to C=C stretching vibrations of aromatic/pyrrole moiety²⁹ (Fig. 3B). The band at $1526\,\mathrm{cm^{-1}}$ can be designated to the N-H bending along with the band at $1414\,\mathrm{cm^{-1}}$ (C-N stretching) suggests the presence of indole/pyrrolic functional groups in the structure of the pigment^{27,29}. Absorption at $1220\,\mathrm{cm^{-1}}$, indicative of –C-OH group of a phenolic or indolic moiety of pigment³⁰ (Fig. 3B). The band at $1048\,\mathrm{cm^{-1}}$ can be ascribed to the CH- in-plane or CH- out plane deformations and abruption below $700\,\mathrm{cm^{-1}}$ corresponds to out of plane carbon-hydrogen bending of the aromatic moiety³⁰. The IR spectroscopic properties of the pigment of strain JA2 closely correlated with eumelanin^{2,5,30}.

Electron Spin Resonance (ESR) analysis of purified brown pigment revealed the singlet ESR signal at 336.46 mT corresponding to a g-value of 2.00634 (Fig. 3C). Singlet ESR signal observed in the ESR spectrum of brown pigment indicates the presence of stable free-radicals (paramagnetic) a characteristic feature used to identify melanins^{7,27}. X-ray diffraction analysis of the purified pigment showed a broad diffraction peak around $2\theta = 10-50^{\circ}$ suggestive of the amorphous nature of the pigment (Fig. 3D) and this in agreement with previous reports on

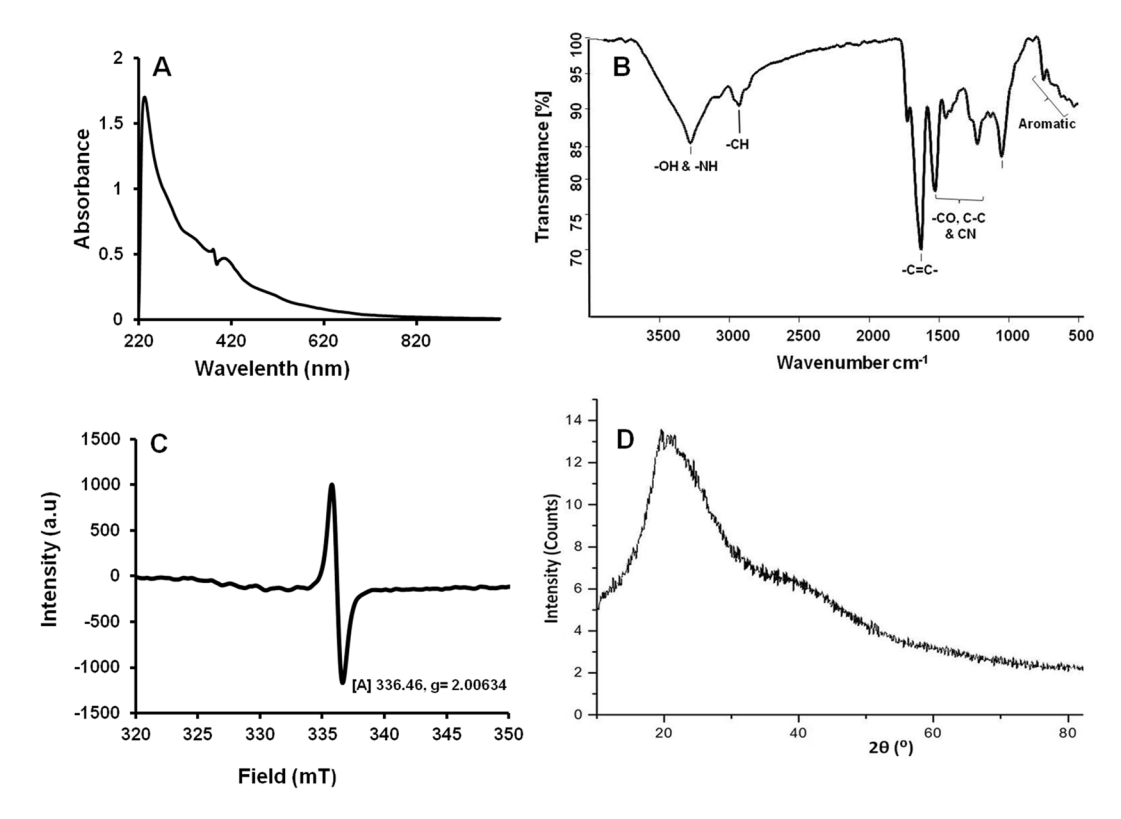


Figure 3. Spectroscopic characterization of purified brown pigment. (**A**) UV-Visible spectrum; (**B**) FTIR spectrum; (**C**) ESR spectrum; (**D**) X-Ray Diffraction spectrum.

melanins¹⁸. Amorphous compounds like melanins which do not have any regular repeating units display broad diffraction features¹⁸.

¹³C and ¹⁵N solid-state NMR studies. The ¹³C solid-state NMR of purified brown pigment showed the intense signal at 160–180 ppm in carboxyl region is usually designated as carbonyl carbon of carboxylates, and quinones possibly associated with a pigment (Fig. 4A)^{2,31,32}. Chemical shifts from 110–150 ppm correspond to aromatic carbons and 100–134 ppm with a broad and weak signal at 126, 110 ppm designated to aromatic carbons of indole/pyrrole moiety^{2,31,32}. Peak around 156 ppm indicates the presence of C-NH- group, possibly of pyrrole/indole moiety². The intense signal from 10–45 ppm is due to side-chain aliphatic carbons correspond to methyl, methylene and methine groups (Fig. 4A)^{2,31,32}. Chemical shifts range from 45–60 ppm can be assigned to backbone carbon of α-C, and β-carbons. The ¹³C solid NMR spectrum of the brown pigment is similar to that of eumelanin spectrum^{2,31,32}.

The solid-state ¹⁵N NMR CP/MAS spectral studies were carried out to further confirm the presence of the nitrogen in the brown pigment. The ¹⁵N NMR spectrum showed an intense broad chemical shift ranging from 110–140 ppm which is consistent with a chemical shift of the nitrogen atom of indole/pyrrole moiety^{31,33} (Fig. 4B). The ¹⁵N spectrum of brown pigment is similar to that of the ¹⁵N spectrum of indole-type Sepia and human hair melanin³¹.

Effect of canonical melanin inhibitors on brown pigment formation. Pigment production by strain JA2 was monitored in the presence of different inhibitors of known melanin biosynthetic pathways. Glyphosate, an inhibitor of tyrosine dependent melanin synthesis¹¹, as well as quercetin, kojic acid, a eumelanin inhibitor² has no effect on pigment production (Fig. 5A). Similarly, pigment production was unaffected in the presence of sulcotrione (visual observation), a pyomelanin inhibitor^{11,18}. Interestingly sodium-azide, a laccase specific inhibitor significantly inhibited the pigment production (Fig. 5A).

HRMS based exometabolite profiling of Trp-fed aerobic cultures. LCMS based exometabolite profiling was carried out to identify the indole derivatives of aerobic tryptophan metabolism and potential immediate precursor/intermediates of pigment synthesis. Typical total ion chromatogram of methanolic extracts of aerobic Trp-amended culture supernatants represented here showing the elution profile of the tryptophan-derived metabolites (Fig. S3). LCMS analysis of a methanolic extract of aerobic Trp culture supernatants revealed metabolite showing identical UV-Visible profile, Rt 7.9 mins having molecular ion mass of 219.0778 [M⁻] corresponding to 5-hydroxytryptophan (Table 1). Metabolite with Rt 14.3 mins also showed identical UV-visible spectrum and molecular ion mass of 190.0509 [M⁻] correspond to 5-hydroxyindole-3-acetic acid (Table 1). Subsequently, metabolites with Rt 7.9 and 14.3 mins were confirmed as 5-hydroxytryptophan and 5-hydroxyindole-3-acetic acid by co-eluting with authentic standards. Metabolites with Rt 10.9, 15.5 and 16.3 mins having molecular ion masses

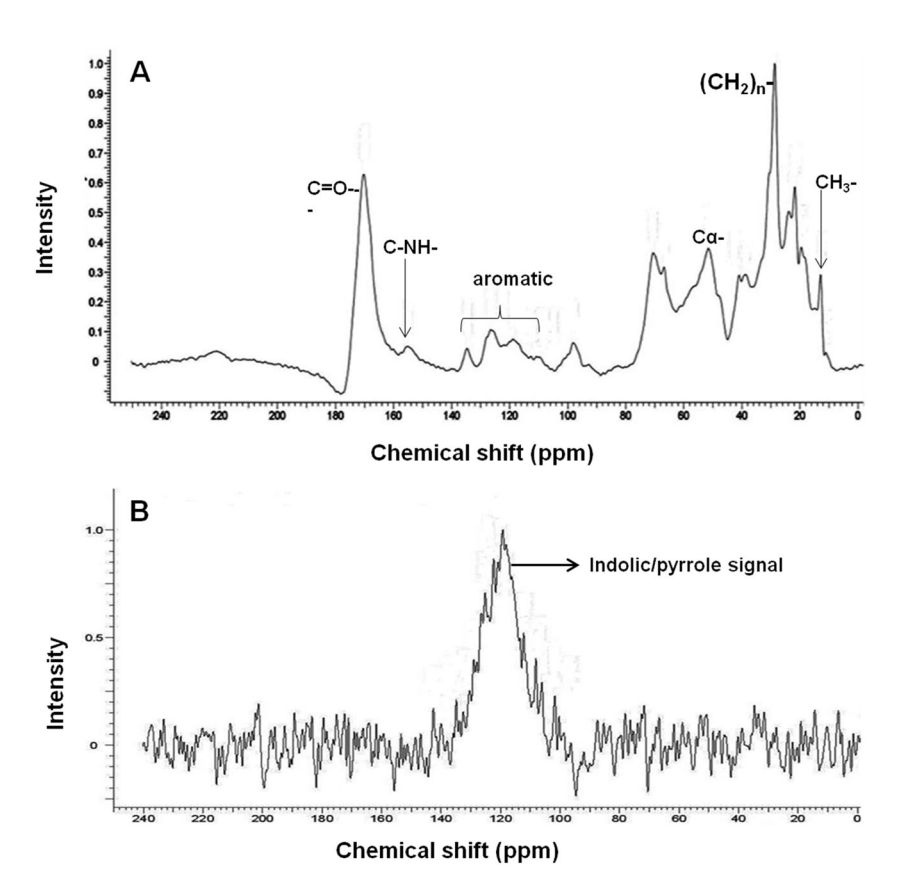


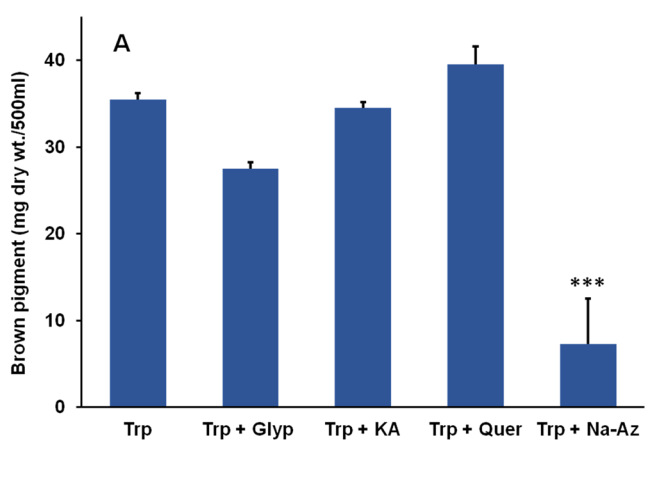
Figure 4. Nuclear Magnetic Resonance spectra of purified brown pigment. **(A)** Solid-state CPMAS ¹³C and **(B)** ¹⁵N NMR spectra.

of 206.04, 218.04, and 147.06[M⁻], were tentatively identified as 5,6-dihydroxyindole-3-acetic acid (DHIAA), 5-hydroxyindole-3-pyruvate (HIPy), and 5-hydroxy-methyl-indole (HMI) respectively based on mass spectra search against database hit and UV-visible profiles.

Brown pigment formation from L-tryptophan and 5-hydroxytryptophan. As we found 5-hydroxytryptophan (OH-Trp) in culture supernatants of Trp-amended cultures, we checked the pigment production in the presence of Trp and OH-Trp in strain JA2. Interestingly, strain JA2 produced intense brown pigment in OH-Trp containing media (Fig. 5B) while no pigment was formed in uninoculated OH-Trp containing media. The pigment production was significantly higher in the presence of OH-Trp compared to tryptophan (Fig. 5B). Pigment purified from OH-Trp-containing cultures showed similar physicochemical properties and UV-Visible profile with that of pigment obtained from Trp cultures (data not shown).

In vitro pigment formation by strain JA2. Strain JA2 showed *in vivo* pigment formation from Trp as well as OH-Trp containing media under aerobic conditions. Here we tried to replicate the pigment formation *in vitro* by exogenously supplying L-Trp and OH-Trp to cell-free extracts obtained from tryptophan supplied aerobic cultures. *In vitro* study revealed the pigment formation in L-Trp and OH-Trp supplied cell-free reactions while pigment formation was not observed in pre-denatured cell-free extracts or reaction mixture without Trp/OH-Trp (Fig. 6A). Pigment intensity was high in OH-Trp compared to L-Trp supplemented *in vitro* assays and purified *in vitro* pigment displayed similar UV-Visible profile (Fig. 6A). *In vitro* studies on pigment formation revealed simultaneous consumption of L-Trp or OH-Trp and formation of pigment over a period of time. Further, the pigment content was high in case of OH-Trp compared to L-Trp (Fig. 6B).

Brown pigment hydrolysis and chemical oxidation confirms the indolic nature of the polymer. Chemical hydrolysis of the brown pigment was performed to confirm the presence of indole derivatives in brown pigment. TLC analysis and indole specific staining of hydrolyzed products obtained from tryptophan (Trp) and hydroxytryptophan (OH-Trp) brown pigments revealed the identical staining pattern in the form of two purple bands indicative of indole moiety (Fig. S4). While staining was not observed in case of unhydrolyzed fractions (methanolic washout) of Trp and OH-Trp pigments indicating that indoles were indeed derived from hydrolyzed brown pigments (Fig. S4). Further chemical oxidation of brown pigment and subsequent HR-LCMS analysis indicated presence of molecular ion mass of 198.0 [M-H] and 241.8 [M-H] corresponding to the pyrrole-2,3,5-tricarboxylic acid(PTCA) and pyrrole-2,3,4,5-tetracarboxylic acid (PTeCA), respectively (Fig. S5). Further PTCA and PTeCA, were confirmed by mass spectral fragmentation pattern, UV spectra and co-elution



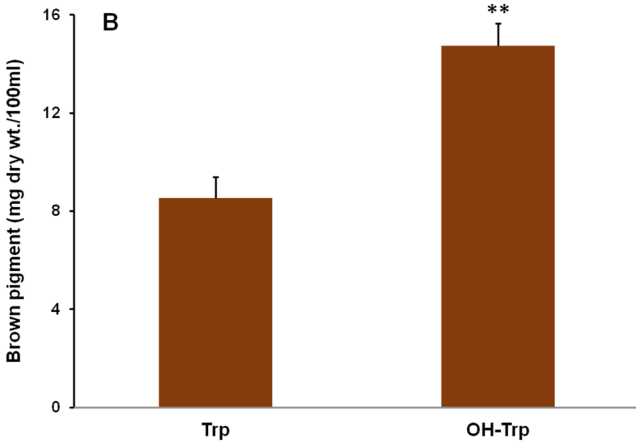


Figure 5. Brown pigment production by strain JA2 in the presence of various inhibitors and substrates. (A) Effect of canonical melanin specific biosynthetic pathway inhibitors on brown pigment production under tryptophan-amended aerobic conditions. (B) Brown pigment production by strain JA2 grown in the presence of tryptophan and 5-hydroxytryptophan. Values are the mean \pm standard deviation of three biological replicates. **P- value <0.005; ***P-val <0.0005 compared to Trp supplemented cultures, calculated using unpaired t-test. Trp, tryptophan; OH-trp, hydroxytryptophan; Glyph, glyphosate: KA, kojic acid; Quer, quercetin; Na-Az, sodium azide.

S. no.	R _t (min)	Generated Mol. formula	Exact Mass	m/z [M ⁻]	Mass accuracy (ppm)	UV-visible Absorbance (nm)	Identification (Confirmed/ Tentative)	
1	7.9	$C_{11}H_{12}N_2O_3$	220	219.0778	0.75	275	5-Hydroxytryptophan	
2	10.9	C ₁₁ H ₉ NO ₄	207	206.0458	0.86	270, 280, 288	5,6-dihydroxyindole-3-acetic acid	
3	14.3	$C_{10}H_9NO_3$	191	190.0509	0.34	275, 300	5-hydroxyindole-3-acetic acid	
4	15.5	C ₁₁ H ₉ NO ₄	219	218.0456	1.42	260, 292	5-Hydroxyindole-3- pyruvate	
5	16.3	C ₉ H ₉ NO	147	146.0609	1.36	290	5-hydroxy-methyl-indole	

Table 1. Tryptophan derived metabolites detected in tryptophan-amended aerobic cultures of strain JA2. Metabolites in italics are confirmed by authentic standards.

with authentic standard (only PTCA). PTCA and PTeCA are oxidative products of 5,6-dihydroxyindole-2-c arboxylic acid (DHICA)^{5,9,34}. Taken together the indole staining of hydrolysed brown pigment and chemical oxidation confirms that brown pigment is indeed an indolic in nature.

Discussion

Melanins are chemically diverse pigments mainly synthesized from two precursors acetyl-CoA (DHN melanin) or tyrosine (eumelanin, pheomelanin, allomelanin, pyomelanin) *via* diverse pathways^{2,8}. Here we identified tryptophan-based melanin (Trp-melanin) synthesis in a bacterium and characterized the pigment and study suggested possible non-canonical Trp-based melanin synthesis. *Rubrivivax benzoatilyticus* JA2 is a metabolically versatile photosynthetic betaproteobacterium and it has remarkable aromatic metabolism evident from a number

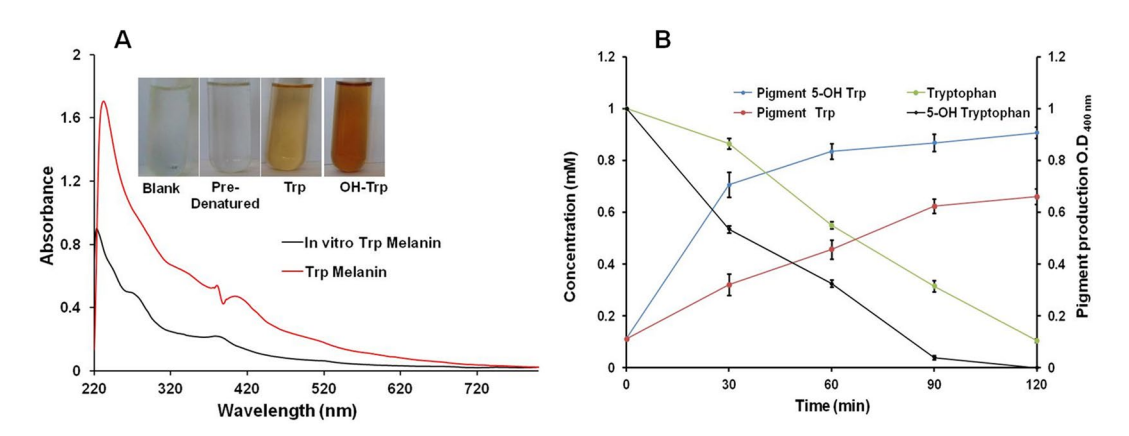


Figure 6. *In vitro* formation of brown pigment in the presence of tryptophan and 5-hydroxytryptophan. (**A**) *In vitro* pigment formation. (**B**) Time-dependent *in vitro* pigment formation. Figure shows UV spectra of pigment obtained from *in vivo* and *in vitro* assays from Trp, Inserts shows *in vitro* pigment formation.

of new biomolecules 16,35,36, catabolic pathways 19,20,22-24,35,37, and enzymes reported 24,36. Recently we designed a new metabolite-centric secondary metabolite mining strategy and employing this tool we successfully demonstrated novel anthocyanin–like pigment production in phenylalanine-amended aerobic cultures of strain JA2¹⁹. Similarly, while working on aerobic metabolism of L-tryptophan, serendipitously we found brown pigment production in strain JA2. Interestingly, only Trp-amended aerobic cultures of strain JA2 produced brown pigment with concomitant utilization of Trp and this suggests that pigment synthesis is Trp-dependent oxidative metabolic process.

Surprisingly, the purified pigment displayed the characteristic properties of melanin such as alkaline solubility, insoluble in organic solvents, positive to polyphenol test and decolorizing to oxidizing agent²⁵ indicating that the brown pigment is melanin (Table S1). Furthermore purified brown pigment showed typical UV-Visible profile of melanin; higher UV absorption and absorbing all the wavelengths in the visible region further confirms that the pigment is melanin (Fig. 3A). Melanins are amorphous polymers with stable free radical centers^{7,27}, in agreement with this, broad diffraction peak and singlet ESR signal displayed by the brown pigment (Fig. 3C,D) of strain JA2 strongly suggests it is an amorphous pigment having free radical centers. Physico-chemical and spectroscopic studies unequivocally confirm that the brown pigment is indeed a melanin. Melanins are known to be synthesized during the oxidative metabolism of phenylalanine/tyrosine^{8,18,24,33}, in contrast, here we report oxidative metabolism of tryptophan leading to Trp-melanin formation in strain JA2. Further, the high nitrogen content (9%) and C/H ratio (8.9%) (typical of aromatic polymers)^{26,28} revealed by elemental analysis of brown pigment indicate that the pigment is a nitrogen-containing aromatic polymer.

This is further supported by IR, NMR analysis wherein brown pigment showed characteristic signals of hydroxy, indolic/pyrrolic and aliphatic moieties. Moreover, a broad signal in ¹⁵N NMR of brown pigment confirms the presence of pyrrole/indolic nitrogen atom (Fig. 4B) and similar ¹⁵N chemical shift was displayed by indole-based eumelanins^{31,33}. In addition, TLC analysis of the degradation products of brown pigment revealed the presence of indole moiety (Fig. S4) confirming the indolic nature of the brown pigment. Presence of high nitrogen and absence of sulfur content further confirms that brown pigment is indole-type melanin and this is in agreement with the previous reports²⁶ and also rules out the possibility of brown pigment being DHN or pheomelanin. Interestingly, brown pigment showed similar spectroscopic features of eumelanin (indole-type melanin) derived from tyrosine. In contrast, here for the first time, we identified and characterized indole-type melanin derived from L-tryptophan in a bacterium.

Tyrosine or acetyl CoA derived melanin biosynthesis is well established while Trp-based melanin biosynthesis is a mystery¹³⁻¹⁵. To gain the insights into the Trp-melanin biosynthesis, first, the genome of strain JA2 was mined for the genes of canonical melanin biosynthesis. Interestingly, strain JA2 genome lacks candidate genes for synthesis of DHN, DOPA, and eumelanin except for the pyomelanin pathway genes. Furthermore, biosynthetic inhibitors of DOPA-melanin/eumelanin (Kojic acid)⁴, pyomelanin (Sulcotrione)¹⁸ and *de novo* tyrosine-based melanin inhibitor glyphosate did not inhibit the Trp-melanin synthesis in strain JA2 (Fig. 5A) suggesting that the Trp-melanin is not synthesized from canonical tyrosine-based melanin biosynthetic process. However, pigment synthesis is inhibited by sodium azide, a laccase inhibitor⁴ and this implies the possible role of laccase in Trp-melanin synthesis. Role of laccase in melanin synthesis is reported in few microorganisms^{4,8}, although we did not find gene coding for laccase, we speculate laccase-like enzyme role in Trp-melanin synthesis by strain JA2 as laccase-like enzyme role is reported in melanin synthesis in few bacteria^{38,39}.

Eumelanin is a polymer of 5,6-dihydroxyindole (DHI) and 5,6-dihydroxyindole-2-carboxylic acid (DHICA), synthesized from tyrosine *via* DOPA, DOPA-chrome finally to DHI, DHICA, and their polymerization lead to eumelanin formation^{3,8}. In contrast, for Trp-melanin, tryptophan acts as a precursor and its oxidative metabolism possibly leading to the formation of hydroxyindoles and their subsequent polymerization to melanin (Fig. 7). In support of this, we found OH-Trp and other hydroxyindole derivatives in the exometabolome of Trp-amended aerobic cultures of strain JA2 (Table 1). Hydroxyindole derivatives and brown pigment formation were not found in anaerobic cultures and on the other hand correlation between hydroxyindoles and pigment formation in aerobic cultures indicates possible role of hydroxyindoles in pigment formation. Furthermore, significantly higher brown pigment production in the presence of OH-Trp compared to Trp (Fig. 5B) suggests that OH-Trp

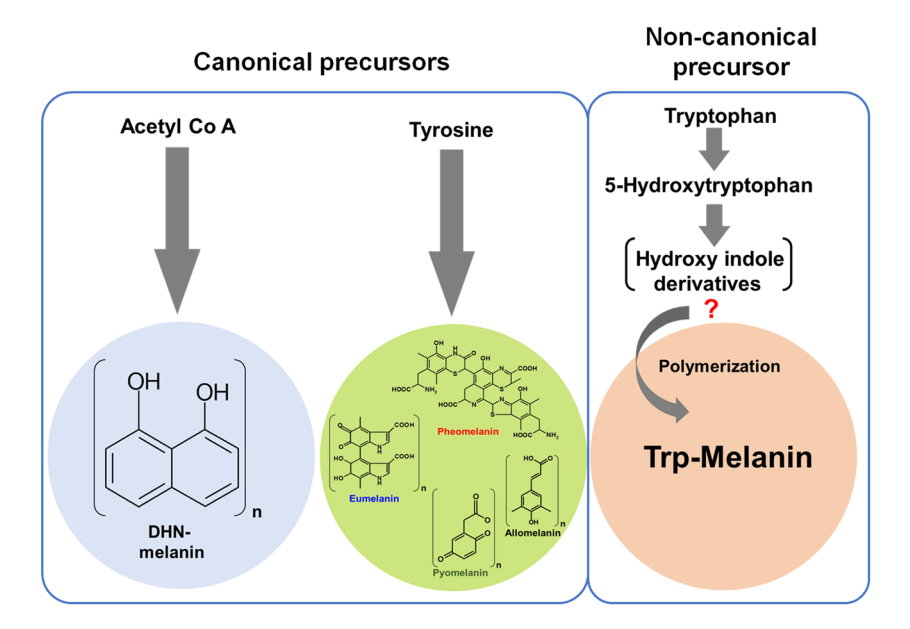


Figure 7. Schematic representation showing melanin synthesis from canonical precursors and non-canonical tryptophan-based melanin synthesis in strain JA2. Predicted trp-based melanin biosynthetic pathway in strain JA2. Metabolites in parenthesis are unknown hydroxyindoles involved in polymerization.

may have readily converted to hydroxyindoles and thereby leading to higher pigment production in strain JA2. Taken together these findings suggest oxidative metabolism of Trp leading to the formation of hydroxyindole derivatives and thereby Trp-melanin formation. Similarly, Vekey *et al.* 1992, reported tryptophan-based melanin formation during chemical oxidation of Trp using perchloric acid and study revealed that polymer consists of hydroxyindoles⁴⁰.

However, our study demonstrates oxidative metabolism of Trp leading to Trp-melanin formation in a biological system. Melanins are natural polymers of phenols or hydroxyindoles mostly derived from tyrosine^{2,3} however in our study hydroxyindole derivatives are derived directly from Trp. Interestingly, alkaline chemical oxidation of Trp-melanin revealed presence of PTCA and PTeCA, which are oxidativate products of 5,6-dihydroxyindole-2-c arboxylic acid (DHICA)^{5,9,34}, thus we speculate that DHICA could be one of the monomer of Trp-melanin. Alternatively, detection of eumelanin markers (PTCA and PTeCA) suggest co-exsitance of eumelanin along with Trp-melanin. Whether DHICA is a involved in Trp-melanin formation needs further investigation, however, the possible role of other hydroxyindole derivatives role in Trp-melanin formation can not be ruled out.

In vitro melanin formation by strain JA2 from Trp or its derivative OH-Trp (Fig. 6) and significantly higher pigment synthesis from OH-Trp suggests (Figs. 5B and 6) that OH-Trp is a possible immediate precursor of pigment synthesis. Higher pigment content in the presence of OH-Trp is possible because of availability of high levels of hydroxyindoles derived from OH-Trp and their subsequent polymerization may have resulted in higher melanin synthesis. Previous study on *Planaria* larval eye melanogenesis demonstrated that formation of OH-Trp is essential for pigment synthesis and suggested possible role of OH-Trp in melanogenesis¹³. Similarly, *in vitro* peroxidase, mediated OH-Trp based melanogenesis is reported elsewhere suggesting the role of OH-Trp in melanogenesis^{14,15}. Based on findings from the current study we hypothesize Trp-melanin synthesis, wherein during oxidative metabolism, tryptophan, is possibly converted to OH-Trp, thereafter into hydroxyindoles and these subsequently polymerized to melanin (Fig. 7). Although few chemical oxidation and *in vitro* studies revealed Trp-melanin formation, for the first time, our study revealed *in vivo* Trp-melanin synthesis, characterized the melanin and study provided important clues on the possible biochemical route of Trp-melanin synthesis.

In conclusion, our study revealed tryptophan-based melanin synthesis by aerobic cultures of photosynthetic bacterium, *Rubrivivax benzoatilyticus* JA2. Traditionally indole-type melanins (eumelanin) are known to synthesize from tyrosine, however, our study demonstrated novel indole-type melanin (named as Trp-melanin) synthesis from a non-canonical precursor, Trp possibly through an alternative route in strain JA2. Future investigations on the identification of monomeric constituents and transcriptome studies would reveal chemical diversity and possible candidate genes involved in Trp-melanin synthesis in strain JA2. Findings from our study strongly supports the view that tryptophan can be a physiological precursor for melanin synthesis and organisms may have evolved mechanisms to use non-canonical precursors for melanin synthesis based on their physiological conditions. Our study indicates that enigmatic melanin pigment chemical and biosynthetic diversity are far from over and suggests possible occurrence of non-canonical melanin biosynthetic process in other life forms.

Methods

Organism, growth conditions and pigment production. Rubrivivas benzoatilyticus JA2 (ATCC BAA-35) was used as a model organism for all the experiments and pure culture was maintained and grown photoheterotrophically (under anaerobic condition, pH 6.8, $30\pm2\,^{\circ}$ C; light 2,400 lux) on minimal media containing 22 mM of malate (carbon source) and 7 mM of ammonium chloride as a nitrogen source in completely filled culture bottle (250 ml). Photoheterotrophically grown mid-log phase culture (O.D- 0.4 at 660 nm) was used as inoculum(10%) and culture was grown aerobically in 500/1000 ml conical flasks and incubated at $30\pm1\,^{\circ}$ C, 180 rpm in shaker incubator (Innova Eppendorf) for 48 h. Ammonium chloride was replaced with 1 mM of L-tryptophan as a nitrogen source for induction of pigment synthesis. The growth was measured as a change in optical density (OD) at 660 nm, while pigment production was measured spectrophotometrically against uninoculated media as a blank at 400 nm. To check the effect of different melanin inhibitors on brown pigment production by strain JA2, glyphosate (1 mM), sodium azide (1 mM), Kojic acid (0.5 mM) and quercetin (0.15 mM) were added to the aerobic cultures containing L-tryptophan. All the inhibitor studies were carried out with mid-log phase aerobic cultures of strain JA2. Whenever required 1 mM L-tryptophan replaced with 5-hydroxytryptophan(1 mM; Himedia chemicals) as a nitrogen source to check the pigment production.

Extraction and purification of brown pigment. L-tryptophan amended aerobic cultures of strain JA2 was used to isolate the pigment and after 48 h of incubation, culture was harvested by centrifugation (10,000 rpm for 10 mins at 4 °C). Later the supernatant was collected and acidified to pH 2.0 using 5 M HCl and acidified supernatant was stored at 4 °C for 2–4 days. The brown precipitate settled at the bottom of the flask was collected by centrifugation at 10,000 rpm for 10 mins at 4 °C. The brown pigment was further purified by serial washings using different organic solvents (10 ml of hexane, acetonitrile, acetone, ethyl acetate, ethanol, and methanol) and finally with Milli-Q water. The purified pigment was dried under freeze drier (Labcanco, USA) and dried pigment was used for physicochemical and spectroscopic studies.

Scanning Electron Microscopic (SEM) and UV visible spectroscopic analysis. SEM analysis of purified pigment was carried out according to Prasuna *et al.*²⁴ with slight modifications, In brief, 1 mg of pigment was suspended in 1 ml of acetonitrile, 100 µl of suspended solution or sonicated solution was mounted on a glass slide and fixed on to the stubs. Samples were subjected to gold sputtering and examined using SEM (Philips XL30 series). UV-Visible spectroscopic studies of purified pigment were done on a spectrophotometer (SHIMADZU, Japan) and the spectra were recorded from 200–800 nm using 1 M NaOH as blank.

FTIR, the spectrum of brown pigment was recorded on alpha ATR-FTIR spectrometer (ALPHA T model, Bruker Optics, Germany) Dried sample was loaded on diamond crystal and the spectrum was recorded from the range of $400-4000\,\mathrm{cm^{-1}}$ at resolution $4\,\mathrm{cm^{-1}}$ with 20-30 scans in transmittance mode. ESR and XRD analysis of purified pigment was done according to Prasuna *et al.*¹⁸. Briefly, dried pigment (20 mg) was loaded into the ESR quartz tube and spectra were recorded on JEOL X-band ESR spectrometer at room temperature. X-ray Diffraction spectrum of purified pigment was recorded using Bruker D8 Advance, Germany X-Ray Diffractometer. Spectrum was recorded by scanning the pigment using the CuKα radiation at wavelength 1.5406 A° with a step size of 0.04°, voltage $40\,\mathrm{kV}$, current $40\,\mathrm{mA}$ and $20\,\mathrm{range}\ 10-90^\circ$.

Solid-state ¹³C **and** ¹⁵N **NMR analysis.** The Solid-state ¹³C and ¹⁵N spectra of purified brown pigment were acquired on an Avance III Bruker Spectro spinning as 800 MHz spectrometers operated using as a triple resonance probe with 5 mm. Purified melanin packed (20–30 mg) in ¹³C and ¹⁵N probe Bruker operating as resonance probe with the operating conditions; spinning speed -7 kHz: 1 H 90°; pulse length was 2.83 μ s and the ¹³C 180° pulse length was 6.52 μ s. The contact time -2000 μ s, acquisition time was 33 ms and the recycle delay-8 s with total 10000 scans. The ¹³C chemical shifts were calibrated relative to tetramethylsilane (0 ppm). The solid-state ¹⁵N NMR CP/MAS spectrum was obtained with the same instrument using N-15 probe Bruker polarization depends on the ¹⁵N—H dipole interaction.

Brown pigment hydrolysis, alkaline oxidation and TLC analysis. The brown pigment degradation products were identified by hydrolysis of the pigment as described by Ellis and Griffiths 1974^{41} with slight modifications. Five milligrams of the dried pure brown pigment was added to $0.5\,\mathrm{g}$ of KOH in a 5 ml tightly sealed screw cap glass tube. The mixture was brought to boil on hot water bath $(1\,\mathrm{h})$ and the dark color residue thus formed was allowed to cool. To the dried residue $1.5\,\mathrm{ml}$, distilled water was added and acidified (pH 2) with concentrated HCl and metabolites were extracted with diethyl ether and dried under rota evaporator (Heidolph, Germany) finally dissolved in HPLC grade methanol. To detect the indoles, the hydrolyzed fraction was run on TLC (Merk, Silica gel $60\,\mathrm{F}_{254}$, $20\times10\,\mathrm{cm}$, $0.2\,\mathrm{mm}$,) using a mixture of Chloroform: Methanol: Glacial acetic acid $(9:0.95:0.05\,\mathrm{v/v})$ as a solvent system and TLC plate was developed using indole-specific TLC reagent prepared as described by Ehmann *et al.*⁴². Alkaline hydrogen peroxide oxidation of brown pigment was carriedout according to Ito et al. 2011 and LCMS analysis was performed as described in HRLC-MS.

Extraction of metabolites and HRLC-MS analysis. Metabolites were extracted from the tryptophan-amended aerobic cultures of strain JA2 and culture was harvested after 48 h of incubation by centrifugation (10,000 rpm, 4 °C, 10 mins). The supernatant was collected and, the supernatant was dried under vacuum using rotary flash evaporator (Heidolph, Germany). The dried supernatant was dissolved in 5 ml of HPLC grade methanol and centrifuged (12,000 rpm, 5 mins), the clear methanolic fraction was collected and freeze dried under vacuum. Finally, the dried methanolic extract was redissolved in 1 ml MS grade methanol and used for HPLC and LCMS analysis.

HRLC-MS ESI analysis was performed according to Prasuna *et al.*²⁴, Briefly, analysis was performed on 6520 Accurate-Mass Q-TOF LC-MS system(Agilent Technologies) equipped with Agilent 1200 series HPLC with a photodiode array detector; an auto sampler was used to inject (2μ l) the sample and chromatographic separation was carried out at 25 °C. Reverse phase column (Phenomenex) C-18 (Luna, $5\,\mu$ m, $150\times4.6\,\text{mm}$) was used to separate the metabolites using a constant flow rate 0.8 ml/minute of mobile phase consisting of 0.1% glacial acetic acid in water (v/v) (eluent A) and acetonitrile (eluent B). The gradient program was used to elute the metabolite (60 mins): starting with 1% eluent B followed by 55% within 48 min then step gradient to 100% within 55 min and held for 5 minutes. The separated analytes were infused into the ESI ion source under full-spectrum scan mode ($50-1000\,\text{m/z}$). Data were collected under negative and positive modes in independent runs. Mass Hunter Qualitative software (version 6.0, Agilent Technologies) was used to analyze the raw data. The standards PTCA and PDCA were generously gifted by Prof. Shosuke Ito and Prof. Kazumasa Wakamatsu, Fujita Health University, Japan. 5-hydroxyindole-3-acetic acid standard was purchased from Sigma-Aldrich (Sigma-Aldrich, H8876).

In vitro melanin production by strain JA2. Log phase aerobic cultures grown on L-tryptophan containing media were used for *in vitro* melanin production studies and cell-free extracts were prepared according to Prasuna *et al.*¹⁸. Briefly, the culture was harvested by centrifugation at 4°C for 10 min 10,000 rpm, collected pellet was washed thrice with 50 mM Tris-buffer and resuspend in 4 ml of 50 mM (pH 7.5) Tris-HCl buffer. The cell lysate was prepared by sonicating the cells using sonicator (BANDELIN, Germany 8 cycles, 55% amplitude) and cell lysate was centrifuged at 16,000 rpm for 20 minutes. The pellet was discarded, the clear supernatant was collected and was used as an enzyme source for *in vitro* pigment production. The *in vitro* assay was carried out in 4 ml final volume consisting of 1 mM L-tryptophan or OH-Trp as substrate and appropriate amount cell-free extract and reaction mixture was incubated at 180 rpm, 37 °C for 1 hour in a incubator shaker (Innova). The reaction was terminated by adding the 300 µl of concentrated HCl and pre-denatured enzyme (with conc. HCl) and reaction mixture without cell-free extract were used as blanks. After the reaction was terminated the brown pigment was purified as described in material and methods earlier. For time-dependent *in vitro* pigment production studies, same procedure was followed as described above except, 1 ml sample was withdrawn periodically (at 30 mins). Samples were centrifuged and the supernatants were analyzed for Trp or OH-Trp using HPLC. The pigment produced was analyzed spectrophotometrically at 400 nm.

Data availability

Melanin samples and spectral data available from the corresponding author on request.

Received: 1 February 2020; Accepted: 8 May 2020;

Published online: 02 June 2020

References

- 1. Narsing Rao, M. P., Xiao, M. & Li, W. J. Fungal and bacterial pigments: Secondary metabolites with wide applications. Front Microbiol 8, 1113, https://doi.org/10.3389/fmicb.2017.01113 (2017).
- 2. Banerjee, A., Supakar, S. & Banerjee, R. Melanin from the nitrogen-fixing bacterium Azotobacter chroococcum: a spectroscopic characterization. *PLoS One* **9**, e84574, https://doi.org/10.1371/journal.pone.0084574 (2014).
- 3. El-Naggar, N. E. & El-Ewasy, S. M. Bioproduction, characterization, anticancer and antioxidant activities of extracellular melanin pigment produced by newly isolated microbial cell factories Streptomyces glaucescens NEAE-H. *Sci Rep* 7, 42129, https://doi.org/10.1038/srep42129 (2017).
- Drewnowska, J. M., Zambrzycka, M., Kalska-Szostko, B., Fiedoruk, K. & Swiecicka, I. Melanin-like pigment synthesis by soil Bacillus weihenstephanensis isolates from Northeastern Poland. PLoS One 10, e0125428, https://doi.org/10.1371/journal. pone.0125428PONE-D-15-00099[pii] (2015).
- Glass, K. et al. Direct chemical evidence for eumelanin pigment from the Jurassic period. Proc Natl Acad Sci USA 109, 10218–10223, https://doi.org/10.1073/pnas.1118448109 (2012).
- d'Ischia, M. et al. Melanins and melanogenesis: from pigment cells to human health and technological applications. Pigment Cell Melanoma Res 28, 520–544, https://doi.org/10.1111/pcmr.12393 (2015).
- Eisenman, H. C. & Casadevall, A. Synthesis and assembly of fungal melanin. Appl Microbiol Biotechnol 93, 931–940, https://doi. org/10.1007/s00253-011-3777-2 (2012).
- 8. Plonka, P. M. & Grabacka, M. Melanin synthesis in microorganisms-biotechnological and medical aspects. Acta Biochim Pol 53, 429-443, 20061329[pii] (2006).
- 9. d'Ischia, M. et al. Melanins and melanogenesis: methods, standards, protocols. Pigment Cell Melanoma Res 26, 616–633, https://doi.org/10.1111/pcmr.12121 (2013).
- 10. Langfelder, K., Streibel, M., Jahn, B., Haase, G. & Brakhage, A. A. Biosynthesis of fungal melanins and their importance for human pathogenic fungi. Fungal Genet Biol 38, 143–158 (2003).
- 11. Almeida-Paes, R. *et al.* Biosynthesis and functions of a melanoid pigment produced by species of the sporothrix complex in the presence of L-tyrosine. *Appl Environ Microbiol* **78**, 8623–8630, https://doi.org/10.1128/AEM.02414-12 (2012).
- 12. Geib, E. et al. A Non-canonical melanin biosynthesis pathway protects Aspergillus terreus conidia from environmental stress. Cell Chem Biol 23, 587–597, https://doi.org/10.1016/j.chembiol.2016.03.014 (2016).
- 13. Lambrus, B. G. *et al.* Tryptophan hydroxylase is required for eye melanogenesis in the Planarian Schmidtea mediterranea. *PLoS One* **10**, e0127074, https://doi.org/10.1371/journal.pone.0127074PONE-D-15-04567[pii] (2015).
- 14. Vogliardi, S. et al. An investigation on the role of 5-hydroxytryptophan in the biosynthesis of melanins. J Mass Spectrom 37, 1292–1296, https://doi.org/10.1002/jms.383 (2002).
- Allegri, G. et al. Involvement of 5-hydroxytryptophan in melanogenesis. Adv Exp Med Biol 527, 723-730, https://doi. org/10.1007/978-1-4615-0135-0_85 (2003).
- Mohammed, M. et al. Genome sequence of the phototrophic betaproteobacterium Rubrivivax benzoatilyticus strain JA2T. J Bacteriol 193, 2898–2899, https://doi.org/10.1128/JB.00379-11 (2011).
- 17. Ouchane, S., Picaud, M., Vernotte, C., Reiss-Husson, F. & Astier, C. Pleiotropic effects of puf interposon mutagenesis on carotenoid biosynthesis in Rubrivivax gelatinosus. A new gene organization in purple bacteria. *J Biol Chem* 272, 1670–1676, https://doi.org/10.1074/jbc.272.3.1670 (1997).

- 18. Mekala, L. P., Mohammed, M., Chinthalapati, S. & Chinthalapati, V. R. Pyomelanin production: Insights into the incomplete aerobic l-phenylalanine catabolism of a photosynthetic bacterium, Rubrivivax benzoatilyticus JA2. *Int J Biol Macromol* 126, 755–764, https://doi.org/10.1016/j.ijbiomac.2018.12.142 (2019).
- 19. Mekala, L. P., Mohammed, M., Chintalapati, S. & Chintalapati, V. R. Precursor-feeding and altered-growth conditions reveal novel blue pigment production by Rubrivivax benzoatilyticus JA2. *Biotechnol Lett* 41, 813–822, https://doi.org/10.1007/s10529-019-02682-610.1007/s10529-019-02682-6[pii] (2019).
- 20. Mujahid, M., Sasikala, C. & Ramana, C. V. Aniline-induced tryptophan production and identification of indole derivatives from three purple bacteria. *Curr Microbiol* **61**, 285–290, https://doi.org/10.1007/s00284-010-9609-2 (2010).
- 21. Kumavath, R. N., Ramana, C. V. & Sasikala, C. L-Tryptophan catabolism by Rubrivivax benzoatilyticus JA2 occurs through indole 3-pyruvic acid pathway. *Biodegradation* 21, 825–832, https://doi.org/10.1007/s10532-010-9347-y (2010).
- 22. Mujahid, M., Sasikala, C. & Ramana, C. V. Production of indole-3-acetic acid and related indole derivatives from L-tryptophan by Rubrivivax benzoatilyticus JA2. Appl Microbiol Biotechnol 89, 1001–1008, https://doi.org/10.1007/s00253-010-2951-2 (2011).
- Prasuna, M. L., Mujahid, M., Sasikala, C. & Ramana, C. V. L-Phenylalanine catabolism and L-phenyllactic acid production by a
 phototrophic bacterium, Rubrivivax benzoatilyticus JA2. Microbiol Res 167, 526–531, https://doi.org/10.1016/j.micres.2012.03.001
 (2012).
- 24. Mekala, L. P., Mohammed, M., Chintalapati, S. & Chintalapati, V. R. Stable isotope-assisted metabolic profiling reveals growth mode dependent differential metabolism and multiple catabolic pathways of l-phenylalanine in Rubrivivax benzoatilyticus JA2. *J Proteome Res* 17, 189–202, https://doi.org/10.1021/acs.jproteome.7b00500 (2018).
- Ellis, D. H. & Griffith, D. A. The location and analysis of melanins in the cell walls of some soil fungi. Canadian Journal of Microbiology 20, 1379–1386 (1974).
- Saini, A. S. & Melo, J. S. One-pot green synthesis of eumelanin: process optimization and its characterization. RSC Advances 5, 47671–47680, https://doi.org/10.1039/C5RA01962A (2015).
- 27. Goncalves, R. C., Lisboa, H. C. & Pombeiro-Sponchiado, S. R. Characterization of melanin pigment produced by Aspergillus nidulans. *World J Microbiol Biotechnol* 28, 1467–1474, https://doi.org/10.1007/s11274-011-0948-3 (2012).
- 28. Xun Hu et al. High yields of solid carbonaceous materials from biomass. Green Chemistry 21, 1128-1140 (2019).
- 29. Di Capua, R. et al. Eumelanin Graphene-like integration: The impact on physical properties and electrical conductivity. Front Chem 7, 121, https://doi.org/10.3389/fchem.2019.00121 (2019).
- 30. Silvia, A. Centeno & Shamir, J. Surface enhanced raman scattering (SERS) and FTIR characterization of the sepia melanin pigment used in works of art. *Journal of Molecular Structure* 873, 149–159 (2008).
- 31. Bhavin, B. *et al.* Solid-state cross-polarization magic angle spinning 13C and 15N NMR characterization of Sepia melanin, Sepia melanin free acid and human hair melanin in comparison with several model compounds. *Magnetic Resonance in Chemistry* 41, 466–474 (2003).
- 32. Xiao, M. et al. Elucidation of the hierarchical structure of natural eumelanins. J R Soc Interface 15, https://doi.org/10.1098/rsif.2018.0045 (2018).
- 33. Chatterjee, S. et al. Demonstration of a common indole-based aromatic core in natural and synthetic eumelanins by solid-state NMR. Org Biomol Chem 12, 6730–6736, https://doi.org/10.1039/c4ob01066c (2014).
- 34. Ito, S. et al. Usefulness of alkaline hydrogen peroxide oxidation to analyze eumelanin and pheomelanin in various tissue samples: application to chemical analysis of human hair melanins. Pigment Cell Melanoma Res 24, 605–613, https://doi.org/10.1111/j.1755-148X.2011.00864.x (2011).
- 35. Kumavath, R. N. & Ch Sasikala, C. V. R. Rubrivivaxin, a new cytotoxic and cyclooxygenase-I inhibitory metabolite from Rubrivivax benzoatilyticus JA2. World Journal of Microbiology and Biotechnology 27, 11–16 (2011).
- 36. Kumavath, R. N. et al. Isolation and Characterization of L-tryptophan ammonia lyase from Rubrivivax benzoatilyticus strain JA2. Curr Protein Pept Sci 16, 775–781 (2015).
- 37. Mujahid, M., Sasikala, C. & Ramana, C. V. Carbon catabolite repression-independent and pH-dependent production of indoles by Rubrivivax benzoatilyticus JA2. *Curr Microbiol* 67, 399–405, https://doi.org/10.1007/s00284-013-0378-6 (2013).
- 38. Castro-Sowinski, S., Martinez-Drets, G. & Okon, Y. Laccase activity in melanin-producing strains of Sinorhizobium meliloti. FEMS Microbiol Lett 209, 119–125, https://doi.org/10.1111/j.1574-6968.2002.tb11119.x (2002).
- 39. Lucas-Elio, P., Solano, F. & Sanchez-Amat, A. Regulation of polyphenol oxidase activities and melanin synthesis in Marinomonas mediterranea: identification of ppoS, a gene encoding a sensor histidine kinase. *Microbiology* **148**, 2457–2466, https://doi.org/10.1099/00221287-148-8-2457 (2002).
- 40. Karoly Vèkey, J. T., Somogyi, A., Bertazzo, A., Costa, C. & Allegri, G. Roberta Seraglia, Piero Traldi. Studies on structure characterization of tryptophan melanin: Comparison between filament and curie-point pyrolysis gas chromatography/mass spectrometry. *Journal of Mass Spectrometry* 27, 1216–1219 (1992).
- 41. D. H. ELLIS, D. A. G. The location and analysis of melanins in the cell walls of some soil fungi. *Canadian Journal of Microbiology* **20**, 1379–1386 (1974).
- 42. Ehmann, A. The van urk-Salkowski reagent–a sensitive and specific chromogenic reagent for silica gel thin-layer chromatographic detection and identification of indole derivatives. *J Chromatogr* 132, 267–276, https://doi.org/10.1016/s0021-9673(00)89300-0 (1977).

Acknowledgements

Shabbir Ahmad acknowledges University Grant Commission, Govt. of India for Fellowship (File No:F1–17.1/201415/ MANF-2014-15-MUS- JHA-35979). Ramana thank the Department of Biotechnology (Tata Innovative Fellowship- BT/HRD/35/01/02/2015) and CSIR, Government of India for the award project funding (CSIR/04/0404/2018/01247). We are greatful to Prof. Shosuke Ito and Prof. Kazumasa Wakamatsu, Fujita Health University, Japan for generously gifting the PTCA and PDCA standards.

Author contributions

S.A., L.P.M., M.M. and V.R.C., conceived and designed the research. S.A. performed the experiments. S.A, L.P.M., M.M and V.R.C discussed and analysed the data. S.A and M.M. drafted the manuscript. L.P.M., M.M., V.R.C., and S.C., edited the manuscript. All authors have read and approved the manuscript.

Competing interests

The authors declare no competing interests.

Additional information

Supplementary information is available for this paper at https://doi.org/10.1038/s41598-020-65803-6.

Correspondence and requests for materials should be addressed to V.R.C.

Reprints and permissions information is available at www.nature.com/reprints.

Publisher's note Springer Nature remains neutral with regard to jurisdictional claims in published maps and institutional affiliations.

Open Access This article is licensed under a Creative Commons Attribution 4.0 International License, which permits use, sharing, adaptation, distribution and reproduction in any medium or format, as long as you give appropriate credit to the original author(s) and the source, provide a link to the Creative Commons license, and indicate if changes were made. The images or other third party material in this article are included in the article's Creative Commons license, unless indicated otherwise in a credit line to the material. If material is not included in the article's Creative Commons license and your intended use is not permitted by statutory regulation or exceeds the permitted use, you will need to obtain permission directly from the copyright holder. To view a copy of this license, visit https://creativecommons.org/licenses/by/4.0/.

© The Author(s) 2020

JOURNAL OF SYSTEMATIC AND EVOLUTIONARY **MICROBIOLOGY**

TAXONOMIC DESCRIPTION

Rai et al., Int. J. Syst. Evol. Microbiol. DOI 10.1099/ijsem.0.003962



Paracoccus aeridis sp. nov., an indole-producing bacterium isolated from the rhizosphere of an orchid, Aerides maculosa

Anusha Rai¹, Smita N¹, Suresh G¹, Shabbir A¹, Deepshikha G¹, Sasikala Ch^{2,*} and Ramana Ch.V^{1,*}

Abstract

A Gram-stain-negative, non-motile, coccoid-shaped, catalase- and oxidase-positive, non-denitrifying, neutrophilic bacterium designated as strain JC501^T was isolated from an epiphytic rhizosphere of an orchid, Aerides maculosa, growing in the Western Ghats of India. Phylogenetic analyses based on the 16S rRNA gene sequence indicated that strain JC501^T belonged to the genus Paracoccus and had the highest levels of sequence identity with Paracoccus marinus KKL-A5^T (98.9 %), Paracoccus contaminans WPAn02^T (97.3%) and other members of the genus Paracoccus (<97.3%). Strain JC501^T produced indole-3 acetic acid and other indole derivatives from tryptophan. The dominant respiratory quinone was Q-10 and the major fatty acid was $C_{18.1}\omega 7c/C_{18.1}\omega 6c$, with significant quantities of $C_{18:1}\omega$ 9c, $C_{17:0}$ and $C_{16:0}$. The polar lipids of strain JC501^T comprised phosphatidylglycerol, phosphatidylcholine, diphosphatidylglycerol, an unidentified glycolipid, two unidentified aminolipids, two unidentified lipids and four unidentified phospholipids. The genome of strain JC501[™] was 3.3 Mbp with G+C content of 69.4 mol%. For the resolution of the phylogenetic congruence of the novel strain, the phylogeny was also reconstructed with the sequences of eight housekeeping genes. Based on the results of phylogenetic analyses, low (<85.9%) average nucleotide identity, digital DNA-DNA hybridization (<29.8%), chemotaxonomic analysis and physiological properties, strain JC501[™] could not be classified into any of the recognized species of the genus Paracoccus. Strain JC501^T represents a novel species, for which the name Paracoccus aeridis sp. nov. is proposed. The type strain is JC501^T (=LMG 30532^T=NBRC 113644^T).

Bacteria residing in the rhizosphere of the plants play a vital role in the holistic development of the plant system [1-3]. Epiphytic orchid-associated bacteria have functional and ecological roles in the development of their host plant [4]. Epiphytes do not interact directly with the soil or its microbiota and thus constitute a unique system of ecology. Therefore, epiphytes have their own distinctive structural system for their sustenance, wherein they take up the nutrients and moisture from the atmosphere on the surface of the host plant aided by the microbial association [5, 6]. While investigating this unique diversity and its subsequent role in the development of the orchids, we have isolated strain JC501^T from the rhizosphere of an epiphytic orchid (Aerides maculosa). This strain belongs to the genus Paracoccus based on 16S rRNA gene sequence analysis. The genus Paracoccus was first described by Davis and his co-workers in 1969 [7] and belongs to the family 'Rhodobacteraceae' of the class Alphaproteobacteria in the phylum *Proteobacteria*. There are more than 50 species of *Paracoccus* with validly published names (www.bacterio.net). Members have been isolated from environmental samples such as soil [8, 9], sediment [10, 11], water [12, 13], sludges [14, 15], foodstuffs [16], clinical specimens [17] and insects [18]. Paracoccus halotolerans [19], Paracoccus salipaludis [20], Paracoccus fontiphilus [13], Paracoccus alimentarius [16], Paracoccus endophyticus [21], Paracoccus haematequi [22] and Paracoccus nototheniae [23] are the valid names published during the year 2018-2019, while Paracoccus jeotgali [24] and Paracoccus indicus [25] are effective publications. Members of this genus are Gram-stain-negative, mostly non-motile and chemoorganotrophs [26]. Their major fatty acid is $C_{18.1}\omega 7c$ and they are metabolically versatile [27]. The members of the genus Paracoccus have a genome size ranging from 2.9 to 5.6

Author affiliations: 1Department of Plant Sciences, School of Life Sciences, University of Hyderabad P.O. Central University, Hyderabad 500046, India; ²Bacterial Discovery Laboratory, Centre for Environment, Institute of Science and Technology, J. N. T. University Hyderabad, Kukatpally, Hyderabad 500085, India.

*Correspondence: Sasikala Ch, sasi449@yahoo.ie; Ramana Ch.V, cvr449@gmail.com

Keywords: Paracoccus; epiphytic orchid; Proteobacteria; indole.

Abbreviations: AIC, Akaike information criterion; ANI, average nucleotide identity; dDDH, digital DNA–DNA hybridization; IAA, indole-3-acetic acid; IAM, indole-3-acetamide; LCB, local collinear block; ML, maximum-likelihood; MLSA, multilocus sequence analysis; NA, nutrient agar. The GenBank/EMBL/DDBJ accession number for the 16S rRNA gene sequence of strain JC501^T is LT799401. The Whole Genome Shotgun project is SELD00000000. The genome sequence of *P. marinus* NBRC 100637^T is VJYZ00000000.

1

Five supplementary tables and ten supplementary figures are available with the online version of this article.

INTERNATIONAL JOURNAL OF SYSTEMATIC AND EVOLUTIONARY MICROBIOLOGY

TAXONOMIC DESCRIPTION

B. et al., Int J Syst Evol Microbiol 2020;70:93–99 DOI 10.1099/ijsem.0.003716



Chryseobacterium candidae sp. nov., isolated from a yeast (Candida tropicalis)

Indu B., ¹ Kumar G., ¹ Smita N., ¹ Shabbir A., ² Sasikala Ch. ^{1,*} and Ramana Ch. V. ¹

Abstract

A Gram-stain-negative, rod shaped, non-motile, aerobic bacterium (strain $JC507^T$) was isolated from a yeast (*Candida tropicalis JY*101). Strain $JC507^T$ was oxidase- and catalase-positive. Complete 16S rRNA gene sequence comparison data indicated that strain $JC507^T$ was a member of the genus *Chryseobacterium* and was closely related to *Chryseobacterium indologenes* NBRC 14944^T (98.7 %), followed by *Chryseobacterium arthrosphaerae* CC-VM-7^T (98.6 %), *Chryseobacterium gleum* ATCC 35910^T (98.5 %) and less than 98.5 % to other species of the genus *Chryseobacterium*. The genomic DNA G+C content of strain $JC507^T$ was 36.0 mol%. Strain $JC507^T$ had phosphatidylethanolamine, four unidentified amino lipids and four unidentified lipids. MK-6 was the only respiratory quinone. The major fatty acids (>10 %) were anteiso-C_{11:0}, iso-C_{15:0} and iso-C_{17:0}30H. The average nucleotide identity and *in silico* DNA-DNA hybridization values between strain $JC507^T$ and *C. indologenes* NBRC 14944^T, *C. arthrosphaerae* CC-VM-7^T and *C. gleum* ATCC 35910^T were 80.2, 83.0 and 87.0 % and 24, 26.7 and 32.7 %, respectively. The results of phenotypic, phylogenetic and chemotaxonomic analyses support the inclusion of strain $JC507^T$ as a representative of a new species of the genus *Chryseobacterium*, for which the name *Chryseobacterium candidae* sp. nov. is proposed. The type strain is $JC507^T$ (=KCTC 52928^T=MCC 4072^T=NBRC 113872^T).

The family Flavobacteriaceae comprises the genus Chryseobacterium which was first established by Vandamme et al. [1]. At the time of writing, more than 100 species of bacteria (www.bacterio.net/chryseobacterium.html) placed in the genus Chryseobacterium and were isolated either from clinical samples [2], fish [3], fresh water [4], sewage and plants [5], soils [6, 7], meat [8] or waste water [9]. New species with valid names added during 2018-2019 included Chryseobacterium salipaludis [10] Chryseobacterium aurantiacum [11], Chryseobacterium phosphatilyticum [12], Chryseobacterium glaciei [13] and Chryseobacterium populi [14]. The typical characteristics of the genus Chryseobacterium include the presence of an aerobic type of metabolism, branched-chain fatty acids, iso-C_{15:0} and iso-C_{17:0}3-OH as the major fatty acids, phosphatidylethanolamine as a major polar lipid, menaquinone-6 (MK-6) as the characteristic respiratory quinone, and production of flexirubin-type pigments [15-17]. Some of the members of this genus are associated as endophytes [12, 17] and during our study on yeast diversity, we have isolated an endobacterium (strain JC507^T) of a yeast (*Candida tropicalis*) which was characterized by a genomic and polyphasic taxonomic approach.

A yeast (strain JY101) was isolated from a soil sample collected from Hyderabad, India (22° 98′ N 71° 47′ E). The soil sample was serially diluted and plated onto a nutrient agar plate containing chloramphenicol (100 µg ml⁻¹). Several white-coloured colonies were observed which were further purified and sequenced using yeast-specific primers used for amplification of the ITS regions and the D1/D2 domain of the 26S rRNA gene. The Internal transcribed spacer (ITS) amplified (5'-GTCGTAAregion was with ITS1 CAAGGTTTCCGTAGGTG-3') TCCTCCGCTTATTGATATGC-3') primers (31). The D1/ D2 domain of the 26S rRNA gene was amplified using NL1 (5'-GCATATCAATAAGCGGAGGAAAAG-3') and NL4 (5'-GGTCCGTGTTTCAAGACGG-3') primers. NCBI/CBS BLAST analysis of strain JY101 for D1/D2 (599 bp; NCBI accession numberLT999794) and ITS (340 bp; NCBI accession number LT795043) showed 100 % sequence similarity

Author affiliations: ¹Department of Plant Sciences, School of Life Sciences, University of Hyderabad, P.O. Central University, Hyderabad 500046, India; ²Bacterial Discovery Laboratory, Centre for Environment, Institute of Science and Technology, J. N. T. University Hyderabad, Kukatpally, Hyderabad 500085, India.

*Correspondence: Sasikala Ch., cvr449@gmail.com or sasi449@yahoo.ie Keyword: Chryseobacterium .

Abbreviations: EDTA, Ethylenediaminetetraaceticacid; EMSA, ElectrophoreticMobility Shift Assay; SPI-1, SalmonellaPathogenicityIsland 1; MR/P, Mannose-Resistant/Proteus; PAGE, PolyacrylamideGel Electrophoresis; PBS, PhosphateBuffered Saline; PCR, PolymeraseChain Reaction; UAS, UpstreamActivating Sequence.

The GenBank/EMBL/DDBJ accession number for the 16S rRNA gene sequence of strainJC507^T is LT838865. The GenBank/EMBL/DDBJ accession for the whole genome shotgun sequence is SDLV00000000.

One supplementary table and three supplementary figures are available with the online version of this article.

ORIGINAL PAPER



Descriptions of *Roseiconus nitratireducens* gen. nov. sp. nov. and *Roseiconus lacunae* sp. nov.

Dhanesh Kumar¹ · Gaurav Kumar¹ · Jagadeeshwari Uppada² · Shabbir Ahmed¹ · Chintalapati Sasikala² · Chintalapati Venkata Ramana¹

Received: 19 June 2020 / Revised: 25 August 2020 / Accepted: 1 October 2020 © Springer-Verlag GmbH Germany, part of Springer Nature 2020

Abstract

Two pink-coloured, oxidase–catalase-positive, salt and alkali-tolerant planctomycetal strains (JC635^T and JC645^T) with pear to spherical-shaped, Gram-stain-negative, motile cells were isolated from Chilika lagoon, India. Both strains share highest 16S rRNA gene sequence identity with members of the genus *Rhodopirellula* (<94%) and *Roseimaritima* (<94%) of the family *Pirellulaceae*. The 16S rRNA sequence identity between the strains JC635^T and JC645^T is 96.1%. Respiratory quinone for both strains is MK6. Major fatty acids are $C_{18:1}\omega$ 9c and $C_{16:0}$. Major polar lipids are phosphatidylethanolamine, phosphatidylcholine, unidentified amino lipids and an unidentified lipid. The genomic size of strain JC635^T and JC645^T are 7.95 Mb and 8.2 Mb with DNA G+C content of 55.1 and 60.0 mol%, respectively. Based on phylogenetic, genomic (ANI, AAI, POCP, *d*DDH), chemotaxonomic, physiological and biochemical characteristics, we conclude that both strains belong to a novel genus *Roseiconus* gen. nov. and constitute two novel species for which we propose the names *Roseiconus nitratireducens* sp. nov. and *Roseiconus lacunae* sp. nov. The two novel species are represented by the type strains JC645^T (=KCTC 72174^T = NBRC 113879^T) and JC635^T (=KCTC 72164^T = NBRC 113875^T), respectively.

Keywords Chilika lagoon · *Planctomycetes* · *Pirellulaceae* · Gen. nov. · Sp. nov.

Communicated by Erko stackebrandt.

Dhanesh Kumar and Kumar Gaurav share equal authorship and are considered as first authors.

Electronic supplementary material The online version of this article (https://doi.org/10.1007/s00203-020-02078-5) contains supplementary material, which is available to authorized users.

- Chintalapati Sasikala sasi449@yahoo.ie; sasikala.ch@gmail.com
- Chintalapati Venkata Ramana cvr449@gmail.com

Published online: 12 October 2020

- Department of Plant Sciences, School of Life Sciences, University of Hyderabad, P.O. Central University, Hyderabad 500046, India
- Bacterial Discovery Laboratory, Centre for Environment, Institute of Science and Technology, J. N. T. University Hyderabad, Kukatpally, Hyderabad 500085, India

Introduction

Members of the phylum Planctomycetes are widely distributed and are most commonly isolated from aquatic habitats (Wiegand et al. 2018). Species of this phylum have unique physiology and cell morphology compared to other bacteria (Lage et al. 2013; Wiegand et al. 2020). Phylogenetically, the phylum *Planctomycetes*, along with *Chlamydiae*, *Ver*rucomicrobia and others sister phyla forms the PVC superphylum (van Niftrik and Devos 2017). The phylum Planctomycetes is subdivided into three classes: Planctomycetia, Phycisphaerae and "Candidatus Brocadiae". Members of "Candidatus Brocadiae" are capable of performing anaerobic ammonium oxidation (anammox) (Strous et al. 1999) and thereby convert toxic ammonium to dinitrogen gas. The class Planctomycetia has the highest number of species and in the past decade, a large number of strains representing new taxa were isolated from aquatic habitats (Storesund and Øvreås 2013; Bondoso et al. 2014, 2017; Vollmers et al. 2017; Kallscheuer et al. 2019a, b, 2020; Boersma et al. 2019; Peeters et al. 2020a, b; Schubert et al. 2020; Dedysh et al. 2020; Kumar et al. 2020a, b; Waqqas et al. 2020). The



INTERNATIONAL JOURNAL OF SYSTEMATIC AND EVOLUTIONARY MICROBIOLOGY

TAXONOMIC DESCRIPTION

Kumar et al., Int. J. Syst. Evol. Microbiol.
DOI 10.1099/ijsem.0.004211



Gimesia chilikensis sp. nov., a haloalkali-tolerant planctomycete isolated from Chilika lagoon and emended description of the genus Gimesia

MOI Dhanesh Kumar¹†, Kumar Gaurav¹†, Sreya PK¹, Shabbir A.¹, Jagadeeshwari Uppada², Sasikala Ch.².* and Ramana Ch.V.¹.*

Abstract

A Gram-stain-negative, aerobic, non-motile, salt- and alkali-tolerant, pear to oval shaped, rosette-forming, white coloured, bacterium, designated as strain JC646^T, was isolated from a sediment sample collected from Chilika lagoon, India. Strain JC646^T reproduced through budding, grew well at up to pH 9.0 and tolerated up to 7% NaCl. Strain JC 646^T utilized α -D-glucose, fumarate, lactose, sucrose, fructose, D-galactose, mannose, maltose and D-xylose as carbon sources. Peptone, L-isoleucine, L-serine, L-lysine, L-glutamic acid, L-aspartic acid, DL-threonine and L-glycine were used by the strain as nitrogen sources for growth. The respiratory quinone was MK6. Major fatty acids were $C_{16:1}\omega 7c/C_{16:1}\omega 6c$ and $C_{16:0}$. The polar lipids of strain JC646^T comprised phosphatidyl-dimethylethanolamine, phosphatidylcholine, diphosphatidylglycerol, an unidentified amino lipid and two unidentified lipids. Strain JC646^T had highest (97.3%) 16S rRNA gene sequence identity to the only species of the genus *Gimesia*, *Gimesia* maris DSM 8797^T. The genome of strain JC646^T was 7.64 Mbp with a DNA G+C content of 53.2 mol%. For the resolution of the phylogenetic congruence of the novel strain, the phylogeny was also reconstructed with the sequences of 92 housekeeping genes. Based on phylogenetic analyses, digitalDNA–DNA hybridization (19.0%), genomeaverage nucleotide identity (74.5%) and averageamino acid identity/percentageof conserved proteins (77%) results, chemotaxonomic characteristics, and differential physiological properties, strain JC646^T is recognized as representing a new species of the genus *Gimesia*, for which we propose the name *Gimesia chilikensis* sp. nov. The type strain is JC646^T (=KCTC 72175^T=NBRC 113881^T).

In 1976, Bauld and Staley [1] reported a marine, stalked and budding bacterium as *Planctomyces maris*. Later, in 2014, Scheuner and co-workers [2] on the basis of the results of further chemotaxonomic and phylogenomic analyses reclassified the genus *Planctomyces* and emended the description of the family *Planctomycetaceae*. They proposed the genus *Gimesia* under which *Gimesia maris* is the only species. The genus *Gimesia* comes under order *Planctomycetes* and family *Planctomycetaceae* having characteristic features of reproduction by budding. The genus *Gimesia* is characterized by the presence of sym-homospermidine as the polyamine, diphosphatidylglycerol, phosphatidyl-monomethyl-ethanolamine and phosphatidyl-dimethylethanolamine as major polar lipids, and $C_{16:0}$ and $C_{16:1}$ $\omega 7c/C_{16:1}$ $\omega 6c$ as major fatty acids.

G. maris is a slow-growing, obligately aerobic, mesophilic, heterotrophic marine bacterium with spherical to ovoid, rosette-forming cells. It reproduces by budding at the opposite pole of the cell, exhibiting longitudinal symmetry and has a single fibrillar appendage located at one pole of mature cells [1]. During our survey of planctomycetes from Chilika lagoon, strain JC646^T was isolated and its 16S rRNA gene sequence identity value was highest (97.3%) with *G. maris* DSM 8797^T. Strain JC646^T was characterized by using a polyphasic approach together with genomic information.

Author affiliations: ¹Department of Plant Sciences, School of Life Sciences, University of Hyderabad, P.O. Central University, Hyderabad 500046, India; ²Bacterial Discovery Laboratory, Centre for Environment, Institute of Science and Technology, JNT University Hyderabad, Kukatpally, Hyderabad-500085, India.

*Correspondence: Sasikala Ch., sasikala.ch@gmail.com; Ramana Ch.V., cvr449@gmail.com

Keywords: planctomycetes; Gimesia chilikensis sp. nov.; Chilika lagoon.

Abbreviations: AAI, average amino acid identity; ASW, artificial seawater; dDDH, digital DNA–DNA hybridization; gANI, genome average nucleotide identity; LCB, local collinear block; ME, minimum-evolution; ML, maximum-likelihood; NJ, neighbour-joining; POCP, percentage of conserved proteins. The GenBank/EMBL/DDBJ accession number for the 16S rRNA gene sequence of the strains JC646^T is LR132072. The GenBank/EMBL/DDBJ accession for the whole genome shotgun sequence is VTSR00000000.

†These authors contributed equally to this work

Four supplementary tables and six supplementary figures are available with the online version of this article.

ORIGINAL PAPER



Paludisphaera soli sp. nov., a new member of the family Isosphaeraceae isolated from high altitude soil in the Western Himalaya

Rishabh Kaushik · Meesha Sharma · Kumar Gaurav · U. Jagadeeshwari · A. Shabbir · Ch. Sasikala · Ch. V. Ramana D · Maharaj K. Pandit

Received: 8 June 2020/Accepted: 1 September 2020 © Springer Nature Switzerland AG 2020

Abstract A novel strain of Planctomycetes, designated JC670^T, was isolated from a high altitude (~ 2900 m above sea level) soil sample collected from Garhwal region in the Western Himalaya. Colonies of this strain were observed to be light pink coloured with spherical to oval shaped cells having crateriform structures distributed all over the cell surface. The cells divide by budding. Strain JC670^T was found to grow well at pH 7.0 and pH 8.0 and to tolerate up to 2% NaCl (w/v). MK6 was the only

Rishabh Kaushik and Meesha Sharma having equal authorship and consider as first authors.

Electronic supplementary material The online version of this article (https://doi.org/10.1007/s10482-020-01471-w) contains supplementary material, which is available to authorized users.

R. Kaushik · M. Sharma · M. K. Pandit (☒) Department of Environmental Studies, University of Delhi, Delhi 110007, India e-mail: rajkpandit@gmail.com

K. Gaurav · A. Shabbir · Ch. V. Ramana (⋈)
Department of Plant Sciences, School of Life Sciences,
University of Hyderabad, P.O. Central University,
Hyderabad 500046, India
e-mail: cvr449@gmail.com

U. Jagadeeshwari · Ch. Sasikala Bacterial Discovery Laboratory, Centre for Environment, Institute of Science and Technology, J. N. T. University Hyderabad, Kukatpally, Hyderabad 500085, India

Published online: 16 September 2020

respiratory quinone identified. The major fatty acids of strain JC670^T were identified as $C_{18:1}\omega 9c$, $C_{18:0}$ and C_{16:0}, and phosphatidylcholine, two unidentified phospholipids and six unidentified lipids are present as the polar lipids. The polyamines putrescine and sym-homospermidine were detected. Strain JC670^T shows high 16S rRNA gene sequence identity (95.4%) with *Paludisphaera borealis* PX4^T. The draft genome size of strain $JC670^{T}$ is 7.97 Mb, with G + C content of 70.4 mol%. Based on phylogenetic analyses with the sequences of ninety-two core genes, low dDDH value (20.6%), low gANI (76.8%) and low AAI (69.1%) results, differential chemotaxonomic and physiological properties, strain $JC670^{T}$ (= KCTC 72850^{T} = NBRC 114339^T) is recognised as the type strain of a new species of the genus Paludisphaera, for which we propose the name Paludisphaera soli sp. nov.

Keywords Soil bacteria · Western himalaya · Planctomycetes · Isosphaeraceae · *Paludisphaera* · High altitude

Abbreviations

NCBI	National Center for Biotechnology
	Information
ANI	Average Nucleotide Index
AAI	Average Nucleotide Index
dDDH	Digital DNA-DNA Hybridization
HPLC	High-Pressure Liquid Chromatography
KCTC	Korean Collection for Type Cultures



ovel insights into chemotropic L-tryptophan metabolism of ubrivivax benzoatilyticus JA2

privivax bei	nzoatilyticus JA2			
ENALITY REPORT				
4% LARITY INDEX	9% INTERNET SOURCES	12% PUBLICATIONS	1% STUDENT PAPER	S
ARY SOURCES				
baadals Internet Source	g.inflibnet.ac.in			3%
Prasuna Ramana canonica based m	Ahmad, Mujahid Mekala, Sasikala Chintalapati. "Tr al melanin precurs nelanin production ilyticus JA2", Scie	a Chintalapati, yptophan, a no sor: New L-try n by Rubriviva:	Venkata on- ptophan x	2%
WWW.NC Internet Source	bi.nlm.nih.gov		Prof. Ch. Venkaces school of Lind Prof. Ch. Venkaces school of Lind Department of Plant Sciences Apo. Central Univ Department of Plant Sciences School of Lind University of Hyderabad - 500 046, Indiversity of Hyderabad - 500 046, Indiversity of Lind	2 %
Sasikala Chintala	i Prasuna Mekala a Chintalapati, Ve pati. " Stable Isot ic Profiling Revea	nkata Ramana ope-Assisted	a.	2%

Catabolic Pathways of -Phenylalanine in JA2 ",

Journal of Proteome Research, 2017

Publication

_	Mujahid, Md, M Lakshmi Prasuna, Ch Sasikala,
5	and Ch Venkata Ramana. "Integrated
	metabolomic and proteomic analysis reveals
	systemic responses of Rubrivivax
	benzoatilyticus JA2 to aniline stress", Journal of
	Proteome Research, 2014.
	Dudilization

1%

Publication

Lakshmi Prasuna Mekala, Mujahid Mohammed, Sasikala Chinthalapati, Venkata Ramana Chinthalapati. "Pyomelanin production: Insights into the incomplete aerobic I-phenylalanine catabolism of a photosynthetic bacterium, Rubrivivax benzoatilyticus JA2", International Journal of Biological Macromolecules, 2019

1%

Md Mujahid, M Lakshmi Prasuna, Ch Sasikala, Ch Venkata Ramana. "Integrated Metabolomic and Proteomic Analysis Reveals Systemic Responses of JA2 to Aniline Stress ", Journal of Proteome Research, 2014

1%

Publication

Casadevall, Arturo, Antonio Nakouzi, Pier R. Crippa, and Melvin Eisner. "Fungal Melanins Differ in Planar Stacking Distances", PLoS ONE, 2012.

1%

Publication

Lakshmi Prasuna Mekala, Mujahid Mohammed,

Sasikala Chintalapati, Venkata Ramana Chintalapati. "Precursor-feeding and alteredgrowth conditions reveal novel blue pigment production by Rubrivivax benzoatilyticus JA2", Biotechnology Letters, 2019 Publication

<1%

Xueyan Hu, Yunbing Shen, Shengnan Yang, 10 Wei Lei, Cheng Luo, Yuanyuan Hou, Gang Bai. "Metabolite identification of ursolic acid in mouse plasma and urine after oral administration by ultra-high performance liquid chromatography/quadrupole time-of-flight mass spectrometry", RSC Advances, 2018

<1%

Publication

M. Lakshmi Prasuna, Md. Mujahid, Ch. 11 Sasikala, Ch.V. Ramana. "I-Phenylalanine catabolism and I-phenyllactic acid production by a phototrophic bacterium, Rubrivivax benzoatilyticus JA2", Microbiological Research, 2012

<1%

Publication

S J.W.H.. "Sulfate reduction in methanogenic 12 bioreactors", FEMS Microbiology Reviews, 10/1994

<1%

Publication

Ranjith N. Kumavath, Ch. V. Ramana, Ch. 13 Sasikala. "I-Tryptophan catabolism by

Rubrivivax benzoatilyticus JA2 occurs through indole 3-pyruvic acid pathway", Biodegradation, 2010

Publication

Maik Böhmer. "Quantitative transcriptomic analysis of abscisic acid-induced and reactive oxygen species-dependent expression changes and proteomic profiling in Arabidopsis suspension cells: ABA- and ROS-regulated expression changes", The Plant Journal, 07/2011

Publication

Mohammed, Mujahid, Sasikala Ch, and Ramana V. Ch. "Aniline Is an Inducer, and Not a Precursor, for Indole Derivatives in Rubrivivax benzoatilyticus JA2", PLoS ONE, 2014.

Publication

Ranjith N. Kumavath. "Production of Phenols and Alkyl Gallate Esters by Rhodobacter sphaeroides OU5", Current Microbiology, 10/14/2009

Publication

K. Glass, S. Ito, P. R. Wilby, T. Sota et al.
"Direct chemical evidence for eumelanin pigment from the Jurassic period", Proceedings of the National Academy of Sciences, 2012

Publication

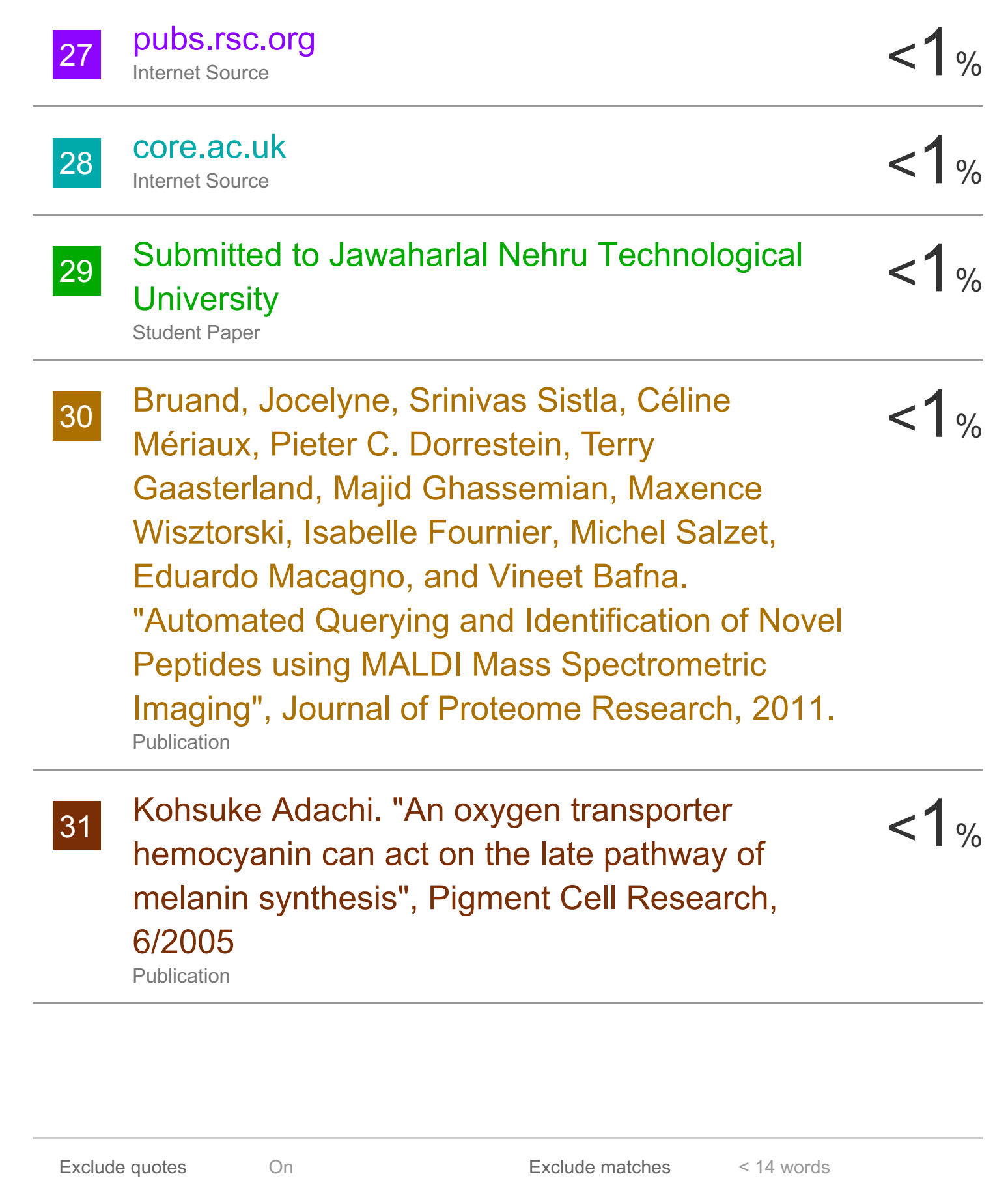
<1%

<1%

<1%

<1%

18	www.mcponline.org Internet Source	<1%
19	Mujahid Mohammed, Sasikala Ch, Ramana V. Ch. "Aniline Is an Inducer, and Not a Precursor, for Indole Derivatives in Rubrivivax benzoatilyticus JA2", PLoS ONE, 2014 Publication	<1%
20	www.livrosgratis.com.br Internet Source	<1%
21	refubium.fu-berlin.de Internet Source	<1%
22	www.mdpi.com Internet Source	<1%
23	duepublico.uni-duisburg-essen.de:443 Internet Source	<1%
24	res.mdpi.com Internet Source	<1%
25	link.springer.com Internet Source	<1%
26	S. Bertaux, R. G. Harrison. "Purification of Prephenate Dehydratase from by Affinity Chromatography ", Preparative Biochemistry, 1991 Publication	<1%



Exclude bibliography Or